MECHANISTIC AND EQUILIBRIUM STUDIES OF MACROCYCLIC COMPOUNDS

A Thesis

submitted for the degree of

DOCTOR OF PHILOSOPHY

in the Faculty of Science of the

University of St. Andrews

by

Mansour M. Hassan B.Sc., M.Sc.

April 1992

United College of St. Salvator

and St. Leonards College

To my

Parents,

family, and

Teachers

with gratitude

DECLARATION

I, Mansour M. Hassan, hereby certify that this thesis has been composed by myself, that it is a record of my own work, and that it has not been accepted in partial or complete fulfilment of any other degree or professional qualification .

I was admitted to the Faculty of Science of the University of St. Andrews under Ordinance No. 12 In October, 1988.

Signed April 1992

CERTIFICATION

I hereby certify that the candidate has fulfilled the conditions of the Resolutions and Regulations appropriate to the degree of Ph.D.

Signed . April 1992

COPYRIGHT

ACKNOWLEDGEMENTS

I wish to thank my supervisor R.W. Hay for his limitless supply of patience, cooperation and guidance over the duration of my degree. I also sincerely thank, Professor M.S. El-Ezaby for his supervision and assistance during the course of this work, Professor Y. Sulfab for fruitful discussions and Dr B. Jeragh for general advice. I am grateful also to Drs. H. Marafie and N. Shuaib for the use of equipment and research laboratories.

I thank the Chemistry departments of St. Andrews University, Kuwait University, and Stirling University for providing research facilities, and Aden University for providing financial support. I wish to thank the British Council which contributed funds towards a six months study period. Special thanks are also due to Drs. J. Crayston and D. Richens for discussions and assistance. Many thanks go to my fellow researchers for their friendship, happy memories and moral support. I also thank Drs. A. Patel, M. Nasreldin, S. Miller and S. Bajbaa for their help. Dr. M. Khanna is also thanked for the typing of this thesis.

Finally, and most importantly, I wish to thank my parents, family, brothers and sisters for their encouragement throughout my academic career.

CONTENTS

ABBREVIATIONS

The following abbreviations are used for convenient nomenclature of the various ligands.

2,2,2-tet	1,8-diamino-3,6-diazaoctane
2,3,2-tet	1,9-diamino-3,7-diazanonane
3,2,3-tet	1,10-diamino-4,7diazadecane
3,3,3-tet	1,11-diamino-4,8-diazaundecane
[12]aneN$_4$	1,4,7,10-tetra-azacyclododecane
[13]aneN$_4$	1,4,8,10-tetra-azacyclotridecane
[14]aneN$_4$	1,4,8,11-tetra-azacyclotetradecane
[15]aneN$_4$	1,4,8,12-tetra-azacyclopentadecane
[16]aneN$_4$	1,5,9,13-tetra-azacyclohexadecane
[15]aneN$_5$	1,4,7,10,13-penta-azacyclopentadecane
Me$_2$cyclam	C-meso-5,12-dimethyl-1,4,8,11-tetra-azacyclotetradecane
tet a	C-meso-5,7,7,12,14,14-dimethyl-1,4,8,11-tetra-azacyclotetradecane
tet b	C-rac-5,7,7,12,14,14-dimethyl-1,4,8,11-tetra-azacyclotetradecane
dioxocyclam	5,7,-dioxo-1,4,8,11-tetra-azacyclotetradecane
hexacyclen	1,4,7,10,13,16-hexa-azacyclooctadecane
TMC	N, N', N", N'"-tetramethyl-1,4,8,11-tetra-azacyclotetradecane
THEC	N, N', N", N'"-tetrakis(2-hydroxyethyl)-1,4,8,11-tetra-azacyclotetradecane
TCEC	N, N', N", N'"-tetrakis(2-cyanoethyl)-1,4,8,11-tetra-azacyclotetradecane
THPC	N, N', N", N'"-tetrakis(2-hydroxypropyl)-1,4,8,11-tetra-azacyclotetradecane
glygly	glycylglycine
glyglygly	glycylglycylglycine
glyglyhis	glycylglycylhistidine
$2_N.1_O.1_O$	1,4,7,10-tetra-aza-13,18,-dioxabicyclo[8.5.5]eicosane

ABSTRACT

This thesis is divided into two main parts. Part 1 covering Chapters 1, 2, and 3 deals with the dissociation, formation, and ligand exchange kinetics of macrocyclic compounds. The effects of ring size and ring substitution have been examined. Chapter 1 deals with the kinetics of the acid dissociation reactions of nickel(II) and copper(II) complexes of six macrocycles containing 14-, 15-, 16-, and 18- membered rings and one open-chain tetraamine.

At high acidities, all the macrocyclic complexes, with the possible exception of $[Cu(hexacyclen)]^{2+}$ and the copper complex of an N_3O_2 macrocycle, show a nonlinear dependence on $[H^+]$ with $k_{obs} = A[H^+] / (1+ B[H^+]) s^{-1}$. A mechanism involving rapid preequilibrium protonation and slow dissociation is proposed for these reactions. The (hexacyclen) and the (mixed-donor N_3O_2) copper(II) complexes show a linear dependence on $[H^+]$ with $k_H = k_{obs} / [H^+] = 75.0$ dm^3 mol^{-1} s^{-1} and $k_H = (k_{obs} - k_d) / [H^+] = 40.17$ dm^3 mol^{-1} s^{-1} respectively.

At low acidities, the reactions of copper(II) and nickel(II) complexes of some ligands show second order dependence on $[H^+]$, with the following rate constants (dm^6 mol^{-2} s^{-1}): copper(hexacyclen)$^{2+}$, 8.5 x 10^3; nickel(hexacyclen)$^{2+}$, 97.0 for the first fast step and 24.7 for the second slow step; and copper(2,2,2-tet)$^{2+}$, 8.5 x 10^5.

Chapter 2, deals with the formation kinetics of copper(II) with [14]aneN_4, [15]aneN_4, [16]aneN_4, C-meso Me_2cyclam, C-meso Me_6 cyclam (tet a), C-rac Me_6 cyclam (tet b), dioxocyclam, and THPC in strongly basic media (0.05 - 0.4 mol dm^{-3} NaOH) at 25.0 °C. Under these conditions the copper is present as $Cu(OH)_3^-$ and $Cu(OH)_4^{2-}$ with $Cu(OH)_3^-$ being the more reactive species. The comparative kinetic behaviour indicates that (1) the formation rates increase as the ring size increases, (2) methyl substitution in C-meso Me_2cyclam, tet a, and tet b leads to significant decreases in the formation rates. Oxygen substitution at the carbon atoms of cyclam (dioxocyclam)

and the hydroxypropyl substitution at the nitrogen donor atoms of cyclam (THPC) have only a relatively small effect upon complexation rates. The effect of ring size and substitution at carbon and nitrogen on the formation rate constants are discussed and the mechanism commented on in detail.

Chapter 3 deals with the ligand exchange kinetics of [14]aneN$_4$, [15]aneN$_4$, and [16]aneN$_4$, with the copper(II) complex of diglycine ($CuH_{-1}G_2$), in the pH range 7.5 - 9.5 at 25.0 ^oC. The rates of displacement of diglycine from copper(II) by the macrocycles are rapid with no observable intermediates. The rate expression is rate = k_{obs} $[CuH_{-1}G_2]$ $[MAC]_T$ where $[MAC]_T$ is the total concentration of the macrocycle and $[CuH_{-1}G_2]$ is the total concentration of copper(II)glycylglycinate. All three macrocycles react with both the aqua- and hydroxo-copper diglycylglycinate species { $[Cu(H_{-1}G_2)(OH_2)]$ and $[Cu(H_{-1}G_2)(OH)]^-$ }. Rate constants for reaction with the hydroxo-complex are 14 - 41 times greater than those for the aqua- complex, presumably due to eletrostatic effects as the monoprotonated macrocycle (HL^+) is the reactive species in the pH range of the measurement. The reaction of HL^+ with { $[Cu(H_{-1}G_2)(OH_2)]$ and $[Cu(H_{-1}G_2)(OH)]^-$ } presumably involves initial displacement of H_2O (OH^-) followed by displacement of the peptide carboxylate group. The reactions of [14]aneN$_4$, [15]aneN$_4$, and [16]aneN$_4$, with the copper(II) complex of triglycine $(CuH_{-2}G_3)^-$ have been studied in the pH range 7.5 - 9.5 at 25.0 ^oC. The macrocycles react rapidly with the doubly deprotonated (triglycinato)cuprate(II) complex to give $Cu(MAC)^{2+}$ and the free peptide. The rate expression is rate = k_f [Cuglyglygly] [MAC] + k_d where k_d represent the solvolytic pathway. On the basis of the pH dependence it is concluded that various ligand species, L, HL^+, H_2L^{2+} are reactive with copper(II) glycylglycylglycinate and the reactivity decreases in the order $L > HL^+ > H_2L^{2+}$. It was possible to resolve the individual second order rate constants (dm^3 mol^{-1} s^{-1}, I = 0.15 mol dm^{-3}) for the reaction of $Cu(H_{-2}G_3)^-$ with all three macrocycles. Possible

mechanisms involving the formation of a ternary complex of the type [$Cu(H_{-1}G_3)$(MAC)] are considered .

Part 2 (Chapter 4) discusses the determination of protonation constants and formation constants for copper(II) and nickel(II) with the macrocycles [15]aneN_4, [16]aneN_4, dioxocyclam, and N,N'- bis(2- cyanomethyl)-5,7-dioxo-1,4,8,11-tetra-azacyclotetradecane, and the linear ligands glycylglycylhistidine, 2,2,2-tet, 2,3,2-tet, and 3,2,3-tet at 25.0 °C and various ionic strengths. The computer program SUPERQUAD was used to process the potentiometric data, and the program SQUAD II to process data obtained from spectrophotometric measurements .

The first two protonation steps of the macrocyclic tetra-amines are more basic than the corresponding open-chain tetra-amine. Two complexes were found in the copper(II) [15]aneN_4 and [16]aneN_4 systems, the 1:1 complex $[ML]^{2+}$ and a protonated species $[MHL]^{3+}$. In addition nickel(II) and copper(II) give the 2 : 1 : 2 complex $[M(HL)_2]^{4+}$ with the linear tetraamines. Nickel(II) also gives the diprotonated species 1:1:2 $[Ni(H_2$ 3,2,3-tet$)]^{4+}$ and the triprotonated species 1:1:3 $[Ni(H_3$ 3,2,3-tet$)]^{5+}$. Complexation of copper(II) and nickel(II) with dioxocyclam, N,N'- bis(2-cyanomethyl)-5,7-dioxo-1,4,8,11-tetra-azacyclotetradecane, and glycylglycylhistidine induce ionisation of the amide protons. Formation constants for species such as 1:1: -1 $[M(H_{-1}L)]$ and 1:1: -2 $[M(H_{-2}L)]$ were determined.

CHAPTER 1

Kinetics and Mechanism of the Acid-catalysed Dissociation of Polyaza- Macrocyclic Complexes

1.1 INTRODUCTION

The kinetics of the acid-catalysed dissociation of metal complexes is a subject of much interest and recently particular attention has been directed towards the complexes of macrocyclic ligands in an attempt to understand the unusual thermodynamic and kinetic properties of these complexes.

Early workers with complexes of 14-membered macrocyclic tetra-aza ligands recognised that these compounds were both unusually stable in the thermodynamic sense, and were inert towards ligand dissociation, even in strong mineral acids.

The term "macrocyclic effect" was first introduced in 1969 by Cabbiness and Margerum[1] to highlight the large thermodynamic stability found for the macrocyclic complex $[Cu(tet\ \underline{a})]^{2+}$(I) compared with $[Cu(2,3,2)\text{-}tet]^{2+}$(II).

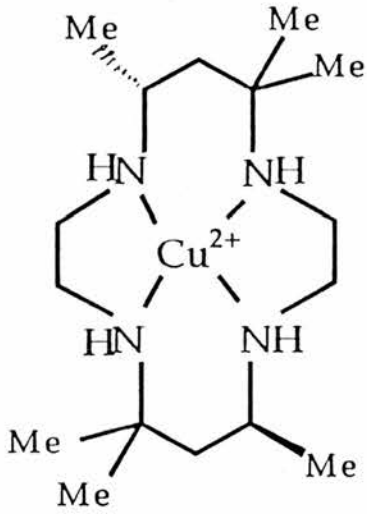

I

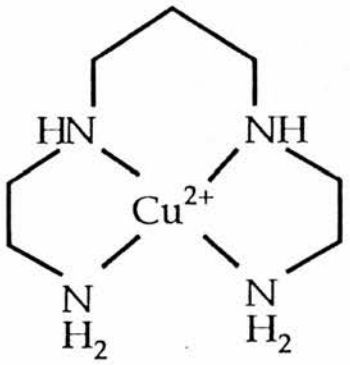

II

In general terms the "macrocyclic effect" refers to the decrease in Gibbs energy for the metathetic reaction.

$$ML_{acyclic}^{n+} + L_{cyclic} \longrightarrow ML_{cyclic}^{n+} + L\,;\quad K\sim 10^{6}$$

and considerable attention has been directed towards separating ΔG^{o} into its component enthalpic and entropic contributions. Early conflicting studies assigned the additional

stability to wholly entropic[2] or wholly enthalpic[3] factors. Further investigations[4,5] have shown that the entropy term is always favourable and that the enthalpy term is dependent on the matching of the macrocyclic ligand aperture to that of the metal ion.

The "macrocyclic effect" can also be considered in kinetic terms, as the formation constant for the equilibrium (1) is given by

$$M_{(solv)} + MAC_{(solv)} \rightleftharpoons M(MAC)_{(solv)} \; ; \; K \qquad (1)$$

$K = k_f / k_r$. Although the rates of formation may sometimes be somewhat slower in the case of macrocyclic complexes (Chapter 2), a much greater decrease normally occurs for the dissociation rates. The latter reflect the enhanced thermodynamic stabilities which are characteristic of the "macrocyclic effect".

For 14- membered tetra-aza macrocycles the acid dissociation reactions are very slow. Thus [Cu(cyclam) $]^{2+}$ is not decomposed in 6 M HCl over a period of several weeks, although copper(II) complexes are normally very labile. The half life of [Ni(cyclam) $]^{2+}$ in 1 M $HClO_4$ has been shown by Billo to be *ca*, 30 years [11].

Relatively few detailed kinetic studies of the acid-promoted dissociation reactions of complexes of nickel(II) and copper(II) with tetra-aza macrocyclic ligands have been reported[6]. The reactions can usually be accommodated within the same general mechanistic framework for complexes of acyclic polyamines (Scheme I). Reaction rates may, however, be slower by many orders of magnitude[7].

Studies of the acid-promoted dissociation of azamacrocyclic complexes of nickel(II) and copper(II) have revealed a variety of dependencies of the rate on the hydrogen ion concentration. Some reactions show a first-order dependence on $[H^+]$, and many also display an acid-independent term, with $k_{obs} = ko + k_H[H^+]$[8-12]. (or consecutive reactions of this type[13]). Copper(II) complexes of some tetra-aza macrocycles with

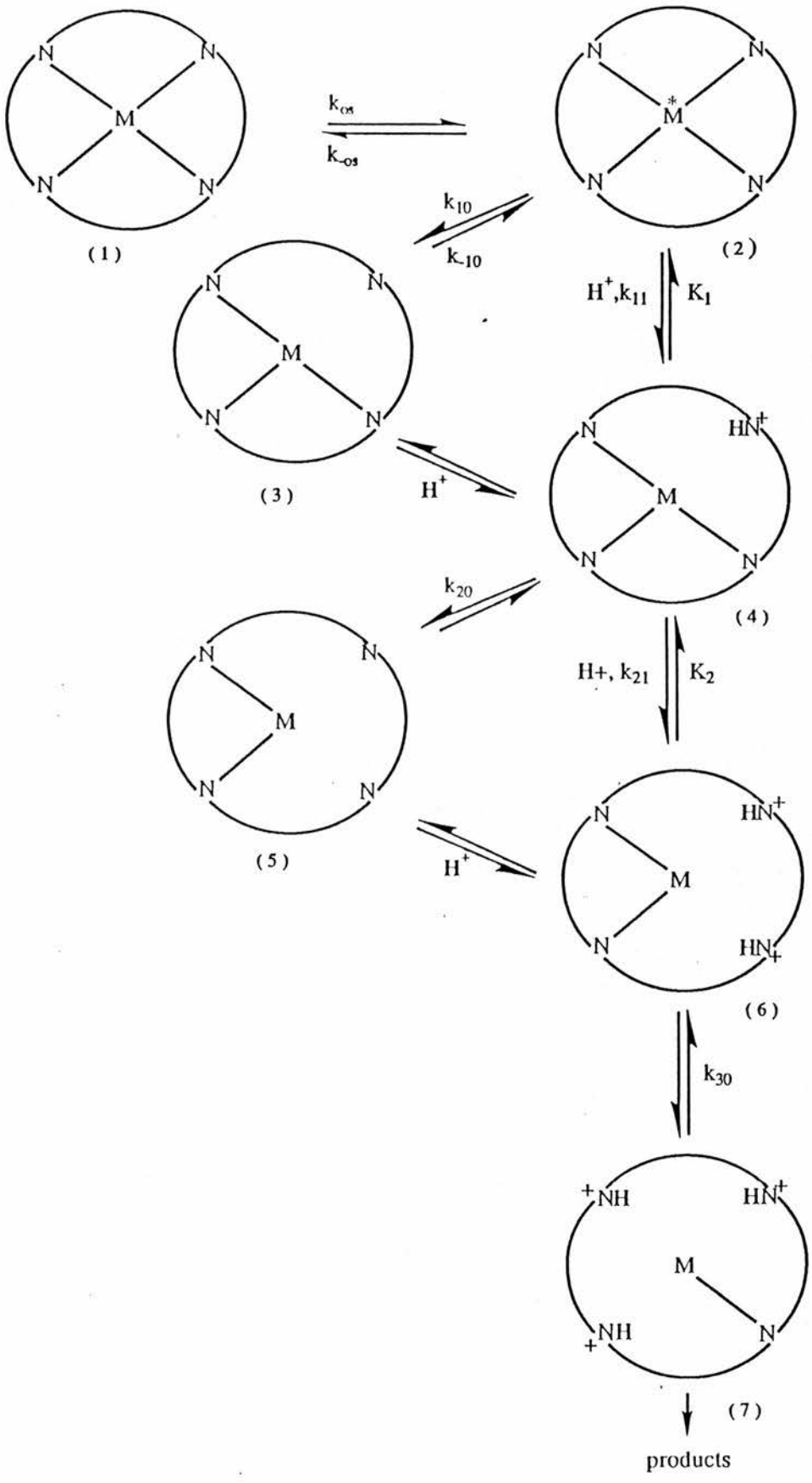

Scheme I Part of the dissociation / protonation reaction sequence for tetra-aza macrocycle complexes .

amido groups[14] and cyclic pentaamines[12,14-16] show a second order dependence on $[H^+]$[15].

For other macrocycles, "acid-limiting" kinetics have been interpreted as indicating the presence of a rapid pre-equilibrium protonation followed by rate-determining dissociation

$$ML + H^+ \rightleftharpoons MLH^+ \quad ; \quad K \text{ (fast)} \qquad (1)$$

$$MLH^+ \longrightarrow M + HL^+ \; ; k \text{ (slow)} \qquad (2)$$

leading to the kinetic expression $k_{obs} = kK / (1 + K[H^+])$ [17,18]. This mechanistic scheme can apply to systems which show a linear dependence of rate on $[H^+]$. When K is small, $k_{obs} = k_o + k_H K [H^+]$ [9,10]. "Acid-limiting" kinetics are also compatible with a mechanism that has a rate-determining reaction of $[H^+]$ with an "activated" species, formed reversibly from the initial complex cation[19,20].

Hydrolysis rates in 0.3 mol dm^{-3} $HClO_4$ for nickel(II) complexes of cyclic tetraamines with 13-16 membered rings show a marked dependence on ring size, with the slowest rate for the 14-membered amine, [14]aneN$_4$[21,20]. However, rates at a single acid concentration are not very informative if the acid dependence is unknown. The dissociation of $[Ni([13]aneN_4)]^{2+}$ has been shown to be complex[20]. The rate of acid hydrolysis is significantly different for nitrogen configurational isomers of the nickel(II) complex with [14]aneN$_4$[11] and TMC[22] and for copper(II) complexes of the hexamethyl derivatives of [14]aneN$_4$[13].

Acid hydrolysis reactions of copper(II) amine complexes are usually more rapid than those of their nickel(II) analogues. Factors of 10^5 fold occur when metal ion-donor atom bond breaking is important in the rate determining step[20]. The complexes of [16]aneN$_4$ 8 and [17]aneN$_4$ 9 (with one large chelate ring of eight and nine members

respectively) react relatively rapidly with acid, and become independent of $[H^+]$ at high acidities with "acid-limiting" kinetics[18].

The copper(II) and nickel(II) compounds of the macrocyclic di-imine of the type *cis*- and *trans*- [14]dieneN$_4$, [15]dieneN$_4$, [16]dieneN$_4$ and [18]dieneN$_4$[18] react slowly with acid. Acid-limiting kinetics were observed except for $[Ni(Me_6[15]dieneN_4)]^{2+}$ where a linear dependence on $[H^+]$ was observed.

This work reports studies of the acid dissociation of nickel(II) and copper(II) complexes of seven macrocyclic ligands. In addition, one open-chain ligand, L^{10}, has also been studied. The aim of the work was to determine the effects of ring size, ring substitution, and the effects of macrocyclic and linear amines on dissociation rates. The structures of the ligands are given in Figure 1.1 along with their systematic abbreviations.

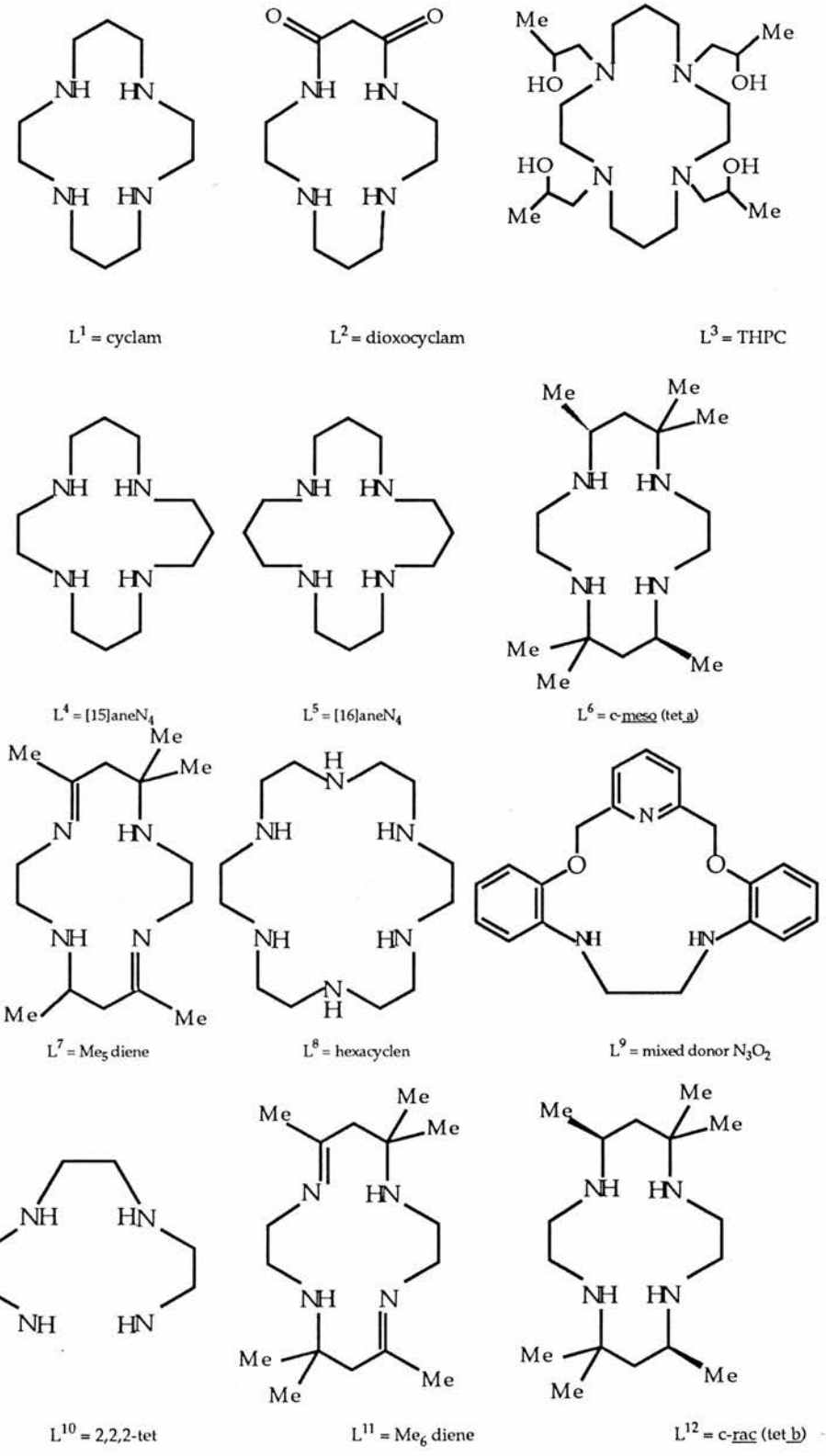

Figure1.1 The ligands studied in this work.

1.2 Acid Dissociation of the Copper(II) Complexes of [15]aneN$_4$ and [16]aneN$_4$.

1.2.1 INTRODUCTION

The acid-promoted dissociation of copper(II) and nickel(II) complexes of macrocyclic ligands containing S_4, O_2N_2, and N_4- donor sets have been studied. The dissociation rates of copper(II) complexes of cyclic polyethers, in 80% methanol/water, do not vary in a regular manner with macrocyclic hole size(56). The kinetic labilities of the acid dissociation rates of the 15- to 17-membered, O_2N_2 ring macrocycles follow the ring size sequence 14 > 15 > 16 < 17(57). For compounds of Cu(II) and Ni(II) with a homologous series of tetra-aza macrocycles of varying ring size, acid-promoted dissociation rates are generally smallest for the 14-membered macrocycle. The ring-size dependence has been attributed to the extent of strain inherent in the square planar coordination of the macrocycles, which is least for the symmetrical 14-membered macrocycle when coordinated to copper(II) or singlet-ground-state nickel(II). However, slow acid dissociation is not only observed in complexes with planar azamacrocycles but also for complexes with tetra-aza macrocycles in folded cis-geometry and for complexes of triazamacrocycles, which must coordinate facially(8). Slow dissociation has also been observed with some cyclic diamines (43). One common factor of cyclic amines is the absence of a terminal amino group that could initiate an "unzipping" mechanism, on cleavage of a metal-nitrogen bond. However, copper(II) compounds of large ring cyclic pentaamines and copper(II) and nickel(II) of cyclic hexaamines react with acid at rates comparable with those of noncyclic polyamines(13, 14, 58), and some nickel(II) and copper(II) compounds of 14-membered cyclic tertiary tetra-aza macrocycles also react rapidly(10, 22, 58, 59), so other factors must be involved in determining the reaction rates. The unusual thermodynamic and ligand field properties of complexes of cyclic tetraamines, compared with those of linear analogues, can largely be attributed to the substitution of two secondary for two primary amino groups upon cyclization, with the increased inter-

and intra ligand strain present when terminal secondary amino groups are present[60]. Some of the enhanced kinetic stability of cyclic amine complexes may arise from the slightly stronger metal nitrogen bonds (Chapter 4). It appears more probable that the very slow reaction rates arise from some organisational process, e.g. a concerted conformational change required to move a dissociated nitrogen away from the coordination site. A process of this nature is likely to be very independent on structural features, such as ring size, ring substitution, and ring unsaturation[20].

1.2.2 EXPERIMENTAL

Preparation of the ligands.

The ligands [15]aneN$_4$ (L^4) and [16]aneN$_4$ (L^5) were obtained by the modified procedure of Richman and Aitkins[24a,24b]. The synthetic routes involve four major steps: (1) tosylation of both reagents [25-28] , (2) conversion of the tosylated linear tetraamine into its disodium salt with sodium hydride (Scheme II), (3) cyclization, where the tosylated amine sodium salt is reacted with the tosylated amine diol in DMF, (4) detosylation of the tetratosylated macrocycle using either 96% H_2SO_4[29], HBr in acetic acid[30] or 80% H_2SO_4[3]. An alternative preparative procedure is shown in Scheme III. In this Scheme, the condensation occurs between the appropriate tosylated amine and the dibromide in DMF.

The starting amine 3,3,3-tet was prepared following the same procedure described below for the preparation of 2,2,2-tet. The resulting amine was purified by vacuum distillation from barium oxide. The tetratosylate of the linear amine was prepared by the dropwise addition of 238.5 g (1.25 mole) of *p* -toluenesulphonyl chloride dissolved in 1.25 litres of diethyl ether to a solution of 40 g (1 mol) of sodium hydroxide and 47.1 g (0.25 mol) of the linear tetraamine in 100 cm^3 of water, the mixture was vigorously stirred during the addition and for an hour after its completion. The resulting sticky paste was

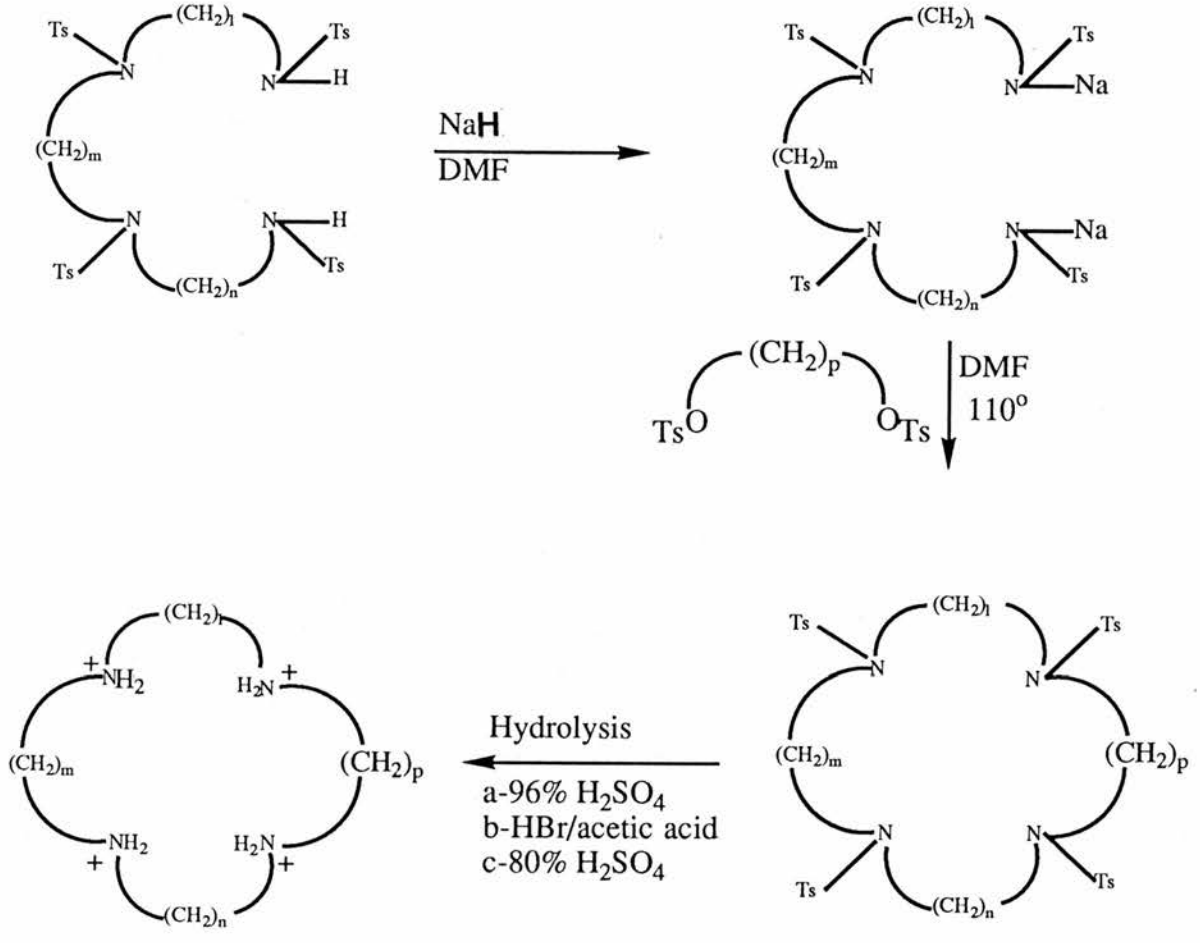

Scheme II Synthetic routes for the preparation of L^4 (l = m = n = 3; p = 2) and L^5 (l = m = n = 3) .

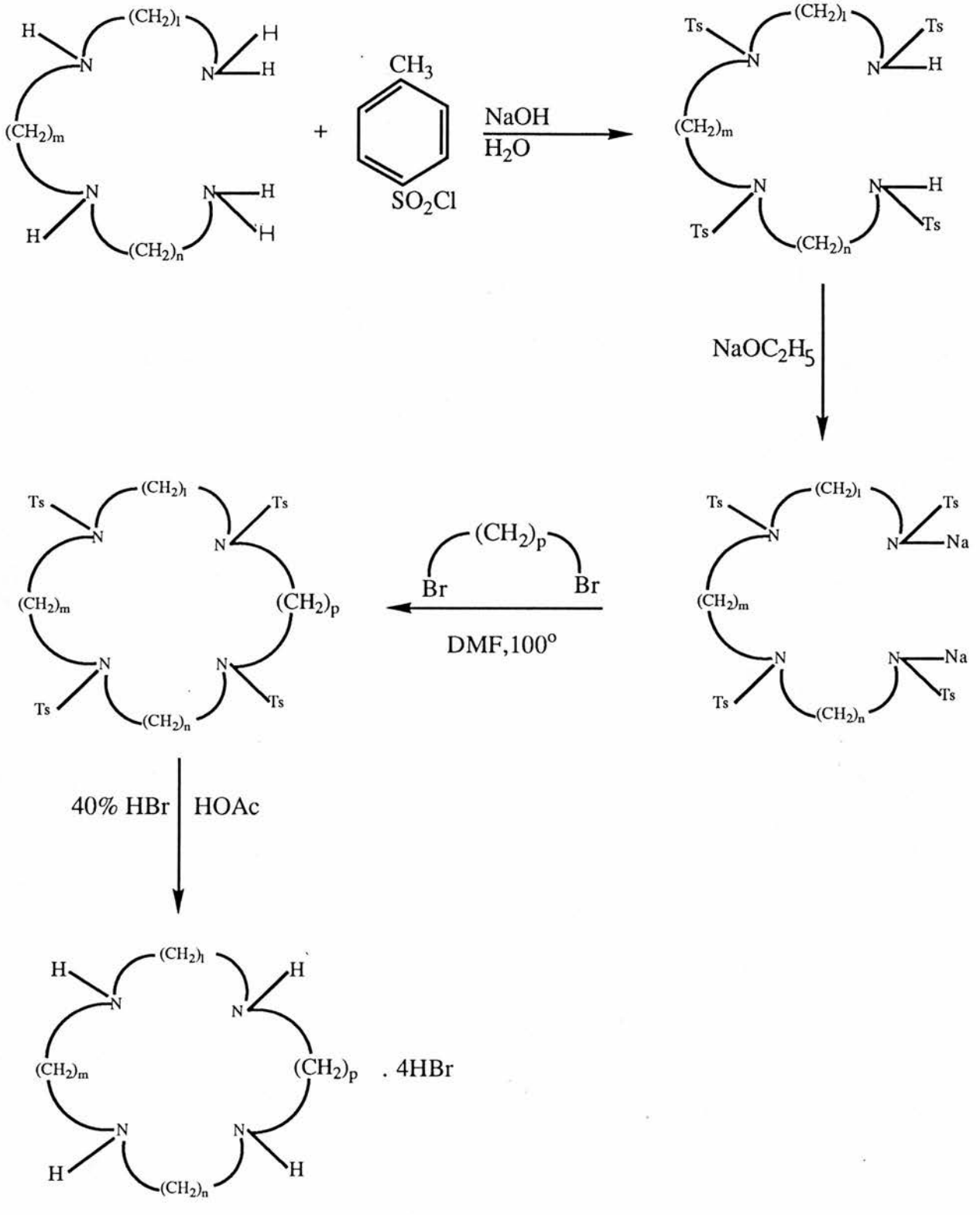

Scheme III Alternative synthetic routes for the preparation of L^4 (l = m = n =3 ; p = 2) and L^5 (l = m = n = 3).

chilled in an ice bath and removed by filtration. It was washed well with diethyl ether and water and thoroughly dried in a *vacuo* at 50 ^{o}C to obtain a white powder.

Small portions of sodium hydride were added to a solution of 40.25 g (0.05 mol) of the tosylated linear amine in 500 cm^3 of DMF until the evolution of hydrogen has ceased. The excess sodium hydride is removed by filtration and the filtrate heated to 110 ^{o}C with continuous stirring. A solution of 19 g (0.05 mole) of the ditosylate of 1,2-dihydroxyethane (or 19.7g (0.05 mol) of the ditosylate of 1,3-dihydroxypropane) in 250 cm^3 of DMF was added dropwise with stirring. Stirring was continued for 2 h at a temperature 110 ^{o}C. The volume was then reduced to 125-120 cm^3 by vacuum distillation and the solution was added to 1 litre of water to cause precipitation. The solid was removed by filtration, washed well with water, and dried at 60 ^{o}C. The free amine was formed by reaction of the tetratosylated [15]aneN_4 (or [16]aneN_4) with 80% H_2SO_4 (2 cm^3 H_2SO_4 /g tetratosylate). The resulting suspension was then heated slowly with stirring to a temperature of 150-160 ^{o}C by use of oil-bath. The temperature was held at 150 ^{o}C for 1 h when all the solids had dissolved. The reaction mixture was cooled and added very slowly, with vigorous stirring, to methanol/diethyl ether (1:1; 400 cm^3) in an ice-bath. The resultant flocculent solid mass was filtered off and washed with diethyl ether. It was then dissolved in the minimum amount of water and brought to pH 10 with sodium hydroxide. The solution was then extracted six times with 30 cm^3 portions of chloroform (or dichloromethane). The extracts were dried with anhydrous sodium sulphate. After removal of the drying agent, the chloroform (or dichloromethane) was stripped on a rotary evaporator to give a light yellow solid. The [15]aneN_4 was recrystallised from hexane to give fine white needles (m.p. 99-100^{o}C; Found: C, 61.4; H, 12.3; N, 26.0. Calc. for $C_{11}H_{26}N_4$: C, 61.6; H, 12.2, N, 26.2%). The [16]aneN_4 was recrystallised from ether to give white crystals (m.p. 83-84 ^{o}C; Found: C, 62.93; H, 12.25; N, 24.29. Calc. for $C_{12}H_{28}N_4$: C, 63.11; H, 12.36; N, 24.53%).

Preparation of Complexes.

$[CuL^4][ClO_4]_2$

Copper(II) perchlorate hexahydrate (0.17 g, 0.46 mmol) was dissolved in hot ethanol (10 cm^3). To this solution was added the macrocyclic ligand L^4 (0.1 g, 0.47 mmol) dissolved in hot ethanol (10 cm^3). The resulting purple solution was heated on a steam bath for 15 minutes then cooled for several hours at 4 °C. The purple crystals which formed were filtered off, washed with ethanol then ether and dried *in vacuo*.

$[CuL^5][ClO_4]_2$

Copper(II) perchlorate hexahydrate (0.17 g, 0.46 mmol) was dissolved in hot ethanol (10 cm^3). To this solution was added the macrocyclic ligand L^5 (0.1 g, 0.44 mmol) dissolved in hot ethanol (10 cm^3). The resulting purple solution was heated on a steam bath for 15 minutes then cooled for several hours at 4°C. The purple crystals which formed were filtered off, washed with ethanol then ether and dried *in vacuo*.

The electronic and i.r. spectra of the ligands and their metal complexes are summarised in Tables 1.1 and 1.2. I.r. spectra were obtained on a Perkin Elmer 457 instrument using KBr discs.

Reagents

Ionic strength was adjusted using $NaClO_4.H_2O$ (Fluka; puriss > 99 %) and NaCl (Fluka; puriss > 99.5 %). Stock solutions of these salts were prepared by accurate weighing.

The copper(II) perchlorate hexahydrate ($Cu(ClO_4)_2.6H_2O$, BDH, AR) was recrystallised twice from water and standardised potentiometrically against standard EDTA solution using a Cu-selective electrode (Russell ISE94-4299/57) as the indicator electrode. Solutions of nitric and hydrochloric acids were prepared from BDH CONVOL ampoules. Stock solution of perchloric acid (BDH, Analar, 71-73 %) was standardised by pH titration against sodium hydroxide using a combined glass electrode (Radiometer, GK 2311C).

Table 1.1 The principal absorption bands and molar absorptivities of the copper(II) and nickel(II) complexes.

Complex	λ_{max}/nm	$\varepsilon/M^{-1}cm^{-1}$
$[CuL^2]$	510 [a](506) [b]	62.4 [a] (86) [b]
	510 [c]	94 [c]
	260 [c]	4900 [c]
$[CuL^4][ClO_4]_2$	571	140
$[CuL^5][ClO_4]_2$	603	253
blue$[CuL^3][ClO_4]$ H_2O	645 (650) [d] (636) [e]	263 (195) [d]
red$[CuL^3][ClO_4]$ H_2O	520 (500) [d] (515) [e]	(124) [d]
$[CuL^8][ClO_4]$ H_2O	800 (sh) 649	89
green$[CuL^9(NO_3)]$ NO_3 $0.5H_2O$	752 212	
$[CuL^{10}][ClO_4]_2$ H_2O	575 257	149.4
$[Cu(H_2O)_6]^{2+}$	810 [f] (810) [g]	11.41 [f] (11.4) [g]
$[NiL^2]$	464 [b]	77 [b]
	438 [h]	61 [h]
$[NiL^7][ClO_4]_2$	438 (433) [i]	90 (82) [i]
$[NiL^8][ClO_4]_2$ H_2O	546	10
	350	18
$[NiL^{10}][ClO_4]_2$ H_2O	922 (922) [j]	12.54 (12.54) [j]
	565 (565) [j]	6.3 (6) [j]
	357 (357) [j]	9 (9) [j]
$[Ni(H_2O)_6]^{2+}$	720 (720) [j]	2.1 (2.1) [j]
	660 (660) [j]	1.8 (1.8) [j]
	395 (395) [j]	5.1 (5.0) [j]

[a](pH=5; $[L^2]=10[Cu^{2+}] = 5x10^{-3}M$); [b]Ref.36; [c](pH = 11;$[L = 10[Cu^{2+}] = 5x10^{-3}M$); [d]Ref. 39; [e]Ref. 47; [f] as perchlorates in 0.5 M $NaClO_4$ (or as nitrates in 0.1M $NaNO_3$); [g]Ref. 45; [h] at pH=12.5; [i]Ref 34; [j]Ref. 40.

Table 1.2 Prominent i.r. absorption in the macrocyclic ligands and their metal complexes (KBr).

Compound	ν(C=O) cm^{-1}	ν(C=N) cm^{-1}	ν(N-H) cm^{-1}	$\nu(ClO_4^-)$ cm^{-1}
L^2	1660_s 1560_s		3260, 3200 3130, 3050	
L^3 a			absent at 3280	
$L^4.2H_2SO_4$			several(3300-3200)	
$L^5.4HCl$				
$L^6.2H_2O$		absent at 1660	3280_s, 3250_s	
$L^7.2HClO_4$		1660_{vs}	$3150_{s,br}$	$1110_{vs,br}$
$L^{11}.2HBr.2H_2O$		1670_{vs}	$3280_{(s)}$	$580_{(s)}$
$L^{12}.H_2O$		absent at 1660	$3300_{(m)}$, $3280_{(s)}$	
$[CuL^2]1.5H_2O$ b			3160	
$[CuL^6][ClO_4]H_2O$			3280_m, 3250_m	1089_{sh},610_s
$[CuL^8][ClO_4].2H_2O$			3300, 3260	1100,628
$[CuL^{12}][ClO_4]H_2O$			3250_s, 3225_w	
$[NiL^2][ClO_4]1.5H_2O$ b			3160	
$[NiL^7][ClO_4]$		1650_s	$3180_{s,br}$	$1085_{br, vs}$
$[NiL^8][ClO_4]_2.2H_2O$			3318, 3280	1100,628

vs = very strong, s = strong, m = medium, sh = shoulder, w = weak, br = broad.

a (OH) 3440

b Other bands (CuL^2, amide bonds = 1580s, 1550m; (OH)3440br; NiL^2, amide bands, 1640m, 1595m, 1535s; (OH)3450b).

Kinetic Measurements

Absorbance and repetitive scan measurements were made using Hewlett Packard 8452 photodiode array spectrophotometer interfaced with a Hewlett Packard Vectra PC(EC) provided with a Hewlett Packard kinetic analysis software. Dissociation rates of the [16]aneN$_4$ copper(II) complex were fast ($t_{1/2}$ = 0.46 s at [H^+] = 0.2 mol dm^{-3}) and were followed using a Union Giken RA-401 stopped-flow spectrophotometer, provided with an RA-451 data processor, an RA-453 monitor scope, and an RA-452 x-y recorder. The experimental rate constants were obtained using a program written for the Guggenheim method, followed by fitting the calculated rate curves with experimental curves. Further details about the instrument calibration and other features are given in Appendix 1.

In the case of [15]aneN$_4$, the dissociation rates ($t_{1/2}$ = 5 min; [H^+] = 0.5 mol dm-3) were too slow to be followed by stopped-flow methods and too fast to be followed by conventional spectrophotometry. The reactions were therefore monitored using the Hewlett Packard photodiode array spectrophotometer. Pseudo-first-order conditions were maintained by using at least a tenfold excess of acid in each run. All kinetic measurements were made at 25.0 $^+$ 0.2 ^{o}C unless otherwise specified. Each k_{obs} is the average of at least three replicates determined over more than 4 half-lives. The detailed experimental conditions for the acid dissociation of the ([15]aneN$_4$) and ([16]aneN$_4$) are summarised in Table 1.3. The parameters for the acid dependence of the rate constants were computed by least-squares linear fitting of $1/k_{obs}$ *vs.* $1/[H^+]$ or $1/(k_{obs} - k_o)$ vs. $1/[H^+]$. In the latter case an initial fitting of $k_{obs} = k_o + A[H^+] / (1+ B[H^+])$ showed that k_o was not significant . Curve fitting was carried out with Grafit program (Erithacus Software) using a Zenith PC.

Table 1.3 Experimental conditions for the acid catalyzed decomposition, and oxidation of the macrocyclic and linear tetramines of copper(II) and nickel(II) at 25 °C.

Compound	Concentration				Ionic strength M	Method of preparing the solution of the complex	Method of initiating the reaction	Monitoring wavelength (nm)
	Compound M	$HClO_4$	Acid/M HNO_3	HCl				
CuL^{2}	$1.0x10^{-3}$		0.01-0.11		1.0 (HNO_3+ $NaNO_3$)	By mixing stoichiometric quantities of the ligand and metal ion solutions (1.1:1), pH adjusted to 7.5.	Stopped-flow rapid mixing.	510
$CuL^{3\ 2+}$	$3.5x10^{-4}$	0.05-1.0			2.0 ($HClO_4$+$NaClO_4$)	The solid complex dissolved in water.	Stopped-flow rapid mixing.	636
		0.02-0.5			1.0 ($HClO_4$+$NaNO_3$)			
$CuL^{4\ 2+}$	$2.4x10^{-4}$	0.05-1.0			2.0 ($HClO_4$+$NaClO_4$)	The solid complex dissolved in water.	By mixing equal volumes of the acid and the complex solutions.	272
$CuL^{5\ 2+}$	$2x10^{-4}$	0.01-0.5			1.0 ($HClO_4$+$NaClO_4$)	The solid complex dissolved in water.	Stopped-flow rapid mixing.	656
		0.01-0.5			1.0 ($HClO_4$+NaCl)			
$CuL^{6\ 2+}$	$1.1x10^{-3}$		0.8-4.7		5.0 (HNO_3+ $NaNO_3$)	The solid complex dissolved in acetonitrile.	By injecting small aliquotes of the complex solution to the equillibrated acid solution.	620
$CuL^{8\ 2+}$	$8\text{-}9x10^{-5}$			$1\text{-}2x10^{-3}$	1.0 (HCl+$NaClO_4$)	The solid complex dissolved in 95% water and 5% acetonitrile	By injecting small aliquotes of the complex solution to the equillibrated acid solution.	265
	$5.5x10^{-3}$			0.05-0.3			Stopped -flow rapid mixing.	610
$CuL^{9\ 2+}$	$1.5x10^{-5}$	0.01-0.5			1.0 (HCl+$NaClO_4$)	The solid complex dissolved in water.	Stopped-flow rapid mixing.	752
$CuL^{10\ 2+}$	$1x10^{-4}$	$1\text{-}5x10^{-3}$			0.5 ($HClO_4$+$NaClO_4$)	The solid complex dissolved water.	Stopped-flow rapid mixing.	575
	$5x10^{-3}$	$5\text{-}50x10^{-3}$						
			$5\text{-}50x10^{-3}$		1.0 (HNO_3+ $NaNO_3$)			
NiL^{2}	$2.5x10^{-4}$		$5x10^{-3}$-0.13		1.0 (HNO_3+ $NaNO_3$)	By mixing stoichiometric quantities of the ligand and metal ion solutions (1:1), pH adjusted to 9.0.	Stopped-flow rapid mixing.	450

$NiL^{7\ 2+}$	$4x10^{-3}$		0.2-0.5		2.0 (HNO_3+ $NaNO_3$)	The solid complex dissolved in water.	By injecting small aliquotes of the complex solution to the equillibrated acid solution.	380
$NiL^{8\ 2+}$	$0.9\text{-}1x10^{-3}$			0.01-0.05	1.0 (HCl+NaCl)	The solid complex dissolved in 95% water and 5% acetonitrile.	By injecting small aliquotes of the complex solution to the equillibrated acid solution.	225
$NiL^{8\ 2+}$	$5x10^{-4}$			0.05-0.4	1.0 (HCl+NaCl)	The solid complex dissolved in water.	Stopped-flow rapid mixing.	240
$NiL^{10\ 2+}$	$2.5x10^{-3}$	0.05			0.5 ($HClO_4$+$NaClO_4$)	The solid complex dissolved in water.	Stopped-flow rapid mixing.	420, 450, 550
$NiL^{10\ 2+}$	$2.5x10^{-3}$	0.25			0.5 ($HClO_4$+$NaClO_4$)	The solid complex dissolved in water.	Stopped-flow rapid mixing.	420, 450, 550
$NiL^{10\ 2+}$	$2.5x10^{-3}$	0.05			0.5 ($HClO_4$+$NaClO_4$)	By mixing stoichiometric quantities of the ligand and metal solutions, pH adjusted to 7.8.	Stopped-flow rapid mixing.	420, 450, 550
$NiL^{10\ 2+}$	$2.5x10^{-3}$	0.25			0.5 ($HClO_4$+$NaClO_4$)	By mixing stoichiometric quantities of the ligand and metal solutions, pH adjusted to 7.8.	Stopped-flow rapid mixing.	420, 450, 550
$NiL^{10\ 2+}$	0.025	0.25			0.5 ($HClO_4$+$NaClO_4$)	By mixing stoichiometric quantities of the ligand and metal solutions, pH adjusted to 7.8.	Stopped-flow rapid mixing.	420, 450
$NiL^{10\ 2+}$	0.01		0.05		1.0 (HNO_3+$NaNO_3$)	The solid complex dissolved in water.	Stopped-flow rapid mixing.	370, 400, 450, 460
$NiL^{10\ 2+}$			0.5		1.0 (HNO_3+$NaNO_3$)	The solid complex dissolved in water.	Stopped-flow rapid mixing.	370, 400, 450, 550, 650
$NiL^{10\ 2+}$			0.14		1.0 (HNO_3+$NaNO_3$)	The solid complex dissolved in water.	Stopped-flow rapid mixing.	370, 400, 420, 450, 550

1.2.3 RESULTS and DISCUSSION

The 14- membered tetra-aza macrocyclic complexes of the type L^1 (cyclam) are highly stable towards acid, and the acid hydrolysis proceeds at a very slow rates, even at very high acidities[1,41]. The enhanced stability of these complexes, compared with the analogous complexes with acyclic ligands of the same denticity has been interpreted in terms of the "macrocyclic effect" (Section 1.1). It may be noted that this stability is dependent on the ring size, degree of unsaturation, and ligand conformation . The copper complexes of the cyclam derivatives L^2 and L^3 and the larger rings L^4 and L^5 are labile in acid. The acid hydrolysis proceeds rapidly even at low acidities, with $t_{1/2}$ at 25 °C of the order of milliseconds. The hexa-aza macrocycle (L^8), the mixed donor macrocycle N_3O_2 (L^9), and the linear ligand (L^{10}) all form labile complexes with copper(II). Typical repetitive scan spectra for the acid hydrolysis of the complexes CuL^4 , and CuL^5 at 25 °C are shown in Figures 1.2 and 1.3.

Acid dissociation rates may be affected by the reaction medium. For example, some tetra-aza macrocyclic complexes of nickel(II) are reported to react at similar rates in 0.7 mol dm^{-3} HCl and 6 mol dm^{-3} $HClO_4$[22], while the reaction of [Cu(*trans*-[18]diene]$^{2+}$ is appreciably faster in HCl than in HNO_3[17].

Media effects have been observed in this work. The hydrolyses of the complexes $[CuL^3]^{2+}$ and $[CuL^5]^{2+}$ were found to be 1.5 to 2 times faster in NaCl than in $NaClO_4$. Also $[CuL^{10}]^{2+}$ dissociates 1.2 times faster in 1.0 mol dm^{-3} (HNO_3 + $NaNO_3$) than in 0.5 mol dm^{-3} ($HClO_4$ + $NaClO_4$).

The copper(II) complexes of the [15]aneN_4 and [16]aneN_4 are bluish violet and show a single d-d band in the visible region (Table 1.1). The band position compares quite well with those of other copper(II) tetra-aza macrocycles. The infrared spectra (Table 1.2) show a sharp ν_{NH} band (*ca.* 3270 cm^{-1}) and the characteristic perchlorate bands (*ca.* 1110 and 620 cm^{-1}). The large differences (*ca.* 30 nm) in the visible (d-d) spectra of the

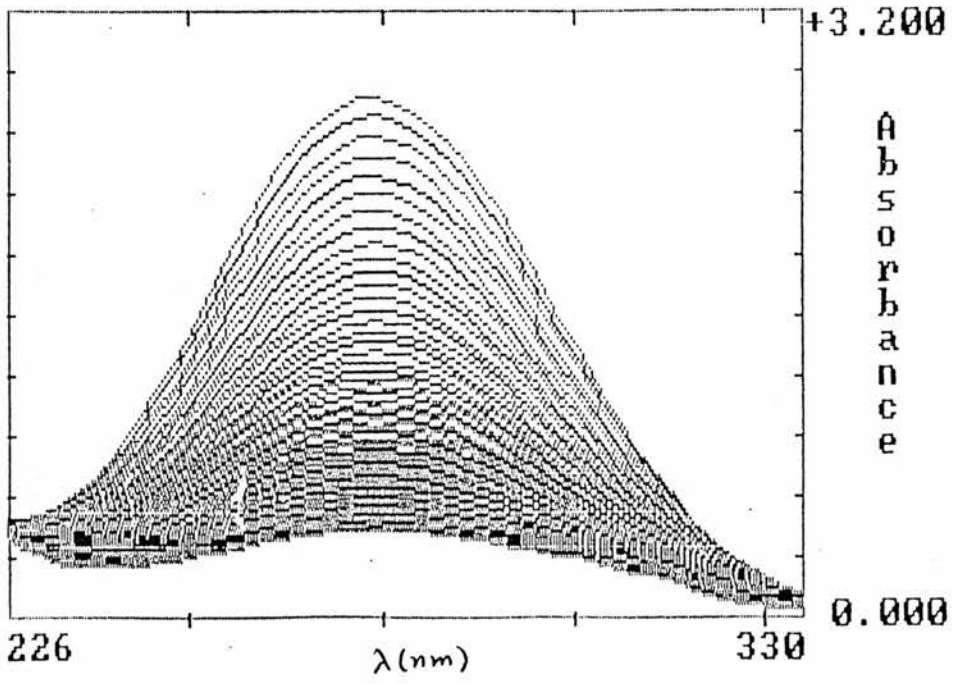

Figure1.2 Repetitive scan spectra for the acid catalysed dissociation of the copper(II) complex of [15]aneN$_4$; [H$^+$] = 0.32 at 25.0 °C . The time interval between scans is 20 s .

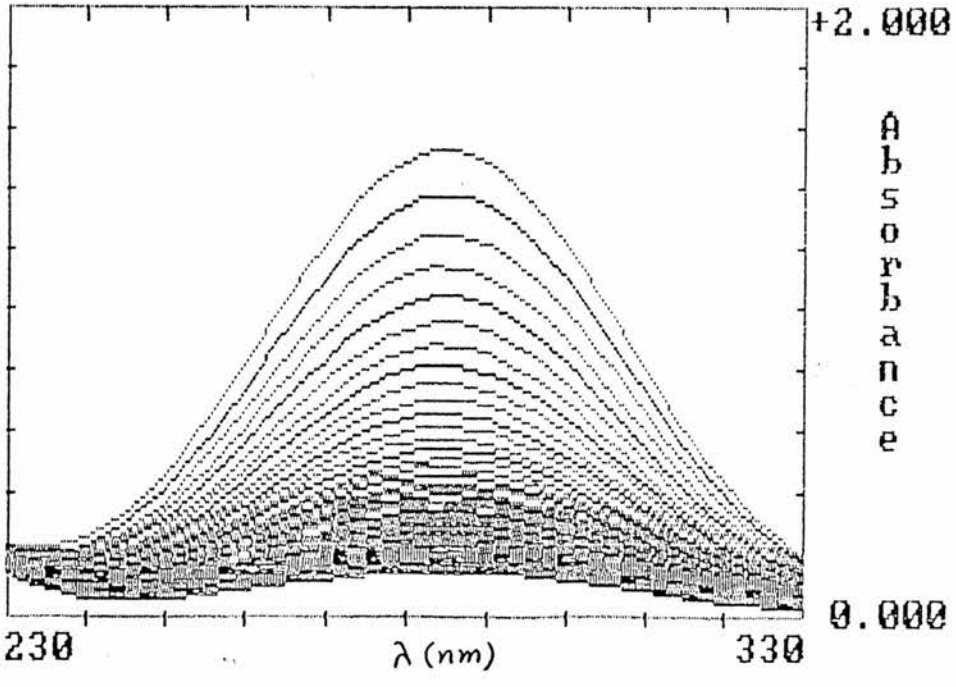

Figure1.3 Repetitive scan spectra for the acid catalysed dissociation of the copper(II) complex of [16]aneN$_4$; [H$^+$] = 0.017 at 25.0 °C . The time interval between scans is 2 s .

two complexes may be attributed to a change in the coordination geometry. Such differences in the coordination geometry are expected to be reflected in the relative dissociation rates of the complexes. Thus the copper(II) complex of L^5 dissociates *ca.* 23 times faster than the copper(II) complex of L^4. Values of k_{obs} at 25 °C, and other temperatures as a function of hydrogen ion concentration for the acid hydrolysis of the complexes CuL^4, and CuL^5 are listed in Tables 1.4 and 1.5, and the corresponding plots of k_{obs} *vs* $[H^+]$ are shown in Figures 1.4 and 1.5. There is initially a linear dependence on $[H^+]$, but at higher hydrogen ion concentrations the reaction becomes independent of $[H^+]$. Both reactions show no solvolytic pathway in the acid range employed. The acid catalysed dissociation is consistent with the kinetic scheme (Scheme IV).

$$CuL^{2+} + H^+ \rightleftharpoons CuLH^+ \quad ; K_1(\text{fast}) \qquad (1)$$

$$CuLH^+ \longrightarrow \text{products} \quad ; k_{21}(\text{slow}) \qquad (2)$$

($K_1 = K_{MLH} = k_{11} / k_{-11}$ in Scheme I)

Scheme IV

This mechanism requires a rapid pre-equilibrium protonation of the complex, forming a tridentate species. Protonation is followed by a slow rate determining dissociation of the protonated species (rate constant k_{21}). Protonated species would be expected to have a d-d absorption spectrum significantly different from that of the tetradentate macrocyclic complexes. For copper(II), the change from a CuN_4 to a CuN_3O chromophore would cause a large shift in the band maximum to lower energy (compare the band maxima for $[Cu(pyaz)]^{2+}$, 573 nm[42] and $Cu(tmdz)_2]^{2+}$, 480 nm[43]).

Table 1.4 Observed rate constants values for the dissociation of $CuL^{4\,2+}$ in acid solution.

T ^oC	Ionic Strength M	$[H^+]$ M	$10^4\,k_{obs}$ s^{-1}
25.0	2.0($HClO_4$+$NaClO_4$)	0.050	1.38
		0.110	4.00
		0.170	6.74
		0.287	11.9
		0.406	17.1
		0.525	22.6
		0.644	26.2
		0.763	29.9
		0.880	33.5
		1.000	37.2
9.0	2.0($HClO_4$+$NaClO_4$)	0.525	4.75
15.0		0.525	8.11
20.0		0.525	11.8

Table 1.5 Observed rate constants values for the dissociation of $CuL^{5\,2+}$ in acid solution.

T ^oC	Ionic Strength M	$[H^+]$ M	k_{obs} s^{-1}	
25.0	1.0 ($HClO_4$+$NaClO_4$)	0.010	0.050	
		0.041	0.156	
		0.071	0.210	
		0.133	0.316	
		0.194	0.355	
		0.255	0.420	
		0.317	0.440	
		0.378	0.490	
		0.440	0.510	
		0.500	0.525	
	1.0 ($HClO_4$ + NaCl)	0.010	0.036	
		0.041	0.106	
		0.071	0.156	
		0.133	0.226	
		0.194	0.260	
		0.255	0.280	
		0.317	0.300	
		0.378	0.310	
		0.440	0.330	
		0.500	0.350	
22.0	1.0 ($HClO_4$+$NaClO_4$)	0.130	0.249	(0.25)[a]
27.3		0.130	0.380	(0.39)[a]
33.0		0.130	0.610	(0.62)[a]
37.0		0.130	0.870	(0.84)[a]
47.0		0.130	1.530	(1.55)[a]

[a] k_{obs} calculated from the activation parameter cited in Table 1.8

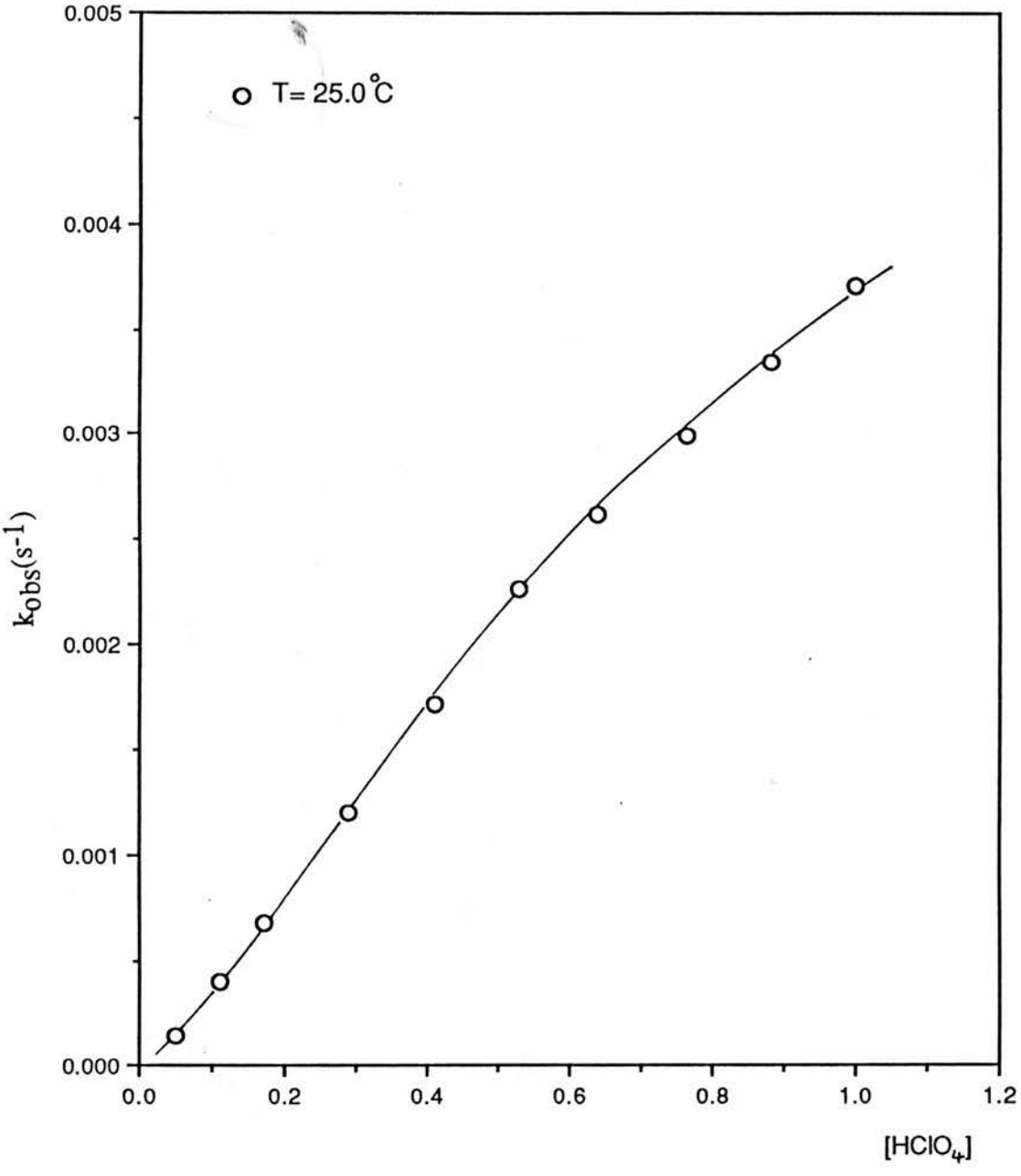

Figure 1.4 Acid dissociation of the copper(II) complex of [15]aneN_4 in acid solution, I = 2.0 M($HClO_4$+$NaClO_4$)

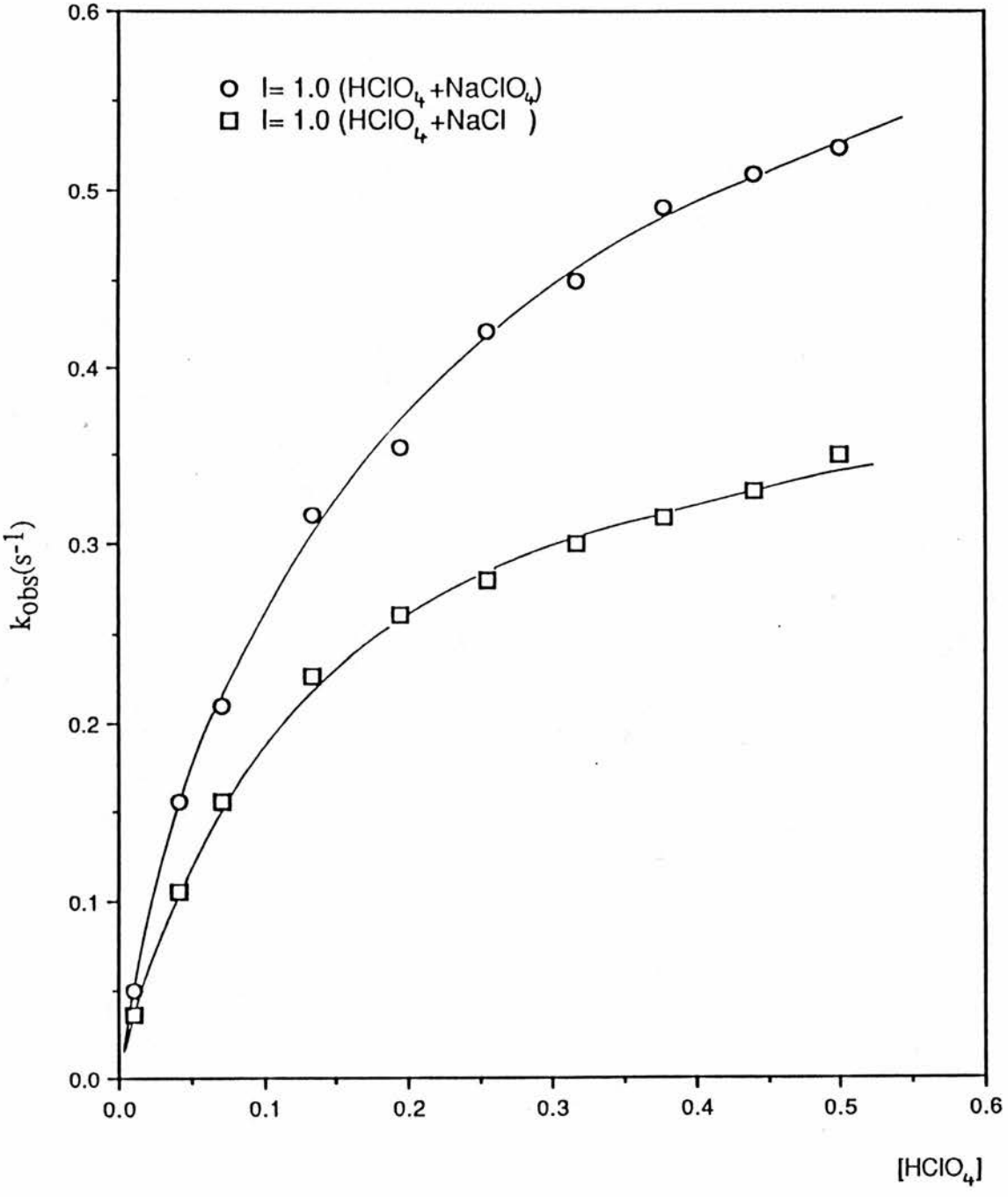

Figure 1.5 Acid dissociation of the copper(II) complex of [16]aneN_4 in perchloric acid solutions , at 25.0 ^oC

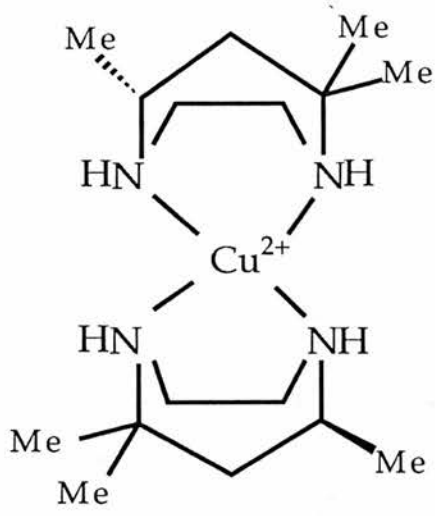

$[M(tmdz)_2]^{2+}$

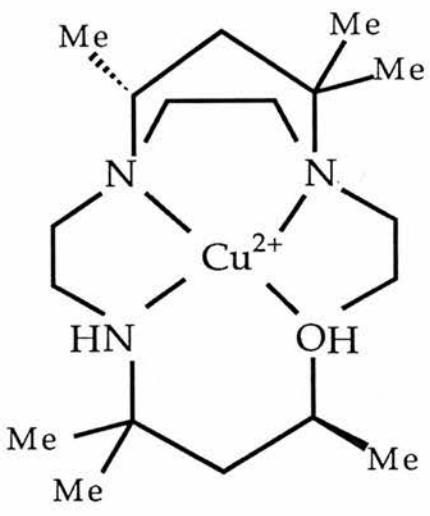

$[M(pyaz)]^{2+}$

The overall rate expression for the above mechanism (Scheme IV) takes the form

,

$$k_{obs} = k_{21}K_1 / \ (1 + k_{21}K_1 [H^+]) \qquad (3)$$

Using equation (3), it can be readily shown that

$$1/k_{obs} = 1/ k_{21}K_1 . \ 1/ [H^+] \ + 1/ k_{21} \qquad (4)$$

The kinetic data for the dissociaton reactions were fitted to the expression k_{obs} = A $[H^+]$ / $(1+B[H^+])$[1] directly and were also checked by linear fitting to the double reciprocal expression $1/ k_{obs}$ *vs.* $1 / [H^+]$, Figure 1.6. The parameters evaluated by the two methods are in reasonable agreement, and the constants shown in Table 1.6 are the mean values calculated by the two procedures. It can be shown from Table 1.6 that k_{21} = 0.017 s^{-1} and K_1 = 0.74 mol^{-1} dm^3 for CuL^4, and k_{21}= 0.59 s^{-1} and K_1 = 9.11 mol^{-1} dm^3 when I = 1.0 mol dm^{-3} ($HClO_4$ + NaCl) , and k_{21} = 0.39 s^{-1} and K_1 = 10.25 mol^{-1} dm^3 when I = 2.0 mol dm^{-3} (HClO4 +$NaClO_4$) for CuL^5. For comparative purposes, it

[1]Parameters are M^{-1} s^{-1} for A and M^{-1} for B .

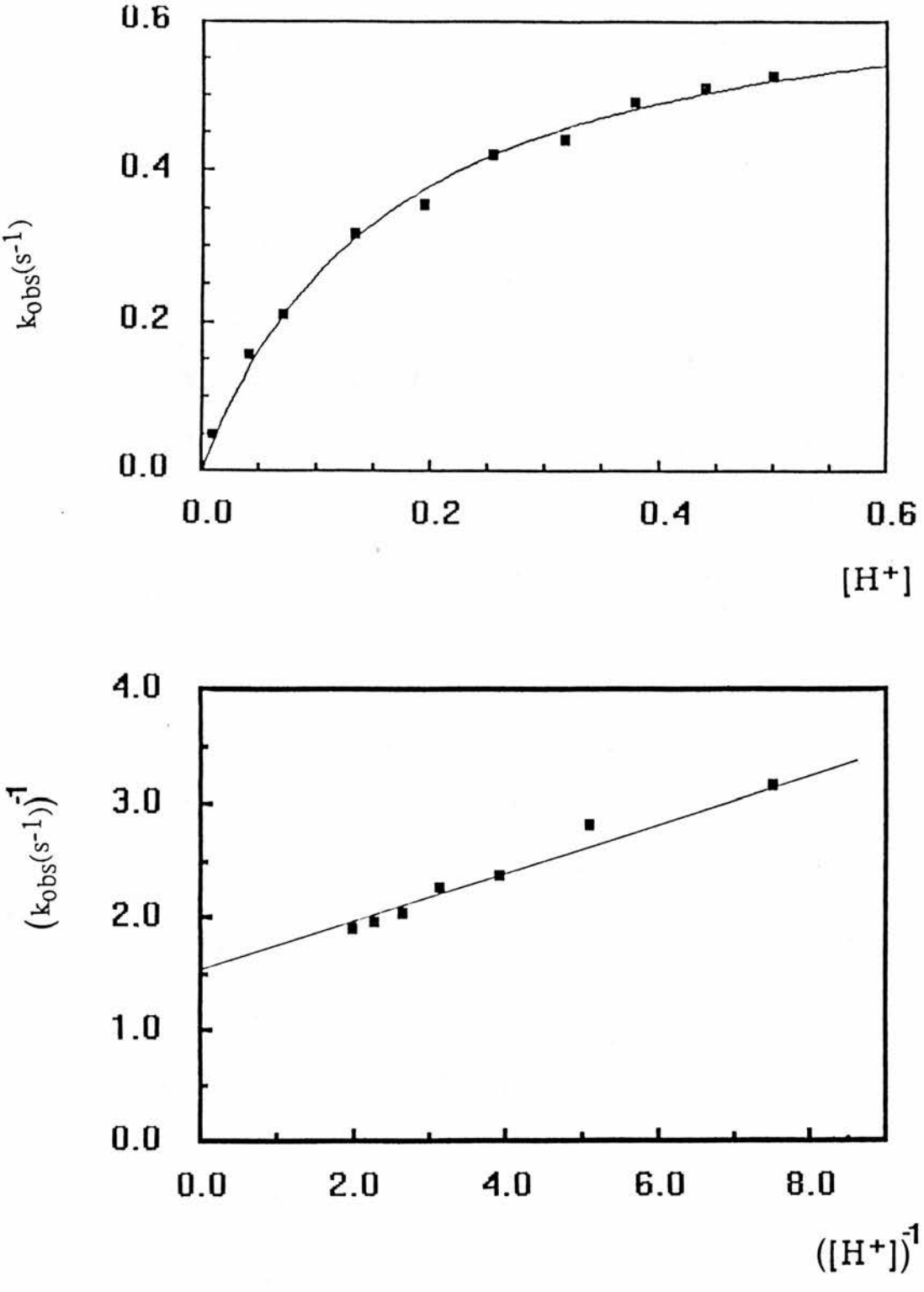

Figure1.6 Observed pseudo-first-order rate constantsfor the acid dissociation of the copper(II) complex of [16]aneN$_4$: (a) represent the results of a non linear least-squares fit of k_{obs} to the function A[H+] / (1 + B[H+]) , (b) represent the results of a linear least-squares fit of the double reciprocal $1/k_{obs}$ vs $1/[H^+]$.

Table 1.6 Kinetic parameters for acid hydrolysis reactions at 25 ^{o}C.

Compound	A = $kK^{a,d}$	B = $K^{b,d,e}$	k_H = $A/B^{c,e}$	k' a,f	k_o' c,f	k_o c,g
CuL^2	$1.6x10^3$ (71)^{d,h}	64.9(4)	24.69			
	$4.48x10^3$ (65)	134.2 (12)	33.4			-10.0 (1.7)
$CuL^{3\ 2+}$	9.57 (0.5)$^{h,\ m}$	1.41 (0.4)	6.79			
	27.7 (2.5)$^{d,\ n}$	3.24 (0.5)	8.6			
	18.7 (4) $^{g,\ n}$	2.14 (0.5)	8.7			0.7 (0.3)
$CuL^{4\ 2+}$	$4.75x10^{-3}$ (0.1)^{o}	0.28 (0.04)	0.017			
	$1.24x10^{-2}$ (0.1)^{p}	0.74 (0.02)	0.017			$1x10^{-3}$ (0.2)
$CuL^{5\ 2+}$	5.33^{m}	9.11 (0.05)	0.59			
	4.0^{n}	10.25 (0.04)	0.39			
$CuL^{6\ 2+}$				$2.24x10^{-4}$ (0.1) ^{f,g}	$2.6x10^{-5}$ (1.2)	
$CuL^{8\ 2+}$		0.12^{k}		$8.5x10^3$ ^{j,r}		
				75.0 ^{l,s}		
$CuL^{9\ 2+}$				40.17	0.52	
CuL^{10}				$8.5x10^5$(0.08) ^{j,s,t}		
				$8.1x10^5$ (0.3) ^{j,u,v}		
	$6.4x10^4$ (0.5) ^{g,w,t}	81.5 (5)	783.8			-335 (24
	$7.7x10^4$ (0.9) ^{g,w,v}	90.7 (5)	850		>200^{x}	-347 (39)
NiL^2	$1.5x10^2$ (6) ^{d,h}	45.2	3.32			
	$2.14x10^2$ (15)^{g}	62	3.45			-0.29 (0.06)
$NiL^{4\ 2+}$				$2.1x10^{-4}$ ^{y}		

$NiL^{5\,2+}$				0.63 [y]	
$NiL^{8\,2+}$				97 (2.3) [j,r,p] 24.7 (0.3) [j,s,o]	
	$1.3x10^2$ (10) [g,s,p]	2.24 (0.3)	58.9		1.1 (0.5)
	$1.17x10^2$ (0.4) [d,s,o]	2.5 (0.1)	6.43		

[a] $M^{-1}S^{-1}$, observed second order rate constant; [b] M^{-1}; [c] s^{-1}; [d] For the expression $k_{obs} = A[H^+]/(1+B[H^+])$; [e] For the expression $k_{obs} = k_H K[H^+]/(1+K[H^+])$; [f] For the expression $k_{obs} = k'_o + k'[H^+](k'=kK)$; [g] for the expression $k_{obs} = k_o + A[H^+]/(1 + B[H^+])$; [h] For the expression $1/k_{obs} = 1/(A/B) + 1/A[H^+]$; [i] For the expression $k_{obs} = k'[H^+]$; [j] For the expression $k_{obs} = k_H[H^+]^2 (k_H = kK)$; [k] For the expression $[CuL^8H_2]^{4+}/[CuL^8H]^{3+}$ at $[H^+] = 10^{-3}$ M; [l] For the expression $k' = k_{obs}/[H^+]$; [m] I = 1.0M($HClO_4$ + $NaNO_3$); [n] I = 2.0M($HClO_4$ + $NaClO_4$); [o] slow step; [p] fast step; [q] Isomerization constant; [r] at low acidities; [s] at high acidities; [t] I = 0.5($HClO_4$ + $NaClO_4$); [u] acid range (0.005-0.01); [v] I = 1.0M(HNO_3 + $NaNO_3$); [w] acid range (0.02 - 0.05 M); [x] Reference 28; [y] Reference 44.

is useful to employ a k_H rate constant, defined as the the slope of the plot of k_{obs} *vs.* $[H^+]$ at low acidities. In this case $k_{II} = 4 \times 10^{-3}$ M^{-1} s^{-1} for CuL^4 and $k_H = 2.6$ M^{-1} s^{-1} for CuL^5 at 25 °C (Table 1.7). The temperature dependence of the reactions was also studied over the temperature range 9 .0 - 25.0 °C for CuL^4 and 25.0 - 47.0 °C for CuL^5. Activation parameters were calculated from the k_{obs} values, Table 1.8. Giving $\Delta H^{\#} = 61.4$ kJ mol^{-1} and $\Delta S^{\#}_{298} = -90.8$ JK^{-1} mol^{-1} for CuL^4, and $\Delta H^{\#} = 59.8$ kJ mol^{-1}, and $\Delta S^{\#}_{298} = -53.8$ JK^{-1} mol^{-1} for CuL^5.

The kinetic expression $k_{obs} = A\,[H^+] / (1 + B\,[H^+])$ can arise with several mechanisms. For the rapid reactions of some copper(II) polyamine cations that show this kinetic form, a mechanism with the acid-dependent reaction of the "activated" species $[M(L)^*]^{2+}$ has been proposed (Scheme V).

$$[M(L)]^{2+} \rightleftharpoons [M(L)^*]^{2+} \quad ; \; k_{os}, k_{-os}$$

$$[M(L)^*]^{2+} + H^+ \longrightarrow \text{products} \quad ; \; k_{11}$$

Scheme V

which results in the kinetic expression

$$k_{obs} = (k_{os} k_{11} / k_{-os})\,[H^+] / (1 + (k_{11} / k_{-os})\,[H^+]) \qquad (11)$$

if the species $[M(L)^*]^{2+}$ is in a low, steady-state concentration. The parameters have the values $A = k_{os} k_{11} / k_{-os}$ and $B = k_{11} / k_{-os}$, so only k_{os} and k_{11}/ k_{-os} can be evaluated from the kinetic data (Scheme I). The spectroscopic evidence indicates that the species $[M(L)^*]^{2+}$ must have a spectrum closely similar to that of $[M(L)]^{2+}$.

Table 1.7 Values of k_H at 25°C.

Compound	k_H (M^{-1} s^{-1})	Intercept s^{-1}
CuL^1		
CuL^2	4.86×10^2 (68)[a] cc. 99	4.6
CuL^3 2+	11.71 (2.2)[a] cc. 98	0.96 (0.4)
CuL^4 2+	4×10^{-3} (0.2)[b] cc. 997	6.7×10^{-5} (11) 0
CuL^5 2+	2.6 (0.5) cc. 98	3.3×10^{-2} (2.5) 0
Red CuL^6 2+	5.9×10^{-8} [c]	
CuL^8 2+	58 (1)[a] cc. 9999	1.6 (0.1)
CuL^9 2+	39.7 (0.2)[a] cc.1	0.38 (0.009)
CuL^{10} 2+	1×10^4 (0.09)[d] cc. 996	-54 (10)
$Cu[16]aneN_4^8$ 2+	1.1[e]	
$Cu[17]aneN_4^9$ 2+	0.6[e]	
$Cu(2,3,2\text{-tet})^{2+}$	0.67[e]	
CuTCE[c][g]	22.5[g]	
CuTHEC[h]	3.4[h]	
NiL^2	85.7 (11)[a] cc. 99	0.13 (0.13) 0
NiL^8 (slow step)$^{2+}$	10.5 (0.9)[a] cc. 997	0.25(0.09)
NiL^8(fast step)$^{2+}$	85 (3) cc. 999	2.8 (0.3)
$Ni(2,2,2\text{-tet})^{2+}$	5[f]	
Ni-cyclam	7.3×10^{-10} j	
NiL^4 2+	2.1×10^{-4} i	
NiL^5 2+	0.63[i]	
Ni(trans-Me_6[15]diene)$^{2+}$	9.6×10^{-6}	

[a]For first three data points; [b]for the acid range 0.2-0.64 M; [c]Reference 17; [d]for the acid range 0.01-0.02 M; [e]Reference 18; [f]calculated for the reaction in 0.5 M HNO_3. Value of $k_H = k_{obs}/[H^+]$; [g]Reference 59; [h]Reference 59; THEC = N, N', N'', N''' - tetra(2-hydroxy-ethyl-1, 4, 8, 11-tetra-azacyclatetradecane. [i]Reference 44; [j]Calculated from data reported (Reference 52).

Table 1.8 Activation parameters for the acid dissociation of some copper(II) and nickel(II) complexes[1].

Compound	$\Delta E_a^{\#}$ kJ mol^{-1}	$\Delta H^{\#}$ kJ mol^{-1}	$\Delta S^{\#}_{298}$ JK^{-1}mol^{-1}	Correlation Coefficiant
$[CuL^2]$	49.1(± 0.47)	46.62 (± 0.47)	-69.8 (± 1.6)	-0.9999
$[CuL^2]$	59.31 [2]	56.83 [2]	-27.5 [2]	-0.998
$[CuL^3]^{2+}$	79.12 (± 1.7)	76.69 (± 1.7)	20.6(± 5.5)	-0.999
$[CuL^4]^{2+}$	63.8(± 3.8)	61.4 (± 3.8)	-90.8(± 13)	-0.997
$[CuL^5]^{2+}$	62.3 (± 1.0)	59.8 (± 1.0)	-53.8 (± 3.3)	-0.9996
$[CuL^8]^{2+}$	33.0(± 0.8) [3]	30.54 (± 0.8) [3]	-124 (± 2.6) [3]	-0.9987
$[CuL^8]^{2+}$	33.0(± 0.8) [2,3]	30.5 (± 0.8) [2,3]	-107 (± 2.1) [2,3]	0.9988
$[CuL^9]^{2+}$	43.4 (± 1.7)	41.0 (± 1.7)	-99.5 (± 5)	-0.997
$[CuL^{10}]^{2+}$	66.0 (± 1.0) [4]	63.3 (± 1.0) [4]	-100 (± 4) [4]	
$[NiL^2]$	66.37 (± 2.3)	63.9 (± 2.3)	-30.0 (± 7.5)	-0.9987
$[NiL^8]^{2+}$	46.9 (± 3) [5]	44.5 (± 3) [5]	-126 (± 10) [5]	-0.994
$[NiL^8]^{2+}$	46.9 (± 3) [2,5]	44.5 (± 3) [2,5]	-70 (± 10) [2,5]	-0.994

[1]Calculated on the basis of k_{obs}, values unless otherwise specified.

[2]Calculated on the basis of $k_H(M^{-1} s^{-1})$.

[3]at high acidities.

[4]Reference 70.

[5]at low acidities.

In the stopped flow work biphasic reactions were observed. The initial reaction (associated with an absorbance increase) is complete within 20-50 ms at 25 ^{o}C and was too fast to measure accurately. The second reaction (associated with an absorbance decrease) is the dissociation step. The magnitude of the absorbance increases on mixing solutions of ML and H^{+} with increasing $[H^{+}]$. This kinetic behaviour can be accounted for in terms of the mechanism in Scheme IV, as it provides evidence for a species such as $CuLH^{3+}$ formed in significant concentrations. A rough estimate of k_{obs} value for the fast step for CuL^{5} is 107 s^{-1} at 25 ^{o}C .

1.3 Copper(II) and Nickel(II) Complexes of N,N',N'',N'''-tetrakis(2-hydroxypropyl)-1,4,8,11-tetra-azacyclotetradecane (THPC) and Dioxocyclam

1.3.1 Acid Dissociation of the Copper(II) Complex of THPC (L^3)

1.3.1.1 INTRODUCTION

Following the discovery of 1,4,8,11-N-tetramethyl-1,4,8,11-tetraazacyclotetradecane (TMC) (I), it was quickly recognised that its metal complexes do not show the usual square planar or octahedral coordination geometry observed in the analogous complexes with cyclam (L^1). Instead the complexes exhibit either square pyramidal or trigonal bipyramidal structures[10].

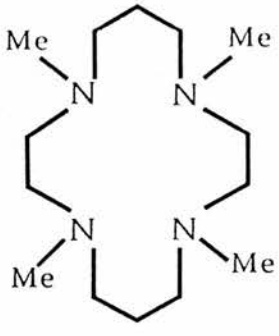

(I) (TMC)

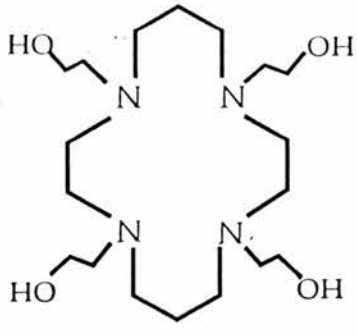

(II) (THEC)

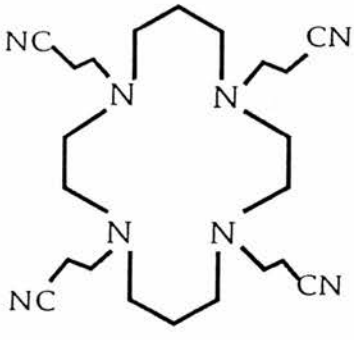

(III) (TCEC)

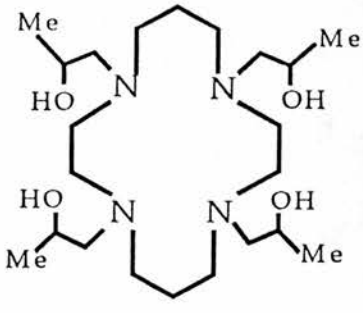

(IV) (THPC)

The nickel(II) complex of TMC has the *trans* I (R,S,R,S) structure (V). Similar behaviour is observed with $Cu(TMC)^{2+}$. By analogy with the TMC complexes, a structure of type (VI) with an RSRS arrangement of the chiral nitrogen centres was suggested for the copper (II) complex of TCEC (III).

The X-ray crystal structure of $Ni(THEC^*)^+$, ($THEC^*$ = deprotonated THEC)[59] confirms that coordination around nickel is almost regular octahedral with four equatorial N

atoms and two axial O atoms of two centrosymmetric hydroxyethyl side arms. The macrocyclic ligand (THEC) adopts the *trans* III stereochemistry (VI).

A ^{13}C NMR study of $Cd(THEC)^{2+}$ and a ^{13}C CPMAS NMR study of solid $Cd(THEC)^{2+}$ show that the most probable structure of this complex is the trans III configuration.

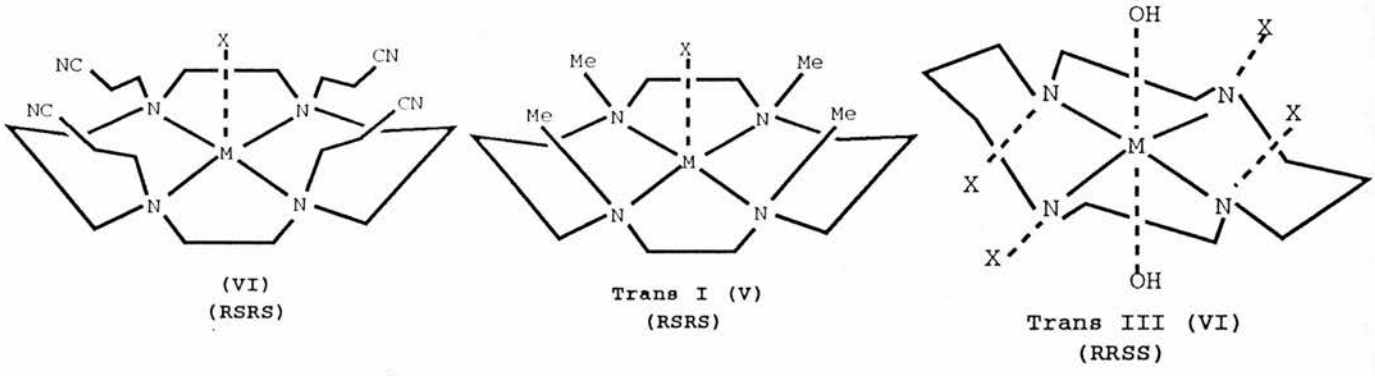

In this structure Cd(II) is above the tetra-aza plane and is trigonally prismatically coordinated by four ring nitrogens and two hydroxyethyl arms attached to the same 1,3-diaminopropane moiety[61]. The study also established that a rapid oscillation of Cd(II) through the macrocyclic ring of THEC[62] occured. The initial work on complexes of TMC[10] showed that N-alkylation of cyclam leads to increased lability of the complexes in both formation and dissociation reactions. Subsequent studies on pendent donor arm polyaza macrocyclic ligands have shown that the resulting metal complexes exhibit a considerable variation in structure and lability which depends substantially on the nature of the arm[10,58,59]. For ligands based on cyclam, metal complexation takes several hours to reach equilibrium when the pendent arms lack donor groups, as in TMC, while equilibrium is reached in seconds when the pendent arms posess donor groups as in TCEC, THEC, and THPC[58]. This increased rate of complexation is probably a

consequence of fast initial coordination of the metal ion by flexible arms. On the other hand the increased rate of acid-promoted dissociation is attributed to the significantly lowered basicity of the tetra-aza ring by N-alkylation (Table A).

Table A. pK_a values of some 14-membered tetra-aza macrocycles at 25 °C.

	Cyclam	TMC[59]	THEC[59]	THPC
pK_1	11.05	9.34	8.83	9.08
pK_2	10.36	8.99	8.3	8.30
pK_3	< 2	2.58	2.65	<2
pK_4	< 2	2.25	<2	<2

A similar effect is observed with simple aliphatic amines, thus the base strength of methylamines in water follows the order $Me_2NH > MeNH_2 > Me_3N$ the appropriate pK_a values being 10.77, 10.64, and 9.80 respectively[59].

Previous studies on the dissociation of copper(II) complexes of both TCEC[10] and THEC[59] have revealed that both reactions show first-order dependence of rate on $[H^+]$, with $k_H^{THEC} = 22.4\ M^{-1}\ s^{-1}$ and $k_H^{TCEC} = 3.44\ M^{-1}\ s^{-1}$ [2]. The increased reactivity of THEC complexes in acid dissociation is probably due to the initial fast protonation of a ring nitrogen, which leads to a molecular rearrangement in which two nitrogen and two oxygen donors are bound to copper(II) (VII).

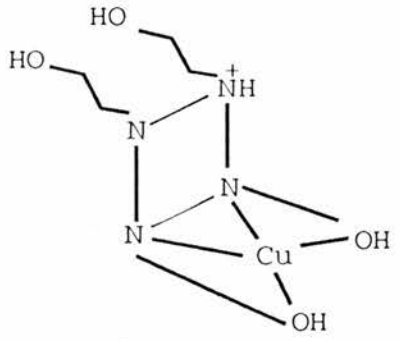

(VII)

[2]The k_{obs} vs $[H^+]$ data given in reference 59 seem to fit "acid limiting" rate kinetics (i.e. $k_{obs} = A[H^+]/1+B[H^+]$) with $kK = 4.4\ mol^{-1}dm^3$, $K = 0.5\ mol^{-1}\ dm^3$.

1.3.1.2 EXPERIMENTAL

Preparation of the ligands

Cyclam (L^1)

Nickel(II) perchlorate hexahydrate 27.4 g (0.675 mol) was dissolved in 400 cm^3 of water in a 1 litre beaker. With adequate stirring, 18 g (0.075 mol) of 3,2,3-tet was added. The resulting red/brown solution was cooled to *ca.* 5 °C in an ice bath, and 15 cm^3 of 40% glyoxal was added with stirring. The beaker was removed from the ice bath and allowed to stand at room temperature for 4 h. The solution was again cooled to 5 °C and treated with 5.5 g (0.15 mol) of sodium tetrahydroborate in small portions over a 1 h period. After complete addition of the tetrahydroborate the solution was removed from the ice bath and heated to 90 °C on a steam bath for 20 minutes. The solution was then filtered hot and the filtrate was transferred to a 500 cm^3 single necked flask with 14.5 g (0.6 mol) of sodium cyanide and the solution mixture refluxed for 2 h. Sodium hydroxide (7.5 g) was added to the cooled solution and evaporated on rotary evaporator until a semi-solid remained. Chloroform (100 cm^3) was added to the flask and the mixture filtered. The solid was washed twice with 50 cm^3 portions of chloroform. The aqueous layer was then separated from the filtrate and washed three times with 50 cm^3 portions of chloroform. The chloroform extracts were dried over anhydrous sodium sulphate and evaporated to dryness. The yellowish solid was recrystallised from 400 cm^3 of chlorobenzene to give white needles (Found: C, 60.3; H, 11.8; N, 28.4. Calc. for $C_{10}H_{24}N_4$: C, 59.99; H, 12.09; N, 28.01 %).

THPC (L^3)

The ligand was prepared by the addition of 2.5 cm^3 (35 mmol) of propylene oxide to a solution of 0.5 g cyclam (2.5 mmol), dissolved in 50% ethanol-water (12.5 cm^3). The solution mixture was then allowed to stand in an open beaker for two days. After this time,

the white crystals which had slowly grown were collected, washed with cold methanol followed by ether and dried *in vacuo*. (Found: C, 61.1; H,11.45; N, 12.8; Calc. for $C_{22}H_{48}N_4O_2$: C, 61.1; H, 11.1; N, 13.0%).

Preparation of the complex $[CuL^3](ClO_4)_2.H_2O$

The copper(II) complex $[CuL^3](ClO_4)_2.H_2O$ was prepared as follows. Copper(II) perchlorate hexahydrate (0.2 g) in ethanol (5 cm^3) was added to a solution of the ligand (0.2 g) in ethanol (5 cm^3). The mixture was heated on a steam-bath for *ca.* 15 min. On cooling the blue/violet complex crystallised and was filtered off, washed with diethyl ether-ethanol (1:1), then diethyl ether and dried *in vacuo* .

Kinetic Measurements.

The kinetic runs were monitored at 636 nm using a Union Giken RA-401 stopped-flow spectrophotometer. The temperature was maintained at 25.0 + 0.1 °C. The dissociation of the copper complex of THPC was studied by using perchloric acid solutions adjusted to I = 1.0 mol dm^{-3} (NaCl) and in another set to I = 2.0 mol dm^{-3} ($NaClO_4$) (Table 1.3). Other experimental details are given in Section 1.2.1.

1.3.1.3 Results and Discussion

The dissociation of the blue complex $[Cu(THPC)]^{+2}$ (λ_{max} 636 nm in water) is quite rapid in acidic solution and the dissociation rates are affected by the ionic strength of the medium.

In the acid hydrolysis of $[Cu(THPC)]^{2+}$ (acidity range 0.05 -1.0 mol dm^{-3} $HClO_4$) two reactions could be detected, the first reaction, associated with absorbance increase, was complete within 20 - 30 ms at 25 °C and was too fast ($k_{obs} \sim 160\ s^{-1}$) to be studied in detail. The second reaction, associated with an absorbance decrease was acid-dependent at low acidities and acid independent at high acidities. At constant hydrogen ion concentration the reaction was first order in the complex. Values of k_{obs} at various acidities and temperatures are listed in Table 1.9 . Plot of k_{obs} *vs* $[H^+]$ is non linear, Figure 1.7, so that the rate expression takes the form

$$k_{obs} = k_{21} K_1 [H^+] / (1+K_1 [H^+]) \qquad (5)$$

Values of $k_{21}K_1 = A$ and $K_1 = B$ are obtained directly from curve fitting of the data to the expression $k_{obs} = A [H^+] / (1+B[H^+])$, Figure 1.8, giving $k_{21} = 6.79\ s^{-1}$ and $K_1 = 1.41\ M^{-1}$ at I = 1.0 mol dm^{-3} (NaCl) and $k_{21} = 8.6\ s^{-1}$ and $K_1 = 3.24\ M^{-1}$ at I = 2.0 mol dm^{-3} ($NaClO_4$) (Table 1.7). The acid catalysed reaction can be rationalised in terms of equations (6) and (7)

$$[CuL^3]^{2+} + H^+ \rightleftharpoons [CuHL^3]^{3+} \quad ; K_1(\text{fast}) \qquad (6)$$

$$[CuHL^3]^{3+} \longrightarrow \text{products} \quad ; k_{21}(\text{slow}) \qquad (7)$$

in which there is a rapid pre-equilibrium protonation step (K_1) and a slow rate-determining dissociation step (k). The temperature dependence of k_{obs} gives $\Delta H^{\#} = 76.69$ kJ mol^{-1} and $\Delta S^{\#}_{298} = 20.60\ JK^{-1}\ mol^{-1}$. The activation parameters indicate that acid catalysis is

Table 1.9 Observed rate constants for the dissociation of $CuL^{3\ 2+}$ in acid solution.

T °C	Ionic Strength M	$[H^+]$ M	k_{obs} s^{-1}
25.0	2.0 ($HClO_4$+$NaClO_4$)	0.050	1.40
		0.169	3.24
		0.289	4.20
		0.406	4.60
		0.525	5.20
		0.644	5.52
		0.763	6.00
		0.880	6.40
		1.000	6.90
15.5	2.0 ($HClO_4$+$NaClO_4$)	0.169	0.95 (0.95) [b]
22.0		0.169	2.08 (1.95) [b]
27.0		0.169	3.44 (3.37) [b]
32.0		0.169	5.74 (5.67) [b]
36.0		0.169	8.63 (8.49) [b]
42.0		0.169	14.6 (15.3) [b]
25.0	1.0 ($HClO_4$+NaCl)	0.025	0.30
		0.084	0.75
		0.144	1.10
		0.203	1.50
		0.263	1.80
		0.322	2.10
		0.382	2.40
		0.440	2.55
		0.500	2.80

[b] k_{obs} calculated from the activation parameter cited in Table 1.8

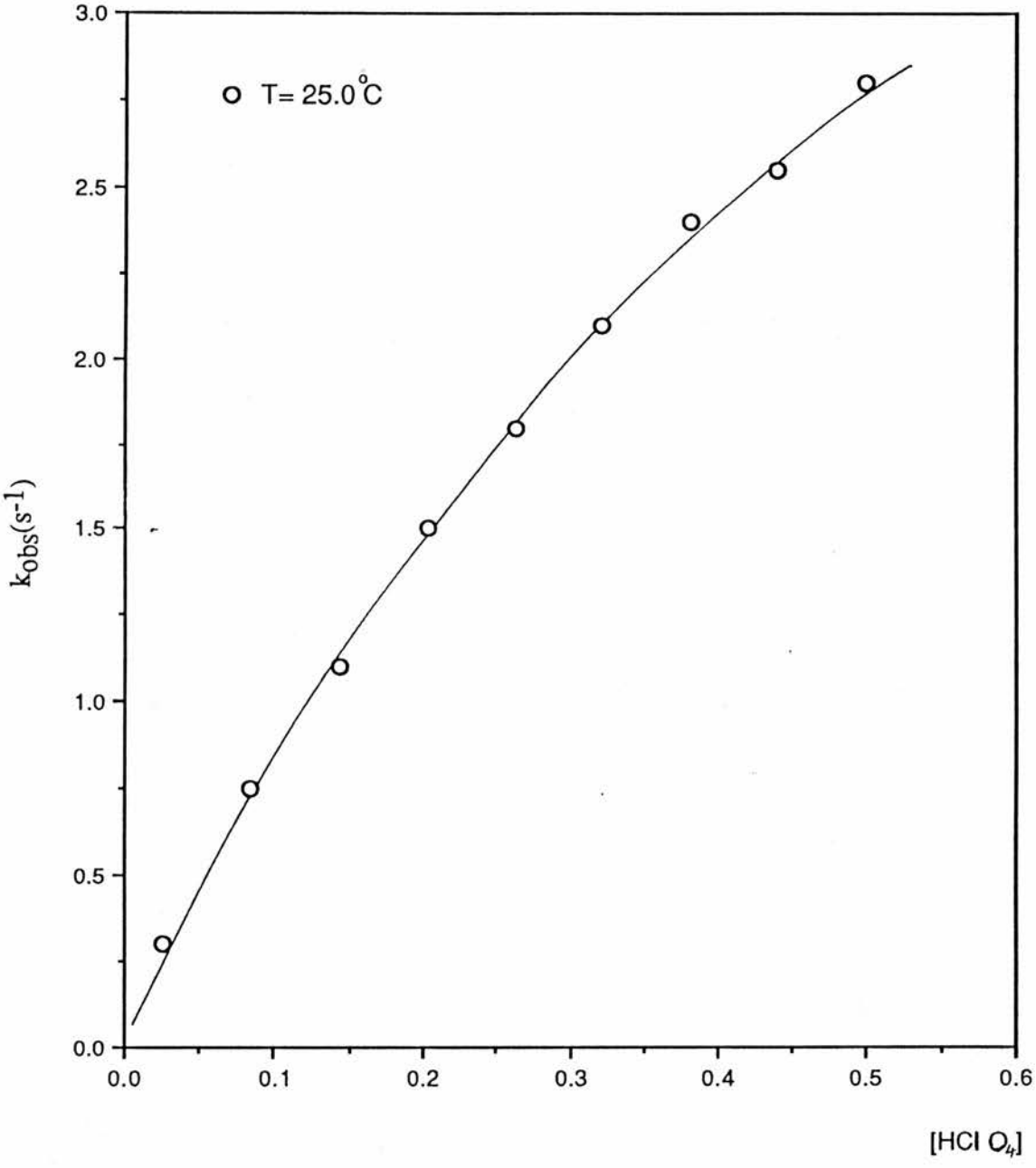

Figure 1.7 Acid dissociation of the copper(II) complex of THPC in perchloric acid solution, I = 1.0 M ($HClO_4$+NaCl) .

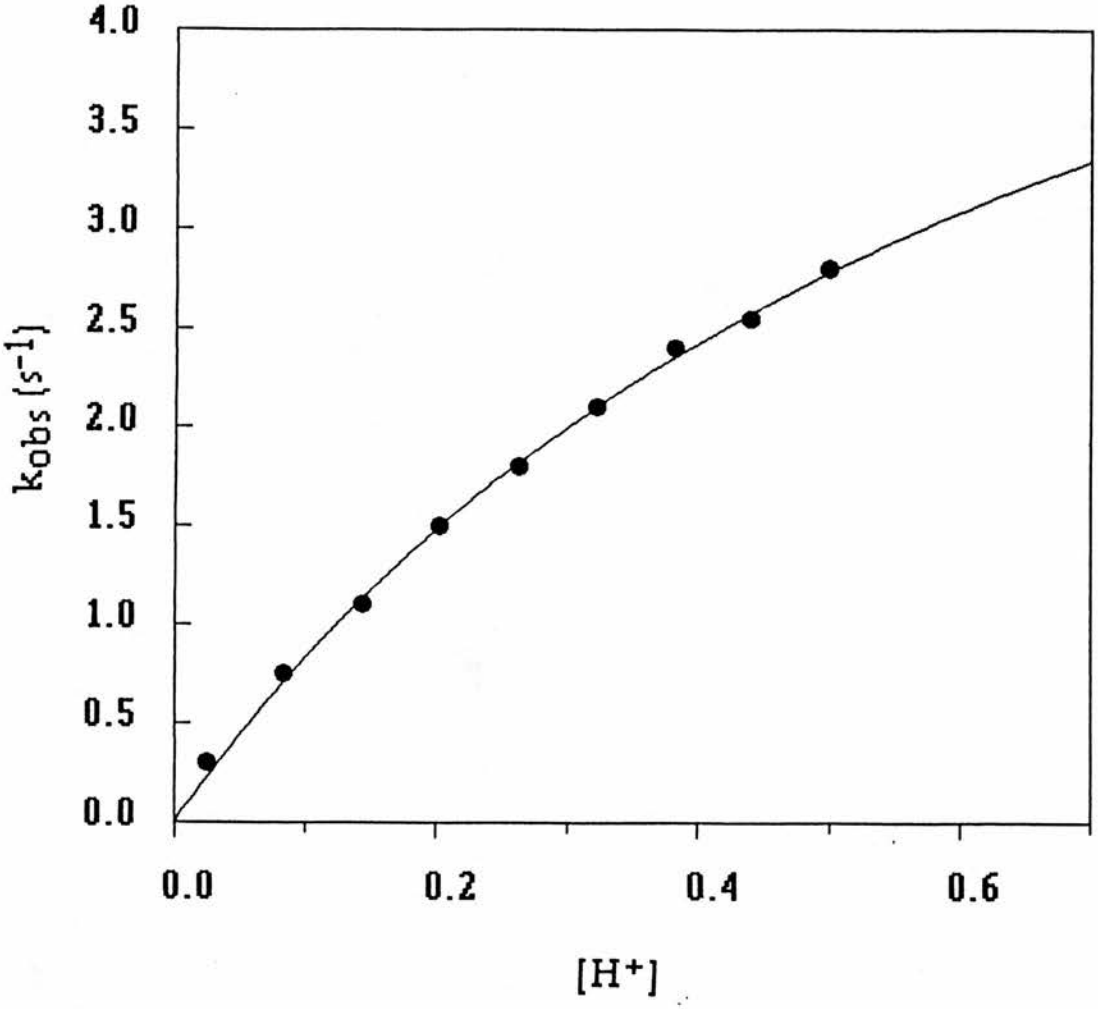

Figure 1.8 Observed pseudo-first-order rate constantsfor the acid dissociation of the copper(II) complex of THPC . A non linear least-squares fit of k_{obs} to the function $A[H^+] / (1 + B[H^+])$, I = 1.0M($HClO_4$+NaCl) .

primarily associated with a much more positive $\Delta S^{\#}$ term compared with other macrocyclic systems (Table 1.7). Such behaviour has been previously observed in the acid-catalysed dissociation of the copper complex of TCEC (59).

The half lives of $[Cu\ (TCEC)]^{2+}$, $[Cu\ (THPC)]^{2+}$, and $[Cu\ (THEC)]^{+2}$ in 0.05 mol dm^{-3} $HClO_4$ are 0.3, 0.5, and 3.5 s at 25.0 °C respectively, although [Cu (cyclam)]$^{2+}$ does not dissociate over a period of weeks in 6 mol dm^{-3} HCl. The kinetic lability of the above complexes in terms of the second order rate constant (k_H) shown in Table 1.7 increases in the order $CuTHEC^{2+} < CuTHPC^{2+} <$ CuTCEC and the ratio $CuTCEC^{2+}$: $CuTHPC^{2+}$: $CuTHEC^{2+}$ is 6.6 : 3.4 : 1. This behaviour may be explained in terms of stabilization of the intermediate species formed on protonation of a ring nitrogen followed by molecular rearrangement in which two nitrogens and two pendent donors bond to copper(II) (Structure VII p. 34).

1.3.2 Acid Catalysed Dissociation of The Copper(II) and Nickel(II) Complexes of Dioxocyclam

1.3.2.1 INTRODUCTION

A previous kinetic study[36] of the CuL^2 and NiL^2 at low acidities (pH 4 - 5) has shown that the dissociation of these complexes displays a second order dependence on $[H^+]$ with $k_{obs} = k_H [H^+]^2$. The observed rate constants ($mol^{-1}\ dm^3\ s^{-1}$) are 1.2×10^7 and 1.2×10^5. Both reactions have insignificant acid-independent terms. The dissociation can be accommodated within a kinetic scheme in which the decomposition of the diprotonated species, formed in successive rapid protonation equilibria (Scheme I), is rate determining. The reaction rate is given by the expression

$$\text{rate} = k_{30} K_1 K_2 [ML] [H^+]^2 / (1 + K_1[H^+] + K_1K_2 [H^+]^2) \quad (1)$$

where K_1 and K_2 are the equilibrium constants for the first and second protonation reactions, and k_{30} is the rate constant for dissociation of the diprotonated species. If the protonation constants are small, so that $(1 + K_1[H^+] + K_1K_2[H^+]^2) = 1$, then the expression simplifies to

$$\text{rate} = k_{30} K_1K_2 [ML] [H^+]^2 \quad (2)$$

Alternatively, the results are compatible with a scheme (Section 1.5) in which the protonation of the monoprotonated species, rate constant k_{21}, is rate-determining, which reduces to the same form if the protonation equilibrium constant, K_1, is small. A pre-equilibrium involving the reactive species ML* would not change the kinetic form if the equilibrium constant k_{os} / k_{-os} was large compared with subsequent values (Scheme I).

These mechanisms would imply rate-determining dissociation of the third (or second) copper-nitrogen bonds, respectively. Any reaction that has successive steps will

show acid independence at high acidities, first-order dependence on $[H^+]$ at intermediate acidities and a second-order dependence on $[H^+]$ at low acidities. The different rate expressions observed for the three compounds may indicate that the different parts of the acid-dependence profile have been examined in the three cases. It is perhaps significant that the observed rate constants at the lower acid concentrations for $CuL^{3\,2+}$ (Section 1.3), and particularly for $CuL^{4\,2+}$(Section 1.2) $^{2+}$, are smaller than predicted from a linear extrapolation of the $1/k_{obs}$ *vs* $1/[H^+]$ plot, which may indicate the beginning of a change over to second-order rate dependence at low acidities. On the other hand the hydrolysis of copper(II) complex of the linear-tetraamine L^{10} (2,2,2-tet) studied in the acidity range (0.001- 0.5 mol dm^{-3}) (Table 1.6) displays the three types of kinetic behaviour (Section 1.6). A change over from one kinetic behaviour to another in a wide range of $[H^+]$ is also displayed by the copper(II) and nickel(II) complexes of the hexadentate ligand L^8 (hexacyclen) in the acidity range (0.001 - 0.4 mol dm^{-3}) (Section 1.5).

1.3.2.2 EXPERIMENTAL

Preparation of dioxocyclam (L^2)

The preparation of dioxocyclam, L^2, is shown in Scheme VI. The ligand is obtained by condensation of the open chain 2,3,2-tet with diethyl malonate, in ethanol solution[35,36]. The linear amine 2,3,2-tet, was prepared following the general procedure described for the preparation of 2,2,2-tet. A mixture of 8.0 g (0.05 mol) of 2,3,2-tet and 8.0 g (0.05 mol) of diethyl malonate was stirred under reflux for 7 days. The solvent was removed on a rotary evaporator and the solid residue obtained was recrystallised from methanol (Found: C, 52.7; H, 8.7: N, 24.3. Calc. for $C_{10}H_{20}N_4O_2$: C, 52.6; H, 8.8; N, 24.5 %).

Scheme VI

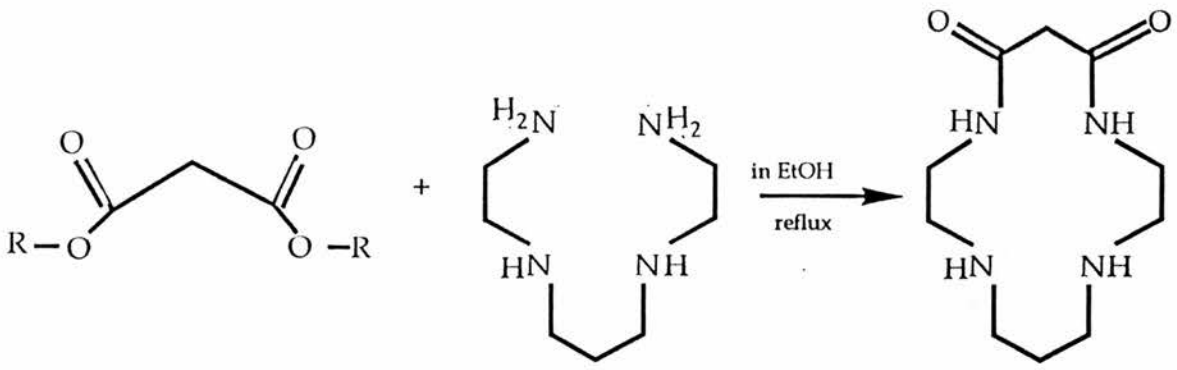

$R = C_2H_5$

Preparation of Complexes.

NiL^2 $1.5H_2O$.

Nickel(II) perchlorate hexahydrate (0.365g, 1 mmol) was dissolved in water (13 cm3). The ligand (0.23 g, 1 mmol) in water (2 cm^3) was added and the solution heated on a steam bath. Aqueous NaOH (2 cm^3, 1 mol dm^{-3}) was added and the initial precipitate which formed, rapidly dissolved with colour intensification of the orange solution. Cooling in ice gave the product as orange plates (0.35 g) which were recrystallised from water and washed with acetone, then diethyl ether and dried *in vacuo* (Found: C, 37.1; H, 6.8; H, 17.2. Calc. for $C_{10}H_{18}O_2N_4Ni$. $1.5H_2O$: C, 37.4; H, 6.9; N, 17.4%).

CuL^2 $1.5H_2O$.

Copper(II) perchlorate hexahydrate (0.37 g, 1 mmol) was dissolved in water (3 cm^3). The ligand (0.23 g, 1mmol) in water (2 cm^3) was added to give a violet solution, from which the complex began to crystallise. Additional water was added and the solution heated to dissolve the complex, and NaOH (2 cm^3, 1 mol dm^{-3}) was added. The product crystallised on cooling (0.4 g) and was recrystallised from water to give purple plates which were washed with acetone, then diethyl ether and dried *in vacuo* (Found: C, 38.0; H, 6.4; N, 17.6. Calc. for $C_{10}H_{18}O_2N_4Cu$. 1.5 H_2O : C, 37.9; H, 6.0; N, 17.7%).

The electronic and i.r. spectra of the ligand and its metal complexes are summarised in Tables 1.1 and 1.2.

Kinetic Measurements.

The kinetics were monitored at 510 nm and 450 nm for the copper(II) and nickel(II) systems respectively using a Union Giken RA-401 stopped-flow spectrophotometer. The temperature was maintained at 25.0 ± 0.1 °C. The dissociation of the copper and nickel complexes of dioxocyclam were studied by using nitric acid solutions adjusted to I = 1.0 mol dm^{-3} ($NaNO_3$) .

1.3.2.3 RESULTS and DISCUSSION

The acid-catalysed dissociation of the copper(II) and nickel(II) complexes of dioxocyclam were studied using nitric acid solutions over a temperature range at I = 1.0 mol dm^{-3}. Two relaxations could be detected in the stopped flow trace. The first relaxation (*ca* 50 ms) is associated with an absorbance increase and is then followed by an absorbance decrease. The initial rapid reaction appears to be associated with protonation of the complex and the second slower process to the dissociation reaction. Values of k_{obs} at various $[H^+]$ and different temperatures for the dissociation of copper(II) and nickel(II) are summarised in Tables 1.10 and 1.11. Plots of k_{obs} *vs* $[H^+]$ for the two cations are curved (Figures 1.9 and 1.10) but plots of $[k_{obs}]^{-1}$ vs $[H^+]^{-1}$ are linear (Figures 1.11(a) and (b)). The acid dissociation can be rationalised in terms of the following Scheme

$$ML + H^+ \rightleftharpoons MLH^+ \quad ; \quad K_1 \qquad (1)$$

$$MLH^+ + H^+ \rightleftharpoons MLH_2^{2+} \quad ; \quad K_2 \qquad (2)$$

$$MLH_2^{2+} \longrightarrow M^{2+} + LH_2^{2+} \quad ; \quad k \qquad (3)$$

Table 1.10 Observed rate constants for the dissociation of CuL^2 in acid solution.

T ^oC	Ionic Strength M	$[H^+]$ M	k_{obs}[a] s^{-1}
18.0	1.0 (HNO_3+$NaNO_3$)	0.0105	5.92
		0.0263	9.20
		0.0525	11.1
25.0	1.0 (HNO_3+$NaNO_3$)	0.0105	9.45
		0.0158	12.7
		0.0210	14.7
		0.0315	17.0
		0.0420	18.4
		0.0525	19.1
		0.0788	20.3
		0.1050	21.3
30.5	1.0 (HNO_3+$NaNO_3$)	0.0105	13.5
		0.0263	22.2
		0.0525	27.0
34.8	1.0 (HNO_3+$NaNO_3$)	0.0105	18.0
		0.0263	31.5
		0.0525	37.1

Table 1.11 Observed rate constants for the dissociation of NiL^2 in acid solution .

T ^oC	Ionic Strength M	$[H^+]$ M	k_{obs}[a] s^{-1}
20.3	1.0 (HNO_3+$NaNO_3$)	0.0105	0.71
		0.0420	1.31
		0.0790	1.51
30.2	1.0 (HNO_3+$NaNO_3$)	0.0105	1.66
		0.0420	3.31
		0.0790	3.98
35.5	1.0 (HNO_3+$NaNO_3$)	0.0105	2.76
		0.0420	5.15
		0.0790	6.14
25.0	1.0 (HNO_3+$NaNO_3$)	0.0053	0.55
		0.0105	1.10
		0.0158	1.45
		0.0210	1.64
		0.0315	1.95
		0.0420	2.22
		0.0520	2.35
		0.0790	2.58
		0.1050	2.67
		0.1313	2.84

[a] Precision in observed rate constants is within ± 3%.

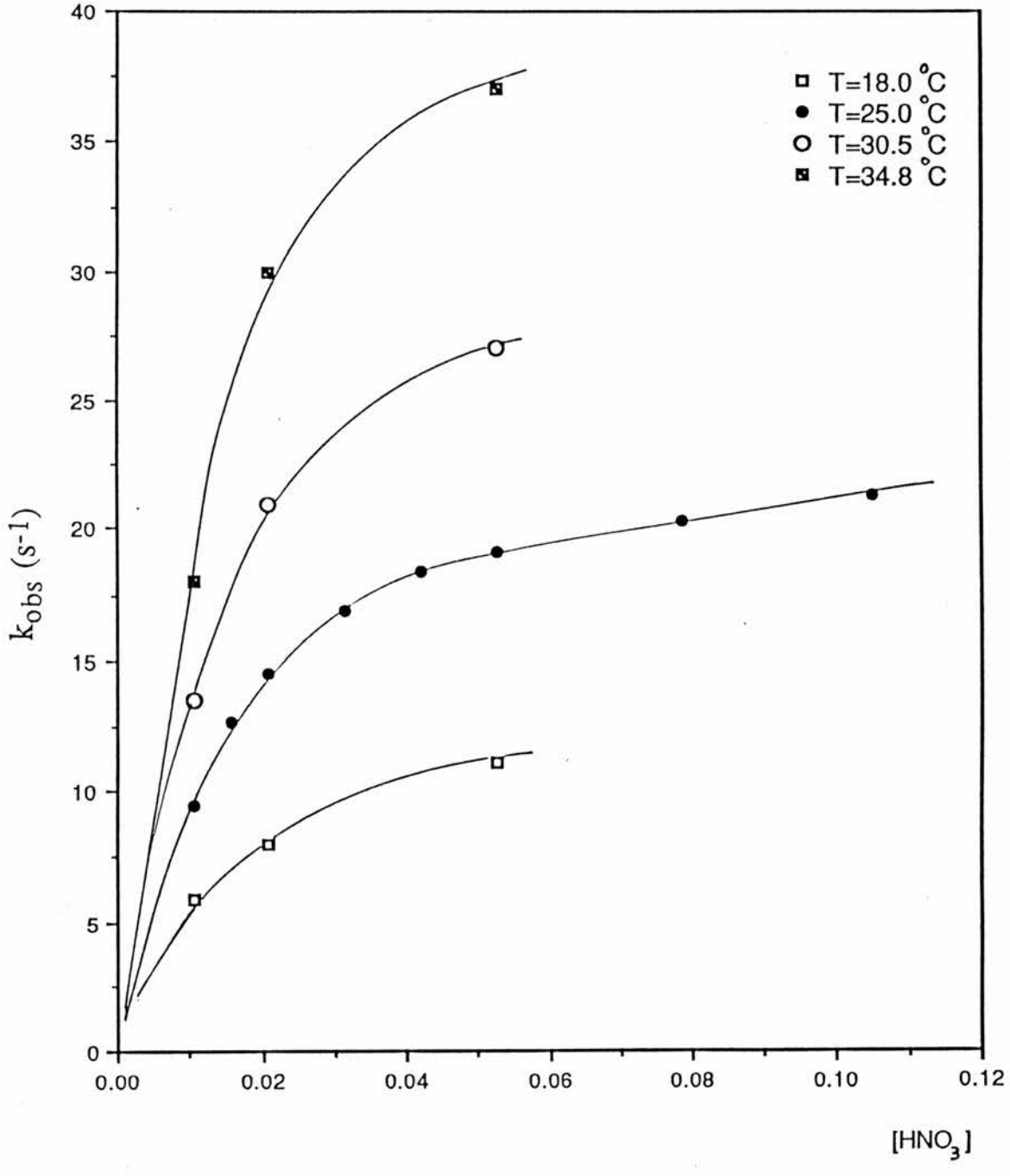

Figure 1.9 Acid dissociation of the copper(II) complex of dioxocyclam in nitric acid solutions, I = 1.0 M (HNO_3+$NaNO_3$) .

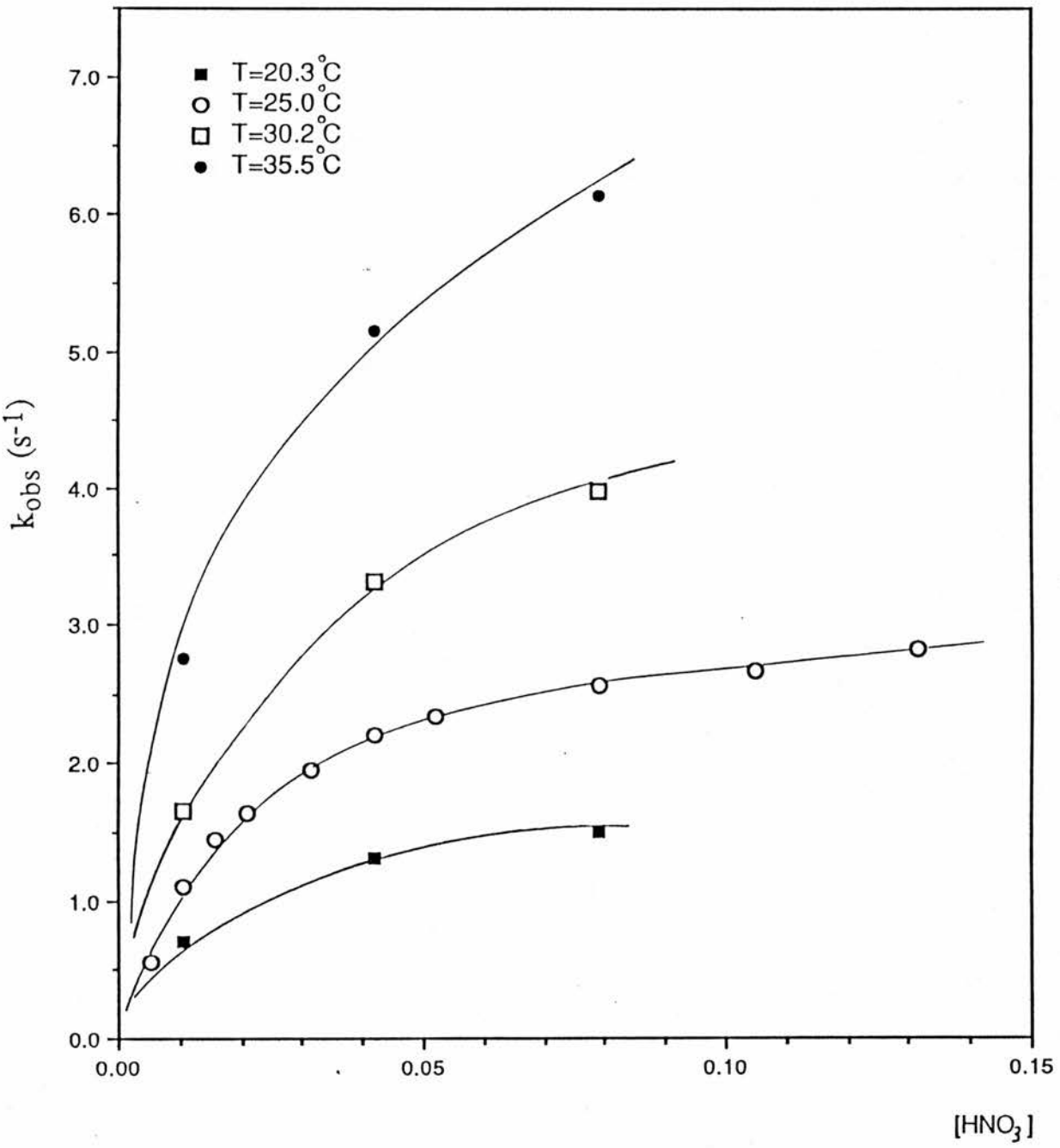

Figure 1.10 Acid dissociation of the nickel(II) complex of dioxocyclam in nitric acid solutions, I = 1.0 M (HNO_3+$NaNO_3$) .

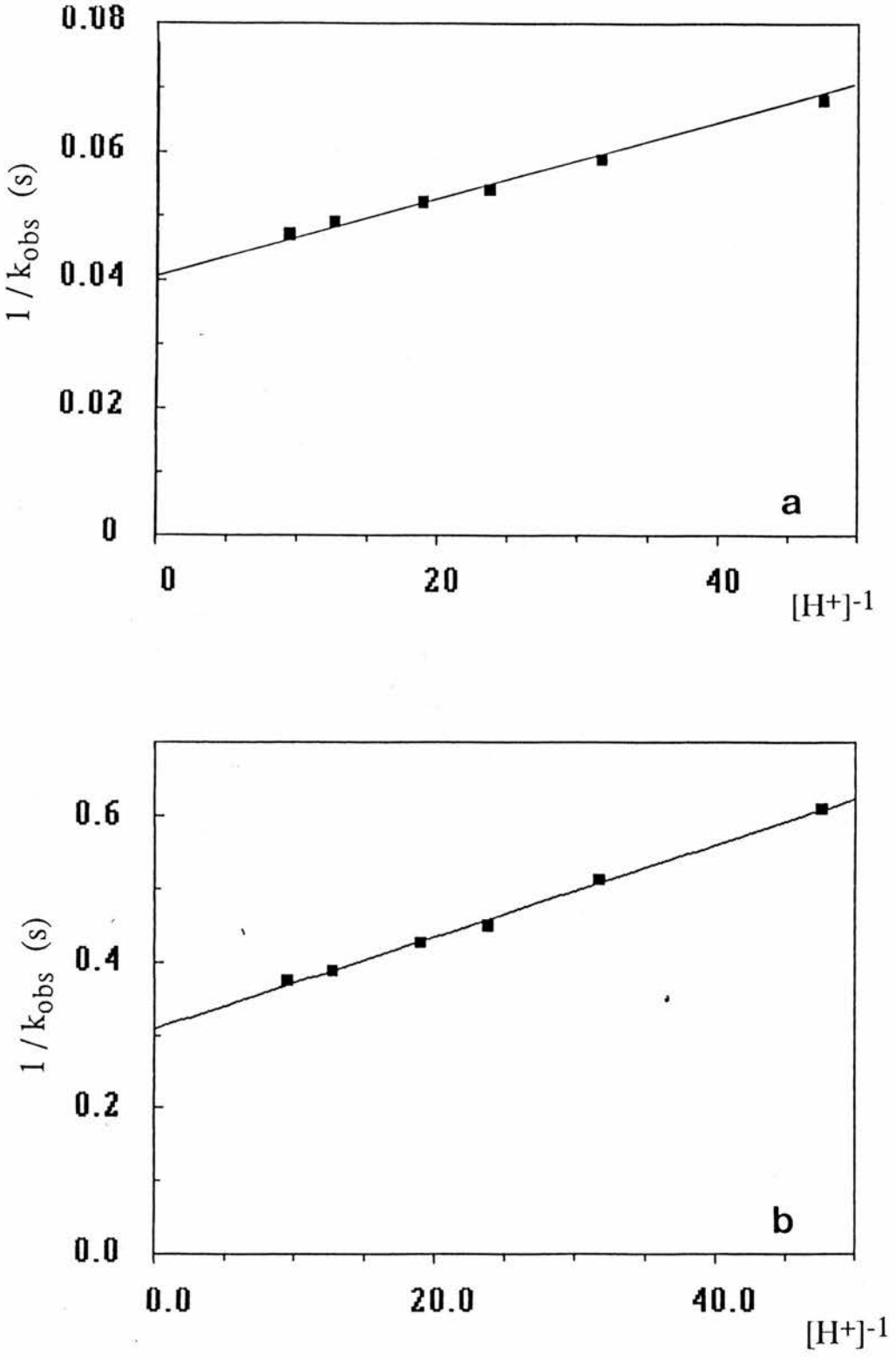

Figure1.11 Linear least-squares fit of the double reciprocal $1/k_{obs}$ *vs* $1/[H^+]$ for : (a) the copper-dioxocyclam system , (b) the nickel-dioxocyclam system .

involving two rapid pre-equilibrium protonations and rate-determining cleavage of the Cu(II)-N(amide) bond. For this Scheme, k_{obs} is the observed first order rate constant at constant hydrogen ion concentration. Under the present experimental conditions it is clear that the complex is completely monoprotonated at all the acidities employed and the kinetic scheme becomes

$$MLH^+ + H^+ \rightleftharpoons MLH_2^{2+} \quad ; \quad K_2 \tag{4}$$

$$MLH_2^{2+} \longrightarrow M^{2+} + LH_2 \; ; \quad k \tag{5}$$

involving a rapid pre-equilibrium protonation of MHL^+ and a slow rate-determining dissociation. In this case,

$$\text{rate} = \frac{kK_2 [MLH^+] [H^+]}{1 + K_2 [H^+]} \tag{6}$$

$$k_{obs} = \frac{kK_2 [H^+]}{1 + K_2 [H^+]} \tag{7}$$

Values of kK_2 and K_2 were obtained by non linear least squares fitting of k_{obs} to the function $A[H^+]/(1+B[H^+])$. An excellent fit is obtained (Figures 1.12 (a) and (b)) giving at 25 °C, k_H^{Cu} = 24.7 $mol^{-1}dm^3\ s^{-1}$ and K_2^{Cu} = 64.8 $mol^{-1}dm^3$ and k_H^{Ni} = 3.2 $mol^{-1}dm^3\ s^{-1}$ and K_2^{Ni} = 51.0 $mol^{-1}dm^3$. These values indicate that copper complex dissociates some 7.5 times more rapidly than the nickel derivative at 25 °C. A similar method of analysis was applied to the data obtained at the other temperatures giving the constants quoted in Table 1.12. The temperature dependence of k_H^{Cu} for the copper complex gives $\Delta H^{\#}$ = 54.5 kJ mol^{-1} and $\Delta S^{\#}_{298}$ = - 35 $JK^{-1}mol^{-1}$, while the temperature dependence of K_2 gives the approximate parameters ΔH = - 9.8 kJ mol^{-1} and ΔS = 1.4

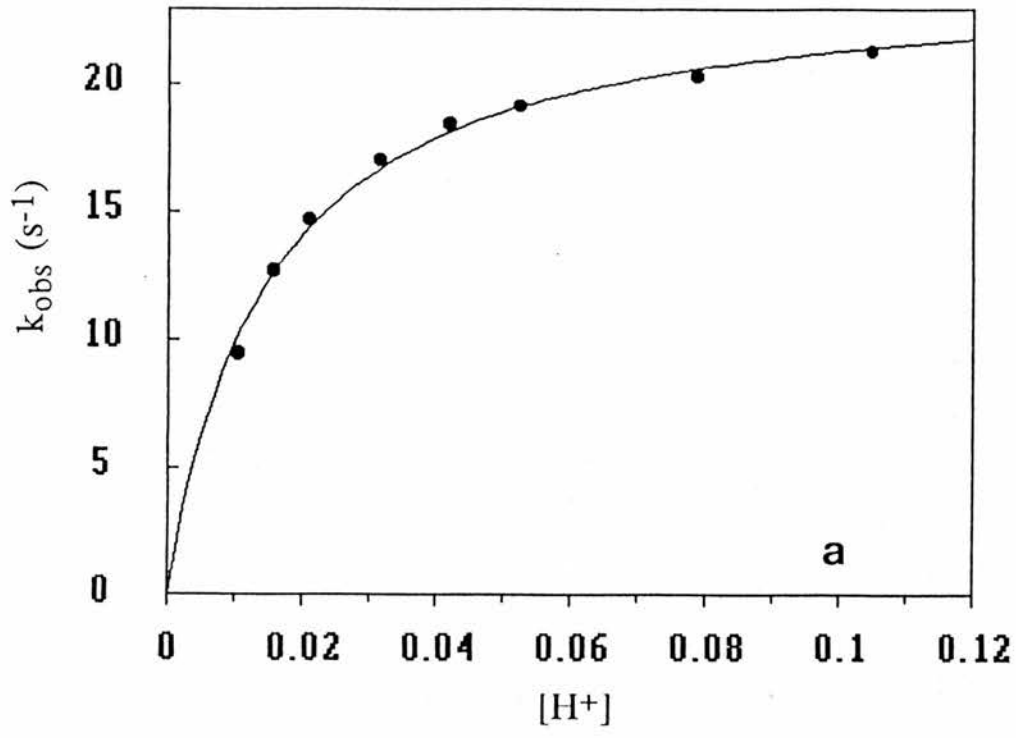

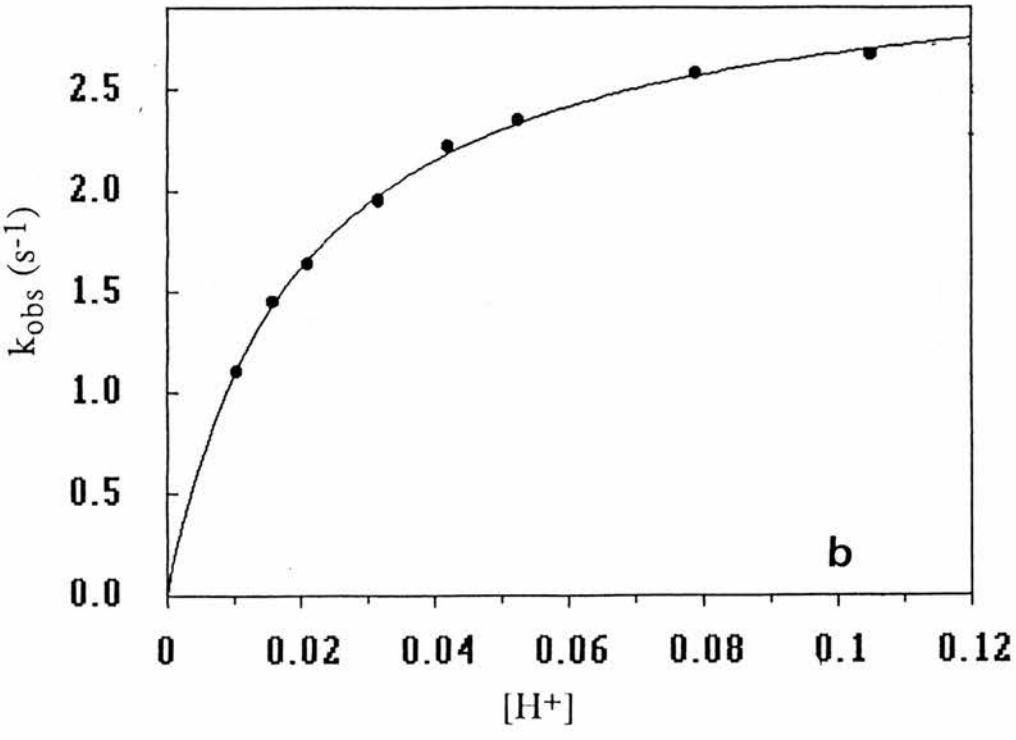

Figure 1.12 Non linear least-squares fit of k_{obs} to the function A[H+] / (1 + B[H+]) for : (a) the copper-dioxocyclam system , (b) the nickel-dioxocyclam system .

Table 1.12 Summary of rate and equilibrium constants for copper(II) and nickel(II) dissociation reactions .

Copper(II)

Temp (^{o}C)	k (s^{-1})	K ($dm^3\ mol^{-1}$)
18.0	14.2	67
25.0	24.7	64.8
34.8	51.3	54

$\Delta H^{\#}$ = 54.5 kJ mol^{-1} $\Delta S^{\#}_{298}$ = - 35 JK^{-1} mol^{-1}

ΔH = -9.8 kJ mol^{-1} ΔS = 1.4 JK^{-1} mol^{-1} .

Nickel(II)

20.3	1.83	60.6
25.0	3.3	45
30.2	5.0	46.7
35.5	7.5	54.8

$\Delta H^{\#}$ = 66.3 kJ mol^{-1} $\Delta S^{\#}_{298}$ = - 13.4 JK^{-1} mol^{-1} .

$JK^{-1}mol^{-1}$. The activation parameters for the nickel complex based on k_H^{Ni} values are $\Delta H^{\#}$ = 66.3 kJ mol^{-1} and $\Delta S^{\#}_{298}$ = -13.4 $JK^{-1}mol^{-1}$ (Table 1.8). Values of K_2^{Ni} are insufficiently precise to derive meaningful thermodynamic parameters for protonation of the nickel complex.

It is significant that the equilibrium constants for protonation of MLH^+ are similar for copper and nickel, as would be expected on the basis of purely electrostatic considerations. Using previously published kinetic data obtained in the pH range 4.7 - 5.3 it has been possible to derive the values $K_1 = 6.6 \times 10^3\ M^{-1}$ at 25.0 °C (copper complex) and $K_1 = 9.3 \times 10^2\ M^{-1}$ at 25.0 °C (nickel complex). It is noteworthy that the kinetic scheme defined in equations (1 - 3) is also observed in the acid decomposition of $[Cu(H_{-2}glyglyhis)]^-$ over the pH range 1 - 5. In this reaction the decomposition rate is independent of $[H^+]$ at high acidities and has a first order dependence on $[H^+]$ at pH 2.5 - 3.5. Above pH 3.5, the hydrogen ion dependence increases and the decomposition rate becomes second order in $[H^+]$ by pH 5. The complicated dependence of the rate on hydrogen ion concentration observed with the copper(II) complexes of dioxocyclam and glycylglycylhistidine indicates that acid decomposition requires more than one protonation. The values of the protonation constants obtained kinetically for glycylglycylhistidine are log K_1 = 4.2 and log K_2 = 2.3 at 25.0 °C, which are similar to those observed with dioxocyclam (log K_1 = 3.97 (30.0 °C) and log K_2 = 1.65 (25.0 °C)). The protonation constants K_1 determined from kinetic measurements ($K_1^{Cu} = 6.6 \times 10^3\ M^{-1}$ and $K_1^{Ni} = 9.3 \times 10^2\ M^{-1}$) differs from those obtained from equilibrium measurements ($K_1^{Cu} = 1.1 \times 10^{-4}\ M^{-1}$ and $K_1^{Ni} = 1.2 \times 10^{-7}\ M^{-1}$ (Chapter 4, using the relation $K_1 = \beta_{11-2} / \beta_{11-1}$). The results indicate that for Cu^{2+} and Ni^{2+} complexes of dioxocyclam, the species MLH^+ observed in the kinetic and equilibrium studies are not same ones. Consequently, the dissociation mechanism is one, in which a rapid stepwise protonation of

the amide oxygens to give MLH^+ (1) and MLH_2^{2+} (2) takes place, followed by the slow dissociation of MLH_2^{2+} to the products.

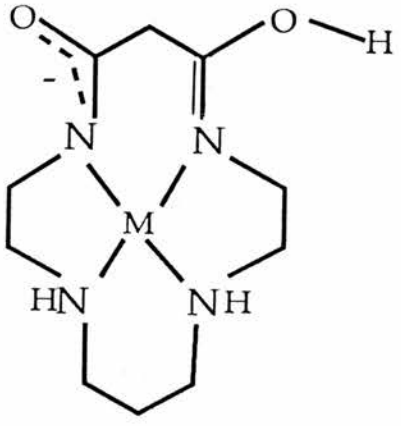

(1)

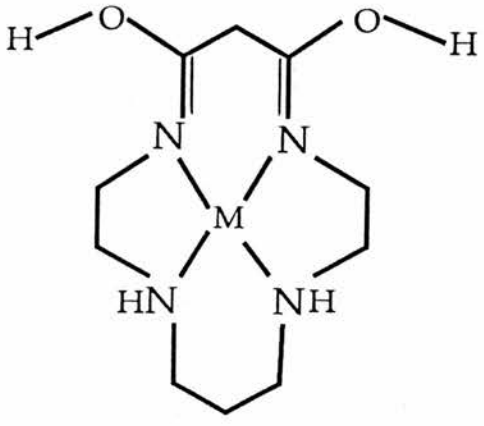

(2)

In MLH_2^{2+} both metal amide bonds are weakened, as protonation of the oxygens increases the double bond character of the carbon- nitrogen bonds. The weakening of the Cu-amide bond allows a partial dissociation which, combined with an intramolecular proton transfer from the oxygen to the nitrogen, finally results in the complete breaking of the metal- nitrogen bond.

Kaden(69) has also observed that in the case mono oxocyclam (3), the copper(II) and nickel(II) complexes display only first- and zero-order dependence on the hydrogen ion concentration, confirming the importance of amide protonation in the dissociation reaction.

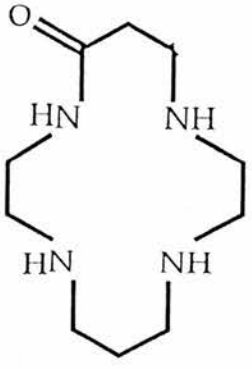

(3)

1.4 Copper(II) and Nickel(II) complexes of the mixed N_3O_2 donor macrocycle (L^9)

1.4.1 INTRODUCTION:

The crystal structures of $[Cu(L^9)(H_2O)](ClO_4)_2$ and $[Ni(L^9)(NO_3)_2]$ $0.5H_2O$ show that the copper is in a tetragonally elongated octahedral enviroment provided by the five ligand donor atoms and a water molecule (65). The formation constants log K = 6.48 (copper complex) and log K < 3 (nickel complex) indicate an enhanced ligand selectivity for Cu (II) relative to Ni(II). The origin of this discriminatory behaviour can be rationalised in terms of the crystal structure. The Ni(II) ion cannot accomodate the complete array of macrocyclic donor atoms while the Cu(II) ion can. The nickel complex is light green and insoluble in water and a variety of organic solvents. In contrast, the green copper complex is readily soluble in water and hence its acid hydrolysis was studied.

1.4.2 EXPERIMENTAL:

The copper(II) and nickel(II) complexes of the mixed N_3O_2 donor ligand L^9 were kindly provided by Professor D.E. Fenton.

Kinetic Measurements.

The kinetic runs were monitored at 752 nm using a Union Giken RA - 401 stopped-flow spectrophotometer. The temperature was maintained at 25.0 ± 0.1 °C. The dissociation of the copper complex of L^9 was studied by using hydrochloric acid solutions adjusted to I = 1.0 mol dm^{-3} ($NaClO_4$) (Table 1.3). Other experimental details are given in Section 1.2.1.

1.4.3 RESULTS and DISCUSSION

The acid dissociation of tetra-azacycloalkane complexes are extremely slow[2] and attention has focused on more labile systems including N_2O_2, N_2S_2, S_4, and N_3 macrocyclic systems [8,28,30,48].

The kinetics of the acid catalysed dissociation of $[CuL^9]^{2+}$ was studied using HCl solutions in the concentration range 0.01- 0.5 mol dm^{-3}, adjusted to I = 1.0 mol dm^{-3} with NaCl. Two reactions are observed at 752 nm; the first reaction was complete within 20 ms at 25 °C and was too fast to study in detail. An approximate value of the observed rate constant is 106 -109 s^{-1}. The second reaction had an acid-dependent rate which suggests that the first reaction possibly corresponds to the breaking of the weak metal-pyridine nitrogen bond, and the slower second reaction involves the opening of the central five-membered chelate ring as the next step in the unwrapping process. The second reaction shows a strict first-order dependence upon $[H^+]$ with a positive intercept k_o at zero $[H^+]$, at 25 °C (Figure 1.13 and Table 1.13). Thus, the rate expression takes the form

$$k_{obs} = k_o + k_H [H^+] \qquad (1)$$

The k_o term can be assigned to non-catalysed solvolytic displacement of the ligand and k_H term to the acid catalysed pathway. This type of behaviour has been noted

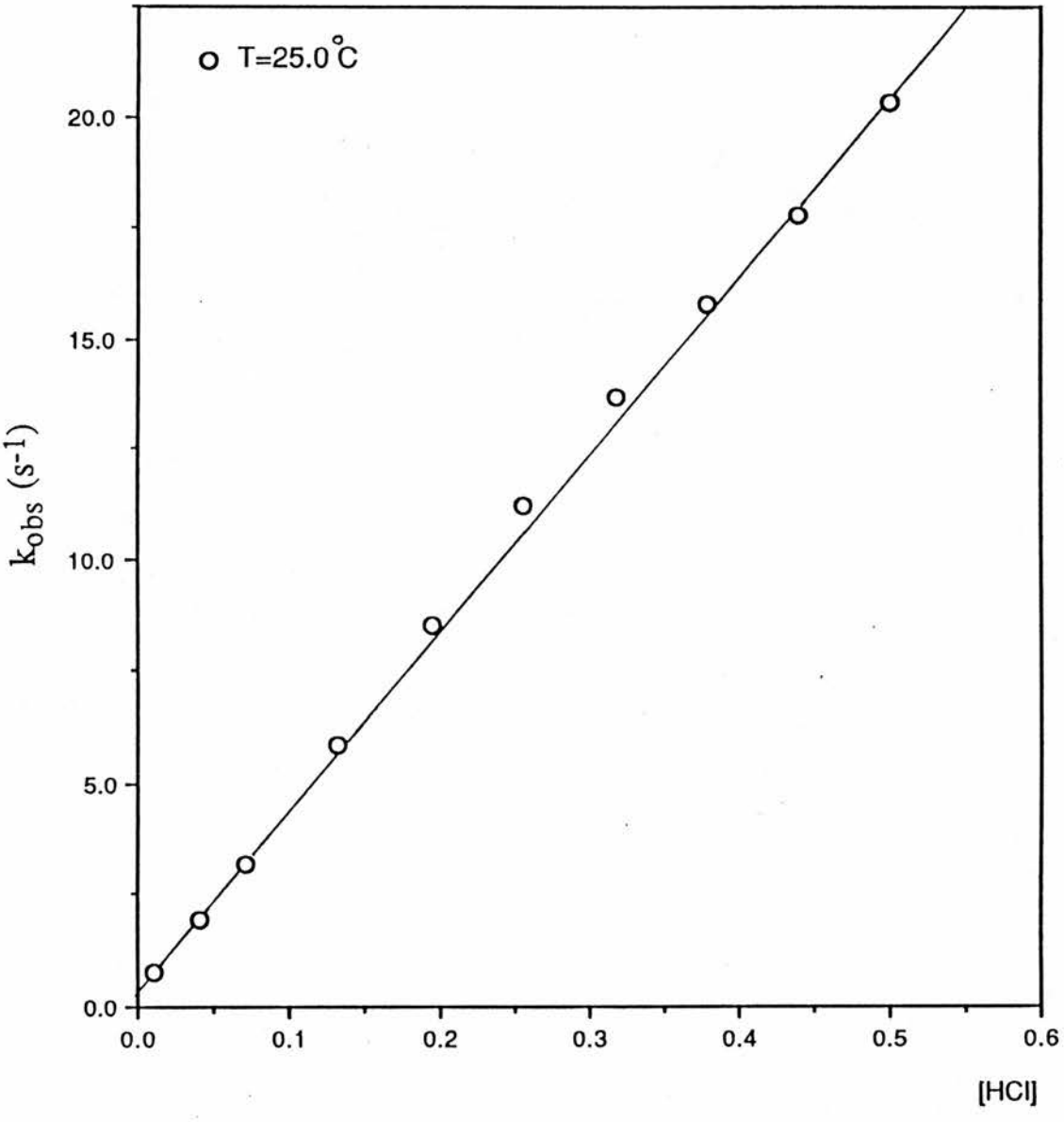

Figure 1.13 Acid dissociation of the copper(II) complex of mixed N_3O_2 donor in hydrochloric acid solution , I = 1.0 M (HCl+NaCl) .

Table 1.13 Observed rate constants for the dissociation of $CuL^{9\ 2+}$ in acid solution.

T ^{o}C	Ionic Strength M	$[H^+]$ M	k_{obs} s^{-1}
25.0	1.0 ($HClO_4$+$NaClO_4$)	0.010	0.78
		0.041	1.96
		0.071	3.20
		0.133	5.88
		0.194	8.50
		0.255	11.2
		0.317	13.7
		0.378	15.8
		0.440	17.8
		0.500	20.3
19.5	1.0 ($HClO_4$+$NaClO_4$)	0.510	1.82
22.5		0.510	2.22
25.0		0.510	2.75
30.2		0.510	3.73
34.5		0.510	4.50
41.5		0.510	6.65

previously for the dissociation of a number of macrocyclic complexes in acidic solution(30).

The kinetic behaviour can be accounted for by the scheme:

$$[Cu\text{-}L^9]^{2+} + H^+ \rightleftharpoons [Cu\text{-}HL^9]^{3+}; \quad K_1(\text{fast}) \qquad (2)$$

$$[Cu\text{-}L^9]^{2+} \; H_2O \longrightarrow \text{products}; \quad k_o \text{ (slow)} \qquad (3)$$

$$[Cu\text{-}HL^9]^{3+} \longrightarrow \text{products}; \quad k_2 \text{ (slow)} \qquad (4)$$

with an overall rate expression

$$k_{obs} = k_o + (k_{21} K_1 [H^+] / 1 + K_1 [H^+]) \qquad (5)$$

Under the conditions of the present experiment $K_1[H^+] << 1$, so that equation (5) can be simplified to

$$k_{obs} = k_o + k_{21} K_1 [H^+] \qquad (6)$$

It can be readily seen from equations (1) and (6) that k_H (= k_{21} K_1) is related to combined rate and equilibrium constants. The linear least-squares analysis of equation (1) gives $k_o = 0.52\ s^{-1}$ and $k_H = 40.17\ M^{-1}\ s^{-1}$ at 25.0 °C. The temperature dependence of k_{obs} values are cited in Table 1.13. The activation parameters based on these values are $\Delta H^{\#} = 41.0$ kJ mol^{-1} and $\Delta S^{\#}_{298} = -99.5$ JK^{-1} mol^{-1} (Table 1.8). The large negative entropy probably reflects the high degree of solvent reorganisation required in the transition state of the reaction.

1.5 Copper(II) and Nickel(II) complexes of the 18-membered hexadentate ligand (hexacyclen; L^8)

1.5.1 INTRODUCTION

Metal complexes of hexacyclen (L^8) can occur as two geometrical isomers the fac- isomer and the mer- isomer. The fac- and mer- isomers with cobalt(III) have been isolated and characterised(54). Standard preparative routes give *ca.* 99% mer and less than 1% fac- isomer. No structural evidence is available on the isomer distribution in the copper (II) and nickel (II) complexes.

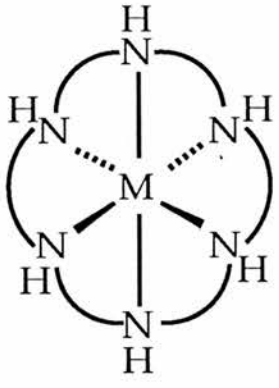

fac

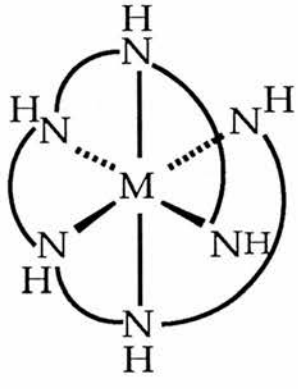

mer

Recent magnetic susceptibility measurements over a range of temperatures and e.s.r. data on $[CuL^8](BPh_4)_2$ indicate a temperature dependent structure(52). At lower temperatures, the e.s.r. data suggests a distorted structure. The g-values are typical for rhombic symmetry with slightly misaligned tetragonal axes, i.e., a compressed tetrahedron with only four nitrogens of the N_6-macrocycle coordinated to copper(II). At higher temperatures a distorted octahedral structure occurs. Magnetic and e.s.r data also suggest that the cobalt(II) complex $[CoL^8](BPh_4)_2$ is planar with only four nitrogen donors coordinated to Co(II) (67). A thermally dependent structure has also been reported for $[NiL^8](BPh_4)_2$(68). Nickel hexacyclen has a typical octahedral spectrum with bands at 351 nm (ε = 20 mol^{-1} dm^3 cm^{-1}), 537 nm (ε = 15 mol^{-1} dm^3

cm^{-1}), and 823 nm (ε = 21 mol^{-1} dm^3 cm^{-1}) in water (Figure 1.14). The dissociation of macrocyclic poly-aza metal complexes appears to differ somewhat from that of linear polyamines. Thus for the dissociation of Ni(2,2,2-tet) at acidities greater than 0.05 mol dm^{-3} the reaction is independent of hydrogen ion concentration and the cleavage of the four individual Ni- N bonds can be detected in stopped flow measurements (Section 1.6). In contrast to $[Cu(hexacyclen)]^{2+}$, the acid hydrolysis of $[Ni(hexacyclen)]^{2+}$ displays two kinetic processes at both low (0.01 - 0.04 mol dm^{-3}) and high (0.05 - 0.4 mol dm^{-3}) hydrogen ion concentrations. Similar kinetic behaviour has been observed with the nickel(II) complex of a 15-membered S_2N_2 donor macrocycle[47]. Both reactions are associated with an abscorbance decrease.

1.5.2. EXPERIMENTAL

Synthesis of the complexes

Hexacyclen.$3H_2SO_4$ was purchased from Aldrich. The copper(II) and nickel(II) complexes were prepared by the following general procedure. To hexacyclen.$3H_2SO_4$ (1 g) in water (20 cm^3) was added an excess of the basic metal carbonate ($NiCO_3.Ni(OH)_2.4H_2O$ or $CuCO_3.Cu(OH)_2.H_2O$). The solution volume was adjusted to 100 cm^3 by the addition of water and the slurry heated on a water bath for 30 minutes. The excess basic carbonate was filtered off and to the filtrate was added saturated sodium perchlorate solution (15 cm^3). The solution volume was reduced to *ca.* 50 cm^3 on a water bath, then cooled in ice. The crystals so obtained were filtered off and dried in *vacuo*. The nickel(II) complex is pink and the copper(II) complex is deep blue in color. Anal . Calc. for $C_{12}H_{32}Cl_2N_6O_9Ni$: C, 26.98; H, 5.99 ; N, 15.74. Found: C, 26.81; H, 5.65; N, 15.45 %. Calc. for $C_{12}H_{32}Cl_2N_6O_9Cu$: C, 26.74; H, 5.94; N, 15.60 . Found : C, 26.78; H, 5.73; N, 15.62 % .

The electronic and i.r. spectra of the metal complexs are summarised in Tables 1.1 and 1.2.

Kinetic Measurements.

Absorbance and repetitive scan measurements were recorded on a Phillips PU 8720 spectrophotometer. Typical interval scan spectra for the reaction of the copper(II)

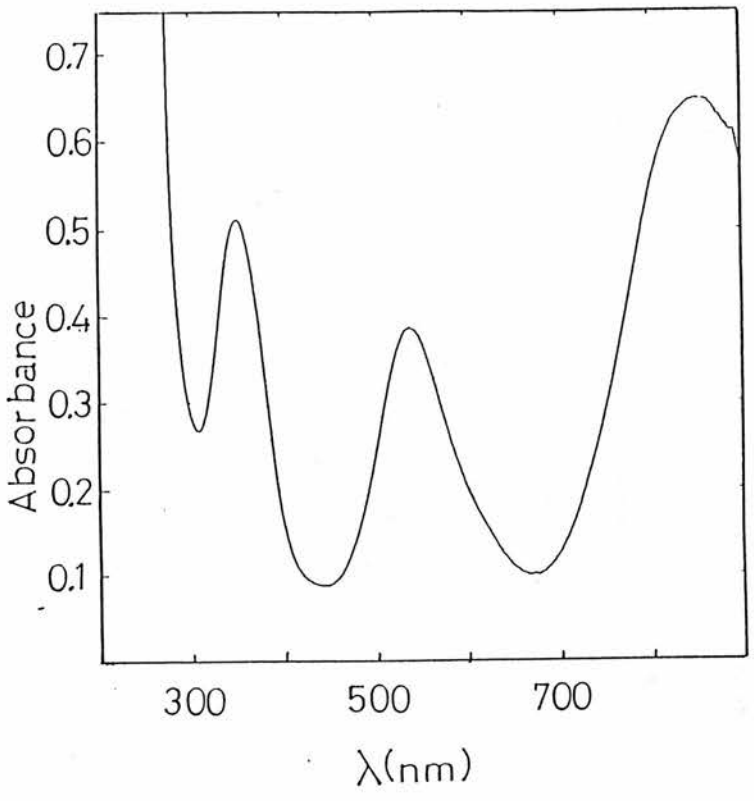

Figure 1.14 Absorption spectrum for the nickel(II) complex of haxacyclen .

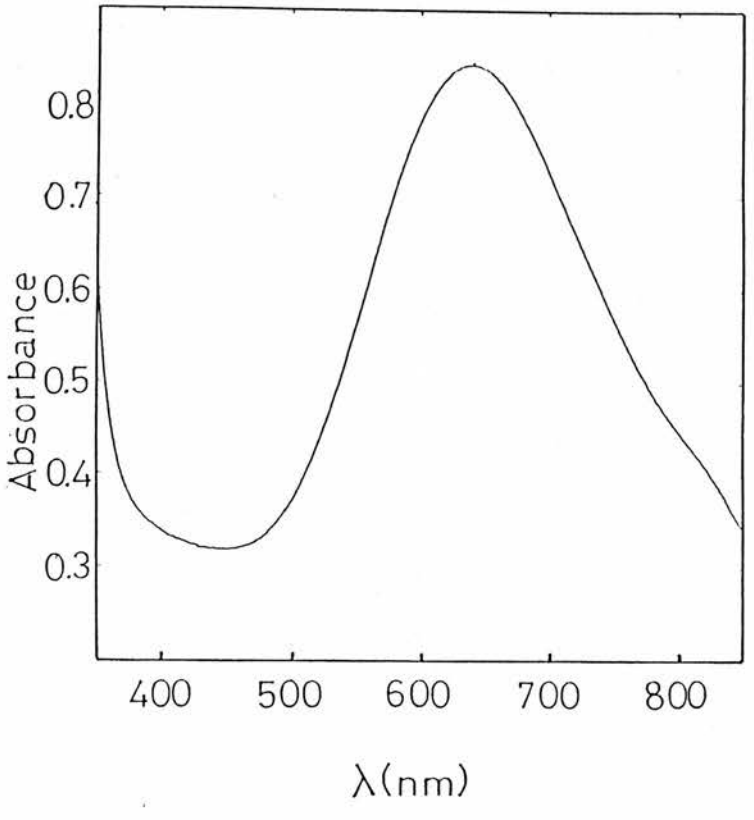

Figure 1.17 Absorption spectrum for the copper(II) complex of haxacyclen .

complex are shown in Figure 1.15. Solutions of hydrochloric acid were prepared from CONVOL ampoules. Dissociation of $[CuL^8]^{2+}$ and $[NiL^8]^{2+}$ were monitored at 265 nm and 225 nm respectively. The reactions were initiated by injecting small aliquots of hydrochloric acid to an aqueous solution of the complex which had previously been equilibrated to 25 ± 0.1 °C. The ionic strength was adjusted to 1.0 mol dm^{-3} in all the reactions by addition of $NaClO_4$ in the case of the copper complex and NaCl in the case of the nickel complex (Table 1.3). Values of k_{obs} were determined by a curve fitting procedure using the " Fitting " program (GW-Basic version 3.2).

Kinetic data at high hydrogen ion concentrations were obtained using a Hi-Tech stopped-flow system. The Hi-Tech system was provided with an SF-40C photomultiplier, Data-Lab DL 901 transient recorder and a DT V12-14 Farnell oscilloscope. Data acquisition and processing were carried out by an Apple II Plus microcomputer using a Hi-Tech system software kinetics package. Rate constants were calculated by a computer program using the Kedzy-Swinbourne[1] method. In this case, the reactions of the copper and nickel complexes were monitored at 610 nm and 240 nm respectively (Table 1.3).

---

[1]F.J. Kezdy, J. Jaz and P. Bruylants, Bull. Soc. Chim. Belges. 67, 687(1958).

1.5.3 RESULTS and DISCUSSION

1.5.3.1 Acid dissociation of copper(II) hexacyclen $(CuL^8)^{2+}$

High Acidities

At high acidities (0.075 - 0.275 mol dm^{-3}), $CuL^{8\,2+}$ is expected to exist as the diprotonated complex $[CuL^8H_2]^{4+}$ (the pK_a values of L^8 are 10.2, 9.2, 8.7, 4.1, ~ 2, ~ 1)(45). Jahn-Teller distortion leads to longer axial Cu-N bonds and the axial nitrogens are readily protonated. At these acidities only a single kinetic process was observed in the dissociation reaction. Values of the observed first-order rate constants at various hydrogen ion concentrations (Table 1.14) show a good first order dependence on $[H^+]$, Figure 1.16(b), with $k_{30} = k_{obs} / [H^+] = 73$ mol^{-1} dm^3 s^{-1} at 25 °C. The reaction is thus

$$[CuLH_2]^{4+} + H^+ \longrightarrow Cu + [H_6L]^{6+} \; ; \; k_{30}\,(slow) \qquad (1)$$

Cleavage of the first equatorial Cu-N bond is slow with all subsequent steps being rapid. The temperature dependence of k_H (Table 1.14) gives $\Delta H^{\#} = 30.5$ kJ mol^{-1} and $\Delta S^{\#}_{298} = -107$ J K^{-1} mol^{-1}. Again the large negative entropy probably reflects the high degree of solvent reorganisation required in the transition state of the reaction.

Low Acidities

At lower acidities (*ca.* 1×10^{-3} $[H^+]$), only the monoprotonated complex $[CuL^8H]^{3+}$ is expected to occur in solution. Existence of such a species in solution is evidenced from the absorption band near 800 nm (Figure 1.17). Copper(II) complexes of [15]aneN_5 with all five membered chelate rings have an extra absorption band near 800 nm, indicative of axial interaction in a five coordinate complex.

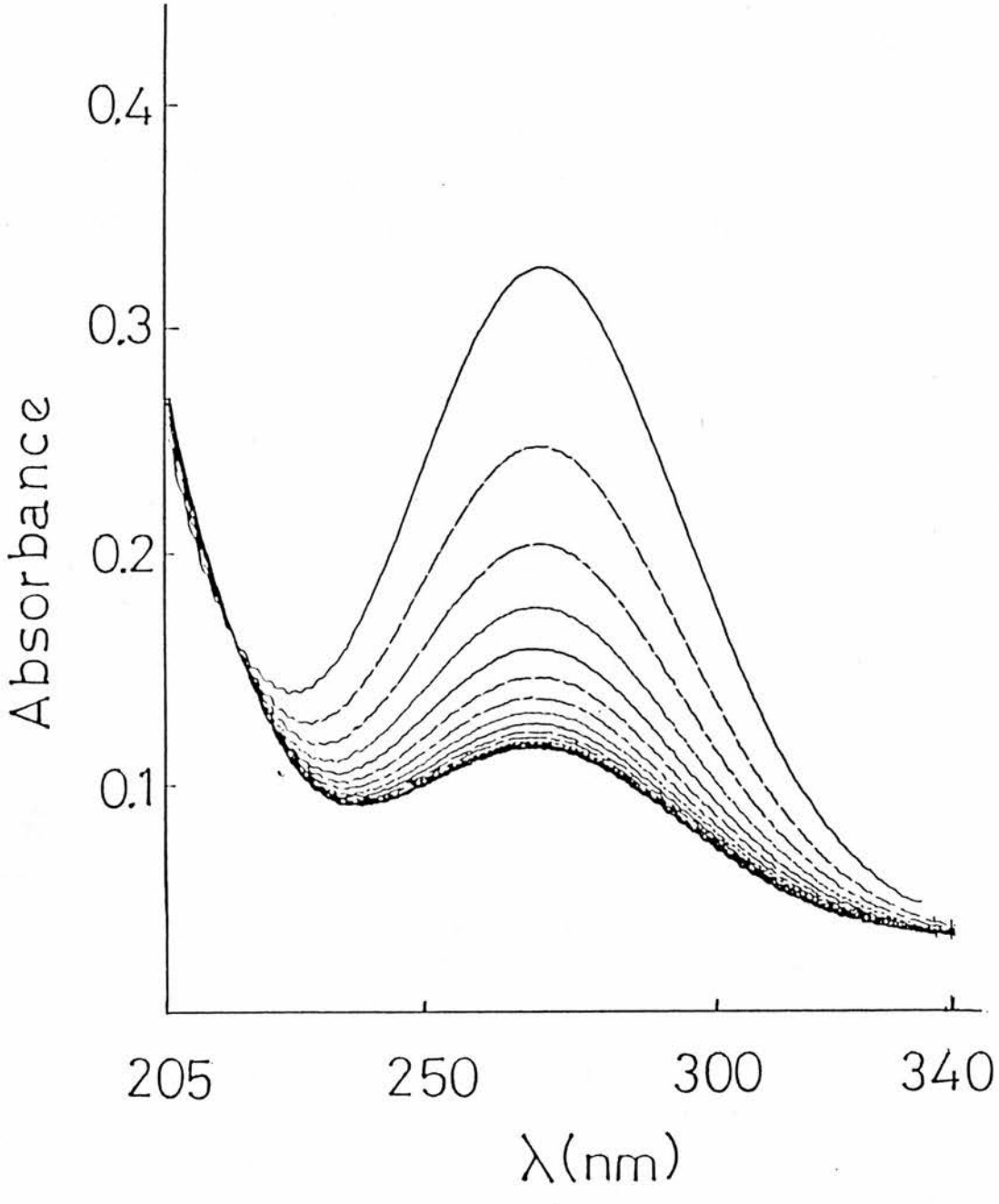

Figure1.15 Repetitive scan spectra for the acid catalysed dissociation of the copper(II) complex of hexacyclen ; $[H^+] = 1.1 \times 10^{-3}$ at 25.0 °C . The time interval between scans is 25 s .

Table 1.14 Observed rate constants for the dissociation of $CuL^{8\ 2+}$ in acid solution.

T °C	Ionic Strength M	$10^4[H^+]$ M	$10^3 k_{obs}$ s^{-1}	k_H $M^{-1}\ s^{-1}$	
25.0	1.0 (HCl+NaCl)	11.70	10.70		
		12.20	13.30		
		13.80	15.60		
		15.30	20.00		
		16.70	23.10		
		[High acidity]	[High acidity]		
		(10^{-4})	(10^{-3})		
		0.075	5.90		
		0.101	7.40		
		0.125	8.80	70.4	(72.5)[f]
		0.150	10.8		
		0.175	12.4		
		0.200	14.5		
		0.225	16.2		
		0.275	20.1		
28.0	1.0 (HCl+NaCl)	0.125	10.2	81.6	(82.5) [f]
32.0		0.125	12.5	100	(98.4) [f]
38.0		0.125	15.6	125	(127) [f]
42.0		0.125	18.6	149	(149) [f]
47.0		0.125	22.0	176	(181) [f]

[f] k_H calculated from activation parametrs cited in Table I.8

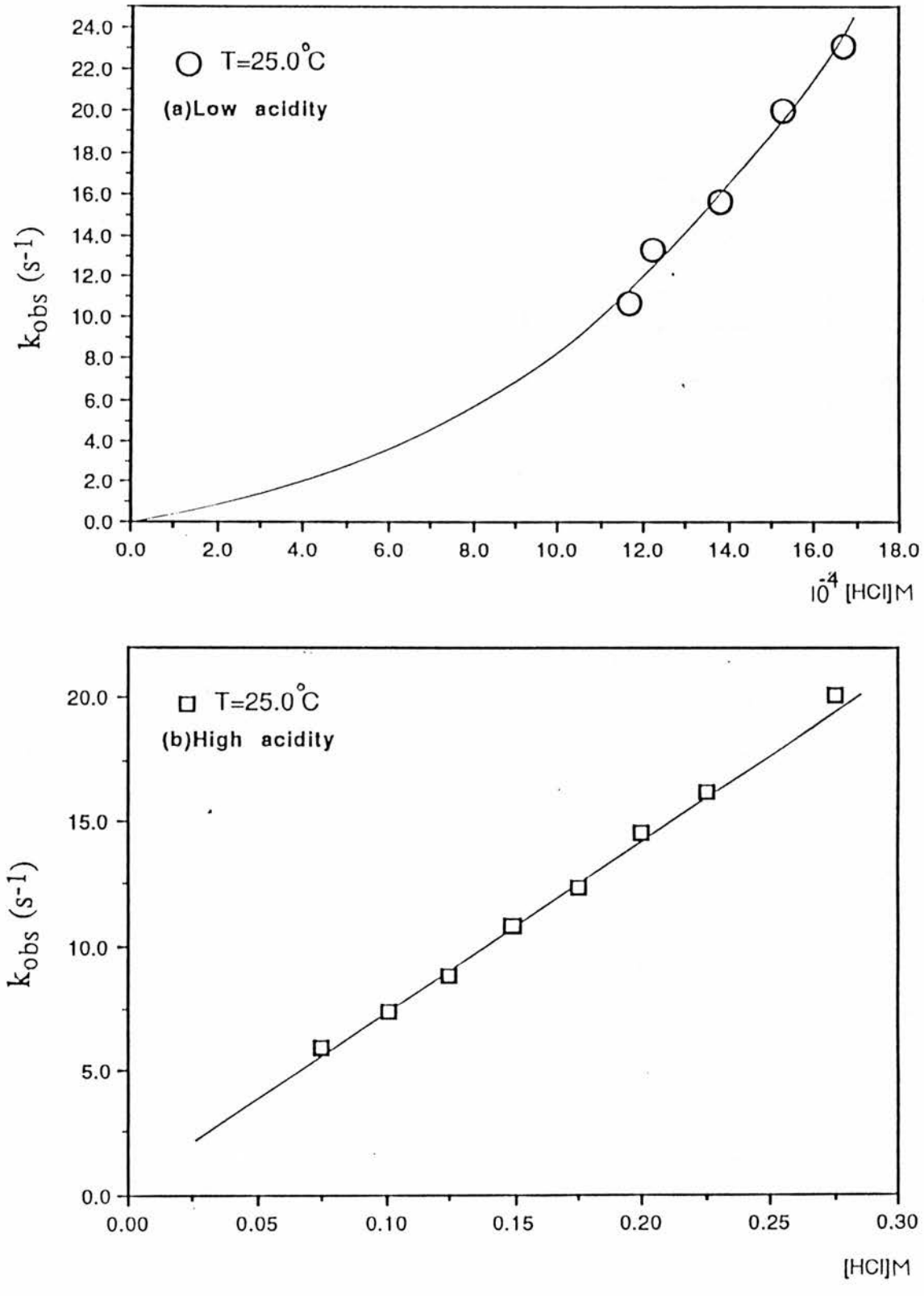

Figure 1.16 Acid dissociation of the copper(II) complex of hexacyclen in hydrochloric acid solutions at (a) low acidity and (b) high acidity .

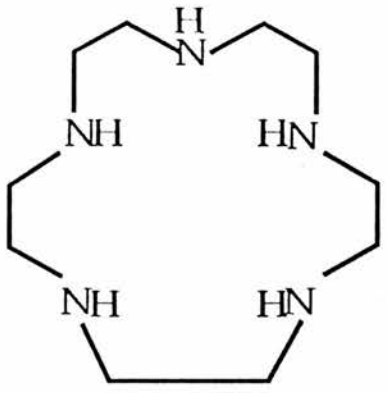

As before only a single kinetic process is observed spectrophotometrically in the dissociation (Table 1.14). However, in this case the reaction displays a second order dependence on $[H^+]$, Figure 1.16a, with $k = k_{obs} / [H^+]^2 = 8.5 \times 10^3$ dm^6 mol^{-2} s^{-1}. The kinetic results indicate that the transition state involves $[CuL^8H]^{3+}$ and two additional protons. Cleavage of an equatorial Cu-N bond is again required before rapid dissociation occurs. The general reaction scheme for dissociation of $[CuL^8]^{2+}$ in acidic solution is summarised below. At low acidities the dissociation can be represented by the equations

$$[CuL^8H]^{3+} + H^+ \rightleftharpoons [CuL^8H_2]^{4+} ; \quad K_2 \text{ (fast)} \qquad (2)$$

$$[CuL^8H_2]^{4+} + H^+ \longrightarrow \text{products} ; \quad k'_{30} \text{ (slow)} \qquad (3)$$

using equations (2) and (3)

$$k_{obs} \{ [CuL^8H]^{3+} + [CuL^8H_2]^{4+} \} = k'_{30} [CuL^8H_2]^{4+} [H^+]$$

and since $[CuL^8H]^{3+} = [CuL^8H_2]^{4+} / K_2 [H^+]$

therefore, $k_{obs} = k'_{30} K_2 [H^+]^2 / (1 + K_2 [H^+])$ (4)

At low acidities where $K_2[H]^+ << 1$, the reaction shows a second order dependence on $[H^+]$, with $k_{obs} = k'_{30} K_2 [H^+]^2$ and $k = k'_{30} K_2$. Since $k'_{30} = k_{30}$ (the rate constant determined at high acidities) the equillibrium constant $K_2 = k / k_{30} = 8.5 \times 10^3 / 73 = 116$ mol^{-1} dm^3 at 25 °C. Using this equilibrium constant, the ratio $[CuL^8H_2]^{4+} / [CuL^8H]^{3+}$ is 0.116 at $[H^+] = 10^{-3}$ mol dm^{-3}, so that some 10% of the complex is diprotonated at this acidity. Formation of $[CuL^8H_3]^{5+}$ will lead to significant electrostatic repulsion forces in the metal complex which results in rapid dissociation of the 3N- bonded intermediate.

A second-order dependence on $[H^+]$ has been reported for compounds of copper(II) with an homologous series of pentaazamacrocyles of varying ring size, and for the nickel complex of [15]aneN$_5$(14, 15). It was found that there is an increase in rate as the ring size increases, the respective k_H (mol^{-1} dm^3 s^{-1}) constants being 0.049 (15-membered), 4.85 (16-membered), and 1.18×10^3 (17-membered). Obviously the more facile dissociation in the latter two complexes is due to the increasing flexibility of the larger rings. In this work k_H for the copper(II) complex of the 18-membered sexadentate ligand (L^8) is 8.5×10^3 mol^{-1} dm^3 s^{-1}, in agreement with the above argument.

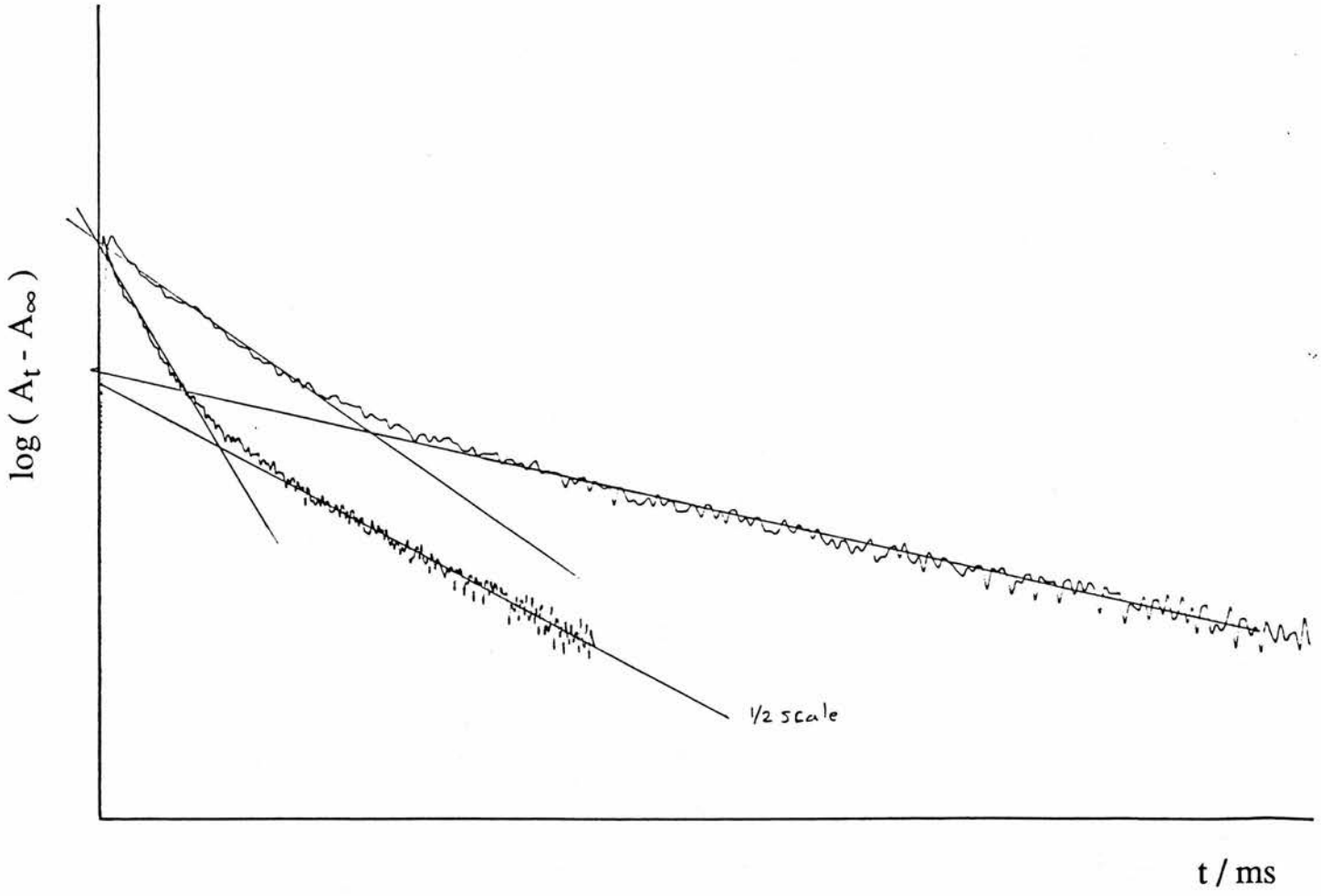

Figure 1.18 Acid dissociation of the nickel(II) complex of hexacyclen in hydrochloric acid solution ($[H^+] = 0.2$) , I = 1.0 mol dm^{-3}, and 25 ^oC , showing the existence of two consequtive kinetic steps .

Table 1.15 Observed rate constants for the dissociation of $NiL^{8\ 2+}$ at I = 1.0 M ($HCl + NaClO_4$).

T ^oC	$[H^+]$ M	$10^3\ k_2(obs)$	$10^3\ k_1(obs)$
25.0	0.010	0.39	1.45
	0.015	1.84	5.53
	0.025	15.1	59.0
	0.030	21.4	84.0
	0.034	27.8	124
	0.040	41.0	150
	0.050	62.0	242
25.0	0.015	1.84	
32.0	0.015	2.56	
38.0	0.015	3.19	
49.0	0.015	3.78	
25.0	0.025	15.1	
31.0	0.025	34.6	
36.5	0.025	36.6	
41.5	0.025	40.0	
47.0	0.025	53.3	
9.00	0.035	8.34	
15.0	0.035	14.0	
20.0	0.035	20.2	
25.0	0.035	26.2	
30.0	0.035	33.5	
25.0	0.050	0.75	7000
	0.100	1.35	11500
	0.150	1.80	15500
	0.200	2.15	19000
	0.250	2.50	22500
	0.300	2.80	24500
	0.350	3.10	26000
	0.400	3.30	28500

1.5.3.2 Acid dissociation of nickel(II) hexacyclen $[NiL^8]^{2+}$

The nickel(II) complex of the sexadentate ligand shows different kinetic behaviour in acid dissociation compared with the copper(II) complex. The acid hydrolysis of [Ni(hexacyclen)]$^{2+}$ displays two kinetic processes at both low (0.01 - 0.04 mol dm^{-3}) and high (0.05 - 0.4 mol dm^{-3}) hydrogen ion concentrations. Figure 1.18 shows a plot of log Abs *vs.* time for the dissociation of Ni-hexacyclen at $[H^+]$ = 0.2 mol dm^{-3}. The plot shows initial curvature and becomes linear at longer times in accordance with the existence of two consequtive first order reactions (k_1(obs) and k_2(obs)) with the second being slower than the first. Both reactions are associated with an absorbance decrease and show the same dependence on $[H^+]$. Similar kinetic behaviour has been reported for the nickel(II) complex of the 15-membered S_2N_2 donor macrocycle[47].

High Acidities

At high acidities (0.05 - 0.4 mol dm^{-3}), the monoprotonated complex $[NiHL^8]^{3+}$ is expected to predominate. Plots of k_2(obs) versus $[H^+]$, Table 1.15 and Figure 1.19b show that the reaction becomes independent of $[H^+]$ at high acidities. The kinetic scheme can be summarised as

$$[NiHL^8]^{3+} + H^+ \rightleftharpoons [NiH_2L^8]^{4+} \quad ; K_2 \text{ (fast)} \qquad (1)$$

$$[NiH_2L^8]^{4+} \longrightarrow \text{products} \quad ; k_{21}\text{(slow)} \qquad (2)$$

Values of K_2 and k_{21} were obtained by curve fitting (using the Grafit program) of k_1(obs) to the function $A\,[H^+] / (1 + B\,[H^+])$, derived from equations (1) and (2), giving K_2 = 2.24 mol^{-1}dm^3 and k_{21} = 58.9 s^{-1} at 25 °C. A similar analysis was applied to the kinetic data k_2(obs) *vs* $[H^+]$. (Table 1.15) giving K_2 = 2.5 mol^{-1}dm^3 and k_{21} = 6.43 s^{-1}. Since rate = k_i(H) [Complex] $[H^+]$ (where k_i(H) is the slope of k_{obs} *vs.* $[H^+]$ at the linear portion of the curve), then $k_i(H) = K_2 k_{21}$ on the basis of

equations (1) and (2) and $k_1(H) = 131$ mol^{-1} dm^3 s^{-1} and $k_2(H) = 16$ mol^{-1} dm^3 s^{-1} for the first and second reactions at 25 °C. The first reaction is eight times faster than the second reaction. The rate constants $k_1(obs)$ and $k_2(obs)$ were calculated by non linear least squares fits of absorbance vs. time to a one exponential function of the form $A = A_o \exp(-k_{obs}\, t) + A_x$ at two different time scales, in which one kinetic step overrides the other.

Low Acidities

In the acidity range (0.01 - 0.04 mol^{-1} dm^3), the monoprotonated complex still predominates. This conclusion can be justified by considering the ratio $[NiH_2L^8]^{4+}$ / $[NiHL^8]^{3+}$ which can be calculated using the value $K = [NiH_2L]^{4+} / [NiHL]^{3+}[H^+]$ = 2.5 mol^{-1}dm^3 obtained above. Thus at $[H^+] = 0.02$ mol dm^{-3} the ratio = 0.05 i.e., only some 5% of the diprotonated complex is present at this acidity.

The kinetic traces (A_s *vs* time), which can be fitted to a double exponential function of the form

$$A = A_o \exp(-k_1(obs)\, t) + A_1 \exp(-k_2(obs)\, t) + A \qquad (3)$$

gave good reproducibility (< 2% standard deviation) .

At the acidity range employed the dissociation reactions display a second order dependence on $[H^+]$ (Figure 1.19(a)). This behaviour can be rationalised in terms of the scheme:

$$[NiL^8H]^{3+} + H^+ \rightleftharpoons [NiL^8H_2]^{4+}; \qquad K \text{ (fast)} \qquad (4)$$

$$[NiL^8H_2]^{4+} + H^+ \longrightarrow \text{products}; \qquad k_{30} \text{ (slow)} \qquad (5)$$

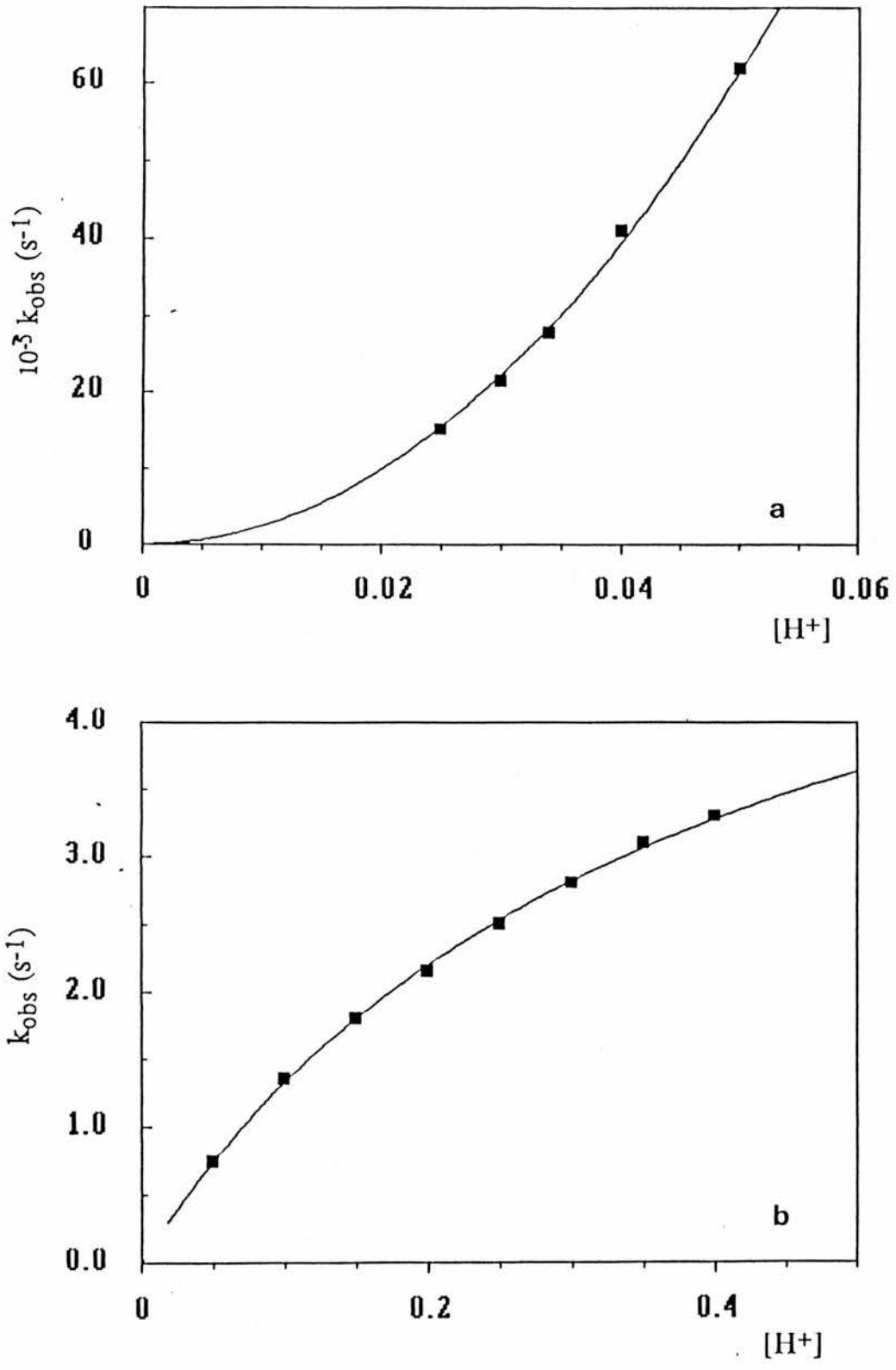

Figure 1.19 Plot of k_1(obs) against [H^+] for the acid catalysed dissociation of the nickel(II) complex of hexacyclen in hydrochloric acid solutions at (a) low acidity ,(b) high acidity

Following the same mathematical treatment described above for $[CuL^8]^{2+}$ at low acidities, it can be readily shown that $k_i(H) = K_2k_{30}$. Analysis of the plots $k_i(obs)$ *vs* $[H^+]$ give $k_1(H) = K_2k_{30} = 97.0\ mol^{-1}dm^3s^{-1}$, and $k_2(H) = K_2k_{30} = 24.7\ mol^{-1}dm^3s^{-1}$ for the $k_1(obs)$ and $k_2(obs)$ reactions respectively. Since $K_2 = 2.24$ and $K' = 2.5\ mol^{-1}dm^3$ (see above) this gives $k_{30} = 43.3\ s^{-1}$ for $k_1(obs)$ and $k'_{30} = 9.9\ s^{-1}$ for $k_2(obs)$. The ratio of the dissociation rates of the first reaction to the second reaction $R_h = k_1(H) / k_2(H) = 97.0 / 24.7 = 3.9$ is almost half the value found under high acidity conditions. The temperature dependence of $k_2(H)$, Table 1.16, gives $\Delta H^{\#} = 44.5\ kJ\ mol^{-1}$ and $\Delta S^{\#}_{298} = -70\ J\ K^{-1}\ mol^{-1}$.

It is thus clear that the copper(II) complex of hexacyclen is much more reactive in acid than is the nickel(II) complex. Indeed the only direct comparison between the two cations occurs at low acidities where both display the same kinetic dependence on $[H^+]$. The ratio of the corresponding second order rate constants ($k_H{}^{Cu} / k_H{}^{Ni}$) is ~ 300 at 25 °C.

The dissociation kinetics of $[Ni(hexacyclen)]^{2+}$ in acidic solution may be rationalised as follows.

At low acidities two protons fastly attack the two axial nitrogens in Ni-hexacyclen , and the dissociation occurs in successive steps for the first and second equatorial nitrogens. At high acidities the nickel complex exists as $[Ni(H\text{-}hexacyclen)]^{+3}$ (square pyramidal) and only one proton is needed to attack the axial nitrogen followed two successive steps. On conclusion the dissociation might be expressed as

$$\text{complex} \xrightarrow{k_1(obs)} \text{intermediate} \xrightarrow{k_2(obs)} \text{products.}$$

1.6 Copper(II) and Nickel(II) Complexes of the Linear Tetraamine ligand 2,2,2-tet(L^{10}).

1.6.1. EXPERIMENTAL

Preparation of the ligand.

The open chain tetraamine, L^{10}, was synthesised by the general methods described in the literature[23] (Scheme VII).

Scheme VII

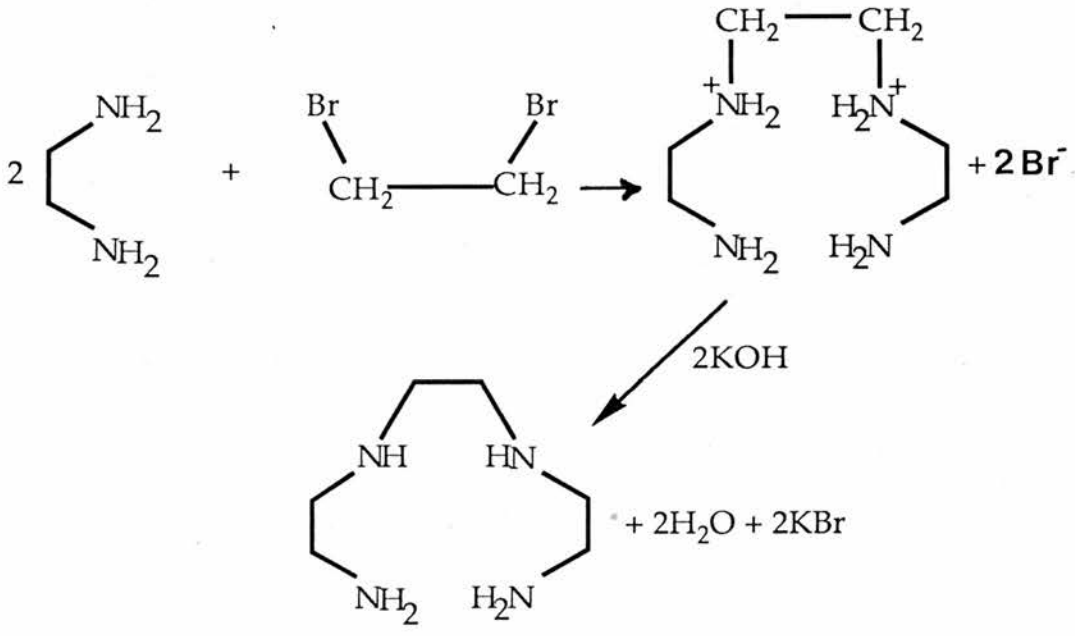

2,2,2-tet(L^{10}).

1,2-Diaminoethane, 445 g (6 mol), was placed in a two litre three-necked flask the diamine was cooled to ice temperature, and 94 g (0.5 mol) of 1,2-dibromoethane was added dropwise with stirring. After the addition was complete (*ca* 0.5 h), the reaction mixture was heated on a steam bath for 1 h and then concentrated to one third of its original volume by removal of excess 1,2-diaminoethane on a rotary evaporator. Potassium hydroxide (150 g) was then added and the mixture heated with efficient stirring for 2 h on a steam bath. After cooling to room temperature, the solids were removed by filtration and washed with several portions of ether to remove adsorbed

product. The ether washings and the filtrate were combined and evaporated to a viscous oil. The oil was separated from any solid which forms by ether extraction and decantation. The decanted ether solution was again stripped on a rotary evaporator. The viscous oil which remains was vacuum-distilled.

2,2,2-tet.4HBr

A solution of 2,2,2-tet. in methanol (200 cm^3) was cooled in an ice bath and concentrated HBr (65 cm^3, 48%) was added dropwise with stirring. The white precipitate was filtered off, washed with n-butanol, then ether and dried in air. The purity of the salt was checked by potentiometric titration against a standard copper(II) solution using a copper selective electrode as the indicator electrode.

Synthesis of the complexes

$[Ni_2(L^{10})_3]Cl_4.2H_2O$ Bis triethylenetetraamine μ–triethylenetetraamine dinickel(II) chloride dihydrate) .

. Nickel(II) chloride hexahydrate (11.85 g) was dissolved in ethanol (25 cm^3) and L^{10} (11 cm^3) diluted with an equal volume of ethanol added slowly with stirring. Heat was evolved and on cooling, the pink complex crystallised. In this complex 2,2,2-tet acts also as a bridging ligand occupying two sites on each central atom (66).

$[NiL^{10}][ClO_4]_2.H_2O$

Nickel(II) chloride hexahydrate (2.5 g) and the complex salt prepared above (7.7 g) were mixed with ethanol (23 cm^3) and water (2.5 cm^3) and the mixture heated under reflux for *ca.* 45 minutes. The resulting blue solution was filtered hot and then evaporated to *ca.* 15 cm^3 on a steam bath. A few drops of a concentrated solution of $NaClO_4$ in water were added and the solution allowed to cool to room temperature. The violet crystals obtained were filtered off and dried (the dried crystals are light blue).

[Cu (L^{10})] $[ClO_4]_2.H_2O$

Copper(II) perchlorate hexahydrate (9.26 g, 0.025 mol) was dissolved in water (10 cm^3) and L^{10} (3.7 g, 0.025 mol) diluted with ethanol (10 cm^3) was slowly added, the deep blue solution formed was filtered and allowed to cool in refrigerator for 24 h. The deep violet crystals obtained were filtered off washed with n-butanol then ether and allowed to dry in air.

Aqueous solutions of the complexes $[ML^{10}]^{2+}$ (M = Cu^{2+} or Ni^{2+}).

These solutions were prepared by mixing appropriate volumes of standard solutions of the metal and the ligand L^{10}.4HBr (1:1) and neutralised to pH 7.8 with NaOH. The solution of the nickel derivative was heated to 60-70° for several hours to ensure the complete conversion to $[NiL^{10}]^{2+}$, (the solution is yellow or light brown when hot and violet at room temperature).

Ultraviolet and visible spectra were recorded on a Shimadzu-160 instrument. Data from the electronic spectra of the metal complexes are summarised in Table 1.1.

Kinetic Measurements

The kinetic runs were monitored at 575 nm and 370, 400, 420, 460, 550, and 650 nm for the copper(II) and nickel(II) systems respectively using a Union Giken RA - 401 stopped-flow spectrophotometer. The temperature was maintained at 25.0 ± 0.1 °C. The dissociation reactions of the copper and nickel complexes of 2,2,2-tet were studied by using nitric and perchloric acid solutions adjusted to I = 0.5 mol dm^{-3} ($NaClO_4$) (unless otherwise specified). The concentration of the copper(II) complex was in the range 1 to 50 x 10^{-4} mol dm^{-3} and that for the acid (HNO_3 or $HClO_4$) 1 x 10^{-3} to 50 x 10^{-3} mol dm^{-3}, and the concentration of the nickel(II) complex was in the range 2.5 to 25 x 10^{-3} mol dm^{-3} and that for the acid (HNO_3 or $HClO_4$) 5 x 10^{-2} to 25 x 10^{-2} mol dm^{-3}.

1.6.2. RESULTS and DISCUSSION

Dissociation of [Cu (2,2,2-tet)]$^{2+}$

The dissociation of [Cu(2,2,2-tet)]$^{2+}$ was studied over a wide range of acid concentrations (0.001 - 0.1 mol dm^{-3}). In this acidity range, the copper complex displays a variety of kinetic behaviour (Figure 1.20). A second order dependence on [H$^+$] in the acidity range 0.001 - 0.005 mol dm^{-3} with rate = k_H [CuL^{10}]$^{2+}$ [H$^+$]^2. A first order dependence on [H$^+$] in the acidity range 0.015 - 0.025 mol dm^{-3} with rate = k'_H [CuL^{10}] $^{2+}$ [H$^+$] and acid independence at high acidity (0.03 - 0.09 mol dm^{-3}) with rate = A [H$^+$] [CuL^{10}] $^{2+}$ / 1 + B [H$^+$] (A = kK and B = K). The study also shows that the reaction is dependent on the nature of the acid used, for example, the copper complex dissociates more rapidly in nitric acid than in perchloric acid (Figure 1.20).

In all cases, at least four kinetic stages could be detected. Stages one and three are associated with absorbance increase while stages two and four are associated with absorbance decrease. The first three stages are fast and overlap each other and are difficult to measure accurately. They are only slightly affected by the hydrogen ion concentration. The fourth kinetic step is assigned to the dissociation step. The initial fast reactions are presumably initial dechelations of copper(II). When the metal ion is relatively inert, for example, Ni^{2+}, all four stages are detectable and could be measured accurately .

Low Acidities

At lower acidities (*ca.* 1x10^{-3} [H$^+$]) the copper complex displays a second order dependence on hydrogen ion concentration. Values of k_{obs} at various [H$^+$] for the dissociation of [CuL^{10}]$^{2+}$ are summarized in Table 1.16. Least-squares analysis of the data gives k_{obs} / [H$^+$]^2 = 8.5 x 10^5 M^{-2} s^{-1} at I = 0.5 mol dm^{-3} ($HClO_4$ + $NaClO_4$) and 8.1 x 10^5 M^{-2} s^{-1} at I = 1.0 mol dm^{-3} (HNO_3+ $NaNO_3$) at 25 ^{o}C.

A possible kinetic scheme for the acid dissociation could involve the steps

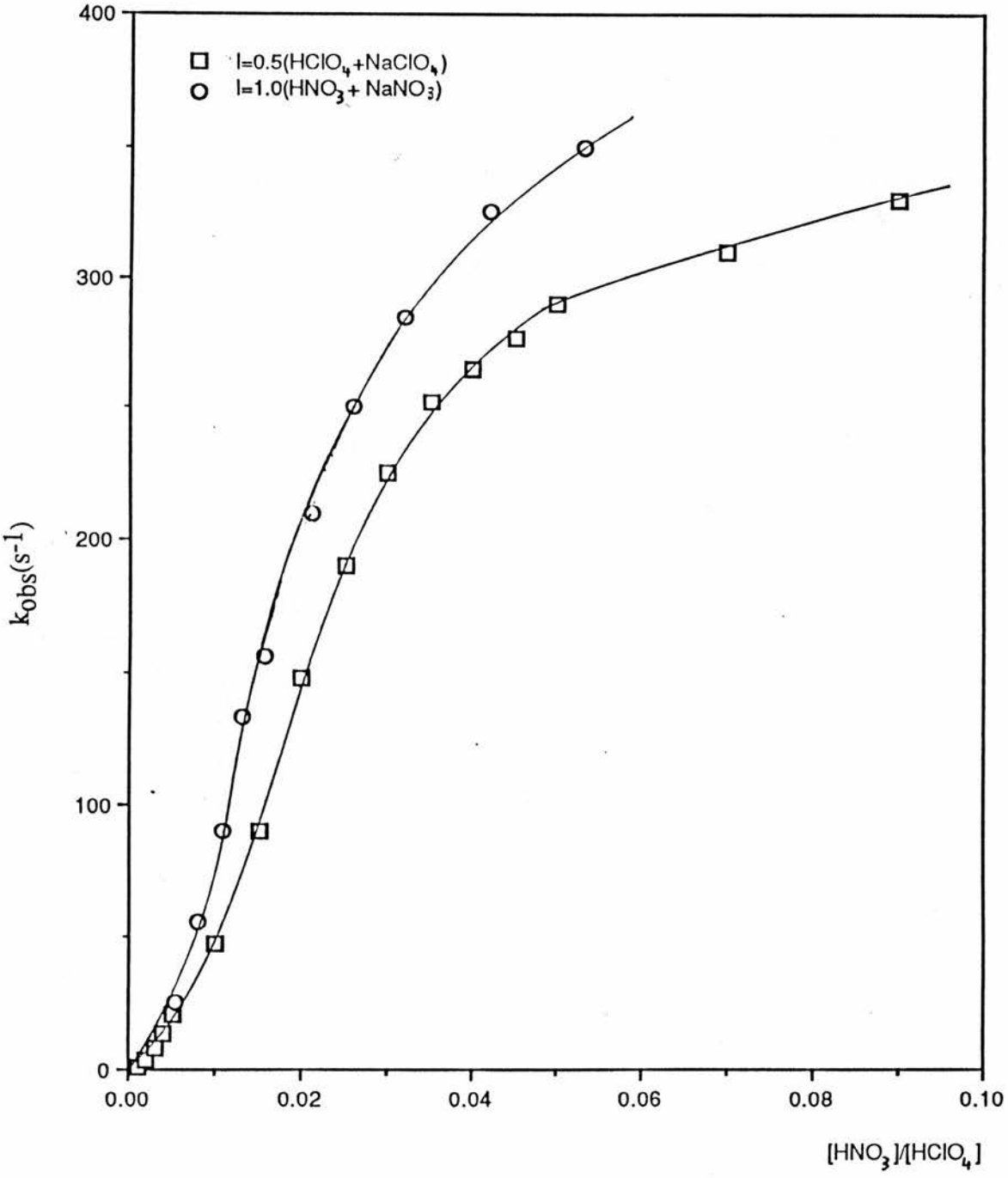

Figure 1.20 Acid dissociation of the copper(II) complex of 2,2,2-tet in perchloric and nitric acid solutions .

Table 1.16 Observed rate constants for the dissociation of $CuL^{10\ 2+}$ in acid solution.

T °C	Ionic Strength M	$[H^+]$ M	k_{obs} s^{-1}
25.0	0.5 ($HClO_4$+$NaClO_4$)	0.001 [g]	0.90
		0.002 [g]	3.50
		0.003 [g]	8.00
		0.004 [g]	13.6
		0.005 [g]	21.0
		0.010 [h]	48.0 [J]
		0.015 [h]	90.0 [J]
		0.020 [h]	148 [J]
		0.025 [h]	190 [J]
		0.030 [h]	225 [J]
		0.035 [h]	252 [J]
		0.040 [h]	265 [J]
		0.045 [h]	277 [J]
		0.050 [h]	290 [J]
		0.070 [i]	310 [J]
		0.090 [i]	330 [J]
		0.110 [i]	365 [J]
		0.250 [i]	430 [J]
		0.050 [g]	287 [J]
25.0	1.0 (HNO_3+$NaNO_3$)	0.005	25.5 [J]
		0.008	55.5 [J]
		0.011	90.0 [J]
		0.013	133 [J]
		0.016	165 [J]
		0.021	210 [J]
		0.026	250 [J]
		0.032	285 [J]
		0.042	325 [J]
		0.053	350 [J]
		0.500	520 [J]

[g] $[CuL^{10\ 2+}] = 1x10^{-4}$;

[h] $[CuL^{10\ 2+}] = 5x10^{-4}$

[i] $[CuL^{10\ 2+}] = 5x10^{-3}$

[J] precision in observed rate constants is within ±5%.

$$ML + 2H^+ \rightleftharpoons MLH_2^{2+} ; \quad K \text{ (fast)} \qquad (1)$$

$$MLH_2^{2+} \longrightarrow \text{products} ; \quad k_{30} \text{ (slow)} \qquad (2)$$

involving a rapid pre-equilibrium protonation (1) and a slow rate-determining step (2). It can be readily shown that

$$k_{obs} = k K [H^+]^2 / (1 + K [H^+]^2) \qquad (3)$$

Under the conditions of the present experiment $K[H]^{+2} << 1$ and $k_{obs} = k_{30}K [H^+]^2$.

High Acidities

At high acidities (0.03 - 0.09 mol^{-1} dm^3), copper 2,2,2-tet is expected to exist as the monoprotonated complex $[Cu(2,2,2\text{-tet}(H))]^{3+}$. At these acidities the copper complex displays initially a linear dependence on $[H^+]$, but at higher hydrogen ion concentrations the reaction becomes independent of $[H^+]$. Values of k_{obs} at various $[H^+]$ for dissociation of $[CuL^{10}]^{2+}$ are summarized in Table 1.16. The kinetic scheme may be considered to be

$$[CuHL^{10}]^{3+} + H^+ \rightleftharpoons [CuH_2L^{10}]^{4+}; \quad K_2 \text{ (fast)} \qquad (4)$$

$$[CuH_2L^{10}]^{4+} \longrightarrow \text{products} ; \quad k_{21} \text{(slow)} \qquad (5)$$

Values of K_2 and k_{21} were obtained by curve fitting (using the Grafit program) of k_{obs} to the function $A [H^+] / (1 + B [H^+])$, derived from equations (4) and (5), giving $K_2 = 81.5$ $mol^{-1}dm^3$ and $k_{21} = 783.8$ s^{-1} at I = 0.5 mol dm^{-3} ($HClO_4$+ $NaClO_4$) and $K_2 = 90.7$ $mol^{-1}dm^3$ and $k_{21} = 850$ s^{-1} at I = 1.0 mol dm^{-3} (HNO_3 + $NaNO_3$) at 25 °C.

Obviously the kinetic behaviour of the copper(II) linear tetraamine complex is similar to that of the copper(II) complexes of macrocycles. The dissociation of $[Ni(2,2,2\text{-tet})]^{2+}$ appears to differ somewhat from that of cyclic tetra- or polyamines.

Acid dissociation of $[Ni(2,2,2\text{-tet})]^{2+}$

The facultative nature of 2,2,2-tet allows the formation of three different octahedral species with nickel (II), α-cis, β-cis, and trans.

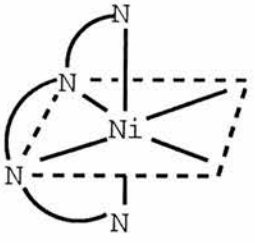

∝− cis

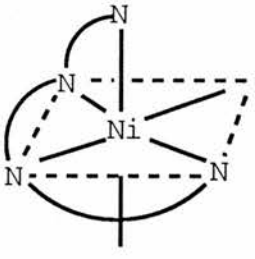

β − cis

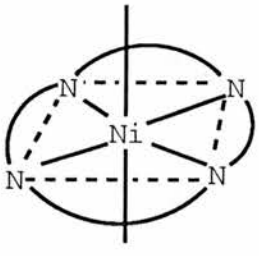

trans

The cis structures are believed to be the more stable in solution at room temperature, but on heating or addition of salt the solution turns brown-yellow and a peak in the visible spectrum at *ca.* 440 nm appears, suggesting that isomerisation to a tetragonal structure is taking place(55).

The dissociation of $[Ni(2,2,2\text{-tet})]^{2+}$ in the acidity range 0.05 - 0.5 mol dm^{-3} $HClO_4$ (or HNO_3) exhibits no specific acid dependence. The dechelation of the four individual Ni-N bond could be detected in the stopped flow measurements. In addition, specific medium effects are observable in these reactions as the dissociation is faster in HNO_3 than in $HClO_4$(Table 1.17).

Table 1.17 Dissociation of $[Ni(2,2,2\text{-tet})]^{2+}$ in perchloric / nitric acid solutions adjusted to I= 0.5 M $NaClO_4$ / 1.0 M $NaNO_3$ at 25 °C .

Wavelength nm	Ni-2,2,2-tet M	Acid [HNO3]	[HClO4]	k^a s^{-1}	k(lit.)[b] s^{-1}
	$[Ni(2,2,2\text{-tet})]^{2+}$			$[Ni(2,2,2\text{-tet})H]^{3+}$	
450	0.01	0.05	-	10.8	
450	0.01	0.14	-	11.7	
450	0.01	0.50	-	11.4	
450	0.005	-	0.05	9.6	16
450	0.005 [c]	-	0.05	9.3	
450	0.005	-	0.25	9.6	
450	0.005 [c]	-	0.25	9.0	
450	0.025	-	0.25	10.0	
	Absorbance decrease				
	$[Ni(2,2,2\text{-tet})H]^{3+}$			$[Ni(2,2,2\text{-tet})H_2]^{4+}$	
550	0.01	0.14	-	8.0	
550	0.01	0.50	-	8.0	
550	0.005	-	0.05	8.2	
550	0.005 [c]	-	0.05	7.7	
550	0.005 [c]	-	0.25	7.5	
550	0.005	-	0.25	8.1	
550	0.025 [c]	-	0.25	8.4	
	Absorbance decrease				
	$[Ni(2,2,2\text{-tet})H_2]^{4+}$			$[Ni(2,2,2\text{-tet})H_3]^{5+}$	
400	0.01	0.05	-	3.30	
400	0.01	0.14	-	3.45	
400	0.01	0.50	-	3.50	4.0
	Absorbance decrease				
	$[Ni(2,2,2\text{-tet})H_2]^{5+}$			$Ni^{2+}(aq)$	
420	0.010	0.14	-	2.45	
420	0.005	-	0.05	0.71	
420	0.005 [c]	-	0.05	0.65	4.0
420	0.005 [c]	-	0.25	0.71	
420	0.005	-	0.25	0.86	
420	0.025 [c]	-	0.25	0.75	
	Absorbance increase				
370	0.01	0.05	-	2.7	
370	0.01	0.14	-	2.6	
370	0.01	0.50	-	2.8	
	Absorbance increase				
650	0.01	0.14	-	2.60	2.2
650	0.01	0.50	-	2.65	
	Absorbance decrease				

[a] Precision in observed rate constant is within ±3.0 %

[b] Ref. 40 ; I = 1M (HNO_3,$NaNO_3$)

[c] $[Ni(2,2,2\text{-tet})]^{2+}$ prepared by mixing stoichiometric amounts of the ligand and metal ion solutions and the pH adjusted to 9 with sodium hydroxide .

The complete dissociation of $[Ni(2,2,2\text{-tet})]^{2+}$ monitored at 420 or 370 nm produces an oscilloscope trace in which at least four stages are apparent, demonstrating the complexity of the reaction. An analysis of these traces at different wavelengths is shown in Table 1.17. Examination of the data in Table 1.17 indicates that the rate constants for the four dechelation steps at a single wavelength, and at different concentrations of HNO_3 are $k_1 = 11.5\ s^{-1}$ (lit. $16\ s^{-1}$) at λ_{450} nm, $k_2 = 8.0$ at λ_{550} nm, $k_3 = 3.5\ s^{-1}$ (lit. $4\ s^{-1}$) at λ_{400} , and $k_4 = 2.5\ s^{-1}$ at λ_{420} nm at 25 °C and I = 1.0 (HNO_3+ $NaNO_3$). These values are the average of the individual values given in Table 1.17.

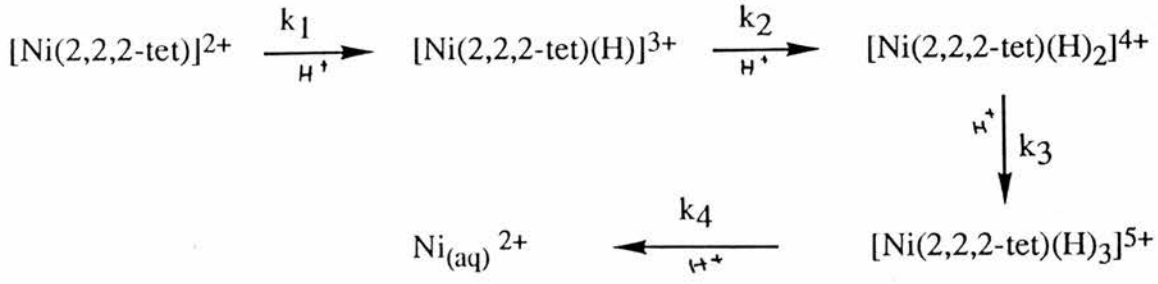

In perchloric acid solutions the rate constants are: $k_1 = 9.6\ s^{-1}$ at λ_{450} nm, $k_2 = 8.0\ s^{-1}$ at λ_{550} nm, and $k_4 = 0.75\ s^{-1}$ at λ_{420} nm, at 25 °C and I = 0.5 ($HClO_4$+ $NaClO_4$) .

Evidence for the existence of mono- and diprotonated species of $Ni(2,2,2\text{-tet})^{2+}$ is available from the equilibrium studies (Chapter 4). It is worth mentioning that the complexity of the dechelation of the $Ni(2,2,2\text{-tet})^{2+}$ species is due to the possibility of concurrent isomerisation pathways. Figure 1.21 shows schematically the possible pathways for the dissociation of α-cis- and β-cis -$[Ni(2,2,2\text{-tet})]^{2+}$ assuming that a primary H_2N-Ni bond is broken first in the ring-opening process(55).

Although there is no direct comparison between the rate of decomposition of the copper(II) and nickel(II) complexes of the linear tetraamine ligand 2,2,2-tet, a lowest second-order rate constant ($1x10^4$ mol $dm^{-3}\ s^{-1}$) for copper(II) with the highest

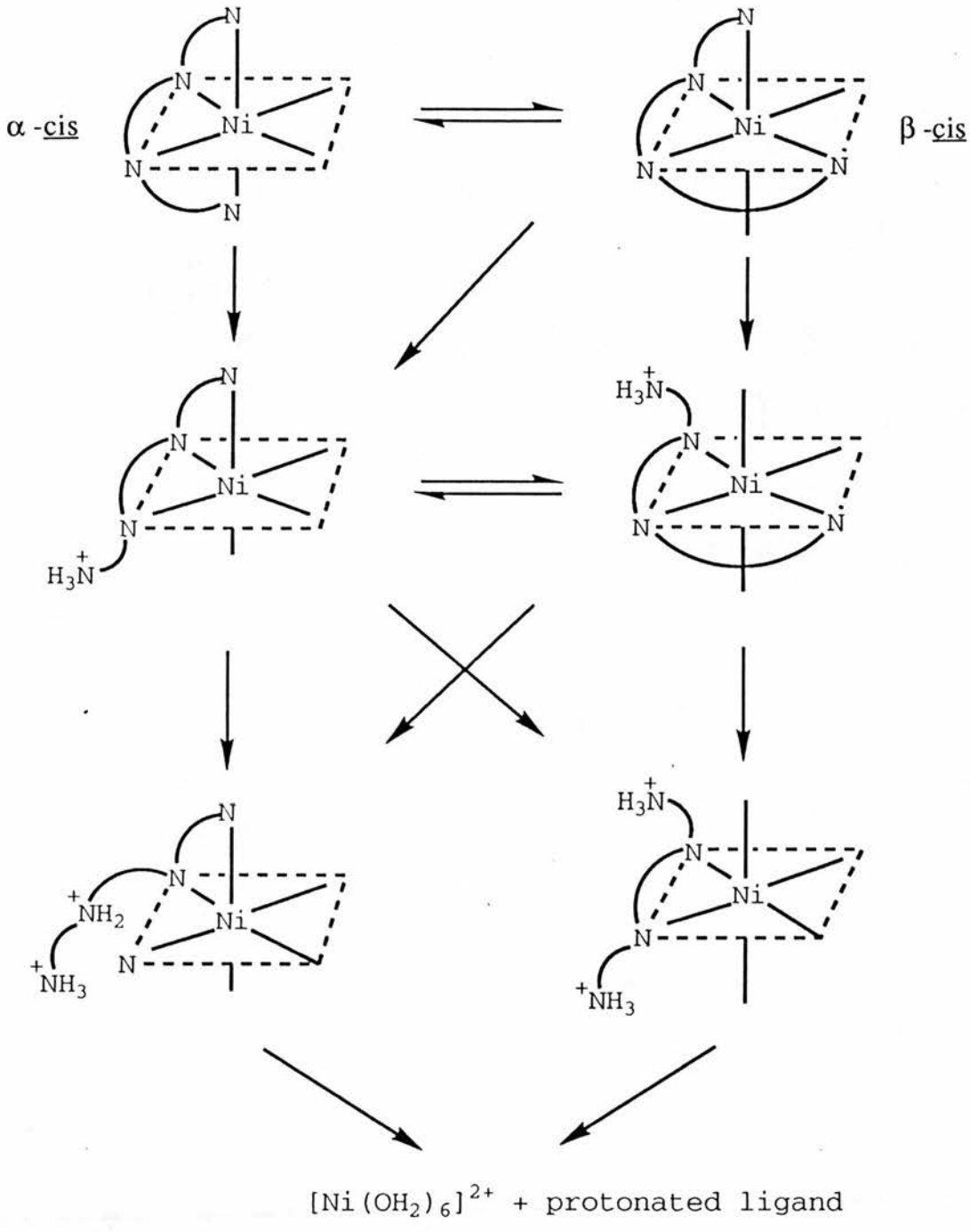

Figure 1.21 Mechanistic scheme for aquation of α -cis and β -cis -$[Ni(2,2,2\text{-tet})(OH_2)_2]^{2+}$.

second-order rate constant value (22.8 mol dm^{-3} s^{-1})[2] for nickel(II), shows that [Cu(2,2,2-tet] $^{2+}$ dissociates some 400 times faster than [Ni(2,2,2-tet)]$^{2+}$ in acidic solution.

[2]calculated for the reaction in 0.5M HNO_3. Value of $k_H = k_{obs}/[H^+]$.

1.7 General Discussion

The kinetic behaviour of the CuL^2, NiL^2, $CuL^{3\ 2+}$, $CuL^{4\ 2+}$, $CuL^{5\ 2+}$, $CuL^{6\ 2+}$, $NiL^{8\ 2+}$, $CuL^{9\ 2+}$, and $CuL^{10\ 2+}$ (at high acidities) can be accounted for by the mechanism (charges omitted)

$$ML + H \rightleftharpoons MHL ; \quad K \text{ (fast)}$$

$$MHL \longrightarrow \text{product} ; \quad k \text{ (slow)}$$

$(M = Cu^{2+}, Ni^{2+})$

in which there is a rapid pre-equilibrium protonation step and a slow dissociation step. For these complexes there is a clear evidence that a species such as $CuHL^{3+}$ is formed in significant concentrations. There is an "absorbance jump" upon mixing solutions of ML^{2+} and H^+. The magnitude of the jump increases with increasing $[H^+]$ (such behaviour is not observed in the system $CuL^{4\ 2+}$ due to manual mixing of the reactants). The slower reaction corresponds to the decomposition of the MHL^{3+} species. Species of the type MHL^{3+} ($M = Cu^{2+}$ or Ni^{2+}) have often been reported in potentiometric studies of copper(II) and nickel(II) complexes, and the values observed for the formation constants show a strong dependence on the distance that the protonated nitrogen can be removed from the metal centre[63]. At very low hydrogen ion concentrations, the kinetic behaviour of the $CuL^{8\ 2+}$, $NiL^{8\ 2+}$, and $CuL^{10\ 2+}$ can be rationalised by the mechanism

$$ML^{2+} + H^+ \rightleftharpoons MHL^{3+} ; \quad K_1 \text{ (fast)}$$

$$MHL^{3+} + H^+ \rightleftharpoons M(H_2L)^{4+} ; \quad K_2 \text{ (fast)}$$

$$M(H_2L)^{4+} \longrightarrow \text{product s} ; \quad k \text{ (slow)}$$

in which there are two rapid pre-equilibrium protonation steps and a slow dissociation step.

Mechanism of Acid Catalysed Dissociation

A general mechanism for the acid catalysed dissociation of polyamine complexes has been proposed[7] and can be adapted for macrocycle complexes (Scheme I). In this scheme, the equilibria (2) ⟶ (3), (3) ⟶ (4), (4) ⟶ (5), and (5) ⟶ (6) are all rapid and never become rate-determining.

In species (3) and (5), the metal-nitrogen bonds have completely broken, and the nitrogens are some distance away from the metal centre. Protonation of the unbound nitrogen in (3) and (5), under the experimental conditions used in this work, should be rapid and therefore (3) ⟶ (4) and (5) ⟶ (6) are rapid equilibria. The acid independent pathway involves the steps (2) ⟶ (3) ⟶ (4) ⟶ (5) ⟶ (6) ⟶ products, with k_{10} as the rate-determining step. All complexes will display such a pathway but as the acid promoted step is much faster, it is only in special circumstances that the acid independent pathway is observed. The acid-dependent pathway involves the path (2) ⟶ (4) ⟶ (6) ⟶ products. Protonation of the partly bound nitrogen in (2) is difficult and the difficulty is reflected both in the slow rates for the protonation reaction k_H (Table 1.8), compared with unbound nitrogen, and the small values of the equilibrium constants K_{MHL}(Table 1.6).These constants are ($dm^3\ mol^{-1}$): $K_{CuHL}{}^2 = 134$, $K_{CuHL}{}^3 = 3$, $K_{CuHL}{}^4 = 0.3$, $K_{CuHL}{}^5 = 9$, $K_{CuHL}{}^{10} = 90$, $K_{NiHL}{}^2 = 62$ and $K_{NiHL}{}^8 = 2$ at 25 °C. The values are very similar to those reported for copper(II) complexes of triazamacrocyles[8] and copper(II) and nickel(II) complexes of trans[14]diene [10, 20], where K_{MHL} falls in the range 0.1 - 10 $mol^{-1}\ dm^3$ at 25 °C. Three interesting points may be extracted from the equilibrium constants. First, the constant $K_{CuL}{}^2 = 134$ $mol^{-1}\ dm^3$ (L^2 = dioxocyclam) is substantially larger compared with other equilibrium constants which suggests that the fast pre-equilibrium protonation step occurs on the

amide oxygen to give the iminol tautomer, followed by intramolecular proton transfer to the nitrogen donors. The same argument can be applied to the Ni dioxocyclam complex (K_{NiL}^2 = 62 mol^{-1} dm^3). Second, the equilibrium constant for the [Cu([16]aneN$_4$)] $^{2+}$ complex, containing a 6,6,6,6 sequence of chelate ring is some 30 times greater than for the [Cu([15]aneN$_4$)]$^{2+}$ complex, with a 5,6,6,6 sequence of chelate rings. This result suggests that the protonated nitrogen is initially at a larger distance from the metal centre in [Cu([16]aneN$_4$)]$^{2+}$ than in [Cu([15]aneN$_4$)]$^{2+}$. The equilibrium results (Chapter 4) supports the kinetic results. The copper complex of [16]aneN$_4$ has K_{CuHL} = 10^6, whereas the copper complex of [15]aneN$_4$ has K_{CuHL} value of 10^2. In Cu[16]aneN$_4^{2+}$ the protonated nitrogen is far enough removed from the metal centre to stabilize the $CuHL^{3+}$ species. The third point concerns K_{CuHL} of the flexible open chain tetraamine, 2,2,2-tet, (K_{CuHL}^{10} = 90 $mol^{-1}dm^3$). This relatively large value suggests that the nitrogen is much further away from copper than in the cyclic polyamines and hence it is easier to stabilize the intermediate protonated species. At high acid concentrations the decomposition of the MHL^{3+} becomes rate determining and the rate constants correspond to k_{21} (Scheme I).

The copper(II) and nickel(II) complexes of the 18-membered sexadentate ligand (L^8) and the copper(II) complex of the linear tetraamine (L^{10}) display 'acid-limiting' kinetics at high [H^+] and second-order kinetics at very low [H^+]. The latter behaviour is indicative of the involvement of two protons in the transition state of the reaction. These reactions can be accommodated within a kinetic scheme in which the dissociation reaction of the diprotonated species, formed in successive rapid protonation equilibria, is rate-determining. The reaction rate is given by the expression:

$$\text{Rate} = k_{30} K_1 K_2 [M(L)] [H^+]^2 / (1+K_1 [H^+] + K_1K_2 [H^+]^2)$$

where K_1 and K_2 are the equilibrium constants for the first and second protonation reactions and k_{30} is the rate constant for dissociation of the diprotonated species

(Scheme I). If the protonation constants are small, so that $(1+K_1[H^+] + K_1K_2[H^+]^2)$ = 1, then the expression simplifies to

$$\text{Rate} = k_{30} K_1K_2 [M(L)] [H^+]^2$$

Alternatively, the results are compatible with a scheme in which the protonation reaction of the monoprotonated species, rate constant k_{21}, is rate-determining, (Section 1.5), which reduces to the same form if the protonation equilibrium constant, K_1, is small.

A second-order dependence of reaction rate on $[H^+]$ has been observed for complexes of copper(II) with a homologous series of penta-aza macrocycles of varying ring size, for the nickel complexes of [15]aneN$_5$[14, 15], and for the copper(II) and nickel(II) complexes of dioxocyclam.

The rate constants from the linear approximation of $k_{obs} / [H^+]$ at low hydrogen ion concentrations, for 14-, 15-, 16-, and 18-membered ring macrocycles together with the linear tetraamine 2,2,2-tet are given in Table 1.8. Dissociation of the 14-membered ring macrocycles is very slow which is indicative of the good fit of the metal ion to the 'hole size' of the ligand. The ideal metal-nitrogen bond length for the saturated 14-membered N_4 ring is 2.07 A[64] and this value corresponds closely to the 'normal' Cu-N bond distance of *ca.* 2.0 A. Comparison of the k_H constants obtained in this and earlier work reveals a correlation between the values of k_H and the size of the tetra-aza macrocyclic ring. Thus the rate increases in the macrocyclic ring size order [14]aneN$_4$ < [15]aneN$_4$ < [17]aneN$_4$9 < [16]aneN$_4$8 < [16]aneN$_4$. If the size of the chelate ring is considered, then the rate increases in the order 5,5,6,6 < 5,6,6,6 < 5,5,6,9 < 5,5,6,8 < 6,6,6,6. Five-membered chelate rings slow down the dissociation rate. This situation is similar to that observed for the copper(II) complexes of 15 - 17 membered N_5-macrocycles[70].

The thermodynamic results (logβ (Cu cyclam) = 28.4; log β (Cu[15]aneN$_4$) = 24.5; log β (Cu[16]aneN$_4$) = 20.0) and the enthalpies of activation (Table 1.7) support the above conclusions. Comparison in terms of chelate size among linear

tetraamines show no correlations between the chelate ring sizes and the rates of Cu-N bond breaking (compare $k_H = 1x10^4$ mol^{-1} dm^3 s^{-1} for (Cu-2,2,2-tet) (5,5,5 chelate) and $k_H = 0.67$ mol^{-1} dm^3 s^{-1} for (Cu-2,3,2-tet) (5,6,5 chelates)). The differences in the rate constants are presumably caused by quite subtle structural and conformational effects within the complex which affect the strength of the Cu-N bond and/or the ease with which the nitrogen is able to rotate away from the metal ion.

Studies with the pendent arm ligands show that the rate of dissociation is dependent on the nature of the arm. When the arms possess weakly coordinating donor groups, the rate of dissociation increases. Based on k_H, values the rate of dissociation increases in the order CuTHEC < CuTHPC < CuTCHC. This behaviour may be explained in terms of stabilization of the intermediate species formed after protonation of a ring nitrogen by molecular rearrangement in which two nitrogens and two pendent donors bond to copper (II).

The complex CuL^9 reacts similarly to the copper complexes of pendent arm macrocycles(10) and small macrocycles (20). The complexes display a first order dependence on $[H^+]$ with a positive intercept at $[H^+] = 0$. The positive intercept is a measure of the non-catalysed solvolytic displacement of the ligand. The activation parameters for the CuL^9 closely resemble those for the copper(II) complexes of triazamacrocycles(7). The increased reactivity of this complex ($k_H = 40$ mol^{-1} dm^3 s^{-1}) is due to the substitution of weaker oxygen donors for the nitrogens.

The reactivities of the various copper(II) complexes in acid solution are

$$\underset{1x10^4}{\text{Cu-(2,2,2-tet)}^{2+}} > \underset{486}{\text{Cu-dioxocyclam}} > \underset{58}{\text{Cu-hexacyclen}^{2+}} > \underset{40}{CuL^9} >$$

$$\underset{22.5}{\text{Cu-TCHC}^{2+}} > \underset{12}{\text{Cu-THPC}^{2+}} > \underset{3.4}{\text{Cu-THEC}^{2+}} > \underset{2.6}{\text{Cu-[16]aneN}_4} >$$

$$\underset{1.1}{\text{Cu[16]aneN}_48} > \underset{0.67}{\text{Cu(2,3,2-tet)}^{2+}} \sim \underset{0.6}{\text{Cu[17]aneN}_49} > \underset{0.004}{\text{Cu[15]aneN}_4} >$$

Red $Cu\text{-teta}^{2+}$ ~ Cu-cyclam.
$6x10^{-8}$

The rates for the nickel(II) complexes of the macrocycles [14]aneN$_4$, [15]aneN$_4$, and [16]aneN$_4$ indicate that there is a clear dependence of dissociation rate on ring size. The rate constants (k_H; Table 1.7) show a progressive increase as the macrocyclic ring size increases from 14- to 16-membered. Hole size considerations suggest that the 14-membered macrocycle provides the best fit for nickel(II). Again, the high reactivity of the nickel(II) complex of hexacyclen can perhaps be rationalised in terms of structural and conformational effects within the complex (due to flexibility of the ligand), which affect the strength of the M-N bond and/or the ease by which the nitrogen is able to rotate away from the metal ion. The reactivity of the various nickel(II) complexes against acid follows the order :

$$\underset{85}{\text{Ni-dioxocyclam}^{2+}} \sim \underset{85}{\text{Ni-hexacyclen (fast step)}} > \underset{10.5}{\text{Ni-hexacyclen (slow step)}} >$$

$$\underset{5}{\text{Ni-(2,2,2-tet)}} > \underset{0.6}{\text{Ni-[16]aneN}_4} > \underset{2\times10^{-4}}{\text{Ni[15]aneN}_4} > \underset{9\times10^{-6}}{\text{Ni(trans-Me}_6\text{[15]diene)}} >$$

$$\underset{7\times10^{-10}}{\text{Ni-cyclam}}$$

The reactions of the nickel complexes are much slower than those of the copper complexes. The only instance where direct comparison between the copper(II) and nickel(II) systems is possible is with the ligands dioxocyclam and hexacyclen. The copper reactions are faster due to a very much more favourable enthalpy of activation counterbalanced by a more negative entropy of activation. Copper(II) hexacyclen exists in solution as five-coordinate species. Jahn-Teller distortions make the axial nitrogen easier to protonate than in the nickel complex, which is six-coordinate in solution. The greater reactivity of the copper complex compared with the nickel complex can be attributed in part to this structural difference.

1.8 References

1. D.K. Cabbiness and D.W. Margerum, *J. Am. Chem. Soc.*, **91**, 6540 (1969). D.K. Cabbiness and D.W. Margerum, *J. Am. Chem. Soc.*,**92**, 2151 (1970).

2. M. Kodama and E. Kimura, *J. Chem. Soc. Dalton Trans.*, 2341 (1976).

3. F.P. Hinz and D.W. Margerum, *Inorg. Chem.*, **13**, 2941 (1974).

4. L. Fabbrizzi, P. Paoletti and R.M. Clay, *Inorg. Chem.*,**17**, 1042 (1978).

5. R.M. Clay, M. Micheloni, P. Paoletti and W.V. Steele, *J. Am. Chem. Soc.*,**101**, 4119 (1979).

6. R.M. Izatta, J.S. Bradshaw, S.A. Nielson, J.D. Lamb, J.J. Christensen, *Chem. Rev.*, **85**, 271 (1985).

7. D.W. Margerum, G.R. Caley, D.C. Weatherburn, G.K. Pagenkopf, ACS in Coordination Chemistry, ACS Monograph 174; American Chemical Society, Washington DC, 1978; vol. 2 pp 1-200. Monogr. 1978, 1-200.

8. P.G. Graham, D.C. Weatherburn, *Aust. J. Chem.*, **34**, 291 (1981). L.J. Murphy and L.J. Zompa, *J. Inorg. Chem.*, **18**, 3278 (1979).

9. R.W. Hay; M.P. Pujari, *Inorg. Chim. Acta,* **100**, L1 (1985).

10. R.W. Hay; R. Bembi, *Inorg. Chim. Acta.*, **65**, L227 (1982).

11. E.J. Billo, *Inorg. Chem.*, **23**, 236 (1984).

12. R.W. Hay; R. Bembi; B. Jeragh, *Transition Met. Chem. (Weinheim, Ger.)* **11**, 385 (1986).

13. B.F. Liang; C.S. Chung, *Inorg. Chem.*, **22**, 1017 (1983).

14. R.W. Hay; M.P. Pujari; F. Mclaren, *Inorg Chem.*, **23**, 3033 (1984).

15. R.W. Hay; R. Bembi; T. Moodie, P.R. Norman, *J. Chem. Soc. Dalton Trans.*, 2131 (1982).

16. R.W. Hay; R. Bembi; F. Mclaren; W.T. Moodie, *Inorg. Chim. Acta,* **85**, 23 (1984).

17. R.W. Hay; R. Bembi, *Inorg. Chim. Acta,* **62**, 89 (1982).

18. R. Bembi; R.S. Bhardwarj; R. Singh; K. Taneja; S. Aftab, *Inorg. Chem.*, **23**, 4153 (1984).

19. S. Siddiqui; R.E. Shepherd, *Inorg. Chem.*, **22**, 3726 (1983).

20. N.F. Curtis; S.R. Osvath, *Inorg. Chem.*, **27**, 305 (1988).

21. D.H. Busch, *Acc. Chem. Res.*, 392 (1977).

22. F. Wagner; K.E. Barefield, *Inorg. Chem.*, **15**, 408 (1976).

23 *Inorganic Syn.* **16**, 220 (1976).

24a. J.E. Richman and T.J. Aitkins, *J. Am. Chem. Soc.*,**96**, 2268 (1974).

24b. W.L. Smith and K.N. Raymond, *Inorg. Syn.*, **20**, 109 (1980).

25. T.J. Aitkins, J.E. Richman and W.F. Oettle, *Org. Synth.*, **58**, 86 (1979).

26. L.F. Fieser and M. Fiesser, in "Reagents for Organic Synthesis" vol. 1, p. 1179 *(John Wiley: New York 1967).*

27. G.H. Searle and M.E. Angley, *Inorg. Chim Acta,* **49**, 185 (1981).

28. P.G. Graham and D.C. Weatherburn, *Aust. J. Chem.*, **36**, 2349 (1983).

29. A. Bencini, L. Fabbrizzi and A. Poggi, *Inorg. Chem.*, **20**, 2544 (1981).

30. P.G. Graham and D.C. Weatherburn, *Aust. J. Chem.*, **34**, 291 (1981). P.G. Graham and D.C. Weatherburn, *Aust. J. Chem.*, **37**, 2243 (1984).

31. R.W. Hay and M.T.H. Tarafdar, *J. Chem. Soc. Dalton Trans.*, 823 (1991).

32. N.F. Curtis, *J. Chem. Soc.*, 2644 (1964).

33. R.W. Hay, G.A. Lawrance and N.F. Curtis, *J. Chem. Soc.*, Perkin Trans. **1**, 591 (1975).

34. R.W. Hay, M.A. Ali and B. Jeragh, *J. Chem. Soc. Dalton Trans,* 2763 (1988).

35. I. Tabushi, Y. Taniguchi and H. Kato, *Tetrahedron Letters,* 1049 (1977).

36. R.W. Hay and P.R. Norman, *Transition Met. Chem (Weinheim. Ger.)* **5**, 232 (1980).

37. R.W. Hay, M.P. Pujari and F. Mclaren, *J. Inorg. Chem.*, **23**, 3033 (1984).

38. R.W. Hay and C.R. Clark, *J. Chem. Soc. Dalton Trans,* 1148 (1977).

39. B. Liang and C. Chung, *Inorg. Chem.*, **20**, 2152 (1981).

40. G.A. Melson and R.G. Wilkins, *J. Chem. Soc.* 2662 (1963).

41. D.K. Cabbiness and D.W. Margerum, *J. Am. Chem. Soc.*, **92**, 2151 (1970).

42. K.R. Morgan, G.J. Gainsford, N.F. Curtis, *Aust. J. Chem.*, **36**, 1341 (1983).

43. N.F. Curtis, *Aust.. J. Chem.*, **39, 239** (1986).

44. D. Busch, *Acc. Chem. Res.* 392 (1977).

45. G.A. Melson and R.G. Wilkins, *J. Amer.Chem. Soc.*, **103**, 3041 (1981).

46. J.D. Viteillo and E.J. Billo, *Inorg. Chem.*,**14**, 3477 (1980).

47. R.M. Clay; P. Murray-Rust; J. Murray-Rust, *J. Chem. Soc. Dalton Trans.*, 1135 (1979).

48. L.F. Lindoy and R.J. Smith, *J. Inorg. Chem.*, **20**, 1314 (1981).

49. B.F. Liang, D.A. Margerum and C.S. Chung, *J. Inorg. Chem.*,**18**, 2001 (1979).

50. P.O. Whimp; M.F. bailry; N.F. Curtis, *J. Chem. Soc.* A, 1956 (1970).

51. B.F. Liang and C.S. Chung, *J. Inorg. Chem.*, **20**, 2152 (1981).

52. M. Mitewa, P.R. Bontchev, K. Kabassanov, D. Vassileva, E. Zhecheva and D. Mechandzziev, *J. Coord. Chem.*, **17**, 287 (1988).

53. A. Bencini, L. Fabbrizzi and A. Poggi, *Inorg. Chem.***20**, 2544 (1981).

54. R.W. Hay, B. Jeragh, S.F. Lincoln and G.H. Searle, *Inorg. Nucl. Chem. Lett.*, **14**, 435 (1978).

55. T.J. Kemp, P. Moore and G.R. Quick, *J. Chem. Soc. Dalton Trans,* 1377 (1979).

56. L.L. Diaddario, L.L. Zimmer, T.E. Jones, L.S.W.L. Sokol, R.B. Cruz, L.E. Yee, L.A. Ochrymowycz and D.B. Rorabacher, *J. Amer. Chem. Soc,* **101**, 3511 (1979).

57. A. Ekstrom; L.F. Lindoy; R.J. Smith, *Inorg. Chem.*, **19**, 724 (1980).

58. This work.

59. R.W. Hay, N.P. Pujari, T.M.S. Craig, D.T. Richens, A. Perotti and L. Ungaretti, *J. Chem Soc. Dalton Trans.*, 2605 (1987).

60. V.J. Thom; J.C.A. Boynes; G.J. McDougall, R.D. Hancock, *J. Am. Chem. Soc.*, **106**, 3198 (1984).

61. P. Clark, A.M. Hounslow, R.A. Keough, S.F. Lincoln and K.P. Wainwright, *J. Inorg. Chem.*, **29**, 1793 (1990).

62. P. Clark, S.F. Lincoln and K.P. Wainwright, *J. Inorg. Chem.*, **30**, 134 (1991).

63. M.Gold, H.K.J. Powell, *J. Chem. Soc. Dalton Trans.*, 230 (1976).

64. L.Y. Martin, L.J. De Hayes, L.J. Zampa and D.H. Busch, *J. Am. Chem. Soc.*, **96**, 4046 (1974).

65. N.a.Baily, D.E.Fenton, S.J.Kitchen, P.A.Tasker and G.G.Williams, *J, Chem. Soc. , Chem. Comm.* ,1575(1988) .

66. N.F. Curtis and D.A.House, *J. Chem. Soc.*, 6195(1965)

67. M.Mitewa, P.R.Bontchev, D.Vassileva, E.Zhecheva, D.Mechandjiev and K.Kbassanov, *Inorg.Chim. Acta.*, **134**, 17 (1987).

68. M. Mitewa, P.R. Bontchev, G.Gencheva, E. Zhecheva, and K. Kabassanov, *Inorg.Chim. Acta.*, **137**, 170 (1990).

CHAPTER 2

Formation Kinetics for the Reaction of Macrocyclic Tetra-aza Ligands With Hydroxycuprate (II) Species.

2.1 Introduction

The enhanced stability of metal complexes formed with macrocyclic ligands compared with those formed with analogous open-chain species has been termed the "macrocyclic effect" (Chapter1) and has sparked much interest in the study of macrocyclic complexes. Thermodynamic studies indicate that the stability constant differences arise primarily from two effects: (i) the diminished flexibility of free macrocyclic ligands, resulting in a less negative entropy term upon complexation(1) and, (ii) in the case of ligands with hydrogen-bonding donor atoms in protolytic solvents, the diminished solvation of the free macrocyclic ligands relative to their open-chain counterparts, resulting in a more favourable enthalpy term upon complexation(2).

Macrocyclic Kinetic Effects:

For simple ligands, the loss of solvent molecules from the primary solvation shell of the metal cation play a key role in the kinetics and mechanism of the formation reaction. As the ligand becomes more complex (for example macrocycles and cryptands) conformational changes within the ligand become of increasing importance. Such reactions can be represented by the general scheme, where $M(MAC)^{n+}(b)$ is the final product of the reaction.

$$M_{(aq)}^{n+} + MAC \underset{\text{outer sphere complex}}{\overset{K_{os}}{\rightleftharpoons}} M_{(aq)}^{n+}.MAC \qquad \text{(pre-association)}$$

$$M_{(aq)}^{n+}.MAC \xrightarrow{k_{ex}} M(MAC)^{n+}\ (a) \qquad \text{(interchange step)}$$

$$M(MAC)^{n+}\ (a) \longrightarrow M(MAC)^{n+}\ (b) \qquad \text{(conformational change)}$$

A mechanism of this type has been termed a 'dissociative interchange" or I_d process. Initially, complexation involves the rapid formation of an 'outer-sphere' complex (of ion-ion or ion-dipole nature), which is characterised by the equilibrium constant K_{os}. The second step is the conversion of the outer-sphere complex to an inner-sphere

complex, which is characterised by the first-order rate constant, k_{ex}, whose value varies widely from one metal to the next. For such a mechanism, the overall second-order formation rate constant is given by the product of the first-order constant k_{ex} and the equilibrium constant K_{os} which may be determined experimentally, or estimated from various equations(3). The solvent exchange rates (k_{ex}) are useful for estimating the rates of formation of complexes of simple monodentate ligands, but the situation for macrocyclic and other polydentate ligands is not straightforward. Chelate ring formation may be rate-limiting for polydentate (and especially macrocyclic) complexes. Further, the rates of formation of macrocyclic complexes are sometimes slower than those for related open-chain polydentate ligands. The additional steric constraints within the cyclic ligand case may restrict the mechanistic pathways available compared with the open-chain case and may even alter the position of the rate-determining step. Indeed, the rate-determining step is not necessarily restricted to the formation of the first or second metal-macrocycle bond but may occur later in the coordination sequence.

The early kinetic studies on the reaction of copper(II) with tetra-azamacrocyclic ligands were conducted at relatively low pH to prevent the formation of hydroxo complexes. As a result, specific rate constants were obtained only for the reaction of the mono- and di-protonated species (4) of the ligand with the metal ion (due to the strongly basic character of the ligand nitrogens). Interpretation of this kinetic data is complicated by electrostatic interactions between the positively charged metal ions and the positively charged protonated ligand. In addition, the pronounced tendency of the protonated macrocycle to form intramolecular hydrogen bonds and intermolecular hydrogen bonds with the solvent, may shift the conformational equilibria toward unreactive "endo" conformers[1].

---

[1]The terms exo and endo relative to macrocyclic conformers are used to indicate whether the lone electron pairs on the ligand donor atoms are oriented away from or towards the central cavity, respectively (5).

Recent work has focused on the formation and isomerisation reactions of Cu(II) with cyclic tetramines in strongly basic media to circumvent some of the problems arising due to ligand protonation. Under these conditions the copper is present as a mixture of soluble hydroxo species, and the ligand is essentially unprotonated(6). Previous work has shown that alkyl substitution on the nitrogen donors has a significant effect on the rate of complexation . Open-chain and cyclic ligands react at similar rates (factor of *ca* 10). It was also found that methyl substitution at the carbon atoms of cyclam (L^1; Figure 2.1) caused significant decreases in the formation rate. The major effect of ligand cyclization appeared to be to shift the rate-determining step for the complexation reaction from the rearrangement following first bond formation to second bond formation as the reactant goes from $Cu(OH)_3^-$ to $Cu(OH)_4^{2-}$ (7). Chung and coworkers have studied the formation reaction of Cu(II) with tet b (L^4; Figure 2.1) in basic solution and have found that the high degree of alkyl substitution appears to shift the rate-determining step of the formation reaction to second-bond formation for both the $Cu(OH)_3^-$ and $Cu(OH)_4^{2-}$ species(8).

Taylor *et al* (6) have studied the complex formation kinetics of copper(II) with Me_4trien, Me_6trien, (N-Me)$_4$Cyclam and the 1,4,7,10-tetra-aza-13,18,-dioxobicyclo[8.5.5]eicosane (cryptand $2_N.1_O.1_O$) in strongly basic media.

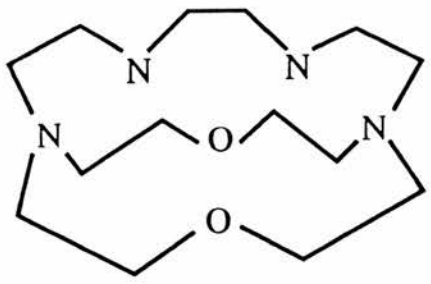

$2_N.1_O.1_O$

Taylor found that :

(1) All ligands (except (N-Me)$_4$cyclam) react with both $Cu(OH)_3^-$ and $Cu(OH)_4^{2-}$, and for a given ligand, $Cu(OH)_3^-$ is 10 to > 300 times more reactive than $Cu(OH)_4^{2-}$.

(2) For Me$_4$trien reacting with either $Cu(OH)_3^-$ or $Cu(OH)_4^{2-}$ and Me$_6$trien reacting with $Cu(OH)_3^-$, the rate determining step is proposed to be Jahn-Teller inversion after formation of the first Cu(II)-nitrogen bond.

(3) The rate-determining step appears to shift to second-bond formation for the reaction of Me$_6$trien with $Cu(OH)_4^{2-}$.

(4) For the cyclic ligands, (N-Me)$_4$ cyclam and $2_N.1_O.1_O$, second-bond formation or multiple desolvation is proposed as the rate-determining step for the reactions with $Cu(OH)_3^-$ and $Cu(OH)_4^{2-}$

The present investigation was undertaken with a four main aims, (1) to study the steric effects resulting from alkyl substitution on the macrocyclic ring, (2) to study the effects of N-substitution on complexation rates, and (3) to study the effect of ring size on the rate of complex formation. Dioxocyclam dissociates readily from copper(II) and nickel(II) (Chapter 1) and formation rate studies were carried out to see if similar effects were observable in the formation kinetics.

The ligands studied include the 14-, 15-, and 16-membered macrocyclic tetraamines, 1,4,8,11-tetra-azacyclotetradecane (cyclam); C-meso-5, 12-dimethyl-1,4,8,11-tetra-azacyclotetradecane (Me$_2$cyclam; C-meso- and C-rac-5,7,7,12,14,14-hexamethyl-1,4,8,11-tetraazacyclotetradecane (tet a and tet b respectively); 1,4,8,12-tetra-azacyclopentadecane ([15]aneN$_4$); 1,5,9,13-tetra-azacyclohexadecane ([16]aneN$_4$) and N, N', N'', N'''-tetra(2-hydroxy-propyl)-1,4,8,11-tetra-azacyclotetradecane (THPC); and the diamide ligand 5,7-dioxo-1,4,8,11-tetra-azacyclotetradecane (dioxocyclam). The structures of these compounds are given in Figure 2.1.

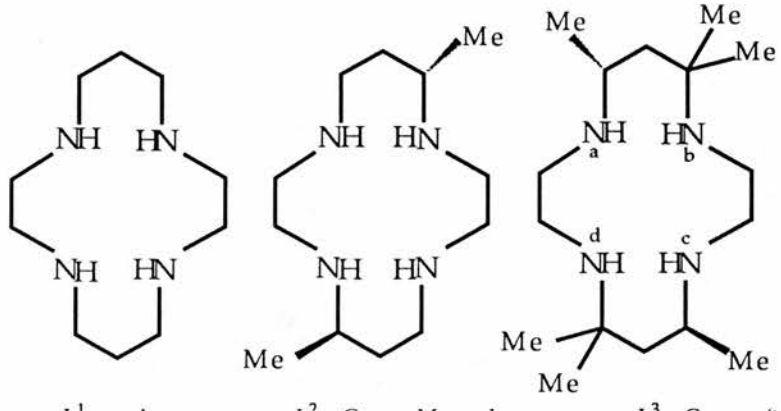

L^1 = cyclam L^2 = C-mesoMe$_2$cyclam L^3 = C-meso (tet a)

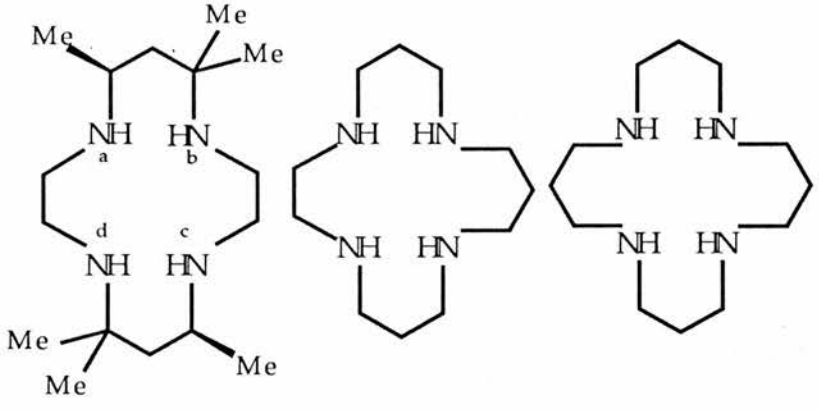

L^4= C-rac(tet b) L^5= [15]aneN$_4$ L^6= [16]aneN$_4$

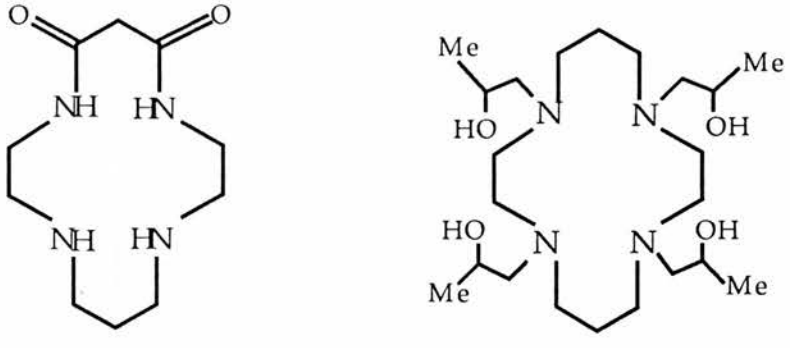

L^7= dioxocyclam L^8= THPC

Figure 2.1 Nitrogen macrocycles used in this study.

2.2 Experimental:

The ligand Me_2cyclam was prepared from the 5,12-dimethyl-1,4,8,11 tetra-azacyclotetradeca-4,11-diene (Me_2[14]diene) by $NaBH_4$ reduction. The dihydroperchlorate salt of Me_2[14]diene was prepared[9] by adding $HClO_4$ (72%, 124.5 cm^3, 1.5 mol) dropwise to a cooled 10% methanolic solution of 1,2-diaminoethane (1000 cm^3 methanol, 100.5 cm^3 1,2-diaminoethane, 1.5 mol). The reaction mixture was cooled to -10° in an ice-salt bath and methyl vinyl ketone (121.5 cm^3, 1.5 mol) in methanol (120 cm^3) added dropwise. When the addition was complete, stirring was continued for 2 hours during which time the white product formed. The mixture was stored in a freezer for *ca.* 1 day. The solid product was filtered off and washed thoroughly with methanol then diethyl ether. The ligand C-meso-Me_2cyclam was prepared as follows[9]. The dihydroperchlorate salt of the diene (50 g) was dissolved in methanol-water (1:1 v/v, 250 cm^3) and $NaBH_4$ (10 g, excess) added in small amounts (*ca.* 0.2 g) with magnetic stirring over a period of *ca.* 1 h. The resulting solution was heated on a water-bath for about 1 h until evolution of H_2 ceased. The methanol was removed on a rotary evaporator and sodium hydroxide solution added to bring the pH ~14. The aqueous solution was then continuously extracted with benzene. The benzene extract was dried (Mg_2SO_4), and after the evaporation of benzene a yellow oil was obtained. This is predominantly the C-meso diastereoisomer and was purified by recrystallisation from xylene. The C-meso isomer had m.p. 143-145°C (lit 144-145°) [9] (Found: C, 62.8; H, 12.5; N, 24.5; Calc. for $C_{12}H_{28}N_4$: C, 63.1; H, 12.35; N, 24.5%). The synthesis and analytical data for the other ligands is given in Chapter 1.

Reagents:

All ligand stock solutions were standardised potentiometrically against standard copper(II) nitrate solution using a Cu-selective electrode (Russell ISE94-4299/57) as indicator electrode and a calomel electrode as reference electrode. The titration was carried out in the presence of an ammonia buffer pH 10. This technique, Figure 2.2 provides a very useful method for the standardization of macrocyclic ligand stock solutions.

Copper(II) perchlorate hexahydrate was recrystallised twice from water and standardised potentiometrically against EDTA (A.R, Aldrich) using a copper electrode and calomel reference.

Sodium perchlorate was recrystallised from water before use. The stock solution of sodium hydroxide (Ampoules, BDH) was standardised potentiometrically against weighed amounts of potassium hydrogen phthalate and was stored in a Nalgene Teflon bottle.

Kinetic Measurements

All reactions were studied using the stopped-flow technique. A Union Giken RA-401 stopped-flow spectrophotometer was used to determine the experimental rate constants by a linear least-squares fit of the data (further details about the instrumentation is given in Appendix 1; and Section 1.2.2). The temperature was maintained at 25.0 $^{o} \pm 0.1$ ^{o}C for all systems. Figure 2.3 shows the individual spectrum of the hydroxy cuprate(II) species(a), the unprotonated THPC(b), and a mixture of the two(c).

Reaction Conditions

Reaction conditions are summarised in Table 2.1. All the metal and the ligand solutions were freshly prepared and used immediately in the measurements. The kinetic

Table 2.1. Summary of experimental conditions used for Cu(II) reacting with macrocycles in basic solution at 25°C and I = 1.0 mol dm^{-3} ($NaClO_4$ + NaOH) (unless otherwise stated).

System	λ_{max} nm	$[Cu^{2+}]$ mol dm^{-3}	[Ligand] mol dm^{-3}	$[OH^-]$ mol dm^{-3}	Method of reactant solutions preparation
$Cu(OH)_n^{n-2}$ vs Cyclam	260	$1.5x10^{-5}$	$(15\text{-}50)x10^{-5}$	0.075-0.43	method 1[a]
$Cu(OH)_n^{n-2}$ vs C-mesoMe$_2$cyclam	270	$(7.5\text{-}9)x10^{-6}$	$(9\text{-}40)x10^{-5}$	0.05-0.4	method 2[b]
$Cu(OH)_n^{n-2}$ vs teta[c]	270	$5.0x10^{-6}$	$(4\text{-}24.5)x10^{-5}$	0.02-0.2	method 1[a,c]
$Cu(OH)_n^{n-2}$ vs tetb	280	$(5\text{-}7.5)x10^{-6}$	$(10\text{-}40)x10^{-5}$	0.05-0.3	method 2[b]
$Cu(OH)_n^{n-2}$ vs [15]aneN$_4$	272	$(5\text{-}40)x10^{-6}$	$(10\text{-}80)x10^{-5}$	0.2-0.8	method 2[b]
$Cu(OH)_n^{n-2}$ vs [16]aneN$_4$	285	$1.5x10^{-5}$	$(15\text{-}50)x10^{-5}$	0.07-0.43	method 1[a]
$Cu(OH)_n^{n-2}$ vs THPC					
$Cu(OH)_n^{n-2}$ vs dioxocyclam	260	$1.5x10^{-5}$	$(16\text{-}48)x10^{-5}$	0.1-0.4	method 2[b]

[a]The ligand solution was prepared in 1.0 mol dm^{-3} $NaClO_4$ and that of copper (II) in the required sodium hydroxide concentration adjusted to I = 1.0 mol dm^{-3} with $NaClO_4$.

[b]Both the metal and the ligand solutions were prepared in the required sodium hydroxide concentration and adjusted to I = 1.0 mol dm^{-3} with $NaClO_4$.

[c]I = 0.5 mol dm^{-3} ($NaClO_4$ + NaOH).

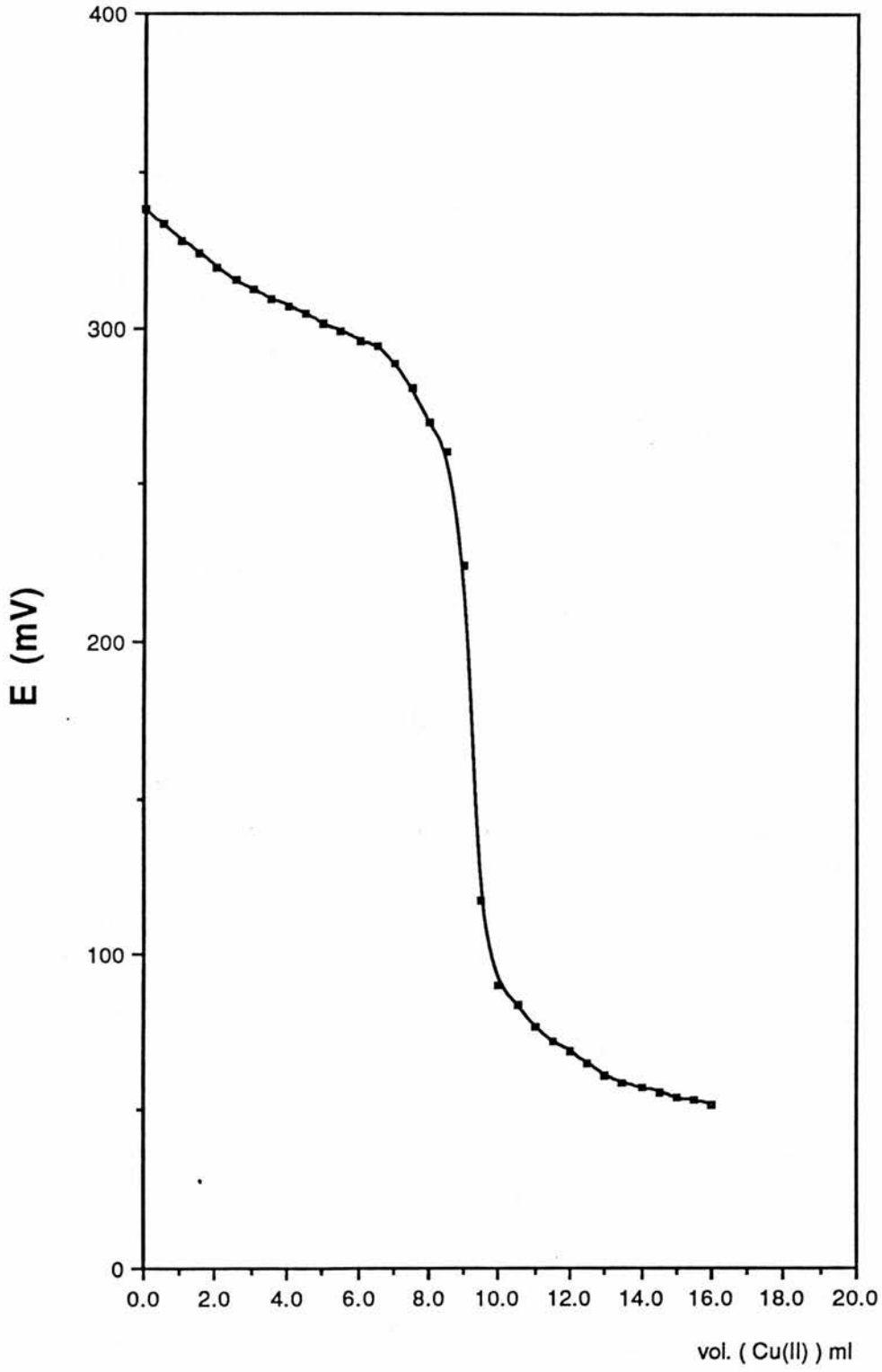

Figure2.2 Potentiometric titration of cyclam in ammonia buffer (pH 10) against standard Cu(II) solution using a copper electrode and calomel reference electrode.

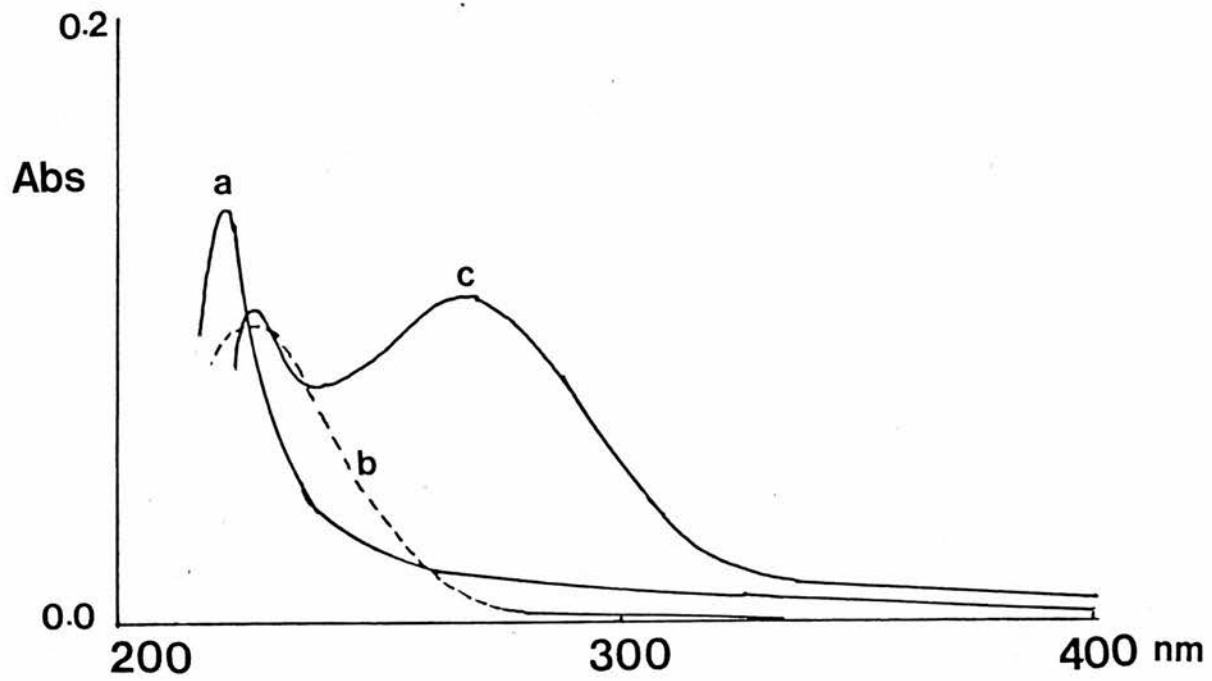

Figure 2.3 Uv. spectra of (a) [THPC] = 2x 10^{-4} in 0.16 M NaOH ; (b) [Cu^{2+}]$_T$ =2x10^{-5} in 0.16 M NaOH ; and 10x [Cu^{2+}] = [THPC] = 1x10^{-4} in 0.08 M NaOH .

studies were carried out under pseudo-first order conditions by using at least a ten fold excess of ligand. Five to ten replicate runs were carried out.

Potentiometric Titrations:

Potentiometric titrations of the macrocyclic ligands were carried out as described in Chapter 4. The protonation constants were calculated using the SUPERQUAD program(10).

2.3 Results

The log β values for the first and the second protonation constants, determined (Chapter 4), for the eight ligands are: Cyclam, 11.05 and 10.31; C-meso Me_2cyclam, 10.8 and 10.3, tet a, 11.23 and 10.36; tet b, 10.9 and 10.7; [15]aneN_4, 11.8 and 10.31; [16]aneN_4, 10.63 and 9.57; THPC, 9.08 and 8.30; and dioxocyclam, 9.78 and 6.12. Therefore, the ligands exist prominently (> 99%) in the unprotonated form under the conditions employed in this study. Copper(II) exists as a mixture of $Cu(OH)_3^-$ and $Cu(OH)_4^{2-}$ at the hydroxide ion concentrations employed, described by the expressions(10)

$$Cu(OH)_3^- + OH^- \rightleftharpoons Cu(OH)_4^{2-} \qquad (1)$$

and

$$K_4^c = [Cu(OH)_4^{2-}]/[Cu(OH)_3^-][OH^-] \qquad (2)$$

The overall reaction of the hydroxocopper species with the various ligands, L, may be represented by the general expression

$$Cu(OH)_n^{2-n} + L \longrightarrow CuL(OH)_m^{2-m} + (n-m)OH^- \qquad (3)$$

Kinetic measurements were made using a series of sodium hydroxide ion concentrations in order to determine the rate constants $k_{Cu(OH)3}^{L}$ and $k_{Cu(OH)4}^{L}$ for the reactions (4) and (5)

$$L + [Cu(OH)_3^-] \longrightarrow [CuL]^{2+} ; \quad k_{Cu(OH)_3}^{L} \qquad (4)$$

$$L + [Cu(OH)_4^-] \longrightarrow [CuL]^{2+} ; \quad k_{Cu(OH)_4}^{L} \qquad (5)$$

Studies were carried out under pseudo-first order conditions by using at least a tenfold excess of the ligand. All of the reactions were found to be first-order with respect to each reactant (the ligand concentration was also varied) and to proceed to completion obeying the rate expression

$$d[CuL]/dt = k_f[Cu]_T [L] \qquad (6)$$

where $[Cu]_T = [Cu(OH)_3^-] + [Cu(OH)_4^{2-}]$ and $k_{obs} = k_f [L]$. The values of k_{obs} are inversely proportional to $[OH^-]$ for all the systems studied. A common feature of the eight systems was the observation of two kinetic steps. One reaction is fast (in the 20 - 50 ms range) and is associated with a decrease in absorbance. This reaction is followed by a slower reaction associated with an increase in absorbance. The latter reaction was considered in detail and is believed to be the metal incorporation step. For all systems (with the possible exception of the tet<u>a</u> system) the initial first step of the biphasic reaction is unaffected by changes in the ligand and sodium hydroxide concentrations. For the tet <u>a</u> system the rate increased with [NaOH]. In the [16]aneN$_4$ and dioxocyclam systems a third slower step (associated with absorbance decrease) was also observed. This latter step, especially in the [16]aneN$_4$ system, is only slightly affected by the ligand concentration at fixed $[OH^-]$ but increases markedly with increased $[OH^-]$ (Figure 2.4). The values of k_{obs} (for the metal incorporation step) for all eight ligands at each hydroxide ion concentration are listed in Tables 2.2 to 2.9. Plots of k_{obs} *vs.* [

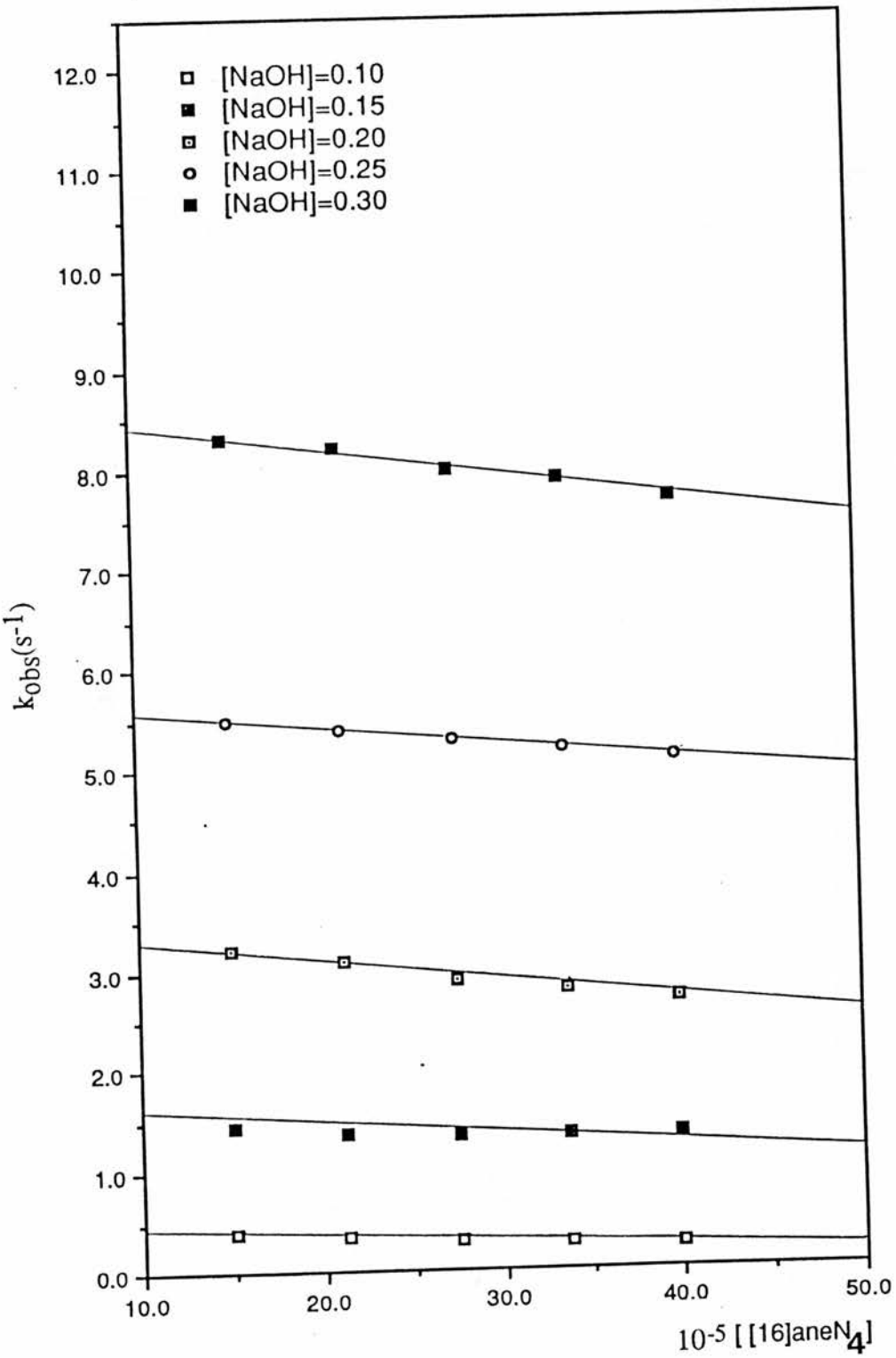

Figure 2.4 Plots of the observed rate constants (k_{obs}) vs. the [16]aneN$_4$ concentration for reactions of Cu(II) in strongly basic media at 25.0 ^{o}C and I =1.0 M ($NaClO_4$+NaOH) (slow step).

L] gave straight lines with slope k_f and zero intercept as shown in Figures 2.5 - 2.12. The temperature dependence of k_{obs} for $Cu(OH)_x^{2-x}$ reacting with tet a is given in Table 2.10.

As shown in Tables 2.2 - 2.9, values of k_{obs} decreased as $[OH^-]$ increased. Thus the rate of formation can be represented by equation (7).

$$\text{Rate} = k_f [Cu]_T [L]$$
$$= k^L_{Cu(OH)3} [Cu(OH)_3]^- [L] + k_{Cu(OH)4} [Cu(OH)_4]^{2-} [L] \qquad (7)$$

where L represent the unprotonated form of the uncomplexed ligand. The suitable mechanism which can accommodate the above rate expression is:

$$Cu(OH)_4^{2-} + L \longrightarrow CuL(OH)_x^{2-x} + (4-x)OH^-$$

$$K_4^c \quad \rightleftharpoons \qquad (8)$$

$$OH^- + Cu(OH)_3^- + L \longrightarrow CuL(OH)_x^{2-x} + (4-x)OH^-$$

since, $K_4^c = [Cu(OH)_4^{2-}] / Cu(OH^-)_3] [OH^-]$ (9)

, $[Cu^{2+}]_T = [Cu(OH)_3^-] + [Cu(OH)_4^{2-}]$ (10)

then from (9) and (10) it can be readily shown that

$$[Cu^{2+}]_T = [Cu(OH)_4^{2-}] (1 + K_4^c [OH^-]) / K_4^c [OH^-] \qquad (11)$$

and

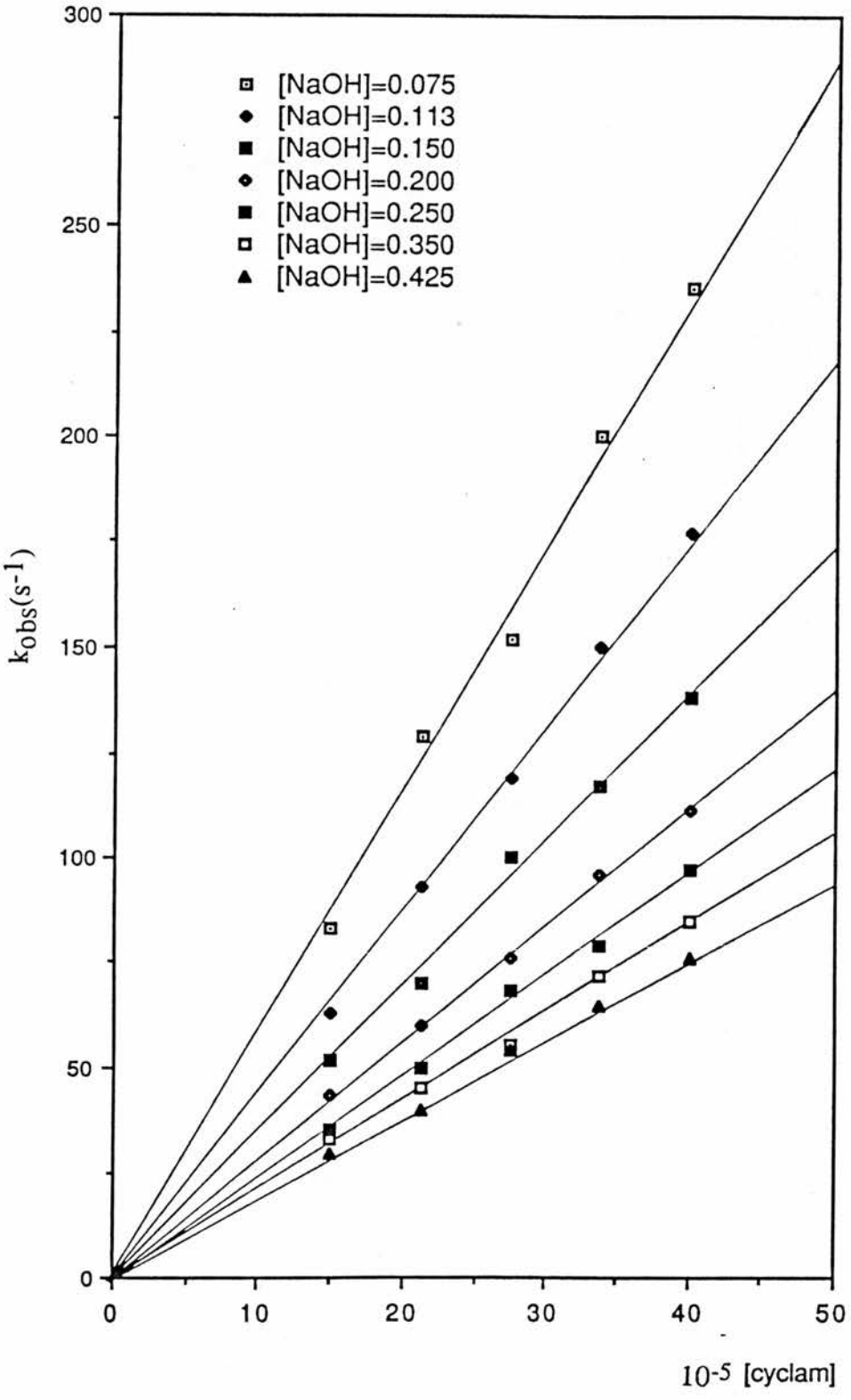

Figure 2.5 Plots of the observed rate constants (k_{obs}) vs. the cyclam concentration for reactions of Cu(II) in strongly basic media at 25.0 °C and I=1.0 M ($NaClO_4$+NaOH) .

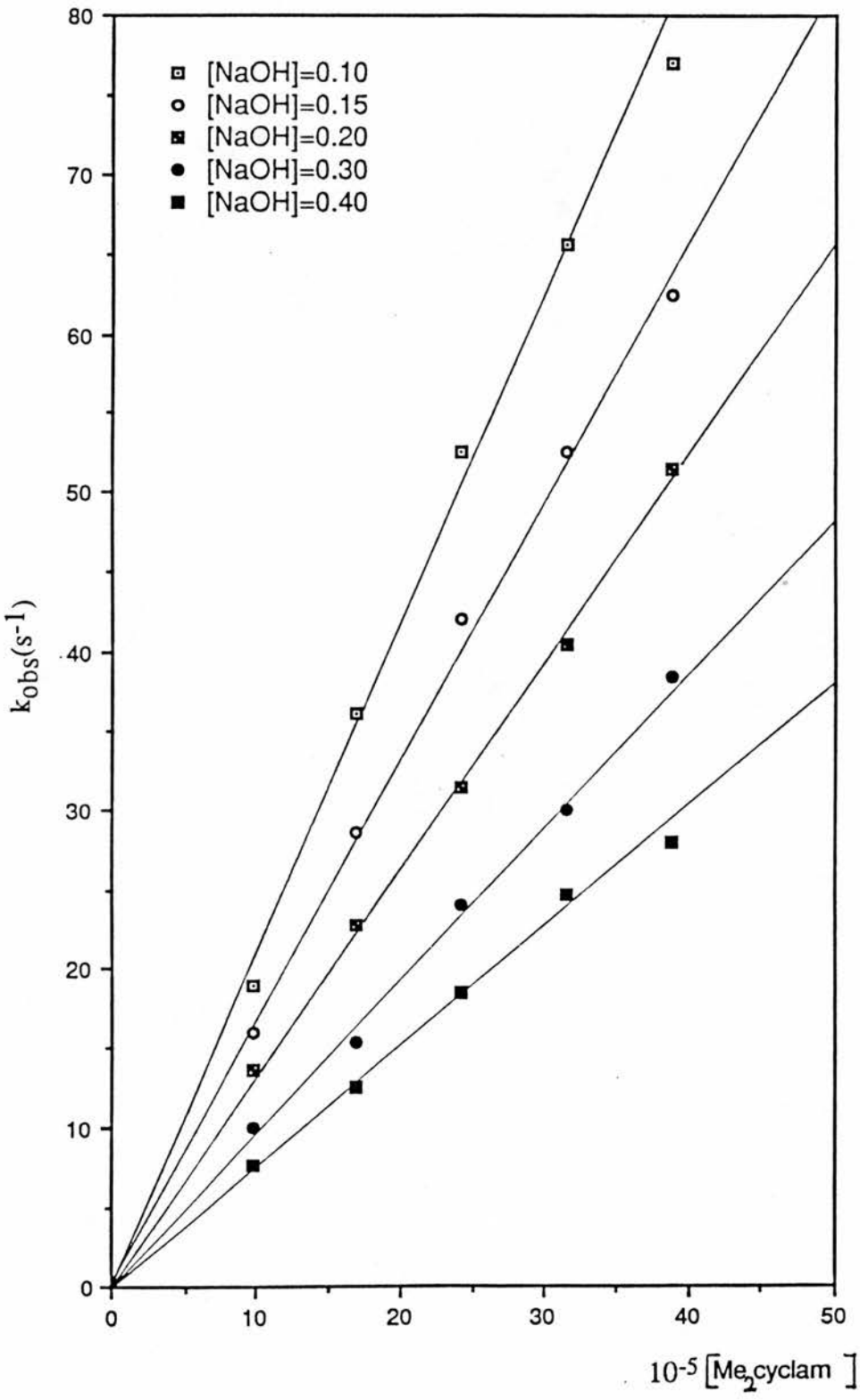

Figure 2.6 Plots of the observed rate constants (k_{obs}) vs. the Me_2cyclam concentration for reactions of Cu(II) in strongly basic media at 25.0 °C and I=1.0 M ($NaClO_4$+NaOH) .

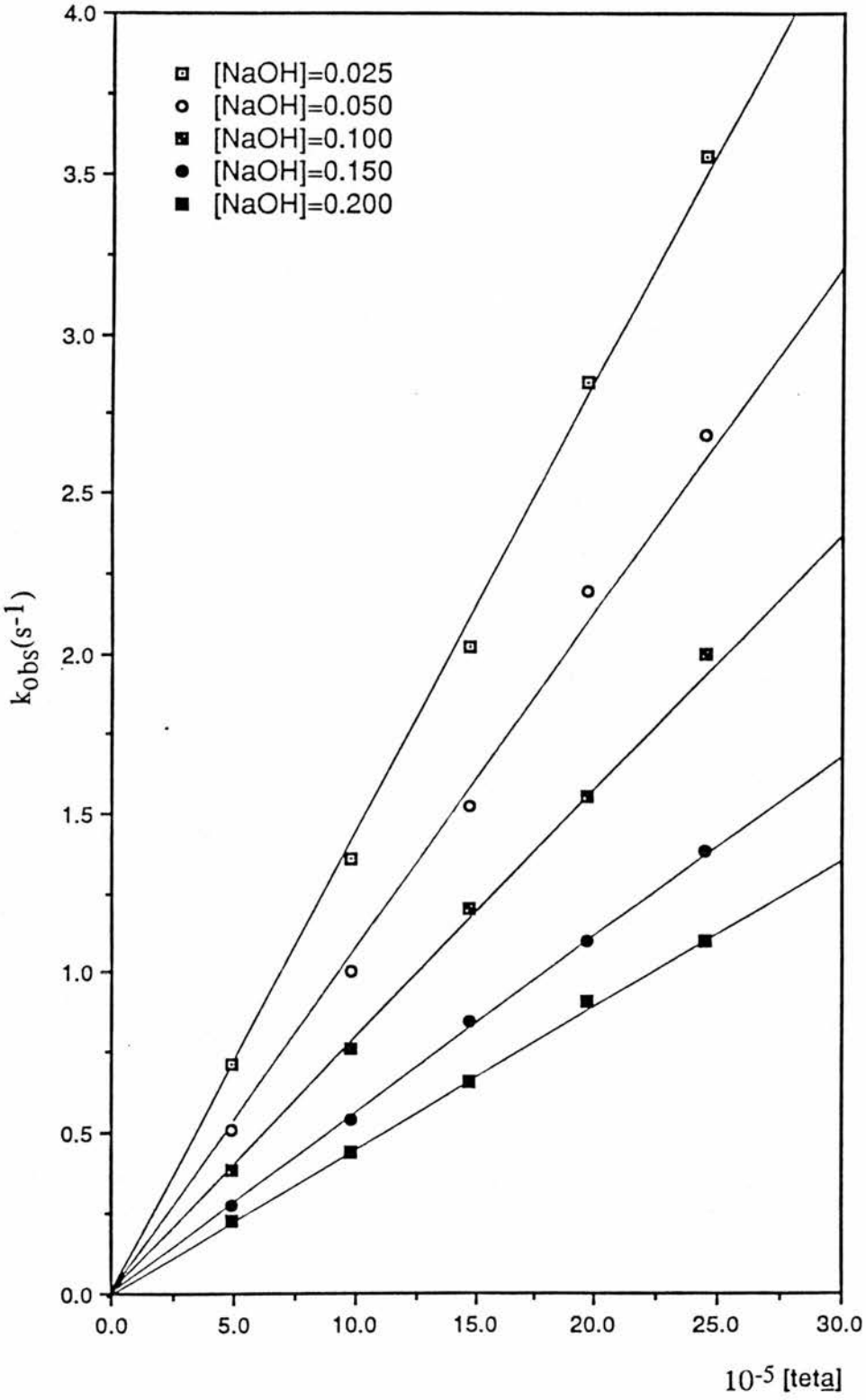

Figure 2.7 Plots of the observed rate constants (k_{obs}) vs. the teta concentration for reactions of Cu(II) in strongly basic media at 25.0 °C and I=0.5 M ($NaClO_4$+NaOH) .

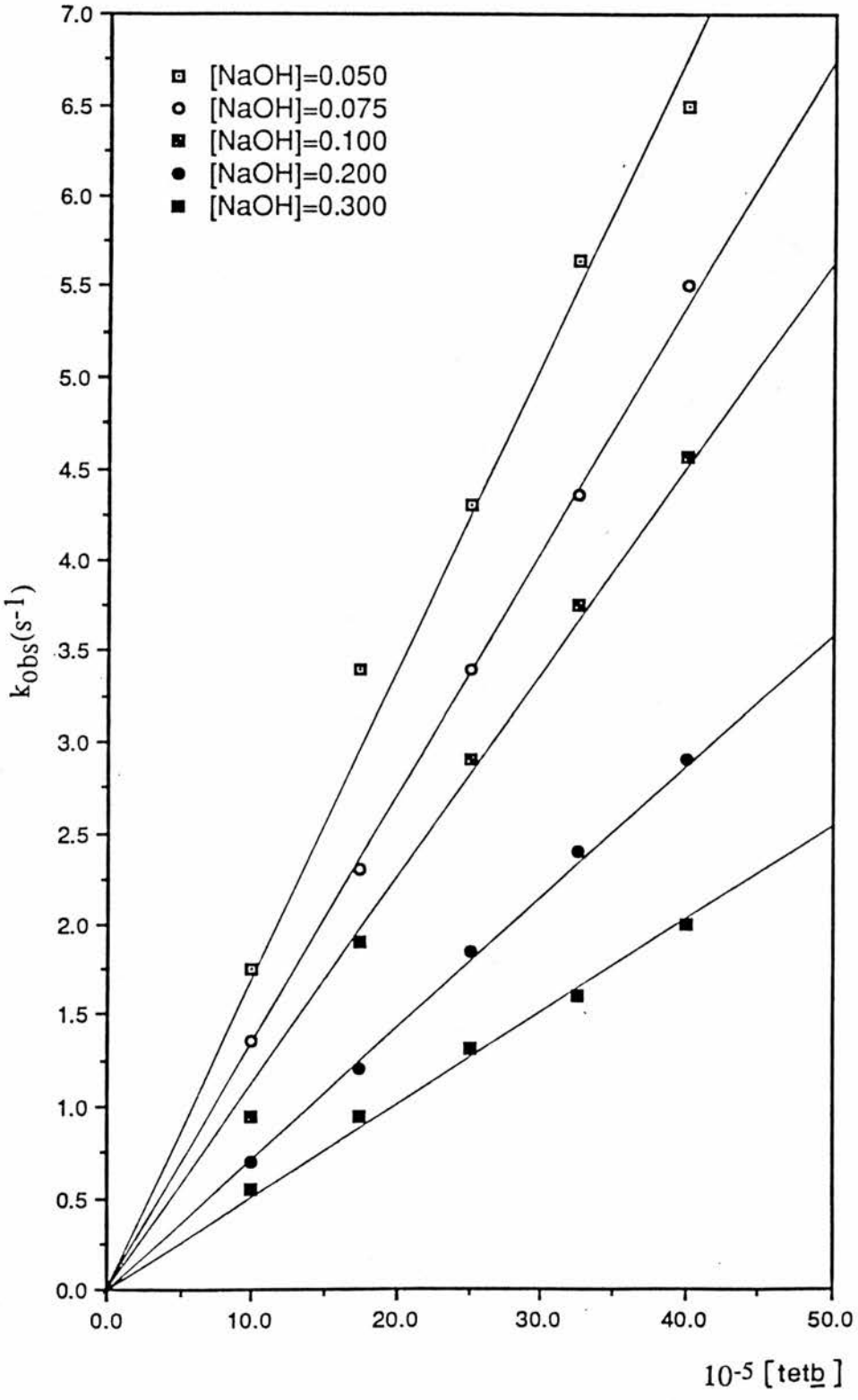

Figure 2.8 Plots of the observed rate constants (k_{obs}) vs. the tetb concentration for reactions of Cu(II) in strongly basic media at 25.0 °C and I=1.0 M ($NaClO_4$+NaOH) .

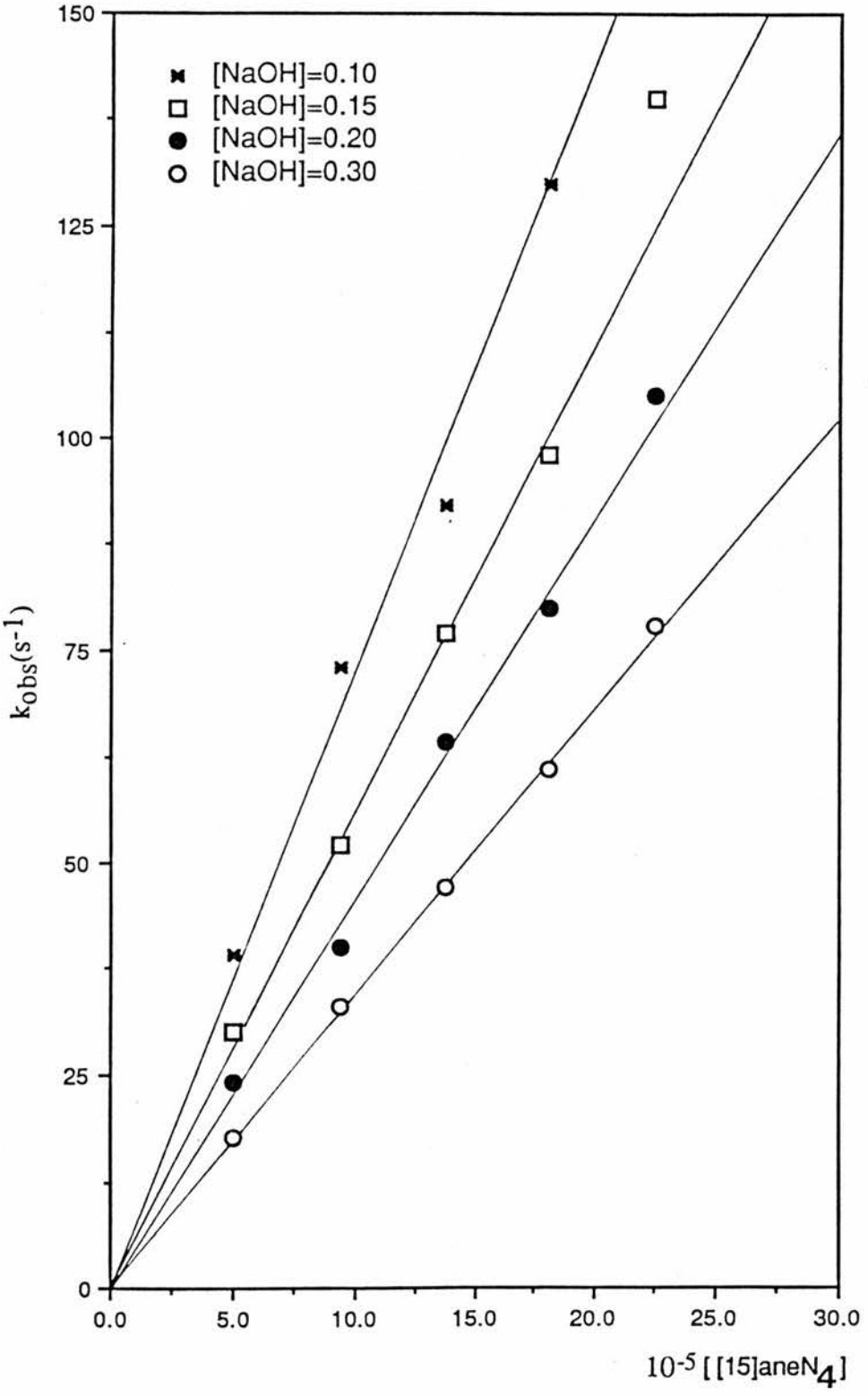

Figure 2.9 Plots of the observed rate constants (k_{obs}) vs. the [15]aneN$_4$concentration for reactions of Cu(II) in strongly basic media at 25.0 °C and I=1.0 M ($NaClO_4$+NaOH) .

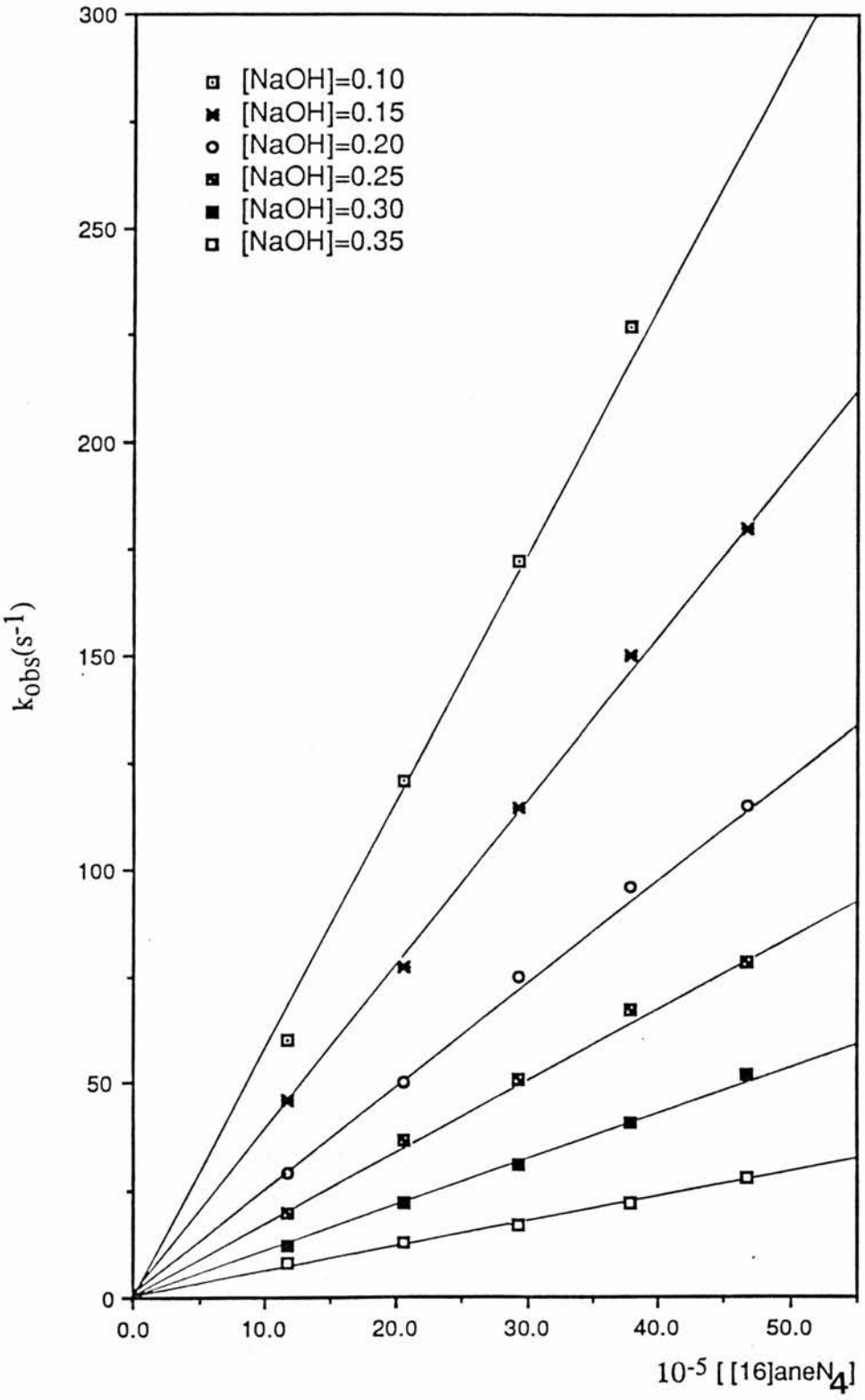

Figure 2.10 Plots of the observed rate constants (k_{obs}) vs. the [16]aneN_4 concentration for reactions of Cu(II) in strongly basic media at 25.0 °C and I=1.0 M ($NaClO_4$+NaOH) .

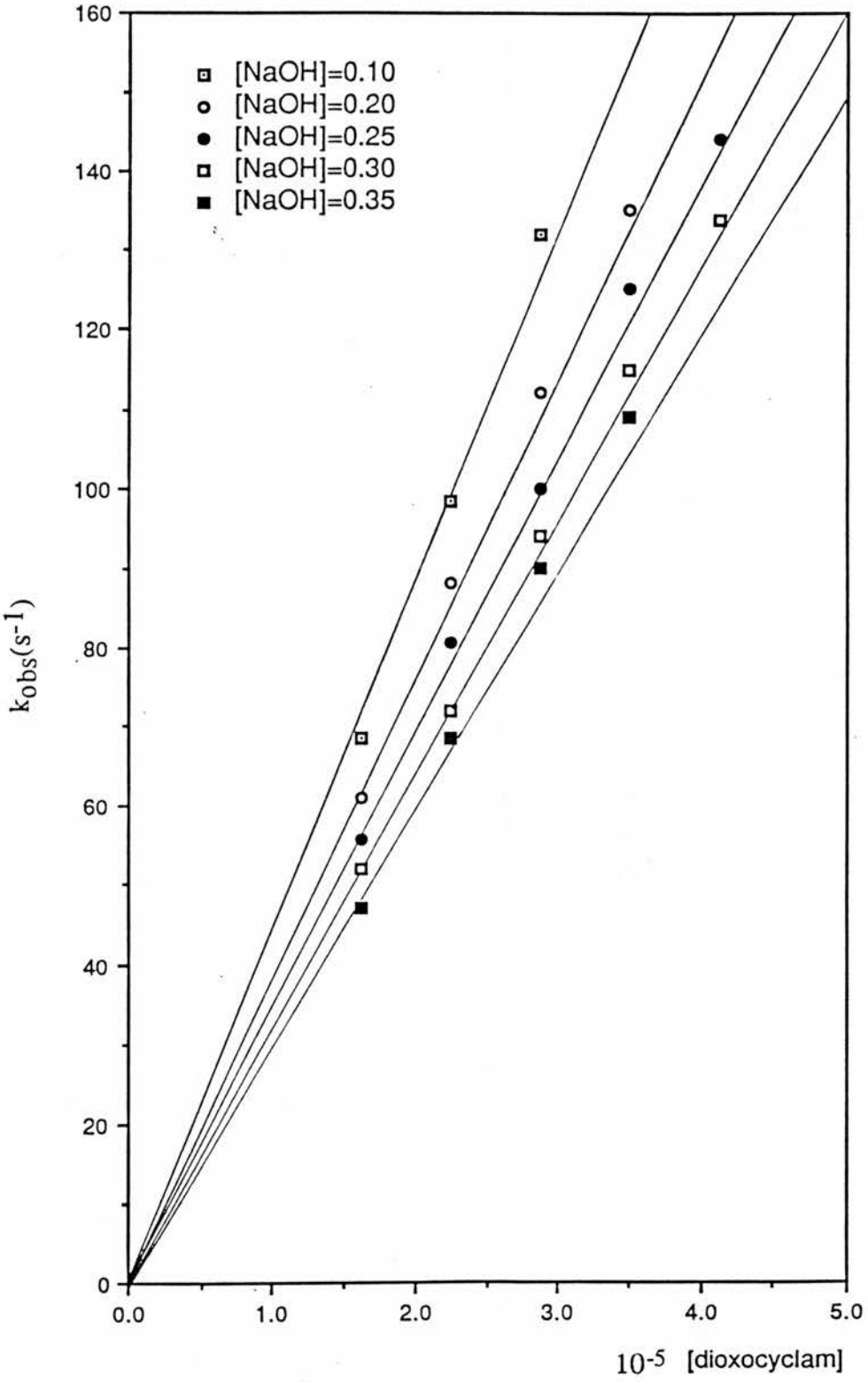

Figure 2.11 Plots of the observed rate constants (k_{obs}) vs. the dioxocyclam concentration for reactions of Cu(II) in strongly basic media at 25.0 °C and I=1.0 M ($NaClO_4$+NaOH)

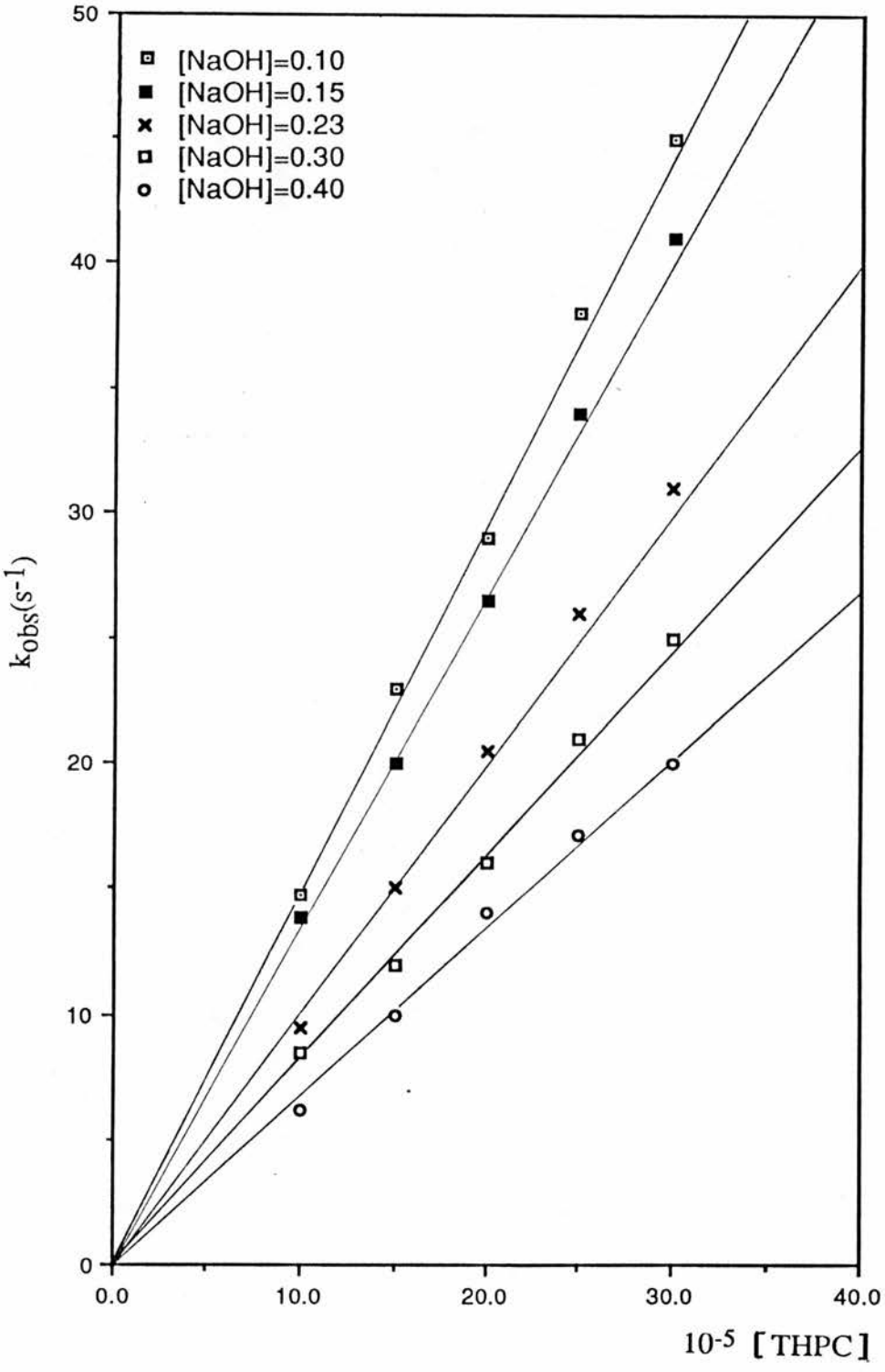

Figure 2.12 Plots of the observed rate constants (k_{obs}) vs. the THPC concentration for reactions of Cu(II) in strongly basic media at 25.0 °C and I=1.0 M ($NaClO_4$+NaOH) .

Table 2.2 Observed Rate Constants for Cu(II) Reacting With Cyclam in Basic Solution at 25.0°C and I= 1mol dm^{-3} ($NaOH+NaClO_4$).

[NaOH] mol dm^{-3}	10^5 $[Cu^{2+}]_T$ mol dm^{-3}	10^5 [cyclam] mol dm^{-3}	k_{obs} s^{-1}	10^{-5} k_f mol dm^{-3} s^{-1}
0.075	1.50	15.00	83	5.5
0.075	1.50	21.25	129	6.1
0.075	1.50	27.50	152	5.5
0.075	1.50	33.75	200	5.9
0.075	1.50	40.00	235	5.9
0.113	1.50	15.00	61	4.1
0.113	1.50	27.50	119	4.3
0.113	1.50	40.00	177	4.4
0.150	1.50	15.00	52	3.4
0.150	1.50	21.03	70	3.3
0.150	1.50	27.50	100	3.6
0.150	1.50	33.75	117	3.5
0.150	1.50	40.00	138	3.4
0.200	1.50	15.00	44	2.9
0.200	1.50	27.50	76	2.8
0.200	1.50	40.00	111	2.8
0.250	1.50	15.00	35	2.6
0.250	1.50	21.25	50	2.5
0.250	1.50	27.50	68	2.5
0.250	1.50	33.75	79	2.3
0.250	1.50	40.00	97	2.4
0.350	1.50	15.00	33	2.2
0.350	1.50	21.25	46	2.1
0.350	1.50	27.50	55	2.0
0.350	1.50	33.75	80	2.3
0.350	1.50	40.00	85	2.1
0.425	1.50	15.00	30	1.9
0.425	1.50	21.25	40	1.9
0.425	1.50	27.50	54	2.0
0.425	1.50	40.00	76	1.9

Table 2.3 Observed Rate Constants for Cu(II) Reacting With Me_2Cyclam in Basic Solution at 25.0°C and I= 1mol dm^{-3} ($NaOH+NaClO_4$).

[NaOH] mol dm^{-3}	10^5 $[Cu^{2+}]_T$ mol dm^{-3}	10^5[Me_2cyclam] mol dm^{-3}	k_{obs} s^{-1}	10^{-5} k_f mol dm^{-3} s^{-1}
0.10	0.75	9.700	19.0	2.0
0.10	0.75	16.98	36.0	2.1
0.10	0.75	24.25	52.5	2.2
0.10	0.75	31.53	65.5	2.1
0.10	0.75	38.80	77.0	2.0
0.15	0.90	9.700	16.0	1.6
0.15	0.90	16.98	28.5	1.7
0.15	0.90	24.25	42.0	1.7
0.15	0.90	31.53	52.5	1.7
0.15	0.90	38.80	62.4	1.6
0.20	0.75	9.700	13.7	1.4
0.20	0.75	16.98	22.8	1.3
0.20	0.75	24.25	31.4	1.2
0.20	0.75	31.53	40.5	1.3
0.20	0.75	38.80	51.5	1.3
0.30	0.75	9.700	8.50	8.8
0.30	0.75	16.98	15.4	9.1
0.30	0.75	24.25	24.0	9.9
0.30	0.75	31.53	30.0	9.5
0.30	0.75	38.80	38.5	9.9
0.40	0.90	9.700	7.70	7.9
0.40	0.90	16.98	12.5	7.4
0.40	0.90	24.25	18.5	7.6
0.40	0.90	31.53	24.7	7.8
0.40	0.90	38.80	28.0	7.2

Table 2.4. Observed Rate Constants for Cu(II) Reacting With teta in Basic Solution at 25.0 °C and I= 1 mol dm^{-3} ($NaOH+NaClO_4$).

[NaOH] mol dm^{-3}	10^5 $[Cu^{2+}]_T$ mol dm^{-3}	10^5 [teta] mol dm^{-3}	k_{obs} s^{-1}	10^{-4} k_f mol dm^{-3} s^{-1}
0.025	0.5	4.90	0.71	1.45
0.025	0.5	9.80	1.36	1.39
0.025	0.5	14.7	2.02	1.37
0.025	0.5	19.6	2.85	1.46
0.025	0.5	24.5	3.55	1.45
0.050	0.5	4.90	0.51	1.04
0.050	0.5	9.80	1.00	1.02
0.050	0.5	14.7	1.52	1.03
0.050	0.5	19.6	2.20	1.11
0.050	0.5	24.5	2.68	1.09
0.100	0.5	5.00	0.38	0.77
0.100	0.5	8.75	0.64	0.73
0.100	0.5	12.5	0.95	0.76
0.100	0.5	16.3	1.25	0.77
0.100	0.5	20.0	1.62	0.81
0.100	0.5	24.5	2.00	0.82
0.150	0.5	4.90	0.27	0.56
0.150	0.5	9.80	0.54	0.55
0.150	0.5	14.7	0.85	0.58
0.150	0.5	19.6	1.10	0.56
0.150	0.5	24.5	1.38	0.56
0.200	0.5	5.00	0.23	0.45
0.200	0.5	8.75	0.41	0.47
0.200	0.5	12.5	0.55	0.44
0.200	0.5	16.3	0.76	0.47
0.200	0.5	20.0	0.91	0.46
0.200	0.5	24.5	1.10	0.45

Table 2.5 Observed Rate Constants for Cu(II) Reacting With tetb in Basic Solution at 25.0 °C and I= 1 mol dm^{-3} ($NaOH+NaClO_4$).

[NaOH] mol dm^{-3}	10^5 $[Cu^{2+}]_T$ mol dm^{-3}	10^5 [tetb] mol dm^{-3}	k_{obs} s^{-1}	10^{-4} k_f mol dm^{-3} s^{-1}
0.050	0.75	10.0	1.80	1.75
0.050	0.75	17.5	3.40	1.94
0.050	0.75	25.0	4.30	1.72
0.050	0.75	32.5	5.65	1.74
0.050	0.75	40.0	6.50	1.62
0.075	0.75	10.0	1.35	1.35
0.075	0.75	17.5	2.20	1.29
0.075	0.75	25.0	3.40	1.36
0.075	0.75	32.5	4.35	1.34
0.075	0.75	40.0	5.50	1.38
0.100	0.75	10.0	1.00	0.95
0.100	0.75	17.5	2.24	1.26
0.100	0.75	25.0	3.11	1.20
0.100	0.75	32.5	3.80	1.17
0.100	0.75	40.0	4.50	1.13
0.200	0.50	10.0	0.86	0.86
0.200	0.50	15.0	1.09	0.73
0.200	0.50	20.0	1.43	0.71
0.200	0.50	25.0	1.85	0.75
0.200	0.50	30.0	2.35	0.76
0.300	0.75	10.0	0.61	0.61
0.300	0.75	17.5	1.00	0.54
0.300	0.75	25.0	1.32	0.53
0.300	0.75	32.0	1.60	0.53
0.300	0.75	40.0	2.07	0.52

Table 2.6 Observed Rate Constants for Cu(II) Reacting With [15]aneN$_4$ in Basic Solution at 25.0 °C and I= 1.0 mol dm^{-3} (NaOH+NaClO$_4$).

[NaOH] mol dm^{-3}	10^5 [Cu^{2+}]$_T$ mol dm^{-3}	10^5[15]aneN$_4$ mol dm^{-3}	k_{obs} s^{-1}	10^{-5} k_f mol dm^{-3} s^{-1}
0.10	0.50	5.000	39.0	7.8
0.10	0.50	9.400	73.0	7.8
0.10	0.50	13.75	92.0	6.7
0.10	0.50	18.13	130	7.2
0.15	0.50	5.000	30.0	6.0
0.15	0.50	9.400	52.0	5.6
0.15	0.50	13.75	77.0	5.6
0.15	0.50	18.13	98.0	5.4
0.15	0.50	22.50	140	6.2
0.20	0.50	5.000	24.0	4.7
0.20	0.50	9.400	40.0	4.3
0.20	0.50	13.75	64.0	4.7
0.20	0.50	18.10	80.0	4.4
0.20	0.50	22.50	105	4.7
0.30	0.50	5.000	17.5	3.5
0.30	0.50	9.400	33.0	3.5
0.30	0.50	13.75	47.0	3.4
0.30	0.50	18.13	61.0	3.4
0.30	0.50	22.50	78.0	3.5
0.40	0.50	5.000	15.0	3.0
0.40	0.50	10.00	29.0	2.9
0.40	0.50	17.50	49.0	2.8
0.40	0.50	25.00	73.0	2.9
0.40	0.50	32.50	85.0	2.6

Table 2.7 Observed Rate Constants for Cu(II) Reacting With [16]aneN$_4$ in Basic Solution at 25.0 °C and I= 1.0 mol dm^{-3} (NaOH+NaClO$_4$) (slow step).

[NaOH] mol dm^{-3}	10^5 [Cu^{2+}]$_T$ mol dm^{-3}	10^5[16]aneN$_4$ mol dm^{-3}	k_{obs} s^{-1}
0.10	1.5	15.00	0.40
0.10	1.5	21.25	0.35
0.10	1.5	27.50	0.30
0.10	1.5	33.75	0.27
0.10	1.5	40.00	0.24
0.15	1.5	15.00	1.45
0.15	1.5	21.25	1.38
0.15	1.5	27.50	1.35
0.15	1.5	33.75	1.35
0.15	1.5	40.00	1.35
0.20	1.5	15.00	3.20
0.20	1.5	21.25	3.10
0.20	1.5	27.50	2.90
0.20	1.5	33.75	2.80
0.20	1.5	40.00	2.70
0.25	1.5	15.00	5.50
0.25	1.5	21.25	5.50
0.25	1.5	27.50	5.50
0.25	1.5	33.75	5.50
0.25	1.5	40.00	5.50
0.30	1.5	15.00	8.30
0.30	1.5	21.25	8.20
0.30	1.5	27.50	8.00
0.30	1.5	33.75	7.85
0.30	1.5	40.00	7.70

Table 2.8 Observed Rate Constants for Cu(II) Reacting With dioxocyclam in Basic Solution at 25.0 °C and I= 1.0 mol dm^{-3} ($NaOH+NaClO_4$).

[NaOH] mol dm^{-3}	10^5 $[Cu^{2+}]_T$ mol dm^{-3}	10^4dioxocyclam mol dm^{-3}	k_{obs} s^{-1}	10^{-5} k_f mol dm^{-3} s^{-1}
0.10	1.50	1.63	68.5	4.2
0.10	1.50	2.25	98.5	4.4
0.10	1.50	2.88	132	4.5
0.20	1.50	1.63	61.0	3.8
0.20	1.50	2.25	88.0	3.9
0.20	1.50	2.88	112	3.9
0.20	1.50	3.50	135	3.9
0.25	1.50	1.63	55.8	3.4
0.25	1.50	2.25	80.7	3.6
0.25	1.50	2.88	100	3.5
0.25	1.50	3.50	125	3.6
0.25	1.50	4.13	144	3.5
0.30	1.50	1.63	52.0	3.2
0.30	1.50	2.25	72.0	3.2
0.30	1.50	2.88	94.0	3.3
0.30	1.50	3.50	115	3.3
0.30	1.50	4.13	134	3.3
0.35	1.50	1.63	47.0	2.9
0.35	1.50	2.25	68.5	3.0
0.35	1.50	2.88	90.0	3.1
0.35	1.50	3.50	113	3.2
0.35	1.50	4.75	151	3.1
0.40	1.50	2.25	70.0	3.1
0.40	1.50	3.50	107	3.0
0.40	1.50	4.75	145	3.0

Table 2.9 Observed Rate Constants for Cu(II) Reacting With THPC in Basic Solution at 25.0 °C and I= 1.0 mol dm^{-3} ($NaOH+NaClO_4$).

[NaOH] mol dm^{-3}	10^5 $[Cu^{2+}]_T$ mol dm^{-3}	10^5[15]aneN_4 mol dm^{-3}	k_{obs} s^{-1}	10^{-5} k_f mol dm^{-3} s^{-1}
0.10	0.75	10.0	14.5	1.4
0.10	0.75	15.0	23.0	1.5
0.10	0.75	20.0	29.0	1.4
0.10	0.75	25.0	38.0	1.5
0.10	0.75	30.0	45.0	1.5
0.15	0.75	10.0	14.0	1.4
0.15	0.75	15.0	20.0	1.3
0.15	0.75	20.0	26.5	1.2
0.15	0.75	25.0	34.0	1.3
0.15	0.75	30.0	41.0	1.4
0.23	0.75	10.0	9.50	0.9
0.23	0.75	15.0	15.0	1.0
0.23	0.75	20.0	20.5	0.9
0.23	0.75	25.0	26.0	1.0
0.23	0.75	30.0	31.0	1.0
0.30	0.75	10.0	9.00	0.9
0.30	0.75	15.0	12.0	0.8
0.30	0.75	20.0	16.0	0.8
0.30	0.75	25.0	21.0	0.8
0.30	0.75	30.0	25.0	0.8
0.40	0.75	10.0	6.20	0.6
0.40	0.75	15.0	10.0	0.7
0.40	0.75	20.0	14.5	0.7
0.40	0.75	25.0	17.1	0.7
0.40	0.75	30.0	20.0	0.6

Table 2.10 Observed Rate Constants for Cu(II) Reacting With teta in Basic Solution at Various Temperatures and I = 0.5 mol dm^{-3} ($NaOH+NaClO_4$).

[NaOH] mol dm^{-3}	10^5 $[Cu^{2+}]_T$ mol dm^{-3}	10^5 [teta] mol dm^{-3}	Temp. ^oC	k_{obs} s^{-1}
0.10	0.5	14.7	15.0	0.41
0.10	0.5	14.7	19.5	0.70
0.10	0.5	14.7	25.0	1.10
0.10	0.5	14.7	30.0	1.71
0.10	0.5	14.7	34.5	2.32

$\Delta H^{\#}$ = 61.55 kJ mol^{-1} ; $\Delta S^{\#}_{298}$= -38 J K mol^{-1} cc. =-0.998 .

$$\text{Rate} = [Cu(OH)_4^{2-}]\,[L]\,(k^{L}_{Cu(OH)3} + k^{L}_{Cu(OH)4}\,K_4^{c}\,[OH^-]) / K_4^{c}\,[OH^-] \quad \text{..... (12)}$$

Assuming that the equilibrium involving $Cu(OH)_3^-$ and $Cu(OH)_4^{2-}$ is rapidly established, the following relationship is obtained by combining equations (2), (11), and (12) ,

$$k_f\,(1 + K_4^{c}\,[OH^-]) = k^{L}_{Cu(OH)3} + k^{L}_{Cu(OH)4}\,K_4^{c}\,[OH^-] \qquad (13)$$

The equilibrium constant for the two copper species at infinite dilution is given in equation 14 (10)

$$K_4 = {}^{a}Cu(OH)_4^{2-} / {}^{a}Cu(OH)_3^{-} \cdot {}^{a}OH^- = K_4^{c} \cdot \gamma^2_{NaOH} = 7.87 \qquad (14)$$

where γ is the mean activity coefficient for NaOH. The values of K_4^{c} utilized were interpolated from the reported equilibrium constant and γ_{NaOH} values at different sodium hydroxide concentrations (Table 2.11 and Figure 2.13)(10, 7) and were used to obtain the concentrations of $Cu(OH)_3^-$ and $Cu(OH)_4^{2-}$ at each NaOH concentration .

For all eight systems included in this work, $[Cu^{2+}]_T$ was kept below the solubility reported by McDowell and Johnston(11), to prevent formation of solid CuO.

A plot of equation (13) for the kinetic data obtained with dioxocyclam (Table 2.12), as a representative example, is shown in Figure 2.14.

The values of $k_{Cu(OH)3}$ and $k_{Cu(OH)4}$ obtained from the least-squares analysis of equation (13) for the eight ligands are listed in Table 2.13 along with some values reported by others(6-8).

Table 2.11 Concentration Equilibrium Constants for Tetrahydroxocuprate(II) Used at Various Sodium Hydroxide Concentrations.

[NaOH] mol dm^{-3}	δ_{NaOH}	K_4^c mol^{-1} dm^3
0.025	0.823	11.60
0.050	0.799	12.30
0.075	0.780	12.90
0.100	0.766	13.40
0.150	0.744	14.20
0.200	0.727	14.90
0.250	0.717	15.30
0.300	0.708	15.70
0.350	0.703	15.90
0.400	0.697	16.20
0.425	0.694	16.28
0.450	0.693	16.35
0.500	0.690	16.50
0.550	0.687	16.65
0.600	0.685	16.80
0.650	0.683	16.85
0.700	0.681	16.90
0.750	0.600	16.98
0.800	0.679	17.00
0.850	0.679	17.00
0.900	0.678	17.10
0.950	0.678	17.10
1.000	0.678	17.10

Table2.12 Kinetic data for the reaction of dioxocyclam with $Cu(OH)_x^{x-2}$ at I= 1.0 mol dm^{-3} and 25.0 °C.

[NaOH] M	K_4^c M^{-1}	K_4^c [OH]	$1+K_4^c$ [OH]	10^{-4} $k_f(1+K_4^c$ [OH]) M^{-1} s^{-1}
0.10	13.4	1.34	2.34	102.96
0.20	14.9	2.98	3.98	153.25
0.25	15.3	3.83	4.83	169.53
0.30	15.7	4.71	5.71	185.00
0.35	15.9	5.57	6.57	203.67
0.40	16.2	6.48	7.48	230.00

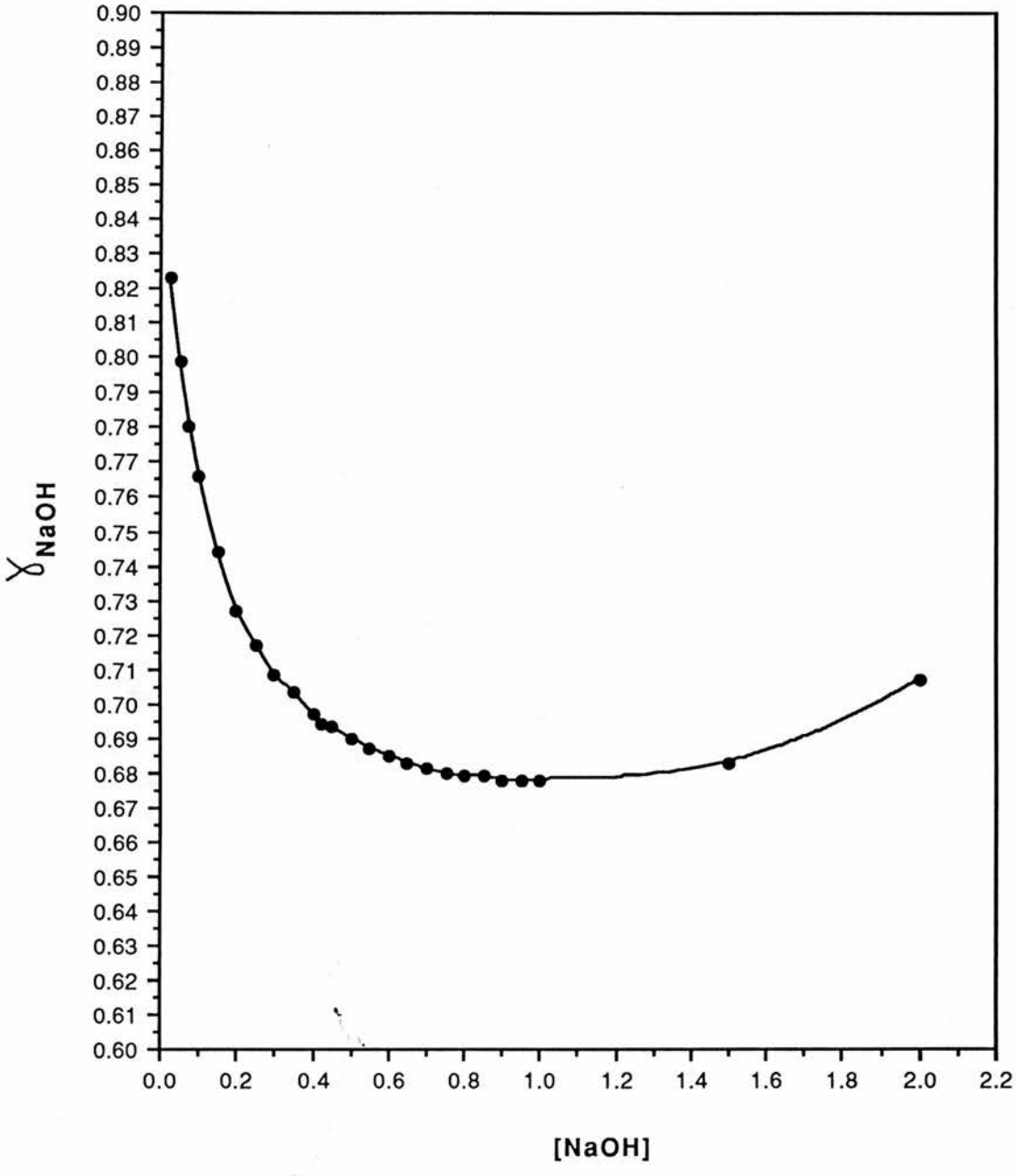

Figure 2.13 Activity coefficients of sodium hydroxide (γ_{NaOH}) at different sodium hydroxide concentrations .

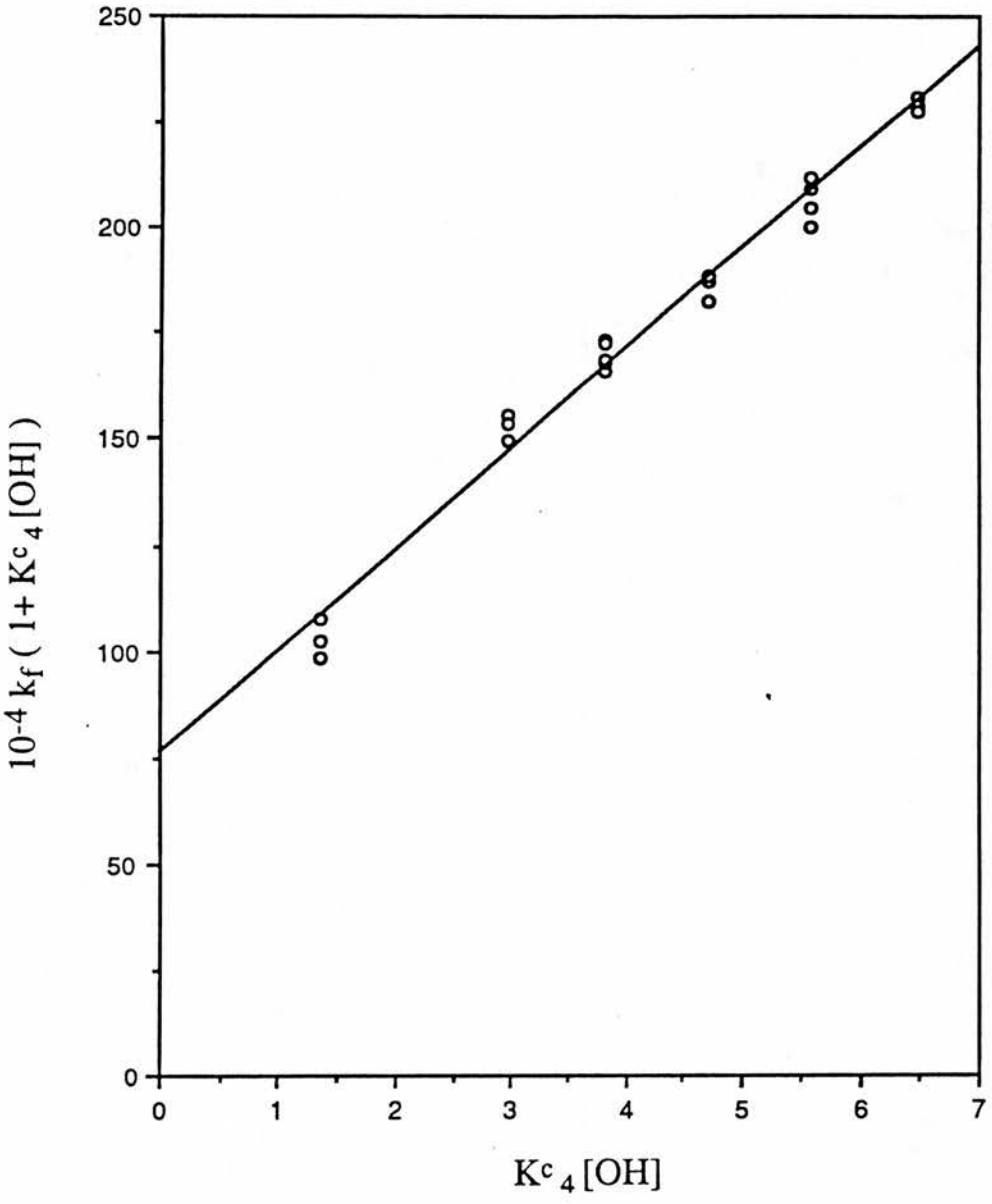

Figure 2.14 Plot of equation 13 to resolve the rate constants for the reaction of dioxocyclam with $Cu(OH)_3^-$ and $Cu(OH)_4^{2-}$.

2.4 Discussion

Inspection of the rate constants listed in Table 2.13 reveals that the ligands utilized in the current study display the following features in common with those from earlier studies.

1) The resolved rate constants are less than the diffusion - controlled limit (~ 10^9 mol^{-1} dm^3 s^{-1}) and are less than the value expected for simple axial H_2O substitution of tetragonal Cu(II).

2) For all ligands, with the possible exception of [16]aneN$_4$, values of $k_{Cu(OH)3}{}^{L}$ are consistently larger than the corresponding values of $k_{Cu(OH)4}{}^{L}$ with the ratio of rate constants $k_{Cu(OH)3}{}^{L} / k_{Cu(OH)4}{}^{L}$ ranging from 3.2 to 32.

3) All ligands, except [16]aneN$_4$, react with $Cu(OH)_4{}^{2-}$. Since a seven-coordinate copper species is unlikely(7), the latter finding suggests that the rate-determining step for reactions involving $Cu(OH)_4{}^{2-}$ occurs before the third Cu-N bond is formed.

As noted in the previous studies(7,8) these observations suggest that the position of the rate-determining step lies after the first axial H_2O substitution and before formation of the third Cu-N bond. A modified version of the reaction mechanism proposed by Lin *et al* (6,7) to explain the reactions of multidentate polyamine ligands with hydroxycuprate (II) species is shown in Figure 2.15.

The Rate-Determining Step:

The actual position of the rate-determining step is important in comparing the reactivities of multidentate ligands with metal centres (12). To assign this step it has been proven useful to examine the rate constant ratios $k^{L}_{Cu(OH)3} / k^{L}_{Cu(OH)4}$ ($R_{3,4}$) for a given ligand L and $k_{Cu(OH)3}{}^{L} / k_{Cu(OH)3}{}^{2,3,2\text{-tet}}$ (R_S) for each ligand reacting with $Cu(OH)_3{}^{-}$ (6,7,8). Values of $R_{3,4}$ listed in Table 2.13, are expected to be greater than unity since the Jahn-Teller inversion step (k_{1b} or k_{2b}) for $Cu(OH)_4{}^{2-}$ requires that two Cu-OH bonds be lengthened instead of one for $Cu(OH)_3{}^{-}$. Small

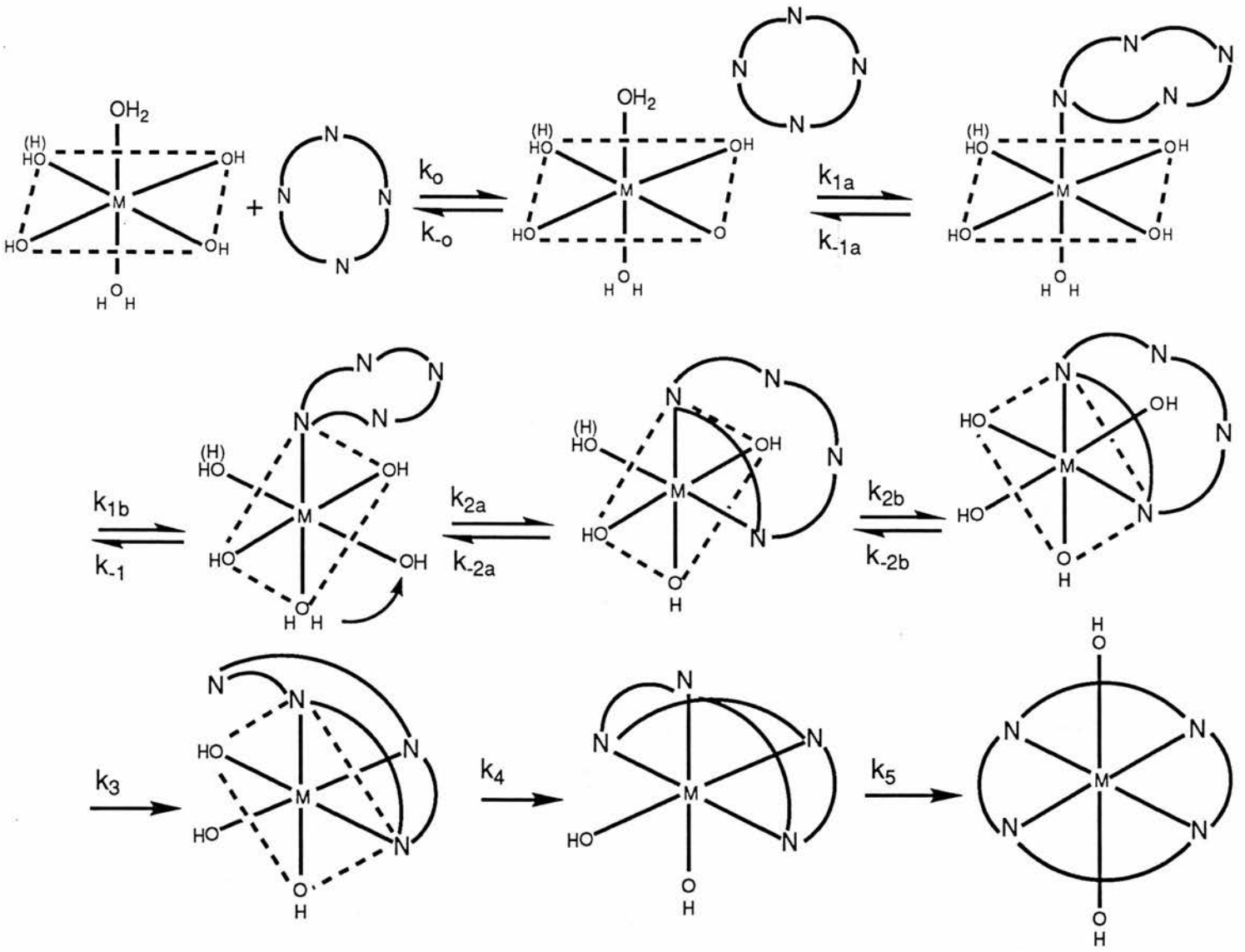

Figure 2.15 Schematic representation of the complexation of $Cu(OH)_n(H_2O)_m^{2-n}$ by a tetradentate polyamine ligand [6] . In this scheme , the first Cu-N bond is formed by replacement of an axial solvent molecule (k_{1a})followed by Jahn-Teller inversion (k_{1b}) to bring the coordinated nitrogen in to an equatorial position . Second bond formation is proposed to occur by a similar two-step sequence (k_{2a} and k_{2b})

Table 2.13 Resolved formation rate constants for hydroxycuprate (II) species reacting with unprotonated macrocyclic tetramines at 25.0°C.

Ligand	$K^{L}_{Cu(OH)3}$ ($M^{-1}s^{-1}$)	$K^{L}_{Cu(OH)4}$ ($M^{-1}s^{-1}$)	$K^{L}_{Cu(OH)3}/K^{L}_{Cu(OH)4}$	Reference
Cyclam	$(9.3\pm0.07)\times10^{5}$	$(7.9\pm0.1)\times10^{4}$	11.8	
	$(2.7\pm0.4)\times10^{6}$	$(3.8\pm0.9)\times10^{4}$	72	7
C-mesoMe_2cyclam	$(4.6\pm0.1)\times10^{5}$	$(1.4\pm0.3)\times10^{4}$	32	
Me_2cyclam	5.6×10^{5}	0.9×10^{4}	60	7
teta	$(1.7\pm0.1)\times10^{4}$	$(4.0\pm0.05)\times10^{2}$	42.5	
	$\sim10^{4}$	$<10^{2}$	>100	7
tetb	$(2.4\pm0.02)\times10^{4}$	$(1.6\pm0.1)\times10^{3}$	15	
	3.1×10^{4}	1.1×10^{2}	281	8
[15]aneN_4	$(1.6\pm0.1)\times10^{6}$	$(7.0\pm0.08)\times10^{4}$	22.9	
[16]aneN_4	$(2.2\pm0.1)\times10^{6}$			
THPC	3.8×10^{5}	1.98×10^{4}	19.2	
$(N\text{-}Me)_4$cyclam	$(3.1\pm0.4)\times10^{3}$	<10	>300	6
Dioxocyclam	$(7.6\pm0.2)\times10^{5}$	$(2.4\pm0.1)\times10^{5}$	3.2	
2,3,2-tet	$(1.0\pm0.7)\times10^{7}$	$(4.3\pm0.2)\times10^{6}$	2.4	

values of $R_{3,4}$ imply that the rate-determining step is the same for $Cu(OH)_3^-$ and $Cu(OH)_4^{2-}$. Large values (i.e. > 10) of $R_{3,4}$ for a given ligand suggest a shift of the rate-determining step from first- to second-bond formation for $Cu(OH)_3^-$ and $Cu(OH)_4^{2-}$, respectively.

If Jahn-Teller inversion following first-bond formation is the rate-determining step for the reactions involving $Cu(OH)_3^-$, the differences among the resolved values of $k_{Cu(OH)_3}^{L}$ may be attributed to C- and N-substitution steric effects or to ring size effects. Table 2.14 lists observed values of R_S for each ligand and the corresponding values predicted on the basis of estimated steric effects of N-substitution. The rate constant for C-meso Me_2cyclam, tet a, and tet b are consistent with the anticipated effects of ring substitution although no quantitative correlation exists.

For those ligands where R_S (observed) << R_S (predicted) steric or ring size factors are not sufficient to account for the difference between $k_{Cu(OH)_3}^{L}$ and $k_{Cu(OH)_3}^{2,3,2\text{-tet}}$, and this may indicate a shift in the rate-determining step to second-bond formation or to the subsequent inversion process.

On the basis of this type of analysis, Lin *et al* [7] have proposed than Jahn-Teller inversion following first-bond formation (k_{1b}) is the rate-determining step for the formation reactions of $Cu(OH)_3^-$ with 2,3,2 - tet, Et_2-2,3,2-tet, cyclam, and Et_4dien (1,1,7,7-tetraethyl-1,4,7-triazaheptane) and of $Cu(OH)_4^{2-}$ reacting with 2,3,2-tet and Et_2-2,3,2- tet. Lin also postulated that the rate-determining step shifts to second bond formation for the reactions of $Cu(OH)_4^{2-}$ with cyclam and Et_4dien. Utilizing the same approach, with cyclam as the reference ligand ($R'_S = k_{Cu(OH)_3}^{L}/k_{Cu(OH)_3}^{Cyclam}$). Chen *et al* [8] proposed that second-bond formation is the rate-determining step for the reaction of tet b with $Cu(OH)_3^-$ and $Cu(OH)_4^{2-}$. Following the same type of analysis used by Lin *et al.* [7], Taylor *et al.* has proposed that Jahn-Teller inversion following first bond formation (k_{1b}) is the rate determining step for the formation reactions of $Cu(OH)_3^-$ with Me_4trien and M_6trien and $Cu(OH)_4^{2-}$ with Me_4trien. The rate-

Table 2.14 Rate constant ratios for cyclic tetramine ligands reacting with $Cu(OH)_3^-$ at 25.0°C.

Ligand	$k^{L}_{Cu(OH)3}/k^{2\,3\,2\text{-tet}}_{Cu(OH)3}$ obsd[a]	predicted[b]	Comments[c]
2,3,2-tet	1.0	1.0	acyclic, PSSP
Cyclam	0.093	0.22	cyclic, SSSS
	0.27 (7)	0.22	cyclic, SSSS
C-mesoMe$_2$cyclam	0.05	0.22	cyclic, SSSS
Me$_2$cyclam	0.056 (7)	0.22	cyclic, SSSS
tet<u>a</u>	1.7×10^{-3}	0.22	cyclic, SSSS
tet<u>b</u>	2.4×10^{-3}	0.22	cyclic, SSSS
	3.2×10^{-3} (8)	0.22	cyclic, SSSS
[15]aneN$_4$	0.16	0.22	cyclic, SSSS
[16]aneN$_4$	0.22	0.22	cyclic, SSSS
THPC	0.038	$(5\text{-}30)\times10^{-3}$	cyclic, TTTT
(N-Me)$_4$cyclam	3.1×10^{-4}	$(5\text{-}30)\times10^{-3}$	cyclic, TTTT
Dioxocyclam	0.08	$(5\text{-}30)\times10^{-3}$ < value < 0.22	cyclic, SSS'S'

[a]Ratios calculated from values from Table 2.13.

[b]Predicted value for each ligand calculated as described in reference (6) from the following steric factors based on reactions of substituted amines: Et'NH$_2$/Et'N(H)ET = 8, Et'N(Me)$_2$/Et'N(Me)ET = 0.4 - 1.2, Et'N(H)Et'/Et'N(Me)Et' = 8 - 50 (Me = -CH_3, Et' = -C_2H_4-, Et = C_2H_5). Thus, for Et$_2$ - 2,3,2 - tet, R_S = (1+1+1+1)/(8+1+1+8) = 0.22, etc.

[c]Ligand type and N-substitution pattern: P = primary, S = secondary, T = tertiary, S' = amide nitrogen.

determining step shifts to second- bond formation for the reactions of $Cu(OH)_4^{2-}$ with Me_6trien. They also propose that second-bond formation or multiple desolvation as the rate-determining step for the reactions of the cyclic ligands $(N\text{-}Me)_4$cyclam and $2_N.1_o.1_o$ with $Cu(OH)_3^-$ and $Cu(OH)_4^{2-}$.

Table 2.15 lists the observed values of R_S' and R_S'' ($k_{Cu(OH)4}^{L}$ / $k_{Cu(OH)4}^{Cyclam}$) for the eight ligands studied in this work.

The rate-determining step for the reactions of cyclam, C-meso Me_2cyclam, [15]aneN_4, [16]aneN_4, THPC, and dioxocyclam with $Cu(OH)_3^-$ appears to be inversion following formation of the first axial Cu-N bond (compare R_S(observed) and R_S (predicted) Table 2.14). The low value (3.2) of $R_{3,4}$ for dioxocyclam suggests the same position of the rate-determining step for the reaction with $Cu(OH)_4^{2-}$. The reaction of $Cu(OH)_4^{2-}$ with cyclam, C-meso Me_2cyclam, [15]aneN_4, and THPC is slower than the corresponding reaction with $Cu(OH)_3^-$ ($R_{3,4} > 10$) implying that the rate determining step shifts to the formation of the second Cu-N bond.

Formation of the first chelate ring is likely to be more difficult for the tetraamines than for the diamide-diamine.

Thus the values of k_{2a} for the tetraamines are expected to be less than the corresponding value for the diamide-diamine. Also the values of k_{-1b} are presumably larger for reactions of $Cu(OH)_4^{2-}$ than those of $Cu(OH)_3^-$ (7). The fact that the observed value of $k_{Cu(OH)3}^{L}$ for the tetraamines is slightly less than that predicted based on steric effects may indicate some influence of the ring closure step. On the other hand $k_{Cu(OH)3}^{L}$ for dioxocyclam and THPC satisfactorily fall in the range predicted indicating that steric effect is minimum in these ligands. Since, the position of the rate-determining step were located and are the same for $k_{Cu(OH)3}^{L}$ and $k_{Cu(OH)4}^{L}$ for all ligands, except $k_{Cu(OH)4}^{L}$ for dioxocyclam and [16]aneN_4, it is of interest to compare the reactivities of these ligands. Based on the observed values of R'_S ($k_{Cu(OH)3}^{L}$ / $k_{Cu(OH)3}^{Cyclam}$), Table 2.14, the reactivities of these ligands

Table 2.15 Rate Constant Ratios for Cyclic Tetraamine Ligands Reacting with $Cu(OH)_x^{x-2}$ at 25.0 °C .

Ligand	$k^L_{Cu(OH)3} / k^{Cyclam}_{Cu(OH)3}$ obsd	$k^L_{Cu(OH)3} / k^{Cyclam}_{Cu(OH)3}$ predicted	$k^L_{Cu(OH)4} / k^{Cyclam}_{Cu(OH)4}$ obsd.
Cyclam	1.0	1.0	1.0
C-mesoMe$_2$cyclam	0.49	1.0	0.18
	0.6 [a]	1.0	0.11 [a]
Tet a	0.018	1.0	5.1×10^{-3}
Tet b	0.026	1.0	0.02
	0.033 [b]	1.0	1.4×10^{-3} [b]
[15]aneN$_4$	1.720	1.0	0.89
[16]aneN$_4$	2.370	1.0	---------
THPC	0.40	0.02 - 0.13	0.250
Dioxocyclam	0.82	0.03 < value > 1.0	3

[a] Ref. (7) ; [b] Ref. (8) .

increase in the order THPC < C-<u>meso</u>Me_2cyclam < dioxocyclam < cyclam < [15]aneN_4 < [16]aneN_4. It is worth mentioning that this order of ligand reactivities is not necessarily the same if comparison is made on the basis of R"$_s$ ($k_{Cu(OH)4}{}^{L}$ / $k_{Cu(OH)4}{}^{Cyclam}$) at least for the ligand [15]aneN_4. The high value (3) of R"$_s$ for dioxocyclam indicates a shift in the position of the rate determining step. The observed values (0.22 and 0.16) of R_s (Table 2.14) for [16]aneN_4 and [15]aneN_4 are almost equal to the calculated values relative to the reference linear ligand 2,3,2-tet. These observations confirm that ligand cyclization itself has only a relatively small influence upon the complex formation rate constants. This influence diminishes as the ring size increases. Previous studies have revealed that the more significant kinetic effects arise from substitution at the nitrogen donor atoms of the linear ligand (e.g. Me_6trien) or of the cyclic ligand (e.g. (N-Me)$_4$cyclam) or on the alkyl backbone of both type of ligands[6-8]. However, THPC with arms possessing donor groups show completely different behaviour in which the steric effects were compensated for by the active arms:

($k_{Cu(OH)3}{}^{THPC}$ / $k_{Cu(OH)3}{}^{(N\text{-}Me)4Cyclam}$ = 123 and $k_{Cu(OH)4}{}^{THPC}$ /$k_{Cu(OH)4}{}^{(N\text{-}Me)4Cyclam}$ > 2000).

This increased rate of complexation is probably a consequence of fast initial coordination of $Cu(OH)_x{}^{2-x}$ by the flexible hydroxypropyl arm followed by the first slow Cu-N bond formation .

Examination of Table 2.16 indicates that the lower formation constants of [16]aneN_4 (log K_{CuL} = 18.9) compared with [15]aneN_4 (log K_{CuL} = 24.5) and of the latter compared with cyclam (log K_{CuL} = 27.2) is thus due to a more rapid dissociation of the 15-, and 16-membered ring from copper(II) and not to formation rate differences (Chapter 1).

The observed values of R'$_s$ for tet <u>a</u> and tet <u>b</u> are about 55 and 38 times smaller than the calculated values. Thus, it appears that the rate-determining step for the

Table 2.16 Kinetic and equilibrium data for copper(II) reacting with macrocyclic ligands at 25.0 °C.

Ligand	log K_{CuL} [a]	$k^{L}_{Cu(OH)_3}$, $M^{-1}s^{-1}$	k_H [b], $M^{-1}s^{-1}$
cyclam	27.2	9.3×10^{5}	very small
[15]aneN_4	24.4	1.6×10^{6}	4×10^{-3}
[16]aneN_4	18.9	2.2×10^{6}	2.6
dioxocyclam	9.50	7.6×10^{6}	4.8×10^{2}
THPC	.....	3.8×10^{5}	11.71

[a] Obtained from equilibrium measurement.

[b] Obtained as the slope of the linear approximation of k_{obs} vs. $[H^+]$.

reaction of these ligands with $Cu(OH)_3^-$ has shifted to the formation of the second axial Cu-N bond. The relatively low value (~15) of $R_{3,4}$ for tet b suggests the same position of the rate-determining step for the reaction with $Cu(OH)_4^{2-}$. The previous study on the tet b system[8] has reported the same conclusion, although the value of $R_{3,4}$ in their results was substantially higher ($R_{3,4}$ = 281). On the other hand, the reaction of tet a with $Cu(OH)_4^{2-}$ is considerably slower than the corresponding reaction with $Cu(OH)_3^-$ ($R_{3,4} > 42$), implying that the rate-determining step, probably, shifts to inversion following second axial Cu-N bond formation .

It is interesting to note that first-bond formation is the rate-determining for the reaction $Cu(OH)_3^-$ with cyclam, C-meso Me_2cyclam, [15]aneN_4, [16]aneN_4, THPC and dioxocyclam. Second-bond formation is rate-determining for the $Cu(OH)_3^-$ reaction with tet a and tet b. This sterically induced shift in the rate-determining step can be explained with reference to Figure 2.1. In the reaction of tet a or tet b, the formation of the Cu-N(b) or Cu-N(d) bond is expected to be faster than the formation of the Cu-N(a) or Cu-N(c) due to steric effects. Accordingly, the first coordinate bond formation with N(b) or N(d) is expected to represent the predominant reaction route with tet a or tet b ($k_{1a} >> k_{2a}$). Second-bond formation involves the formation of the Cu-N(a) or Cu-N(c) bond, and the large steric effects resulting from the methyl groups on tet a (or tet b) related to the crowding of coordinated water molecules is expected to retard the formation of the second Cu-N bond (k_{2a}) and to accelerate the reelongation of the Cu-N bond (k_{-1b}). This would greatly suggest that $k_{-1b} > k_{2a}$, resulting in a shift of the rate-determining step to the point of second-bond formation (k_{2a}). The major difference between the tet a and tet b systems is in the reaction with $Cu(OH)_4^{2-}$. With tet a the rate determining step is shifted to second Jahn-Teller step ($k_{2b} < k_{-2b}$) this effect may be due to the difficulty of folding tet a during complex formation. The tet b ligand is known to readily fold to give *cis* complexes with the (RRRR, SSSS) *sec* NH configuration. Tet a only folds with difficulty and normally gives *trans* complexes with

the ligand occupying the equatorial sites. Since complexation must involve the sequential loss of the solvento ligands from copper(II), a *cis*- complex with the ligand in a folded configuration must be initially formed. Thus tet b reacts with $Cu(OH)_x^{2-x}$ to give initially a blue 5-coordinate complex $[Cu(tet\ b)(OH)(blue)]^+$ with the ligand folded[8] . This kinetically controlled blue product is readily converted to the more thermodynamically stable red isomer, and the kinetics of the blue - to - red conversion have been reported[13]. Unstable blue intermediates were also observed in the reactions of copper (II) with teta and other highly substituted tetramines[14]. The kinetics of the $[Cu(tet\ a)(OH)blue]^+$ to $[Cu(tet\ a)(OH)red]^+$ interconversion have been discussed[8], the conversion involves the intermediacy of the hydroxo-complex which leads to intramolecular specific base catalysis. Some degree of ligand twisting or folding may be necessary to avoid multiple desolvation occuring prior to the rate determining step. The formation of the blue species is due to the folding or twisting of the macrocyclic ligand[8]. Figure 2.16 represents a modified version of the reaction scheme shown in Figure 2.15 expanded to include a possible multiple-desolvation process. Such a process is not likely for the first Cu-N bond formation but may occur prior to the formation of the third Cu-N[6].

It is noteworthy to realise that blue intermediates were not observed for the reaction of less sterically hindered ligands such as cyclam, C-meso-Me_2cyclam...etc. with $Cu(OH)_x^{2-x}$. Steric effects appear to stabilise intermediate of type (I) which are

then converted by the base catalysed inversion of chiral *sec*-NH centres to the planar RSSR (SRRS) diastereoisomers.

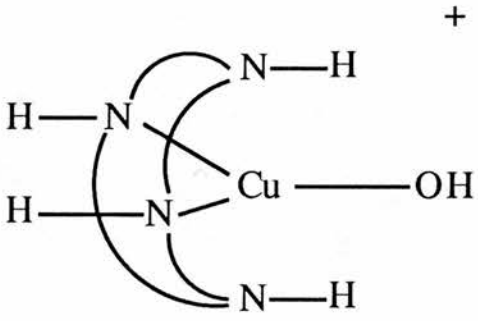

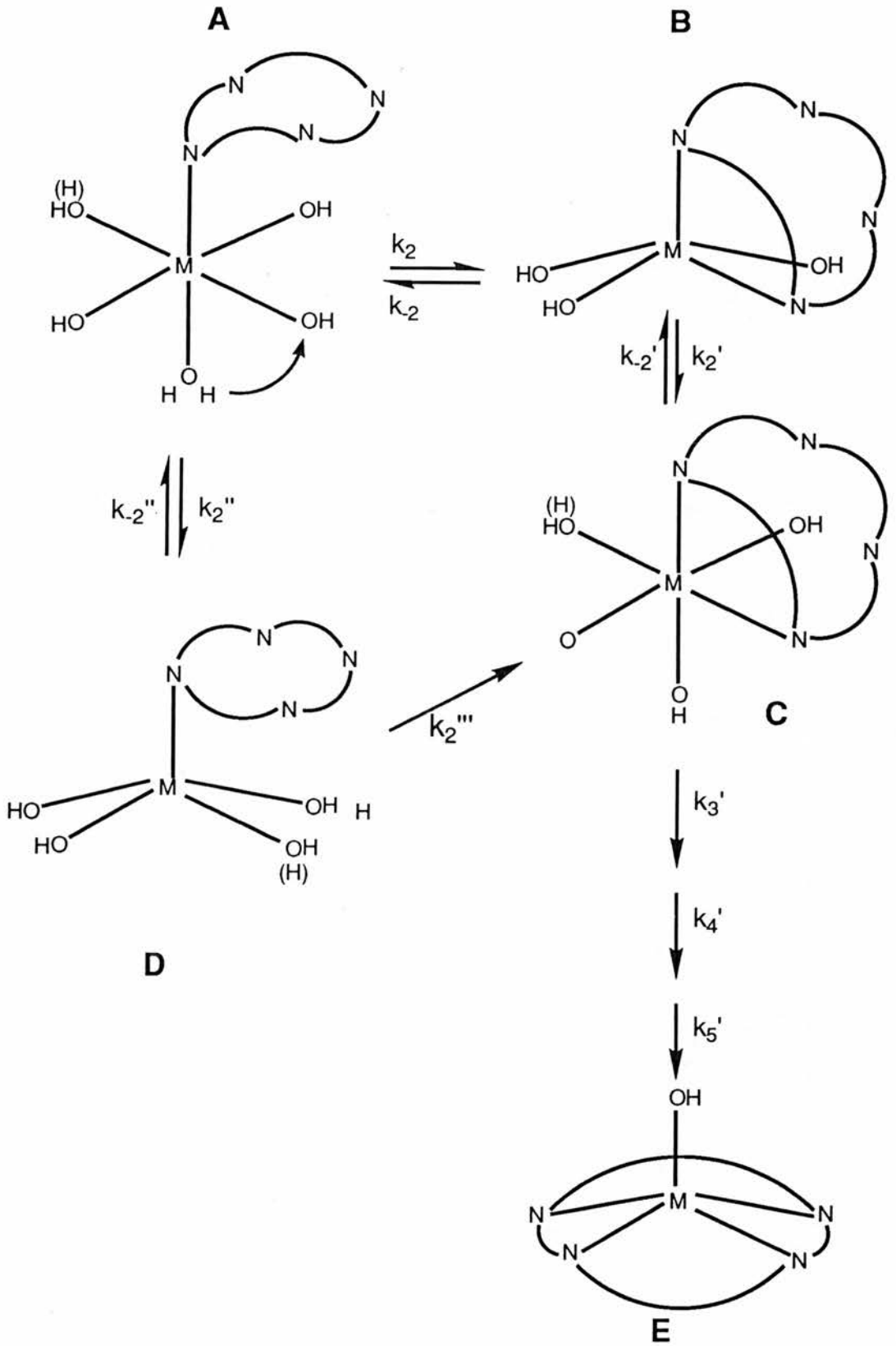

Figure 2.16 Schematic representation of possible multiple-desolvation process in the complexation of Cu(II) by tetradentate polyamine . Only steps subsequent to first bond formation are shown , and Jahn-Teller inversions have been omitted .

As the ligands become more highly substituted, the observed rate constants may reflect an increasing contribution from the multiple-desolvation process due to crowding between the partially bound ligand and the remaining solvent molecules, i.e., $k_2' \simeq k_{-2}$, path ABC or $k_2''' \approx k_{-2}''$, path ADC in Figure 2.16. The large values of $R_{3,4}$ for $(N\text{-}Me)_4$ cyclam, and tet a are also consistent with the scheme shown in Figure 2.16 and suggest that multiple desolvation subsequent to first-bond formation affects reactions involving $Cu(OH)_4^{2-}$ to a larger extent than reactions of $Cu(OH)_3^-$. A multiple-desolvation step for $Cu(OH)_4^{2-}$ subsequent to first Cu(II)-N bond formation would require the loss of at least one coordinated hydroxide molecule from the $Cu(OH)_n$ - ligand intermediate species.

In conclusion, the rate of complexation reactions parallel the ring size, so as the ring size increased the rate of complexation also increased and the rate-determining step appears to shift from the rearrangement following first-bond formation to second-bond formation as the reactant goes from $Cu(OH)_3^-$ to $Cu(OH)_4^{2-}$.

The steric effects attributable to the substituted methyl groups on tet a and tet b retard the forward steps and accelerate the backward steps of the complexation reactions resulting in a shift of the rate- determining step to the point of second-bond formation for $Cu(OH)_3^-$ or $Cu(OH)_4^{2-}$ reacting with tet b and $Cu(OH)_3^-$ reacting with tet a. The rate-determining steps appear to shift to inversion or multiple desolvation for the reaction of $Cu(OH)_4^{2-}$ with tet a.

2.5 References:

1. Cooper has specifically noted that structural constraints within many macrocyclic ligands may predispose the ligands towards geometries that diminish the entropy associated with complex formation: S.R.Cooper and S.C. Rawle, *Struc. Bonding*,**72**, 1 (1989).

2. B.C. Westerby, K.L. Juntunen, G.L. Leggett, V.B.Pett, M.J. Koenigbauer, M.D. Purgett, M.J., Taschner, L.A. Ochrymowycz, and D.B. Rorabacher, *Inorg. Chemistry*, **30**, 2109 (1991) and references therein.

3. D,W,Margerum, G.R. Cayley, D.C. Weatherburn and G.K. Pagenkopf, *Advances in Chemistry Series*, **174**, 1 (1978).

4. R.M. Izatt, J.S. Bradshaw, S.A. Neilsen, J.D. Lamb, and J. Christensen, *J. Chem. Rev.*, **85**, 271 (1985) and references therein.

5. The terms *exo* and *endo* relative to macrocyclic conformers are used to indicate whether the lone electron pairs on the ligand donor atoms are oriented away from or towards the central cavity, respectively: R.E. Desimone and M.D. Glick, *J. Am. Chem. Soc.*, **98**, 762 (1976).

6. J.A. Drumhiller, F. Montavon, J.M. Lehn, and R.W. Taylor, *J. Inorg. Chem.*,**25**, 3751 (1986) and references therein.

7. C.T. Lin, D.B. Rorabacher, G.R. Cayley, D.W. Margerum, *J. Inorg. Chem.*, **14**, 919 (1975).

8. F.T. Chen, C.S. Lee, C.S. Chung, *Polyhedron*, **2**, 1301 (1983).

9. R.A. Kolinski and B. Korybut-Daszkiewicz, *Bull Acad Polon Sci., Ser. Sci Chim.*, **17**, 13 (1969).

10. P. Gans, A. Sabatini, and A. Vacca, *J. Chem. Soc., Dalton Trans.* 1195 (1985).

11. L.A. McDowell and H.L. Johnston. *J. Am. Chem. Soc.*,**58**, 2009 (1936).

12. D.W. Margerum, G.R. Cayley, D.C. Weatherburn, and G.K. Pagenkopf, in "Coordination Chemistry", Vol. 2a, A.E. Martell, Ed., American Chemical Society Publications, Washington, D.C.

13. B.F. Liang and C.S. Chung, *J. Chem. Soc., Dalton Trans* , 1349 (1980).

14. B.F. Liang, Ph.D. Thesis, Tsing Hua University (1980).

CHAPTER 3

LIGAND EXCHANGE REACTIONS. KINETIC STUDIES OF THE REACTION OF [14]aneN$_4$, [15]aneN$_4$ AND [16]aneN$_4$ WITH THE COPPER (II) COMPLEXES OF DIGLYCINE AND TRIGLYCINE.

3.1 INTRODUCTION:

Ligand Exchange with Copper(II) Complexes:

The ligand exchange reactions of Cu(L-histidine) with human serum albumin and glycylglycylhistidine have been studied at pH 7.53[1]. The exchange reactions were found to occur via the formation of a thermodynamically stable ternary complex of the type L-histidine- Cu(II)-albumin or L-histidine-Cu(II)-diglycyl-L-histidine. The exchange rate from L-histidine to albumin was 0.67 s^{-1}. When the exchanging ligand is a strong chelator the exchange occurs without any detectable intermediate. Thus triethylenetetraamine (2,2,2-tet) reacts rapidly with doubly deprotonated (tripeptido) cuprate(II) complexes to give $[Cu(2,2,2\text{-tet})]^{2+}$ and the free tripeptide. The rates of 2,2,2-tet displacement of tripeptides from Cu(II) are very dependent upon the nature of the tripeptide. The replacement reaction proceeds by two general mechanisms: (1) an acid assisted mechanism in which a proton is transferred to a peptide nitrogen to assist the dissociation of the peptide, (2) a nucleophilic mechanism in which the displacing ligand coordinates to copper and accelerates the breaking of the copper-peptide nitrogen bonds[2].

The present work deals with the reaction of the 14-, 15-, and 16- membered macrocyclic tetraamines, [14]aneN$_4$, [15]aneN$_4$, and [16]aneN$_4$ with copper(II) glycylglycinate $CuH_{-1}G_2$ and copper(II) glycylglycylglycinate $CuH_{-2}G_3^-$, in the pH range 7.5 - 10. The compounds studied are shown in Figure 3.1(a) and (b) .

3.2 EXPERIMENTAL

Reagents:

The di- and tripeptides (G_2 and G_3) were obtained from Aldrich. The synthesis, analysis, and standardisation of the 14-, 15-, and 16-membered macrocycles is

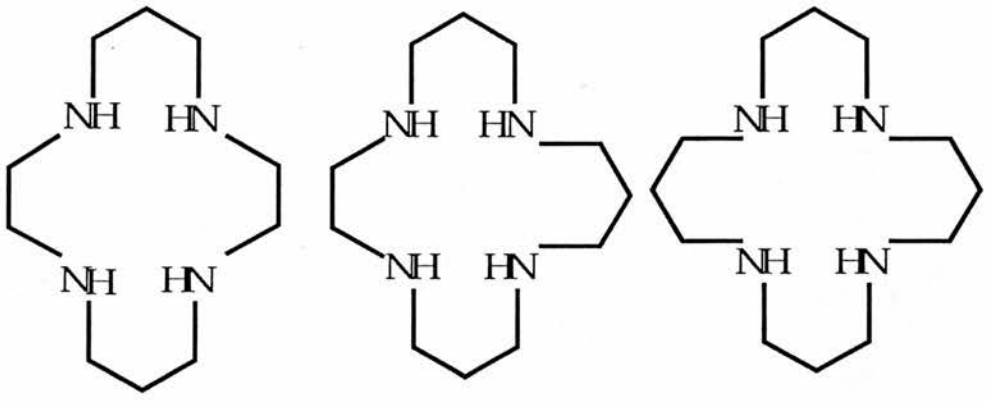

L^1 = cyclam L^2 = [15]aneN$_4$ L^3 = [16]aneN$_4$

Figure3.1a The ligands studied in this work.

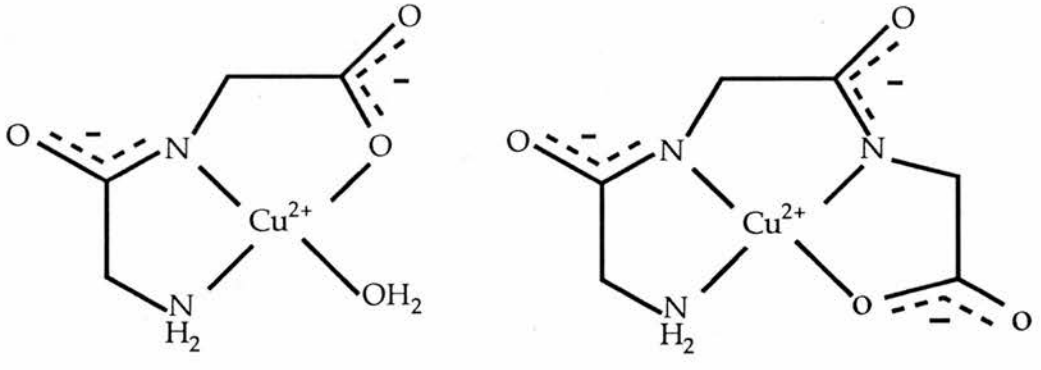

$[CuH_{-1}G_2]$ $[CuH_{-2}G_3]^-$

Figure3.1b The copper(II) di- and tripeptide complexes studied in this work.

described in Chapters 1 and 2. The deprotonated dipeptide and doubly deprotonated tripeptide complexes of copper(II), $CuH_{-1}G_2$ and $CuH_{-2}G_3^-$, were prepared in solution by the slow addition of NaOH to a solution of copper(II) chloride and the peptide (1:2 mole ratio) in 0.02 mol dm^{-3} HEPES buffer until a pH of 7.5 to 10.5 was attained. A colour change from blue to violet occurs on amide deprotonation (above pH 6). The copper peptide solutions were freshly prepared for each set of experiments. The ionic strength was maintained at 0.15 mol dm^{-3} with NaCl.

Methods:

All pH values were measured using Orion Research Ionalyzer type 901 in the pH mode. The pH meter was provided with Orion glass (91-01) and calomel (90-05-00) electrodes. The electrode system was calibrated before use with two NBS buffers pH 9.00 and 6.87 at 25 °C.

The reactions of the macrocycles and the copper(II) peptide complexes were studied under pseudo first-order conditions ([Cu-peptide] > 10 [Ligand]) at 25.0 °C. A Union Giken stopped flow spectrophotometer type RA-401 was used to monitor the kinetics. The initial concentration of the macrocyclic ligand was kept constant at $1x10^{-4}$ mol dm^{-3} and the concentration of the copper(II) dipeptide varied from 1×10^{-3} to 6×10^{-3} mol dm^{-3}. For the tripeptide system the initial ligand concentrations were maintained at 2×10^{-4} mol dm^{-3} while that of $CuH_{-2}G_3^-$ was in the range $(2 - 6)x10^{-3}$ mol dm^{-3}. The reaction monitored is shown in equation (1)

$$\text{Cu-peptide} + L_T \longrightarrow CuL_T + \text{peptide} \qquad (1)$$

where L_T represents the sum of all protonated and unprotonated forms of the uncomplexed ligand and [Cu-peptide] represent all forms of the copper di- and tripeptide complexes. The six systems studied could be fitted to the rate expression (2)

$$\text{Rate} = k_f\,[\text{Cu-peptide}]\,[L_T] + k_d[L_T] \qquad (2)$$

where k_f and k_d represent the rate constants for complex formation and solvolytic path ways respectively. For each system, a series of kinetic determinations were carried out at several pH values under conditions where [Cu-peptide] >> $[L_T]$, to yield the pseudo-first-order rate expression

$$d[CuL_T]/dt = k_{obs}\,[L_T] \qquad (3)$$

for which the observed first-order rate constants, k_{obs} could be obtained from the integrated form

$$\ln [CuL_T]_e / ([CuL_T]_e - [CuL_T]_t) = \ln A_e / (A_e - A_t) = k_{obs} \cdot t \qquad (4)$$

which can then be analysed directly. In this expression, $[CuL_T]_t$ represents the total concentration of the copper complex at time t , $[CuL_T]_e$ represents the equilibrium concentration of the copper complex, A_t and A_e are the corresponding values of the absorbance due to the copper complex measured at λ_{max} (in the range 470 - 550 nm), and t is the elapsed time for each measurement of A_t.

The formation kinetics at each pH value were measured at a minimum of four copper-peptide concentrations. For each set of concentration conditions, an average of six kinetic runs were carried out and the results statistically averaged. The resulting set of k_{obs} values obtained at each specific pH was then resolved to yield the constituent k_f and k_d values by means of the linear relationship

$$k_{obs} = k_f\,[\text{Cu-peptide}] + k_d \qquad (5)$$

Curve fitting was carried out with the Grafit program (Erithacus Software).

Potentiometric Titrations:

Potentiometric titrations of the ligand in the absence and presence of copper(II) chloride were carried out as described in Chapter 4, using a Radiometer Titralab System interfaced with an Apple IIe computer. The formation constants were calculated using the SUPERQUAD program[3] .

3.3 RESULTS

3.3.1 Copper(II) exchange from diglycine to the macrocyclic ligand: The hydroxo complex, $(CuH_{-1}G_2(OH))^-$.

The copper(II) complex with glycylglycine (G_2) is obtained by the addition of the dipeptide to an aqueous solution of Cu^{2+} ion (2 : 1 mole ratio) above pH 6[4] . This complex solution was titrated with 0.1 mol dm^{-3} sodium hydroxide solution at ionic strength of 0.15 mol dm^{-3} maintained with sodium chloride.

The titration curve obtained is shown in Figure 3.2(a). The first buffer zone around pH 5 shows the formation of $[CuH_{-1}G_2]$ with the loss of two protons. The second relatively flat buffer zone and a weak inflection occurs in the higher pH region where deprotonation of a coordinated water occurs[5]. The loss of two protons followed by the third at higher pH is illustrated by the corresponding two peaks in the derivative form of the titration curve (Figure 3.2(b)). At high pH the following two equilibria can be considered.

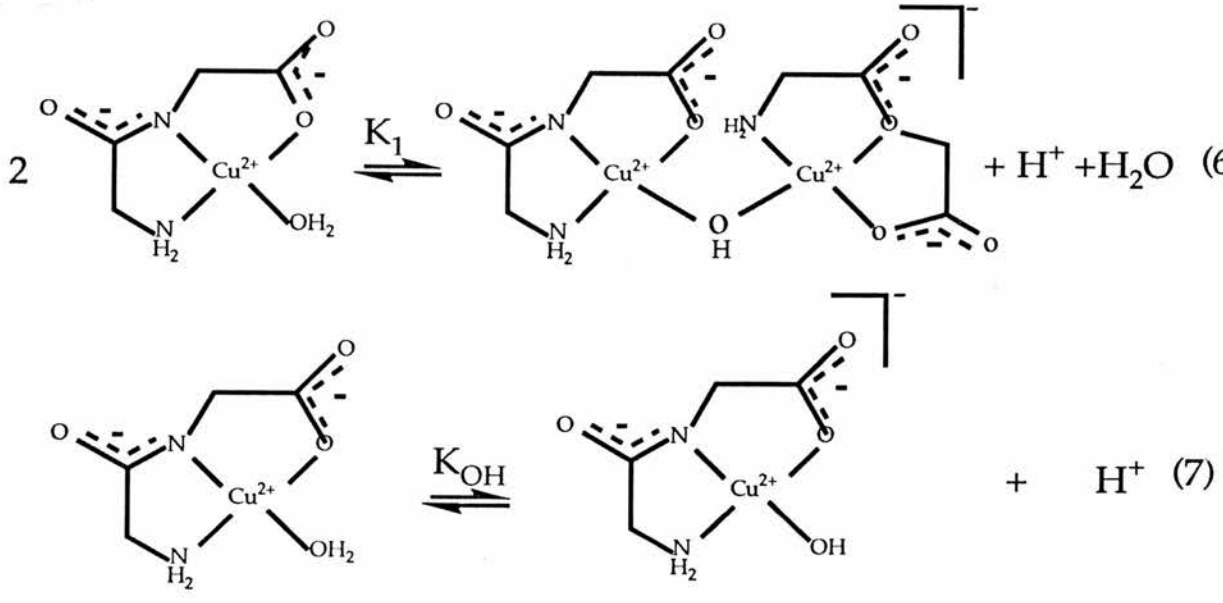

The first equilibrium constant K_1 relates to the formation of the μ-hydroxo binuclear complex (maximum formation is < 5% at pH 9.2, Figure3.3), and the second equilibrium constant K_{OH} to the formation of the hydroxo complex. From the titration pK_1 and pK_{OH} were calculated to be, 5.01 and 9.39 respectively in good agreement

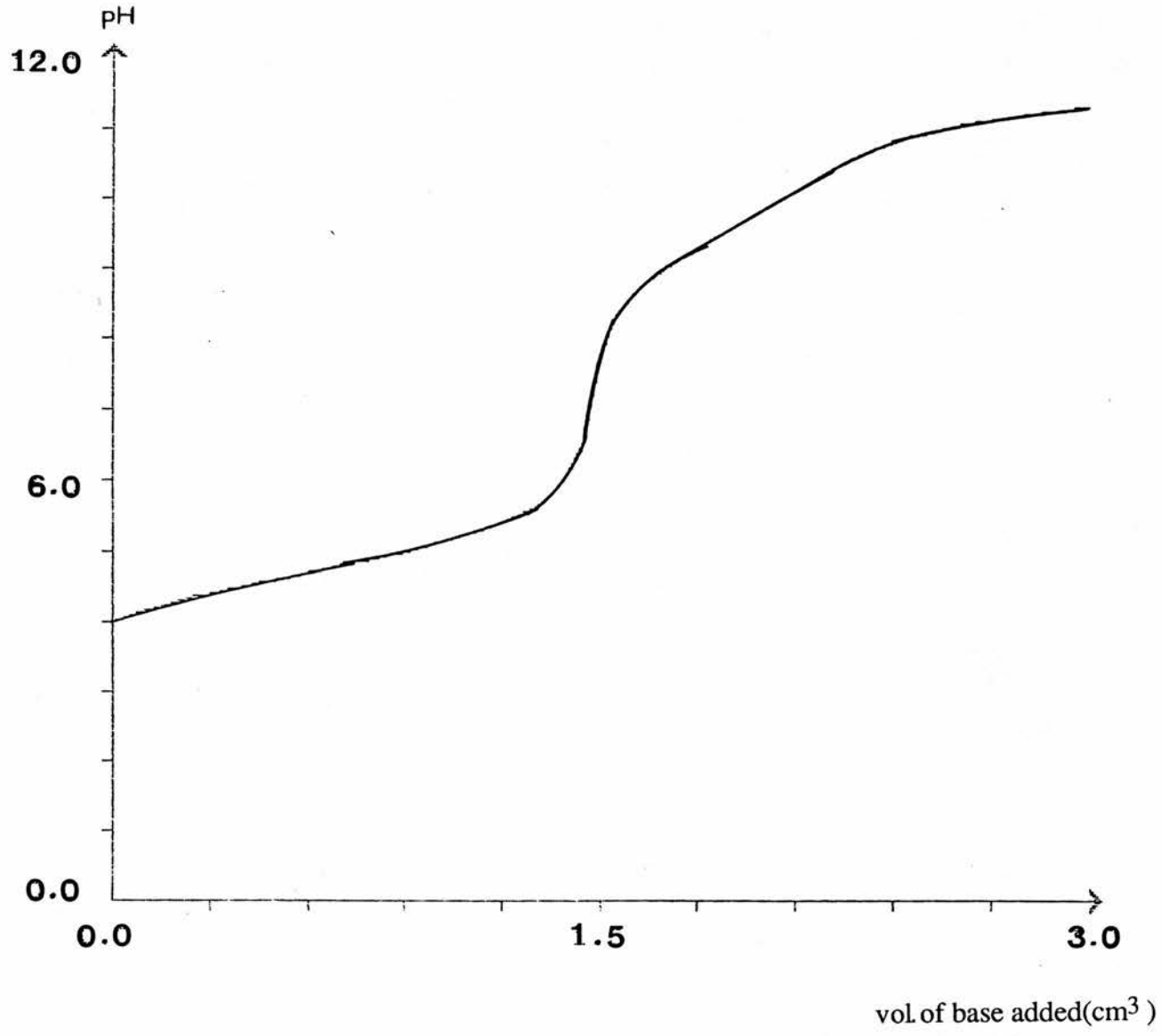

Figure 3.2a Potentiometric titration curve for glycylglycine-cupric chloride system at 25.0 °C and I = 0.15 mol dm^{-3} with NaCl: [copper(II)]= [glycyglycine] = 3.0 x 10^{-3} mol dm^{-3}; [NaOH] = 0.098 mol dm^{-3}.

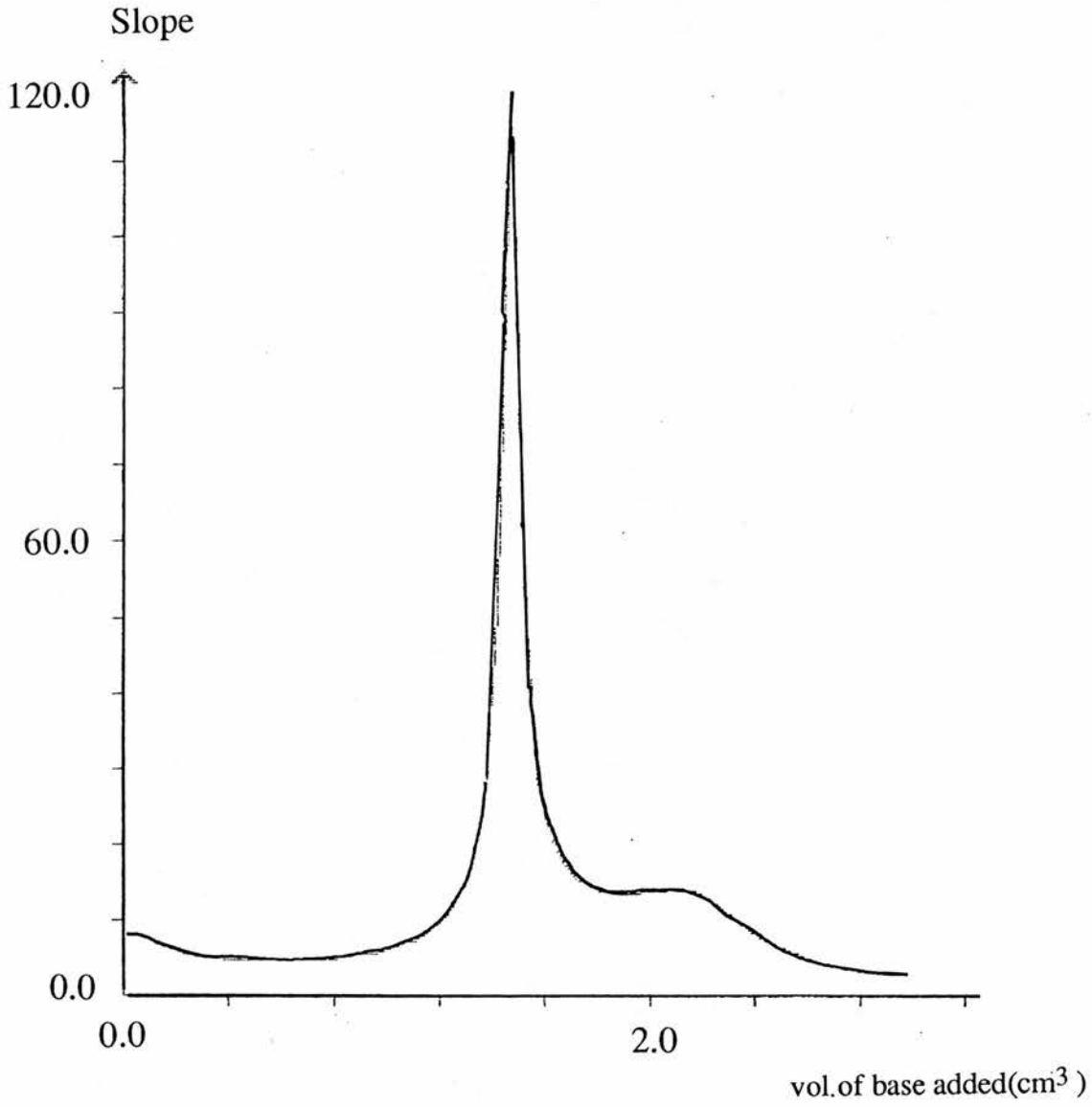

Figure 3.2 b Derivative form of the titration curve in Figure 3.2a .

with previous results (pK_1 = 5.06 and pK_{OH} = 9.31; I = 1.0 M ($NaClO_4$)[5]. The deprotonated complex $CuH_{-1}G_2$ becomes the major species in solution above pH 9.0, Figure 3.3.

Ligand Species.

For the three ligands included in this work, the protonation equilibria of the macrocycle (L) can be represented as follows .

$$L + H^+ \rightleftharpoons HL^+ \quad (8)$$

$$HL^+ + H^+ \rightleftharpoons H_2L^{2+} \quad (9)$$

$$H_2L^{2+} + H^+ \rightleftharpoons H_3L^{3+} \quad (10)$$

$$H_3L^{3+} + H^+ \rightleftharpoons H_4L^{4+} \quad (11)$$

The protonation constants were treated as mixed-mode values as defined by the relationships

$$K_1 = [HL^+]/ a_H[L] \quad (12)$$

$$K_2 = [H_2L^+]/ a_H[HL^+] \quad (13)$$

$$K_3 = [H_3L^{3+}]/ a_H[H_2L^{2+}] \quad (14)$$

$$K_4 = [H_4L^{4+}]/ a_H[H_3L^{3+}] \quad (15)$$

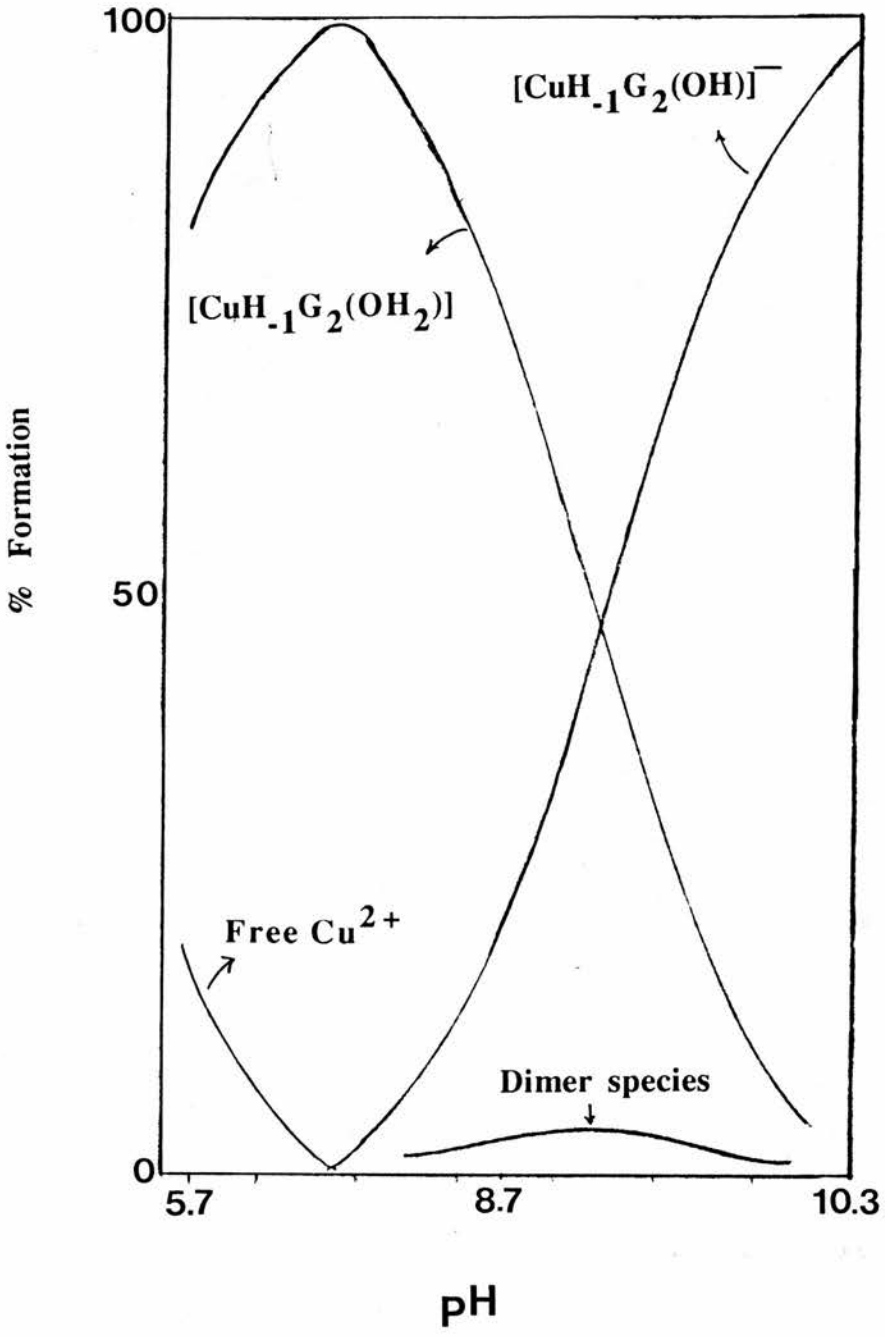

Figure 3.3 Speciation diagram of copper(II) glycylglycinate .

where a_H represents the activity of the hydrogen ion obtained from the pH. The results of Table 3.1 show that log K_3 and log K_4 is strongly influenced by the ring size whereas logK_2 and logK_1 are relatively insensitive to ring size .

Table 3.1 Protonation constants for the macrocyclic tetraamines at 25 °C and I = 0.4 mol dm^{-3} KNO_3[1].

Ligand	log K_1	log K_2	log K_3	log K_4
[14]aneN_4	11.050(0.003)	10.311(0.010)	< 2	< 2
[15]aneN_4	11.180(0.010)	10.310(0.010)	5.210(0.020)	3.550(0.020)
[16]aneN_4	10.630(0.020)	9.570(0.030)	7.480(0.040)	5.780(0.040)

Resolution of specific rate constants:

The exchange kinetics for the reaction of [$CuH_{-1}G_2$] with L to give [CuL^{2+}] were studied at 25.0 °C and I = 0.15 mol dm^{-3} (NaCl). In the pH range of the measurements the predominant ligand species (> 99%) is [H_2L^{2+}] (Chapter 4).The copper(II) glycylglycinate complex exists as a mixture of [$CuH_{-1}G_2(OH_2)$][2] and [$CuH_{-1}G_2(OH)$]$^-$. Kinetic measurements were made over the pH range 7.5-9.0 to determine the rate constants k_A and k_B for the reactions (16) and (17).

$$HL^+ + [CuH_{-1}G_2(H_2O)] \longrightarrow [CuL^{2+}] + G_2 \; ; \; k_A \qquad (16)$$

[1]Standard deviations are given in paranthesis.

[2][$CuH_{-1}G_2(OH_2)$] and [$CuH_{-1}G_2$] are same complex species.

$$HL^{+} + [CuH_{-1}G_2(OH)^{-}] \longrightarrow [CuL^{2+}] + G_2 + OH^{-} ; k_B \qquad (17)$$

As the copper(II) concentration was in large excess, pseudo-first-order conditions were fulfilled and excellent first-order plots for all three systems were observed. At constant copper(II) glycylglycinate concentration, values of k_{obs} increased as the pH increased, suggesting that $[HL^{+}]$ is the reactive species with $[CuH_{-1}G_2]_T$. All of the reactions were found to include a pathway involving H_2O (k_d), following the rate expression

$$\text{Rate} = k_f [CuH_{-1}G_2]_T [HL^{+}] + k_d$$

In the three systems two kinetic steps were detected. The initial reaction is fast, and is associated with decrease in absorbance, and this is followed by a slower reaction which involves an increase in absorbance. The fast step was in the 20 - 50 ms range and was independent of pH or the concentration of copper(II) glycylglycinate. The slow step was dependent on both the pH and the initial concentration of copper(II) glycylglycinate (for example Figure 3.4 for the [14]aneN$_4$ system). An induction period of about 10 - 15 s following the slow step was observed, which was followed by two or more consecutive steps associated with a decrease in absorbance. The slow step only was considered in this work. The values of k_{obs} for the three ligands at various $[CuH_{-1}G_2]$ and pH's are listed in Table 3.2. Plots of k_{obs} *vs* $[CuH_{-1}G_2]_T$ gave straight lines with slope k_f and positive intercept k_d, Figures 3.5 - 3.7.

Table 3.2 show that values of k_{obs} decreased as pH increased , and the rate of the exchange reaction can be represented by equation (18)

$$\text{Rate} = k_f[CuH_{-1}G_2]_T[L_T] + k_d$$

$$= (k_A[CuH_{-1}G_2(OH_2)] [L_T] + k_B[CuH_{-1}G_2(OH)] [L_T]) + k_d \qquad (18)$$

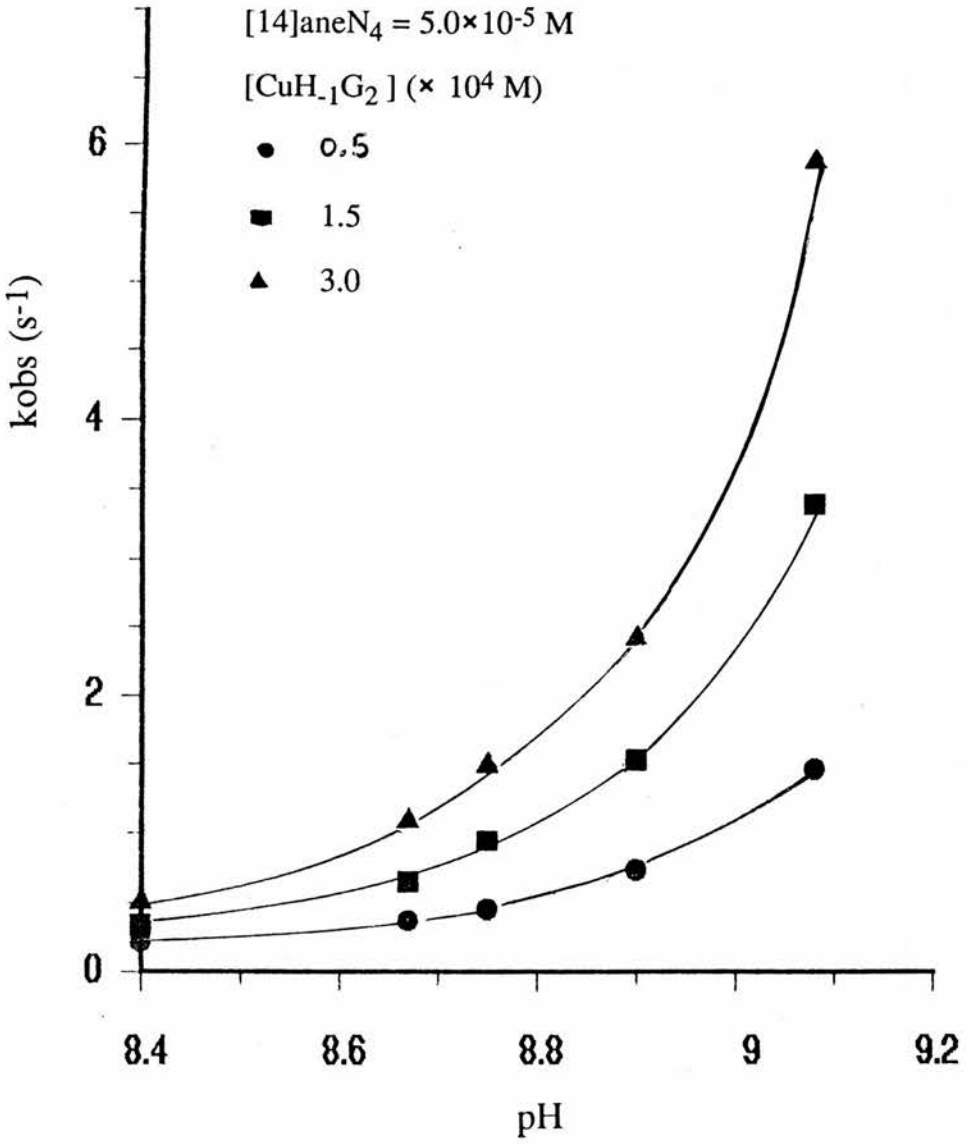

Figure 3.4 Observed pseudo first-order rate constants as function of pH and copper(II)-glycylglycinate .

Table 3.2 Observed Rate Constant Values for Copper(II)-Glycylglycinate Reacting with Tetra-azamacrocycle L (5.0×10^{-5} mol dm^{-3}) at 25.0 °C and I = 0.15 mol dm^{-3}.

pH	10^3x[$CuH_{-1}G_2$] mol dm^{-3}	k_{obs} s^{-1}	pH	10^3x[$Cu_{-1}G_2$] mol dm^{-3}	k_{obs} s^{-1}	pH	10^3x[$CuH_{-1}G_2$] mol dm^{-3}	kobs s^{-1}
	L = [14]aneN_4			L = [15]aneN_4			L = [16]aneN_4	
8.40	0.50	0.20	7.80	0.50	0.34	8.40	0.50	0.13
8.40	1.50	0.33	7.80	1.25	0.52	8.40	1.13	0.21
8.40	2.50	0.45	7.80	2.25	0.75	8.40	1.75	0.35
8.40	3.00	0.50	7.80	3.00	0.96	8.40	2.38	0.44
8.57	0.50	0.36	8.11	0.50	0.40	8.40	3.00	0.61
8.57	1.50	0.65	8.11	1.00	0.63	8.60	0.50	0.24
8.57	3.00	1.10	8.11	2.00	1.10	8.60	1.13	0.46
8.75	0.50	0.45	8.11	3.00	1.65	8.60	1.75	0.70
8.75	1.50	0.94	8.23	0.50	0.60	8.60	2.38	0.89
8.75	2.50	1.28	8.23	1.50	1.34	8.60	3.00	1.07
8.75	3.00	1.49	8.23	3.00	2.70	8.80	0.50	0.39
8.90	0.50	0.73	8.29	0.50	0.70	8.80	1.13	0.93
8.90	1.50	1.53	8.29	2.00	2.25	8.80	1.75	1.40
8.90	3.00	2.42	8.29	3.00	3.42	8.80	2.38	1.95
9.08	0.50	1.46	8.44	0.50	1.10	8.80	3.00	2.50
9.08	1.00	2.15	8.44	1.25	2.70	8.93	0.50	0.70
9.08	1.50	3.39	8.44	2.25	4.10	8.93	1.25	1.40
9.08	3.00	5.88	8.44	3.00	5.20	8.93	1.75	2.30
—	—	—	8.50	0.50	1.57	8.93	2.38	3.10
—	—	—	8.50	1.25	3.40	8.93	3.00	3.70
—	—	—	8.50	2.25	5.60	9.07	0.50	1.30
—	—	—	8.50	3.00	7.25	9.07	1.13	2.50
—	—	—	—	—	—	9.07	1.75	4.60
—	—	—	—	—	—	9.07	2.38	6.00

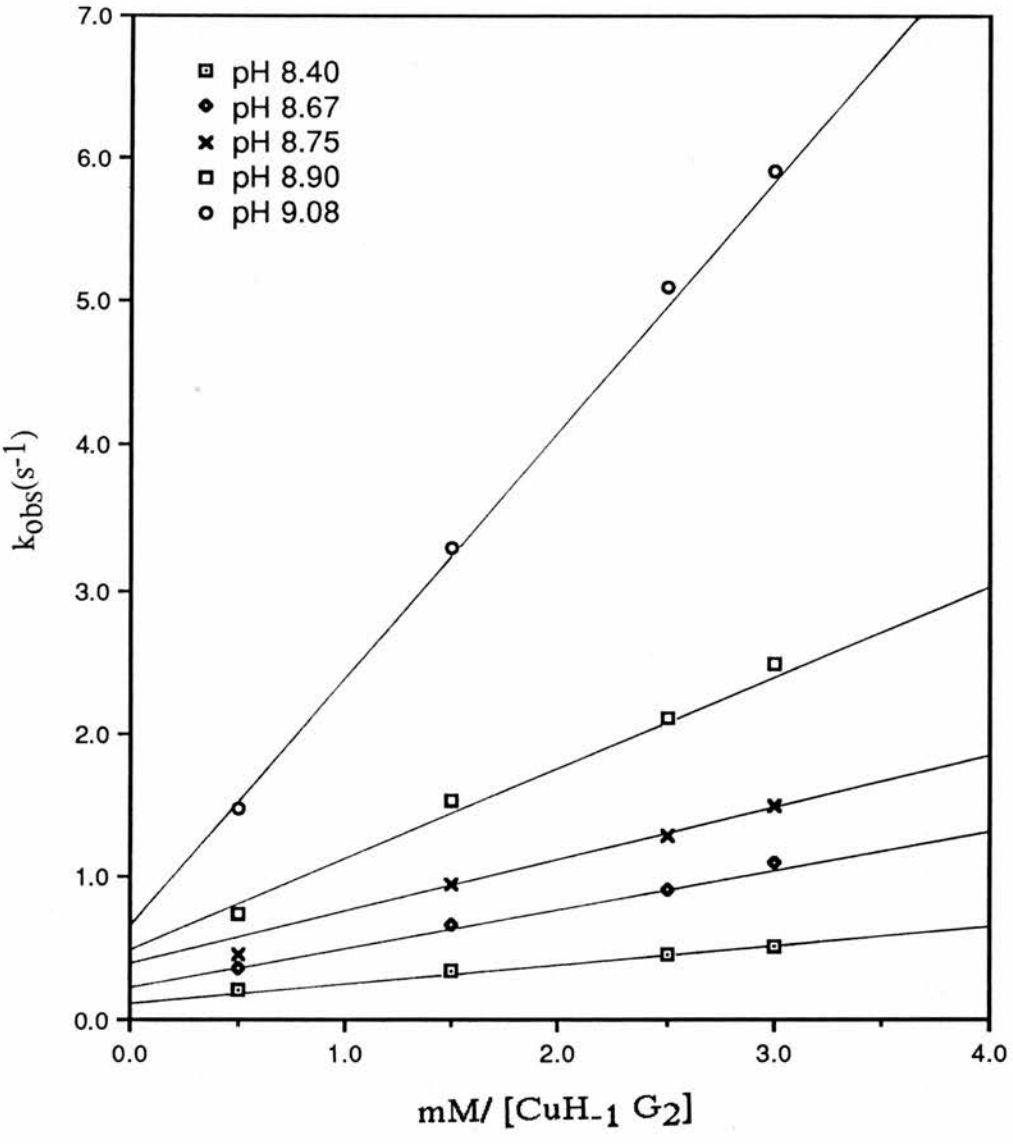

Figure 3.5 Dependence of the first-order rate constants (25.0 °C, I = 0.15 mol dm^{-3}) for the reaction of [14]aneN$_4$, initially 5.0 x 10^{-5} mol dm^{-3}, with excess concentrations of [CuH$_{-1}$G$_2$] at various pH.

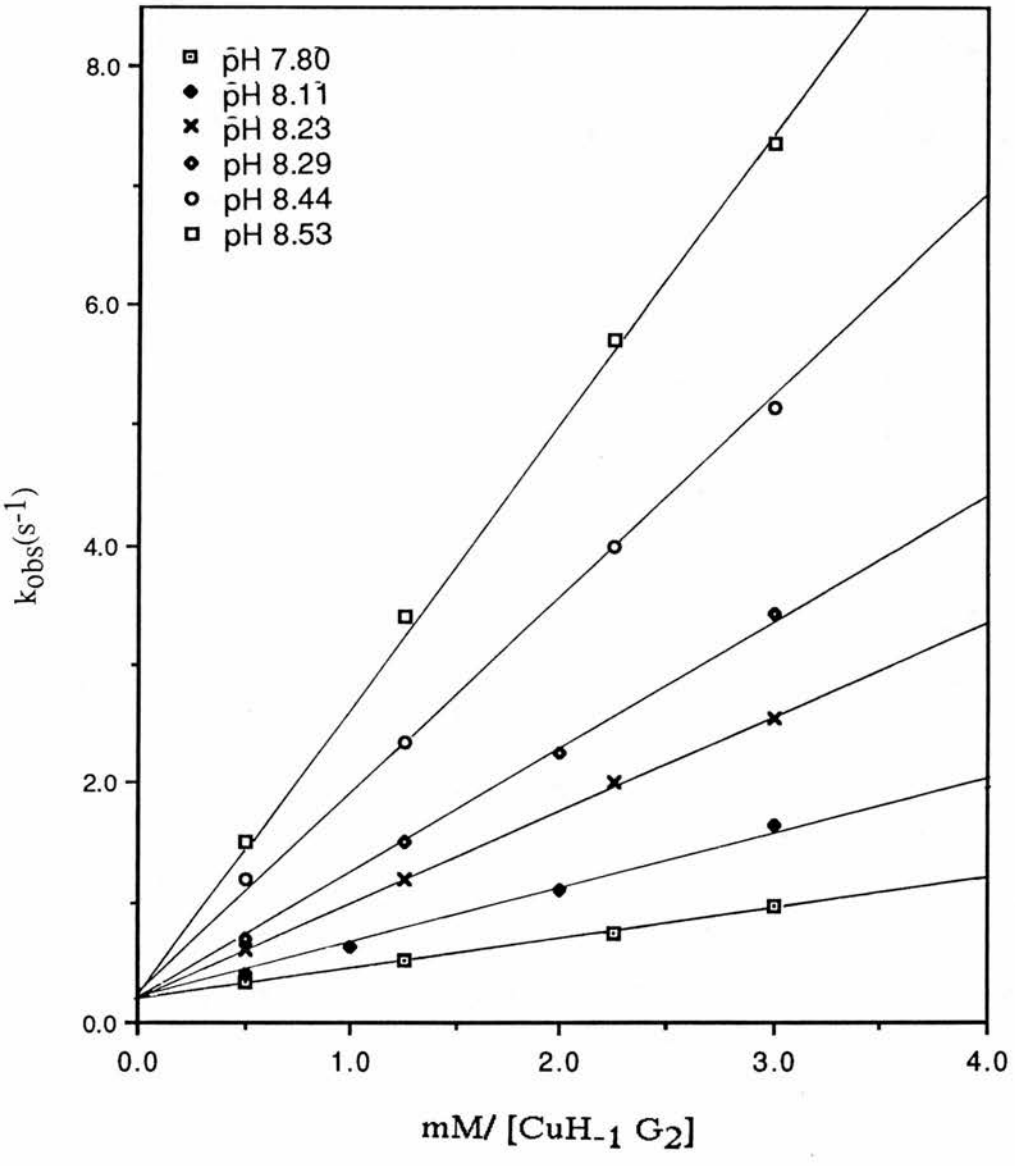

Figure 3.6 Dependence of the first-order rate constants (25.0 °C, I = 0.15 mol dm^{-3}) for the reaction of [15]aneN$_4$, initially 5.0 x 10^{-5} mol dm^{-3}, with excess concentrations of [CuH$_{-1}$G$_2$] at various pH.

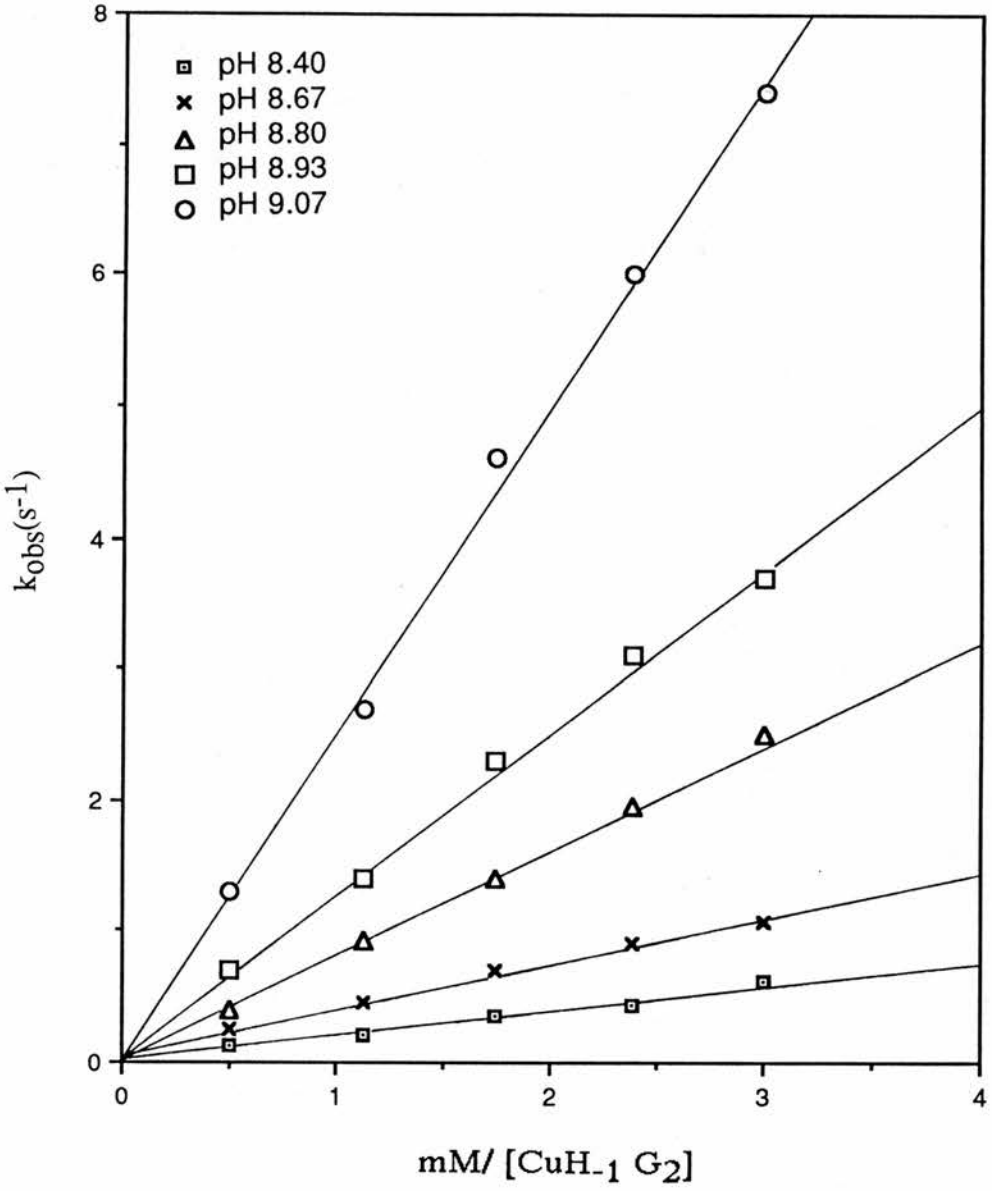

Figure 3.7 Dependence of the first-order rate constants (25.0 ^{o}C, I = 0.15 mol dm^{-3}) for the reaction of [16]aneN$_4$, initially 5.0 x 10^{-5} mol dm^{-3}, with excess concentrations of [CuH$_{-1}$G$_2$] at various pH.

A mechanism which can accommodate the above rate expression is shown in Scheme I

Scheme I

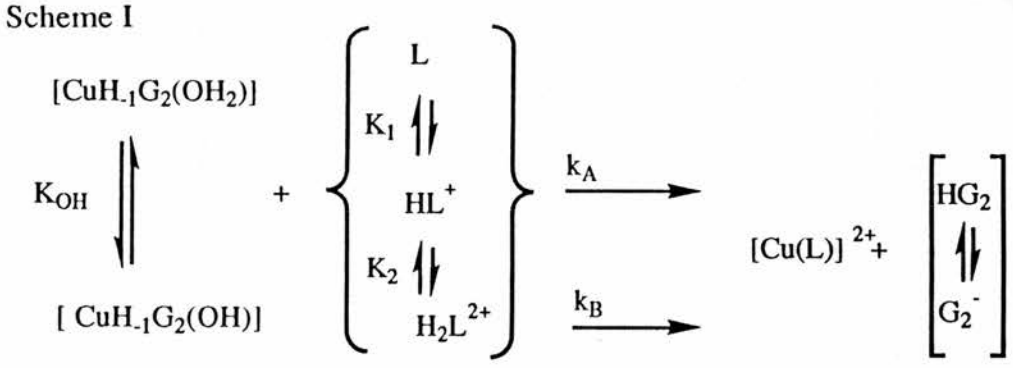

where the reactivities of H_2L^{2+} and L with $CuH_{-1}G_2(OH_2)$ and $CuH_{-1}G_2(OH)^-$ are negligible under the experimental conditions used. In the pH range 8 - 9.5 the total ligand concentration $L_T \sim [H_2L]$ and

$$[L_T] = [H_2L^{2+}] = [HL^+] \cdot {}^{a}H+/ K_a \qquad (19)$$

(where K_a is the reciprocal of K_2 in equation 13) and the total concentration of copper(II) glycylglycinate is given by

$$[CuH_{-1}G_2]_T = [CuH_{-1}G_2(OH_2)] + [CuH_{-1}G_2(OH)]^-$$

or

$$[CuH_{-1}G_2]_T = [CuH_{-1}G_2(OH_2)](1+ K_{OH}/a_{H+}) \qquad (20)$$

Substitution for the corresponding values of L_T and $[CuH_{-1}G_2]_T$ into equation (18) gives (21)

$$k_f[CuH_{-1}G_2](1 + K_{OH} / a_{H+}) [HL^+] a_{H+} / K_a = [HL^+] [CuH_{-1} G_2] (k_A + k_B K_{OH} / a_{H+}) \quad (21)$$

Rearrangement of equation (21) gives

$$k_f (1 + K_{OH}/a_{H+}) / K_a = k_A + k_B K_{OH} \cdot 1/ a_{H+} \quad (22)$$

The individual values of k_f may be calculated from

$$k_f = (k_{obs} - k_d) / [CuH_{-1}G_2]_T \quad (23)$$

A plot of equation (22) should be linear with intercept k_A and slope $k_B K_{OH}$. The plots of equation (22) (Table 3.3) for [14]aneN$_4$, [15]aneN$_4$, and [16]aneN$_4$ are shown in Figures 3.8 - 3.10, and the values of k_A and k_B obtained from the least squares analysis and/or curve fitting of equation (22) are listed in Table 3.4 .

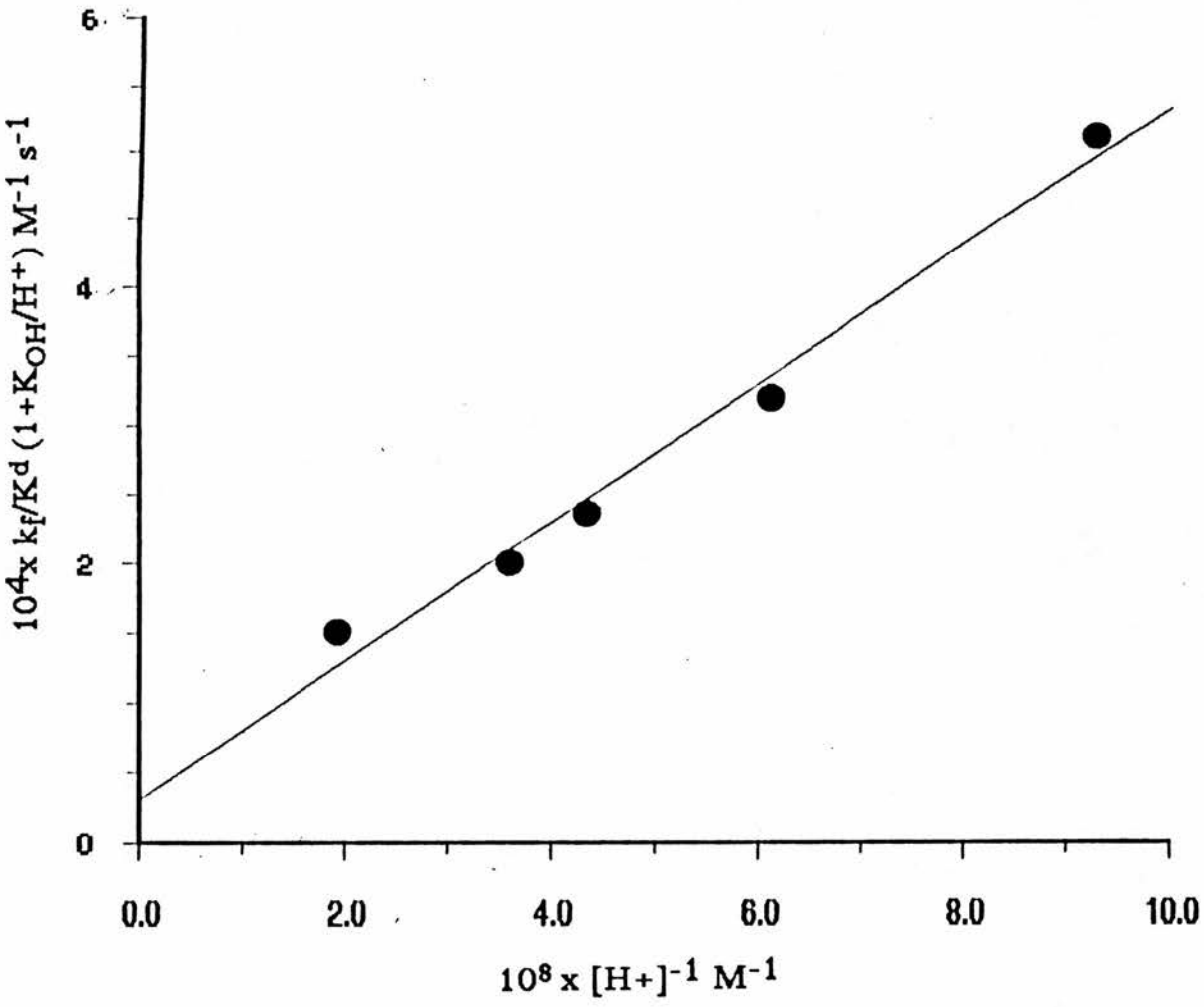

Figure 3.8 Plot of Equation 22 for $[CuH_{-1}G_2]$ *vs.* [14]aneN_4 system.

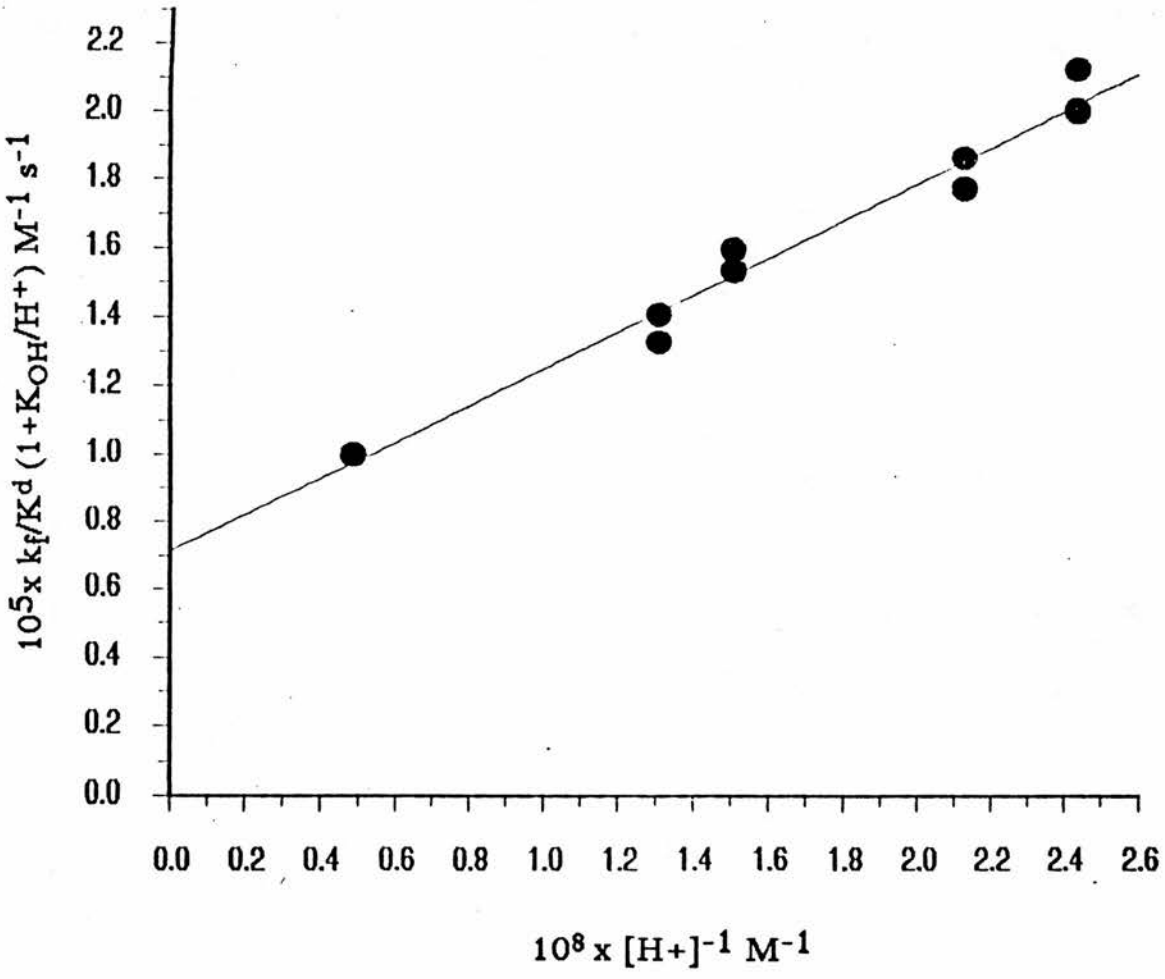

Figure 3.9 Plot of Equation 22 for $[CuH_{-1}G_2]$ *vs.* [15]aneN_4 system.

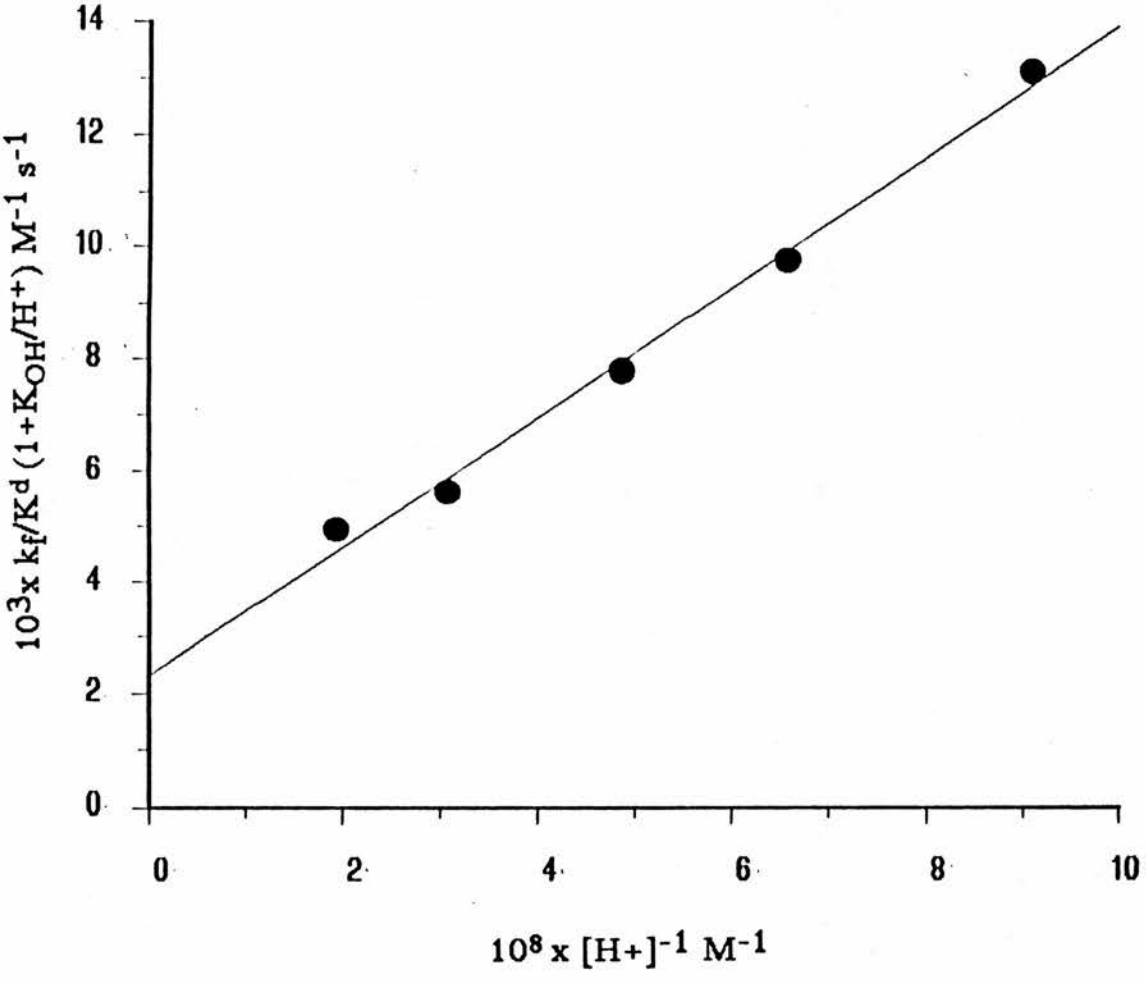

Figure 3.10 Plot of Equation 22 for $[CuH_{-1}G_2]$ *vs.* [16]aneN_4 system.

Table3.3 Kinetic data used for resolution of k_A and k_B for the three macrocycles .

pH	$10^9 x[H^+]$ M	$10^{-8} x[H^+]^{-1}$ M^{-1}	$10^7 x k_f[H^+]$ $M\ s^{-1}$	$1+K_{OH}/[H^+]$	$10^3 x k_f/K^d(1+K_{OH}/[H^+])$ $M^{-1}\ s^{-1}$
			[14]aneN$_4$[a]		
8.40	5.16	1.94	6.85	1.09	15.67
8.67	2.77	3.61	8.30	1.18	20.00
8.75	2.30	4.35	9.50	1.22	23.60
8.90	1.63	6.13	12.0	1.31	32.00
9.08	1.08	9.29	18.0	1.46	55.50
			[15]aneN$_4$[b]		
7.80	20.5	0.49	48.0	1.024	100
8.11	10.1	0.99	52.0	1.050	111
8.23	7.63	1.31	61.0	1.066	133
8.29	6.64	1.51	70.0	1.075	160
8.44	4.70	2.13	83.0	1.106	178
8.50	4.10	2.44	93.0	1.122	201
			[16]aneN$_4$[c]		
8.40	5.16	1.94	12.2	1.097	4.94
8.60	3.25	3.08	13.0	1.154	5.62
8.80	2.05	4.88	13.5	1.244	7.78
8.93	1.52	6.58	19.6	1.330	9.76
9.07	1.10	9.10	24.0	1.455	13.1

[a] $K_{OH} = 5.0 \times 10^{-10}$ M ; $K^d = 4.9 \times 10^{-11}$ M = K^{a}
[b] $K_{OH} = 5.0 \times 10^{-10}$ M ; $K^d = 4.8 \times 10^{-11}$ M = K^{a}
[c] $K_{OH} = 5.0 \times 10^{-10}$ M ; $K^d = 2.7 \times 10^{-10}$ M = K^{a}

Table3.4 Summary of specific rate constants for copper(II) glycylglycinate species reacting with monoprotonated tetra-aza macrocycles at 25.0 °C .

Ligand	k_A $mol^{-1}\ dm^3\ s^{-1}$	k_B $mol^{-1}\ dm^3\ s^{-1}$	k_A / k_B
[14]aneN$_4$	3.0×10^3	1.25×10^5	41
	1.8×10^6 [a]		
[15]aneN$_4$	7.1×10^4	1.08×10^6	15
[16]aneN$_4$	1.75×10^3	2.48×10^4	14
tet a	3.6×10^3 [b]		

[a] Obtained from ref.10 for the reaction [H[14]aneN$_4$]$^+$ with Cu^{2+}(aq) .

[b] Obtained from ref.11 for the reaction [Htet a]$^+$ with Cu^{2+}(aq) .

3.3.2 The Reaction of Macrocycles with Copper-(triglycinate)

Copper(II) triglycinate also forms an hydroxo complex, in which hydroxide ion replaces a carboxylate group in an equatorial coordination site of copper(II). For equimolar amounts of the Cu^{2+} ion and the tripeptide the absorbance of the complex $[CuH_{-2}G_3]^-$ at 555 nm decreases as the hydroxide ion concentration increases, Figure 3.11. This change is accompanied by shift of λ_{max} from 555 nm (ε = 140 mol^{-1} dm^3 cm^{-1}) at pH 10.8 to λ_{max} 574 (ε = 95 mol^{-1} dm^3 cm^{-1}) at high base concentrations (pH = 13). This spectral shift is attributed to the formation of the hydroxo complex (Equation 24).

The diglycine hydroxo complex is formed by loss of a proton from an equatorially coordinated water molecule with a pK_a value of 9.31. The pK_a for the triglycine complex is *ca.* 12.0 because of the need to displace the carboxylate group(6).

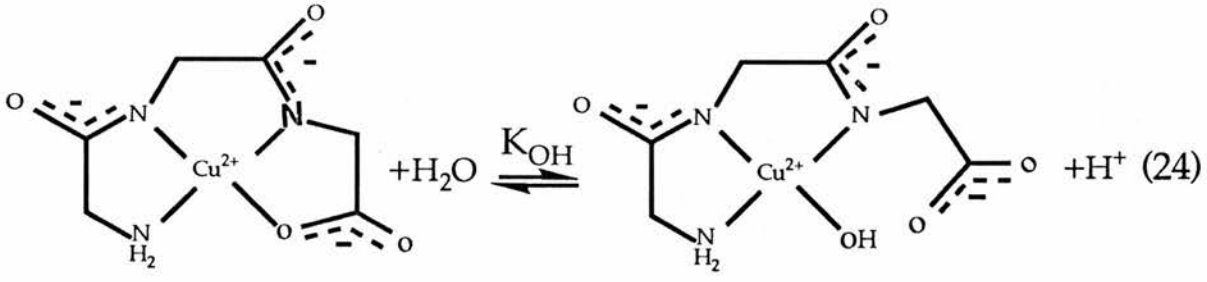

$[CuH_{-2}G_3]^-$ $[CuH_{-2}G_3(OH)]^{2-}$

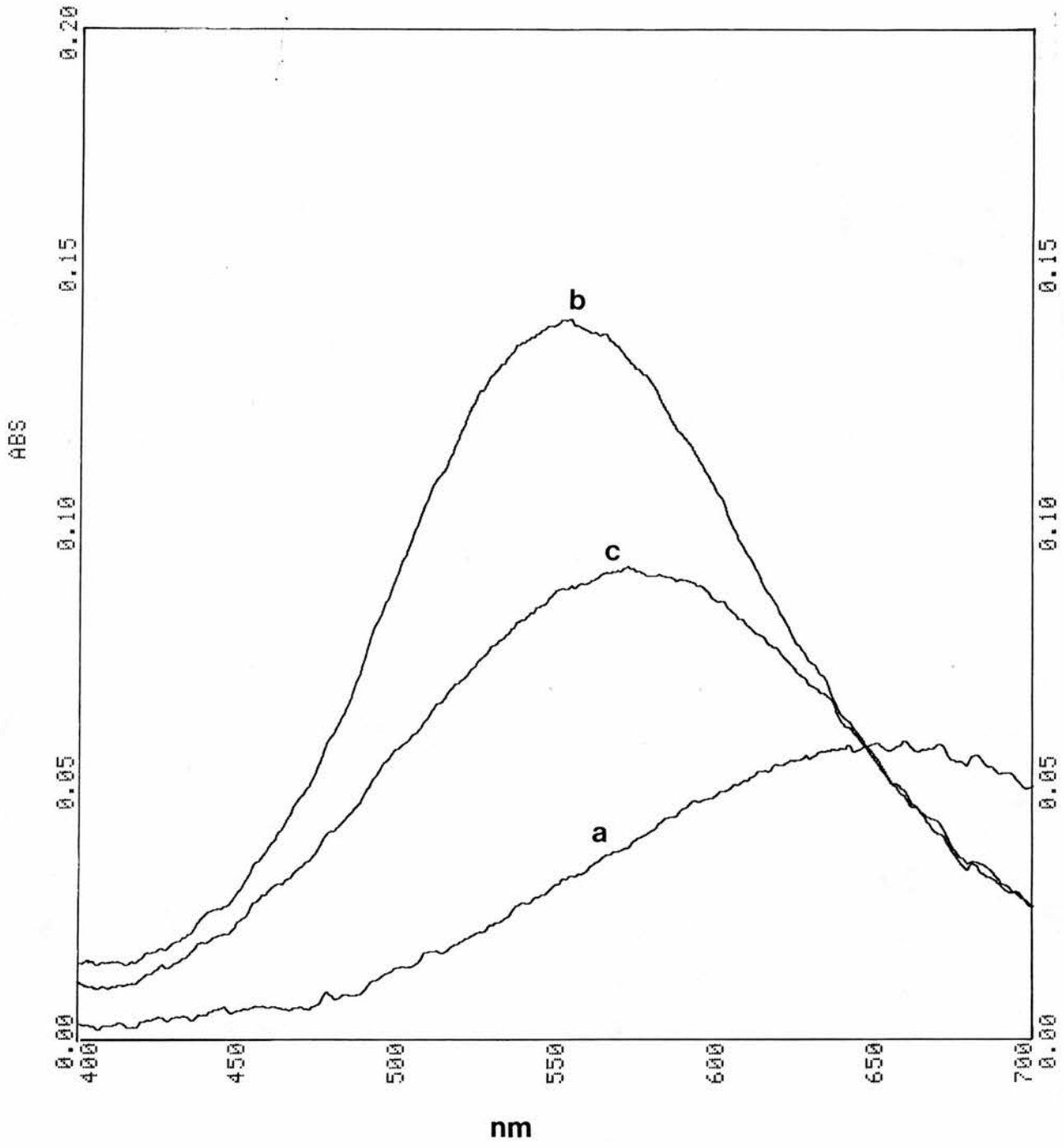

Figure3.11 Absorption spectra of an equimolar mixture of copper (II) and triglycine; $[Cu^{2+}]$ = [triglycine] = 10^{-3} mol dm^{-3} at (a) pH 5.5, (b) pH 10.8, and (c) pH = 13.0.

Table 3.5 Observed Rate Constants Values for Cu-Glycylglycylglycinate Reacting with Tetra-azamacrocycle L (1.0×10^{-4} mol dm^{-3}) and I = 0.15 mol dm^{-3}.

pH	10^3x[$CuH_{-2}G_3$]$^-$ mol dm^{-3}	*k_{obs} s^{-1}	pH	10^3x[$CuH_{-2}G_3$]$^-$ mol dm^{-3}	*k_{obs} s^{-1}	pH	10^3x[$CuH_{-2}G_3$]$^-$ mol dm^{-3}	*k_{obs} s^{-1}
	L = [14]aneN4			L = [15]aneN4			L = [16]aneN4	
9.00	1.00	4.84	9.00	1.00	7.05	8.55	1.00	3.90
9.00	3.00	5.50	9.00	2.00	7.80	8.55	3.00	4.70
9.50	1.00	7.40	9.00	3.00	8.50	8.95	1.00	4.90
9.50	3.00	8.20	9.25	1.00	8.40	8.95	3.00	5.90
9.71	1.00	10.40	9.25	3.00	10.10	9.22	1.00	6.90
9.71	2.00	11.50	9.72	1.00	14.00	9.22	2.00	7.10
9.71	3.00	12.35	9.72	3.00	14.90	9.22	3.00	8.10
9.93	1.00	13.80	9.76	1.00	14.80	9.75	1.00	11.50
9.93	2.00	14.70	9.76	2.00	16.20	9.75	2.00	13.00
9.93	3.00	15.40	9.76	3.00	17.50	9.75	3.00	14.40
10.00	1.00	17.50	9.98	1.00	20.00	10.05	1.00	18.70
10.00	2.00	18.50	9.98	2.00	22.50	10.05	2.00	21.50
10.00	3.00	20.50	9.98	3.00	24.00	10.05	3.00	23.50
10.18	1.00	23.20	10.10	1.00	23.50	10.29	1.00	24.60
10.18	2.00	24.75	10.10	2.00	25.30	10.29	2.00	28.20
10.18	3.00	27.90	10.10	3.00	28.30	10.29	3.00	31.70
10.38	1.00	33.80	10.25	1.00	28.00	10.42	1.00	32.80
10.38	2.00	37.50	10.25	2.00	30.00	10.42	2.00	36.20
10.38	3.00	39.50	10.25	3.00	33.50	10.42	3.00	41.00

*Precision in observed rate constant values is within 5 %

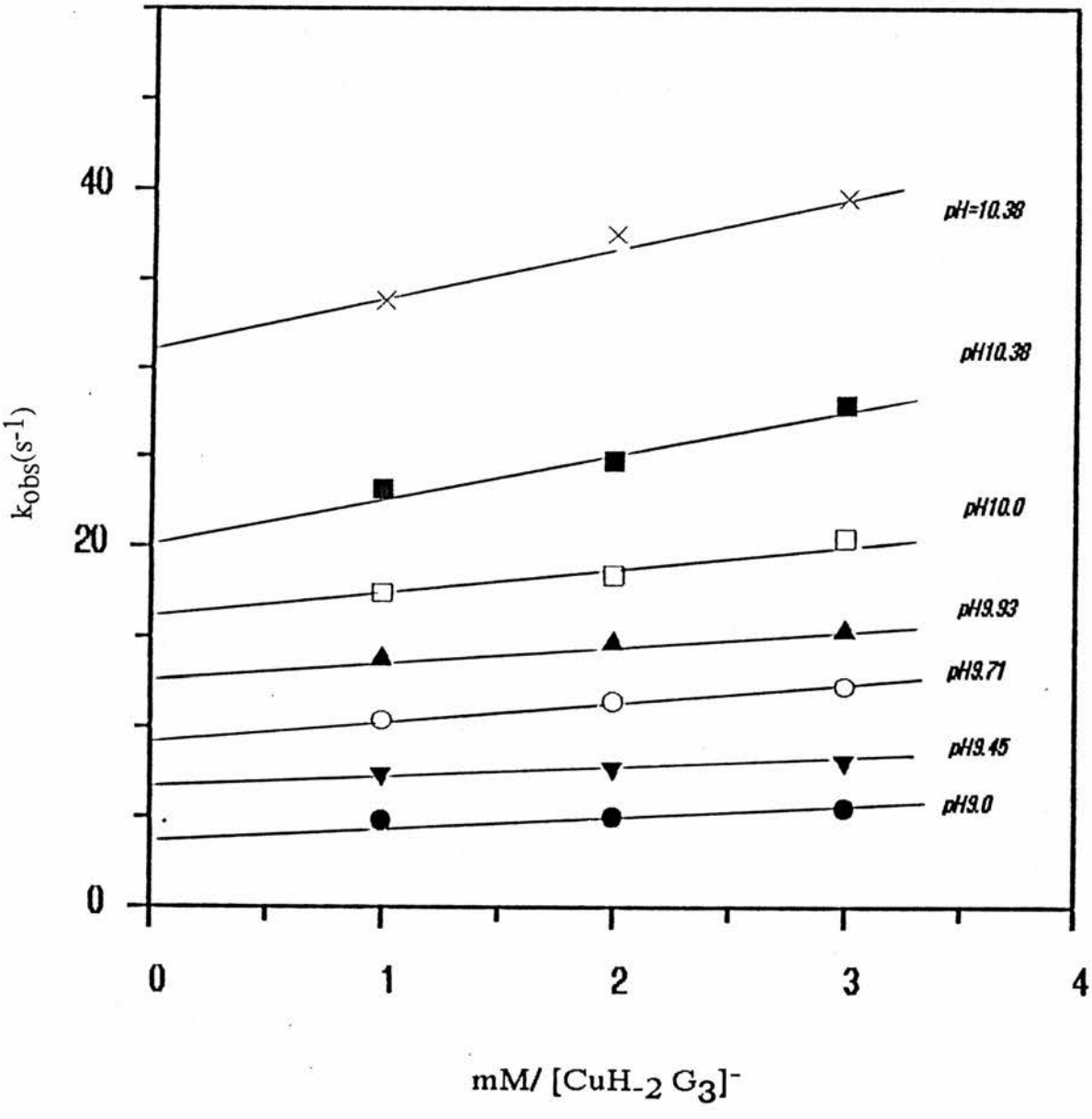

Figure 3.12 Dependence of the first-order rate constants (25.0 ºC, I = 0.15 mol dm^{-3}) for the reaction of [14]aneN_4, initially 1.0 x 10^{-4} mol dm^{-3}, with excess concentrations of $[CuH_{-1}G_2]$ at various pH.

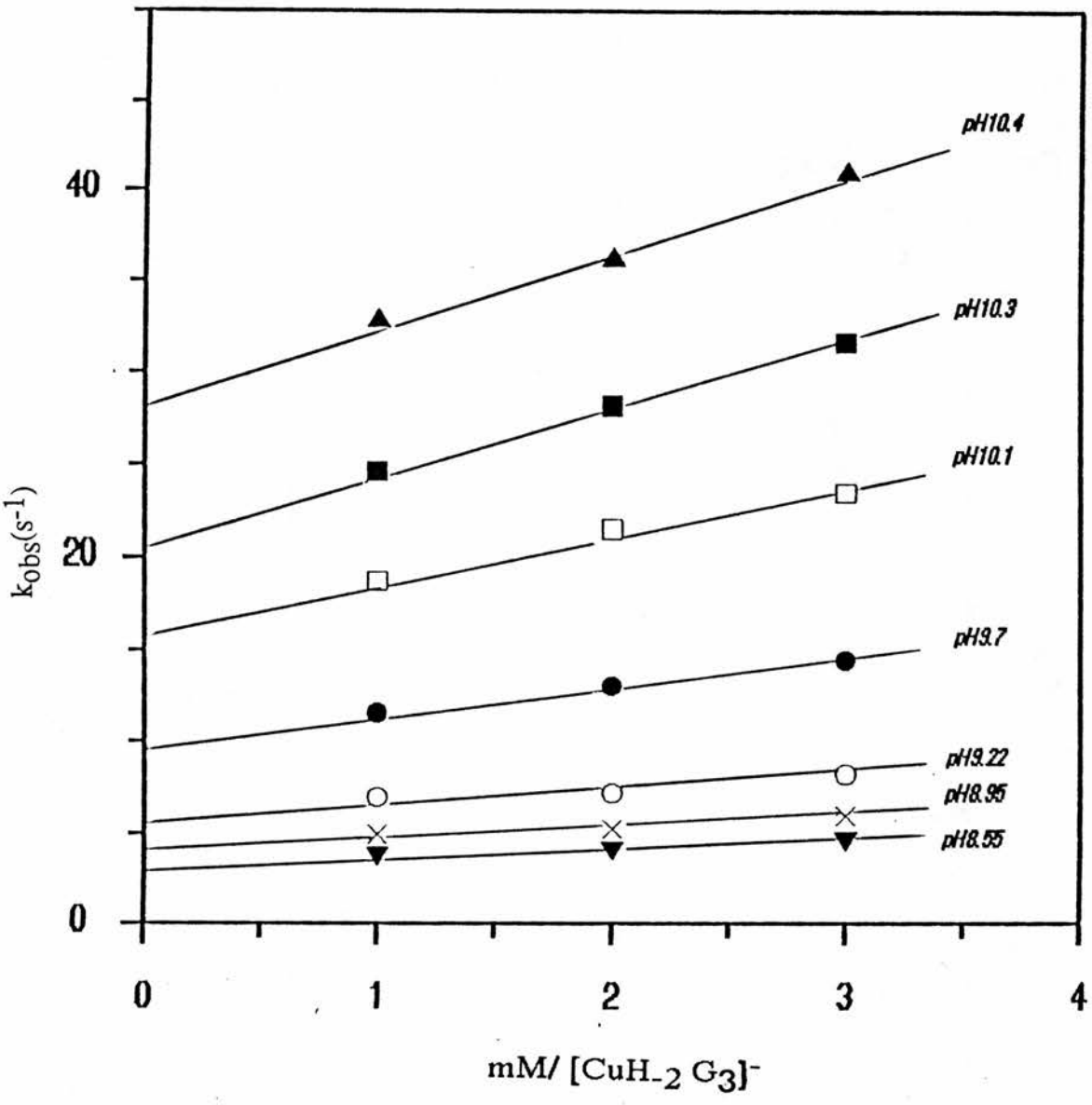

Figure 3.13 Dependence of the first-order rate constants (25.0 °C, I = 0.15 mol dm^{-3}) for the reaction of [15]aneN_4, initially 1.0 x 10^{-4} mol dm^{-3}, with excess concentrations of $[CuH_{-1}G_2]$ at various pH.

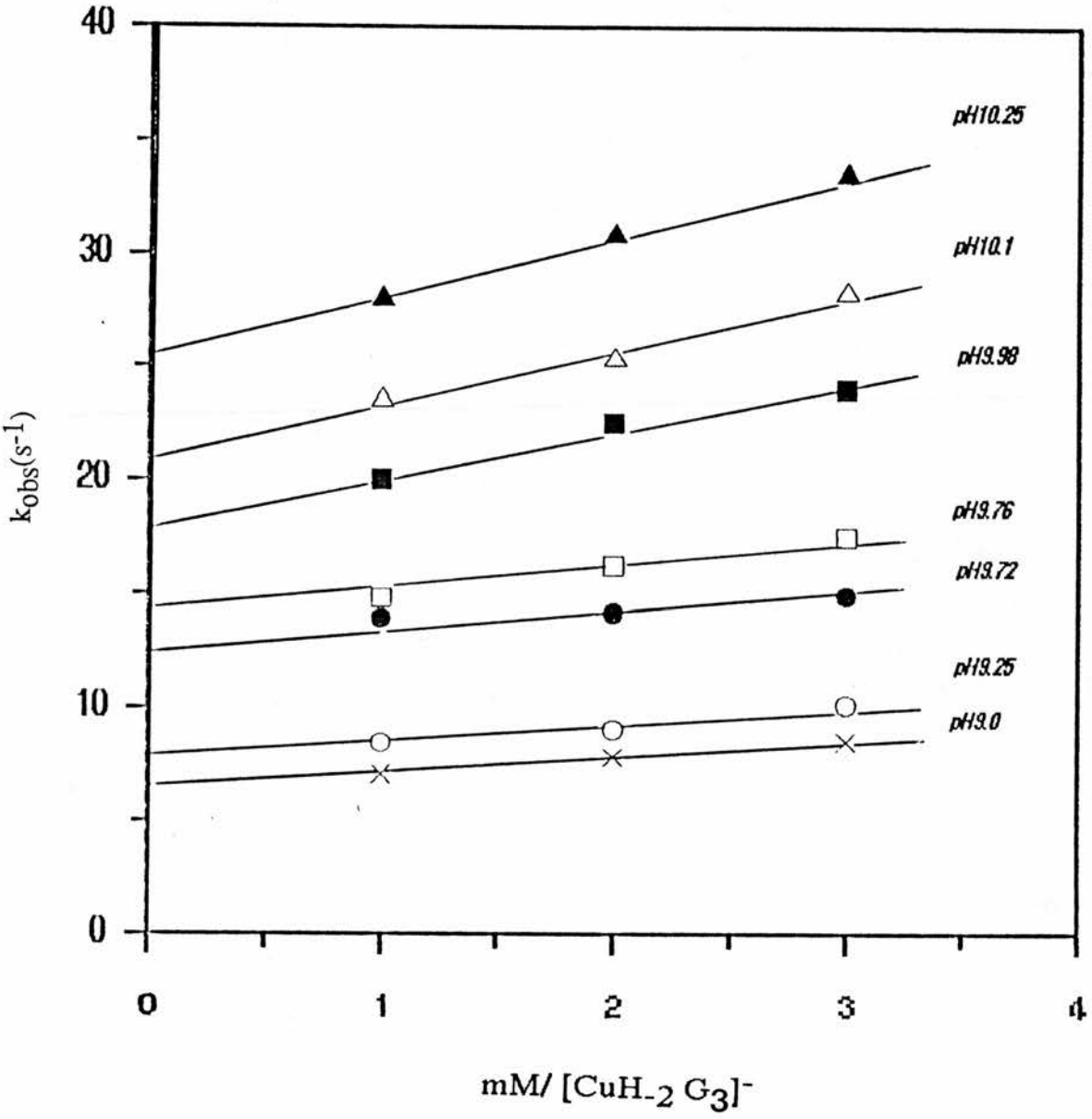

Figure 3.14 Dependence of the first-order rate constants (25.0 °C, I = 0.15 mol dm^{-3}) for the reaction of [16]aneN_4, initially 1.0 x 10^{-4} mol dm^{-3}, with excess concentrations of $[CuH_{-1}G_2]$ at various pH.

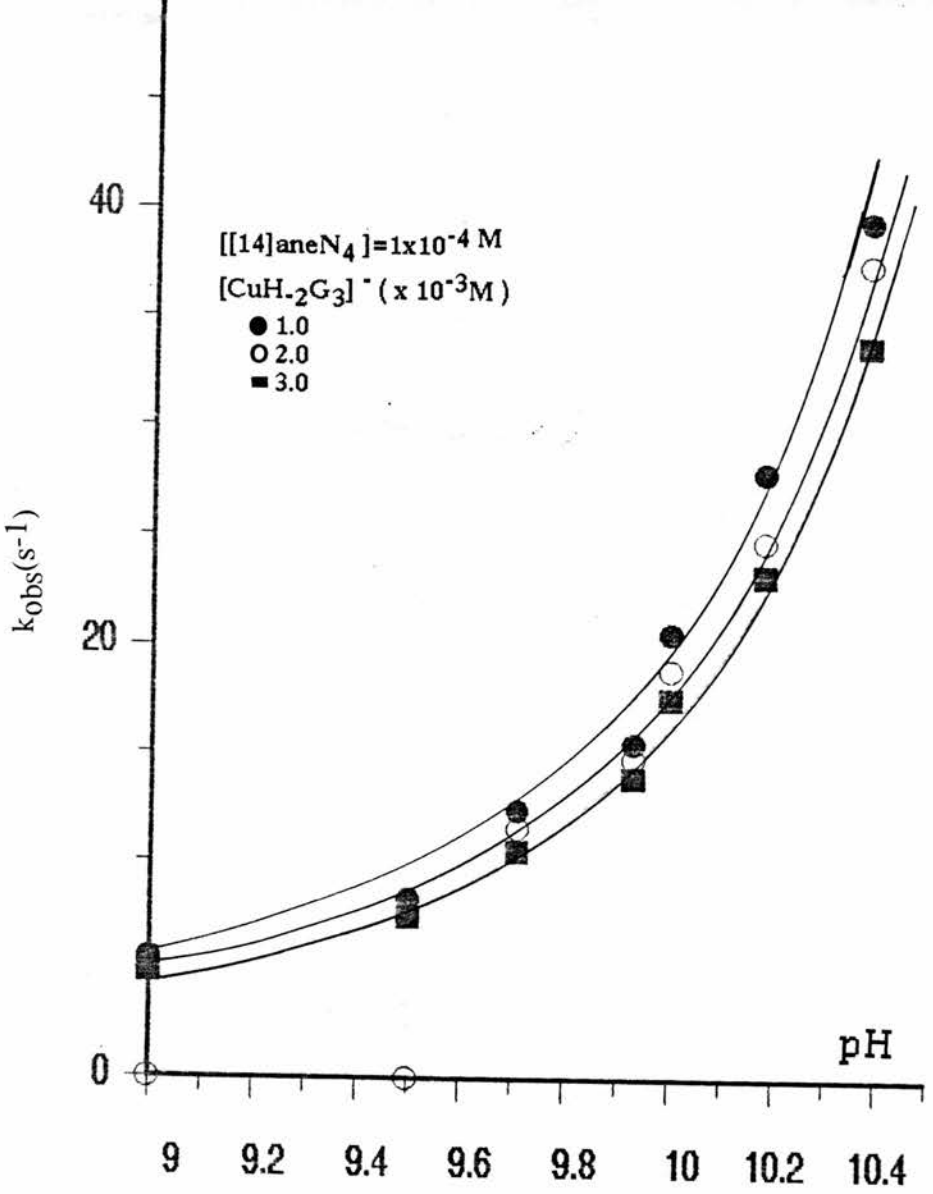

Figure 3.15 Observed pseudo first-order rate constants as function of pH and copper(II)-glycylglycylglycinate.

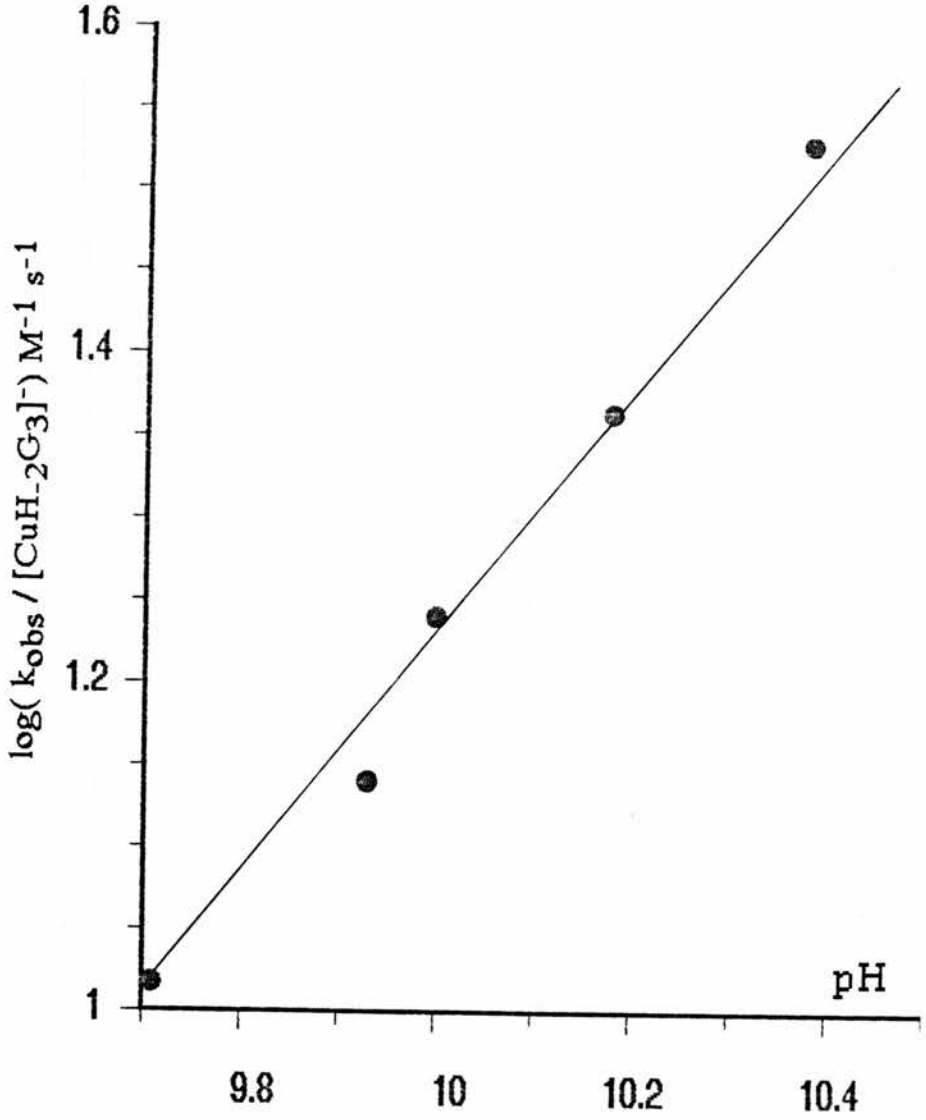

Figure 3.16 Observed pseudo second-order rate constants as function of pH and copper(II)-glycylglycylglycinate.

Resolution of Specific Rate Constants:

The exchange kinetics of the reaction between $[CuH_{-2}G_3]^-$ and L_T to give $[CuL^{2+}]$ were studied at 25 °C and I = 0.15 mol dm^{-3} NaCl. Two successive kinetic steps could be detected. The initial fast step is associated with an absorbance decrease and the second slower reaction to an absorbance increase. This latter reaction is assigned to the metal exchange step and was studied in detail. The reactions of L_T with an excess $[CuH_{-2}G_3]^-$ in the pH range 9 - 10.5 gave excellent first-order plots for all three systems. Table 3.5 lists the observed rate constants obtained for the reaction of $[CuH_{-2}G_3]^{2-}$ with [14]aneN$_4$, [15]aneN$_4$, and [16]aneN$_4$ as a function of pH. The k_{obs} values increase with the total copper (II) glycylglycylglycinate concentration (Figures 3.12 - 3.14) and establish that the reaction is first-order in $[CuH_{-2}G_3]^-_T$. The pseudo first- and second-order rate constant values increase with the basicity of the solution, Figures 3.15 and 3.16. All these reactions were found to include a water dissociation path (k_d) obtained from the data in Table 3.5 as an intercept in the plot of k_{obs} *vs* $[CuH_{-2}G_3]^-_T$ at various pH's indicating the over all rate expression

$$R = k_f [CuH_{-2}G_3]^-_T [L_T] + k_d \qquad (25)$$

In the pH range of the investigation the $[CuH_{-2}G_3]^-$ complex is the only species that contributes significantly to the exchange kinetics at pH < 11. It is presumed that all variations in the observed k_f values as a function of pH may be attributed to the varying ratios of the different protonated species of the ligands as represented in Scheme II.

Scheme II

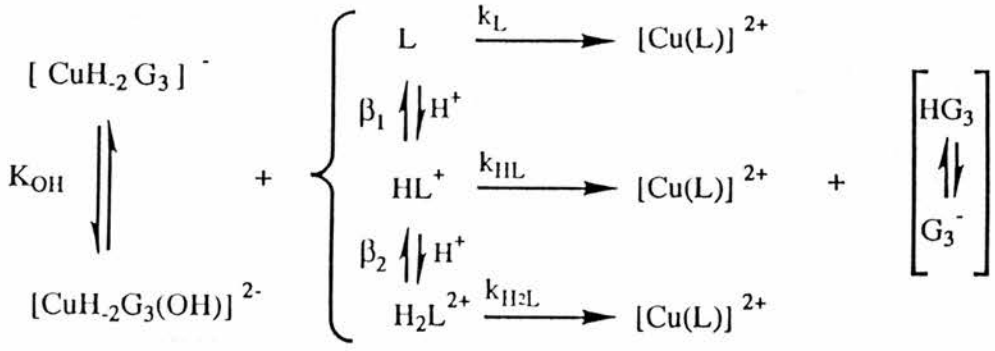

The reactivity of the hydroxo complex $[CuH_{-2}G_3(OH)]^{2-}$ with the various ligand species is negligible. If the ligand species H_3L^{3+} is considered to be kinetically inactive, the expression becomes

$$k_f\,(1 + K_{OH}/[H^+]) = 1/1+\beta_1[H^+]+\beta_2[H^+]^2\ (k_L + k_{HL}\beta_1[H^+] + k_{H2L}\ \beta_2[H^+]^2)^3 \qquad ...(26)$$

Equation (26) was computer fitted with the Grafit program to give the specific rate constants summarised in Table 3.6. The individual values of k_f were calculated from $k_f = (k_{obs} - k_d)/[CuH_{-2}G_3]_T$, Table 3.7. The cumulative protonation constants used in equation (26) are given in Table 3.8.

The kinetic data listed in Table 3.5 may be also rationalised in terms of the formation of a ternary complex $[Cu(H_{-1}G_3)(L)]$ and this is discussed below.

---

[3] $[H^+] = (H^+) = {}^aH_+$ i.e. activity of H^+ as calculated from pH.

On the basis of the pH dependence (Figures 3.12 - 3.14), it is concluded that various ligand species L, HL^+, and H_2L^{2+} are reactive with copper(II) glycylglycylglycinate and the reactivity decreases in the order $L > HL^+ > H_2L^{2+}$. Hydroxo complex formation with copper(II) glycylglycylglycinate is unimportant in the pH range of measurements.

The dependence of the observed rate constants, k_{obs}, on $[CuH_{-2}G_3]^-_T$ for the three systems is shown in Figures 3.12 to 3.14 and is expressed as follows:

$$k_{obs} = A + B\,[CuH_{-2}G_3]^-_T \quad \text{(at a given pH)} \qquad (27)$$

where A and B are constant parameters dependent upon the pH, Table 3.7. The reaction scheme with copper(II) triglycine $[CuH_{-2}G_3]^-$ may be summarised as shown in Scheme III below (charges omitted)

$$CuH_{-2}G_3 + L + H_2O \rightleftharpoons CuH_{-1}G_3.L + OH\,;\, k_L, k_{-L} \qquad (28)$$

$$CuH_{-2}G_3 + HL + H_2O \rightleftharpoons CuH_{-1}G_3.L + H_2O\,;\, k_{HL}, k_{-HL} \qquad (29)$$

$$CuH_{-2}G_3 + H_2L + H_2O \rightleftharpoons CuH_{-1}G_3.L + H_3O\,;\, k_{H2L}, k_{-H2L} \qquad (30)$$

The rate equation can be expressed as follows:

$$d[CuH_{-1}G_3.L]/dt = Q_1(L_T[CuH_{-2}G_3]_T/Q) - [CuH_{-1}G_3.L]\,\{[CuH_{-2}G_3]_T\,Q_1/Q + Q_2\} \qquad (31)$$

where

$Q = 1 + K_{OH}/[H^+]$ (K_{OH} is the equilibrium constant for the reaction $[CuH_{-2}G_3]^- + H_2O \rightleftharpoons [CuH_{-2}G_3(OH)]^- + H^+$ and is 10^{-12} mol dm^{-3})

$$Q_1 = k_L/\alpha_1 + k_{HL}/\alpha_2 + k_{H2L}/\alpha_3$$

$\alpha_1 = (1 + ß_1[H^+] + ß_2[H^+]^2 / ß_2[H^+]^2)$ ($ß_1$ and $ß_2$ are the cumulative protonation constants, i.e. for $H_2L^{2+} ß_2 = [H_2L^{2+}]/[L][H^+]^2$

$\alpha_2 = (1 + \beta_1[H^+] + ß_2[H^+]^2 / ß_1[H^+])$

$\alpha_3 = 1 + ß_1[H^+] + ß_2 [H^+]^2$

$L_T = [H_2L^{2+}] + [HL^+] + [L] + [CuH_{-1}G_3.L]$

$Q_2 = k_{-L}K_w / [H^+] + k_{-HL} + k_{-H2L} [H^+]$ ($K_w = 10^{-13.76}$ at $I = 0.15$ mol dm^{-3})

The integrated form of equation (30)is

$$\ln([CuH_{-1}G_3.L]_e^-/[CuH_{-1}G_3.L]_e^- - [CuH_{-1}G_3.L]^-_t) = \ln(A_e/A_e-A_t) = k_{obs}.t \quad (32)$$

The experimentally observed rate constant, k_{obs} (equation 27) is now correlated as follows

$$k_{obs} = Q_2 + Q_1/Q\ [CuH_{-2}G_3]^-$$

where Q_2 and Q_1/Q stands for the coefficients A (intercepts) and B (slopes) respectively, Table3.7, i.e.

$$A = 1/[H^+] (k_{-L}K_w + k_{-HL}[H^+] + k_{-H2L}[H^+]^2) \quad (33)$$

and

$$B = (1 + K_{OH}/[H^+])^{-1} (k_L / \alpha_1 + k_{HL} / \alpha_2 + k_{H2L} / \alpha_3)$$

or

$$B (1 + K_{OH}/[H^+]) = (1/1 + \beta_1[H^+] + \beta_2[H^+]^2) (k_L + k_{HL} \beta_1[H^+] + k_{H2L} \beta_2[H^+]^2) \quad ....(34)$$

The term $(1 + K_{OH}/[H^+])$ in equation (34) is ~ 1 since the ratio $K_{OH}/[H^+] << 1$. When values of A at different pH values are multiplied by the corresponding $[H^+]$ (Table 3.7) and plotted against $[H^+]$, a linear plot was obtained with significant intercept ($k_{-L}K_w$) and slope (k_{-HL}) and with a value < 1 for the term k_{-H2L} for all three systems. The results of the linear regression analysis of equation (33) are summarised in Table 3.9. The curve fitting of equation (34), using the Grafit program, gave the same specific rate constants summarized in Table 3.6. These specific rate constants now represent the formation rates of the mixed complex $[CuH_{-1}G_3.L]$. The values are summarized in Table 3.9 together with the estimated equilibrium constants of the mixed complex species $[CuH_{-1}G_3.L]$, calculated from the forward and backward reactions of copper(II) glycylglycylglycinate with the various protonated forms of the ligands.

3.4 DISCUSSION:

3.4.1 Copper(II) glycylglycinate:

Inspection of the resolved rate constants k_A and k_B, listed in Table 3.4 reveals that the ligands display the following features.

1. Both the aquo- $[CuH_{-1}G_2(OH_2)]$ and the hydroxo $[CuH_{-1}G_2(OH)]^-$ complex species are reactants with each macrocyclic ligand.

2. For a given ligand, the values of k_B are consistently larger than the corresponding values of k_A with the ratio of the rate constants k_B / k_A in the range 14 to 41 .

3. With the possible exception of [16]aneN$_4$ the exchange rates for both $[CuH_{-1}G_2(OH_2)]$ and $[CuH_{-1}G_2(OH)]^-$ with HL^+ depend upon the the macrocycle and increase with increasing ring size.

A comparison of the stability constants for $[CuH_{-1}G_2(OH_2)]$ (pK = 5.01) and $[CuH_{-1}G_2(OH)]^-$ (pK = 9.39) show that the former complex is more stable by a factor of 10^4 . This result indicates that the replacement of a water molecule by the OH^- group labilizes the copper(II) diglycine complex and hence $k_B > k_A$. The slow rates of ligand exchange with [16]aneN$_4$ may be attributed to the lower formation constant of $[Cu([16]aneN_4)]^{2+}$ (log K_{CuL} = 19.0) compared with $[Cu([15]aneN_4)]^{2+}$ (log K_{CuL} = 24.4) and $[Cu([14]aneN_4)]^{2+}$ (log K_{CuL} = 27.2). The more rapid ligand exchange associated with [15]aneN$_4$, compared with [14]aneN$_4$, may be attributed to the reduced flexibility of the 14-membered ring.

The water dissociation rate constants (k_d) obtained as intercepts from the plots of k_{obs} *vs* $[CuH_{-1}G_2]_T$ are quite small (0.04 - 0.5 s^{-1}) and made a minor contribution to the observed rate constants.

Whereas hydroxo complexes of the type $[Cu\text{-}H_{-2}tripeptide\text{-}(OH)]^{2-}$ of most copper(II) tripeptides inhibit the rate of exchange with polyamines such as 2,2,2-tet,

Table 3.6 Summary of specific rate constants for copper(II) glycylglycylglycinate reacting with various protonated forms of the tetra-aza macrocycles in aqueous solution at 25 ^{o}C, I = 0.15 mol dm^{-3}.

Ligand	k_L mol^{-1} dm^3 s^{-1}	k_{HL} mol^{-1} dm^3 s^{-1}	k_{H2L} mol^{-1} dm^3 s^{-1}	k_L/k_{H2L}
[14]aneN$_4$	(1.6±1)x10^4	(3.8±1)x10^3	8.1x10^1	197
[15]aneN$_4$	(3.3±1)x10^4	(3.5±1)x10^3	(6.0±1)x10^2	55
[16]aneN$_4$	(1.0±0.05)x10^4	(1.7±1)x10^3	(2.5±1)x10^2	40
2,2,2-tet[1]	1.1x10^7	5.1x10^6	1.2x10^5	92

[1]Reference 2

Table 3.7 Summary of the values of k_d = A (intercept) and k_f = B (slope) at different pH^s used in the resolution of k_{HnL} and k_{-HnL} (n = 0, 1, 2) of copper(II) glycylglycylglycinate reacting with tetra-aza macrocycles L at 25 ^{o}C and I = 0.15 mol dm^{-3} NaCl.

pH	10^{10} a_{H+} mol dm^{-3}	k_d = A s^{-1}	k_f = B mol^{-1} dm^3 s^{-1}	10^9 a_{H+} A
		L = [14]aneN$_4$		
9.00	12.95	4.50	330.0	5.83
9.50	4.10	7.00	400.0	2.87
9.71	2.53	9.47	975.0	2.40
10.00	1.30	15.83	1500.0	2.06
10.18	0.856	20.62	2235.0	1.77
10.38	0.540	31.20	2850.0	1.68
		L = [15]aneN$_4$		
9.00	12.450	6.32	710.0	8.18
9.25	7.280	7.57	825.0	5.51
9.76	2.250	14	1175.0	3.15
10.0	1.030	20.90	2400.0	2.15
10.25	0.728	25.33	2750.0	1.84
		L = [16]aneN$_4$		
8.55	36.50	3.43	425.0	12.5
8.95	14.530	4.40	475.0	6.5
9.22	7.810	6.15	615.0	4.8
9.75	2.300	10.00	1450.0	2.3
10.05	1.154	16.20	2500.0	1.87
10.29	0.664	21.30	3350.0	1.41
10.42	0.493	28.70	4000.0	1.41

Table 3.8 Cumulative protonation constant values for the macrocyclic tetraamines at 25 ^{o}C and I = 0.4 mol dm^{-3} KNO_3.

Ligand	logβ_1 (±σ)	logβ_2 (±σ)	logβ_3 (±σ)
[14]aneN$_4$	11.05 (0.003)	21.361 (0.003)	> 21.361
[15]aneN$_4$	11.177 (0.009)	21.487 (0.01)	26.70 (0.02)
[16]aneN$_4$	10.626 (0.02)	20.20 (0.03)	27.680 (0.04)

Table 3.9 Summary of specific forward and backward rate constants for copper(II) glycylglycylglycinate reaction with various species of the tetra-aza macrocycles in aqueous solution at 25 ^{o}C, I = 0.15 mol dm^{-3}.

Ligand	k_L	k_{-L}	k_{HL}	k_{-HL}	k_{H2L}	k_{-H2L}	Magnitude of the equilibrium constant		
	mol^{-1} dm^3 s^{-1}		mol^{-1} dm^3 s^{-1}		mol^{-1} dm^3 s^{-1}		$K = k_L/k_{-L}$	$K = k_{HL}/k_{-HL}$	$K = k_{H2L}/k_{-H2L}$
[14]aneN$_4$	1.6×10^4	8.4×10^4	3.8×10^3	3.5	81	< 1	0.2	1.1×10^3	> 81
[15]aneN$_4$	3.3×10^4	8.2×10^4	3.5×10^3	6.7	6.0×10^2	< 1	0.4	5.2×10^2	$> 6.0\times10^2$
[16]aneN$_4$	1.0×10^4	7.3×10^4	1.7×10^3	4.2	2.5×10^2	< 1	0.12	4.0×10^2	$> 2.5\times10^2$

the hydroxo complex of the diglycine $[CuH_{-1}\ G_2(OH)]^-$ assists the ligand exchange rates for macrocycles . The lack of reactivity of the $[Cu\text{-}H_{-2}tripeptide\text{-}(OH)]^{2-}$ is attributed to the requirement of 2,2,2-tet to coordinate in an equatorial site before the rate-determining step. The hydroxo complex with diglycine appears to assist the displacement of the dipeptide by acting as a second nucleophile. Studies in Chapter 2 show that cyclic tetra-aza ligands can react directly with species such as $Cu(OH)_3^-$ and $Cu(OH)_4^{2-}$. Hydroxide can be displaced by the cyclic ligands utilised in this work and the displacement is faster than a coordinated water.

3.4.2 Copper(II) glycylglycylglycinate

Earlier studies[2] showed that the replacement of triglycine by 2,2,2-tet in $[CuH_{-2}G_3]^-$ is very rapid. Second order rate constants at 25.0 °C of 1.1×10^7, 5.1×10^6, and 1.2×10^5 were obtained for 2,2,2-tet, H(2,2,2-tet)$^+$ and H_2(2,2,2-tet)$^{2+}$, respectively. Ethylenediamine (**en**) and diethylenetriamine (**dien**) also react very rapidly with $[CuH_{-2}G_3]^-$ (4.8×10^6 mol^{-1} dm^3 s^{-1} for **en** and 4×10^6 mol^{-1} dm^3 s^{-1} for **dien**) to form ternary complexes, $[CuH_{-1}G_3(\mathbf{en})]$ and $[CuG_3(\mathbf{dien})]^{2+}$. It is believed that the substitution process begins at the carboxylate terminal residue.

Inspection of the rate constants in Table 3.6 shows that the three macrocyclic ligands display the following general features.

1) When protonated species of the same charge are compared. The ligand exchange for the cyclic ligand is slower than that for the corresponding open chain tetraamine 2,2,2-tet .

2) For a given protonated species the exchange rates do not vary by more than one order of magnitude and do not vary in a regular way with the ring size.

3) For a given macrocycle the exchange rates follow the order $L > HL^+ > H_2L^{2+}$.

The water dissociation rate constants (k_d) for all three ligands were large (4 - 3 s^{-1}), and contributed significantly to the observed rate constants. The rate constant k_d, for 2,2,2-tet reacting with copper(II) triglycine is very small (0.12 s^{-1}) due to the much more favourable nucleophilic 2,2,2-tet path(15). The rate constant k_d represents a solvent pathway corresponding to partial unwrapping of the triglycine residue from copper (the carboxylate group and adjacent N (peptide) group) Figure 3.17, followed by rapid reaction with the macrocycle. A rate dependence of the type Rate = ($k_d + k_f$ [nucleophile]) [complex] is typical of the reactions of square-planar complexes(7).

Proposed Mechanism

The displacement of the tripeptide from copper(II) complexes of the type [CuH_{-2}tripeptide]$^-$ has been shown to occur by two general mechanisms involving either acid attack on the deprotonated ligand or nucleophilic attack on the metal centre(6-8). The ligand 2,2,2-tet reacts by the second mechanism(14). If the macrocycles studied in the present work reacted by the acid-catalysed mechanism the pH dependence would be the opposite to that observed in Figures 3.12 - 3.14. It is concluded that the copper(II) glycylglycylglycinate displacement reactions with the macrocycles occur through a nucleophilic mechanism, in which the displacing macrocycle coordinates to copper and speeds the breaking of the copper-peptide nitrogen bonds. As the unprotonated species react faster than the mono- and diprotonated species, it is clear that the rate-determining step must occur before or during the rupture of the first copper-peptide nitrogen bond. Once the peptide nitrogen is free from the copper it will rapidly add a proton, although this proton is not required in the observed kinetics. Studies (2,6-8) have shown that the equatorial position is very important in the reactions of metal-peptides with nucleophiles. When nucleophiles can react by displacing either an equatorial carboxylate group or water molecule, the reactions are much faster than the displacement of deprotonated peptide groups. When hydroxide occupies the carboxylate

site in a copper tripeptide complex, the reaction with 2,2,2-tet is suppressed, a situation consistent with the need for 2,2,2-tet to coordinate in an equatorial position before the rate determining step. In the pH range where $[CuH_{-2}G_3(OH)]^{2-}$ does not form, 2,2,2-tet reacts with the copper triglycine by attacking the carboxylate end with the rate-determining step being the cleavage of the Cu-N (peptide) bond adjacent to the carboxylate terminal.

The flexible linear polyamine 2,2,2-tet has minimal steric requirements in its coordination to copper. For macrocyclic ligands that coordinate in a planar fashion, the reduced flexibility of the ligand imposes additional constraints upon the exchange process. The first three coordinate bonds must initially occupy sites that are co-facial. A general mechanism for the stepwise complexation of a quadridentate macrocyclic ligand with $Cu(H_2O)_6^{2+}$ has been proposed[9] and can be adapted to ligand exchange reactions with copper(II) triglycine, Figure 3.17.

The copper(II) diglycine reactions may be represented by the same mechanism. In this case, the macrocycle is attacking either water molecules in $[CuH_{-1}G_2(OH_2)]$ or hydroxide ion in $[CuH_{-1}G_2(OH)]^-$.

As with the linear tetraamine 2,2,2-tet , it is presumed that the rate-determining step in the exchange reaction with macrocyclic ligands will not occur beyond the point of second coordinate bond formation (i.e., the closure of the first chelate ring, designated by the constant k_2 in Figure 3.17). The bonding of the third donor atom at a co-facial site should not enter into the observed exchange rate constants but should be manifested solely in the dissociation rate constants (Chapter 1).

In Chapter 2, it is shown that ligand cyclization has only a relatively small influence upon the complex formation rate constants with $Cu(OH)_3^-$ and $Cu(OH)_4^{2-}$. However ligand cyclization has substantial effects upon exchange reactions, Table 3.9. Ligand cyclization effects may be explained in terms of conformational or steric effects. The conformational effect is ruled out because the specific rate constants, Table 3.9 are

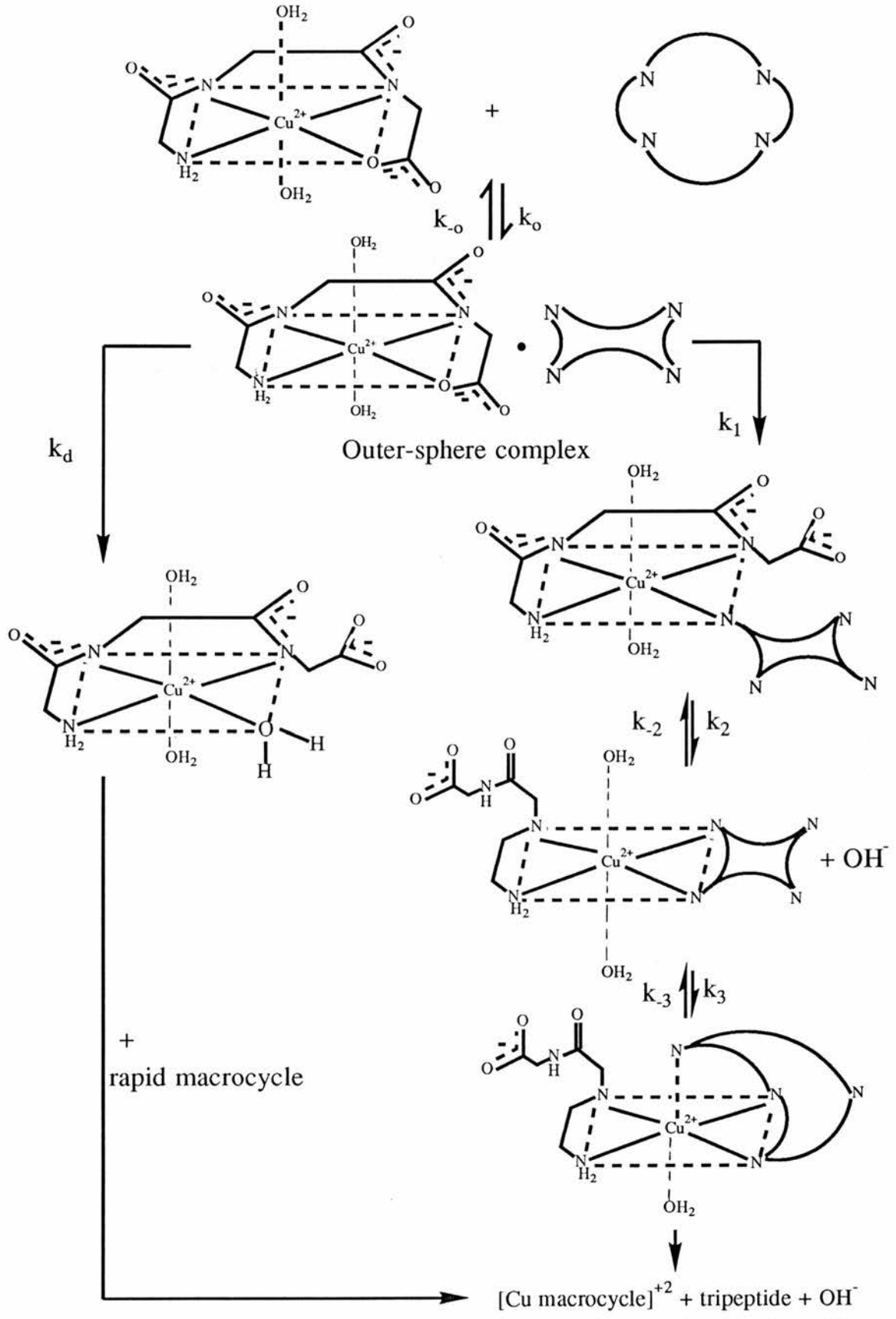

Figure3.17 Proposed mecanism for the macrocycle reaction with $[CuH_{-2}G_3]^-$,where k_2 is the rate-determinig step.

of a similar order of magnitude. Steric effects play an important role in the ligand exchange reactions of cyclic and linear tetraamines.

3.5 References

1. S. Lan and B. Sarkar. *Can. J. Chem.* **53**, 710 (1974).

2. B.E. Schwederski, F.B. Alessandro, P.N. Dickson, H.D. Lee, J.M.T. Raycheba and D.W. Margerum. *Inorg. Chem.* **28**, 3477 (1989), and references therein.

3. P. Gans, A. Sabatini, and A. Vacca, *J. Chem. Soc., Dalton Trans.* 1195 (1985).

4. H.C. Freeman, in J. Peisach, P. Aisen and W.E. Blumberg (eds), 'The Biochemistry of Copper', Academic Press, New York, 1977, p. 77.

5. M. Sato, S. Matsuki, M. Ikeda and J. Nakaya, *Inorg Chim Acta*, **125**, 49 (1986).

6. H. Haver, E.J. Billo, D.W. Margerum, *J. Am. Chem. Soc.*, **93**, 4173 (1971).

7. L.F. Wong, J.C. Cooper, and D.W. Margerum, *J. Am. Chem. Soc.*, **10**, 7269 (1976).

8. G.K. Pagenkopf and D W Margerum. *J. Amer. Chem. Soc.* 2683 (1970).

9. B.C. Westerby, K.L. Juntunen, G.H. Leggett, V.B. Pett, M.J. Koenigbaur, M.D. Purgett, M.J. Taschner, L.A. Ochrymowycz and D.B. Rorabacher. *Inorg. Chem.*, **30**, 2109 (1991).

10. R.W.Hay and C. R. Clark, *J.chem. Soc. Dalton Trans*, 1148 (1977).

11. A.P.Leugger, L.Hertli and T.A. Kaden, *Helv.*, **16**, 2296 (1978).

CHAPTER 4

PROTONATION CONSTANTS AND FORMATION CONSTANTS OF TETRA-AZAMACROCYCLES.

4.1 IONISATION AND COMPLEX EQUILIBRIA

4.1.1 Introduction

There are two major areas of solution chemistry. The first is concerned with the chemical nature and concentration of each of the species present at equilibrium. The second concerns the rate and mechanism by which the species present in solution come to equilibrium. These aspects of solution chemistry are closely related.

Consider a system,

$$A + B \rightleftharpoons C + D \qquad k_f;\ k_r \qquad (1)$$

where k_f and k_r are respectively the forward and reverse rate constants. The rate at which the reaction proceeds in a forward direction, which equals the rate of loss of A (-dA/dt), is given by

$$-dA/dt = k_f [A] [B] \qquad (2)$$

where [X] is the concentration of species X. In addition, the rate of the reverse reaction, which equals the rate of formation of A (dA/dt), is given by

$$dA/dt = k_f[C][D] \qquad (3)$$

At equilibrium the rates of the forward and reverse reactions are equal, and so

$$k_f[A][B] = k_r[C][D] \qquad (4)$$

which may be rearranged to give

$$k_f/k_r = K^o = [C][D] / [A][B] \qquad (5)$$

where k_f / k_r, being a constant, is written as a single constant K^o, known as the equilibrium constant.

STABILITY

A system is said to be thermodynamically stable if its free energy is lower, i.e, more negative, than the sum of the free energies of the products formed when it reacts. Equilibrium studies alone cannot give any information about the reaction rate because, for a reaction to proceed, two criteria must be fulfilled:

(a) there must be a favourable free energy change, and

(b) there must be a pathway of sufficiently low activation energy for it to occur at a measurable rate.

If both criteria are met the system is said to be **labile**. If there is no low activation pathway the reaction will not proceed, even if it is thermodynamically feasible. A system in this state is said to be **inert.**

THERMODYNAMIC STABILITY CONSTANTS:

A fundamental concept in the study of solution equilibria is the equilibrium constant defined by equation (5). There are two particular equilibrium constants that are commonly given special names. Thus when the Lewis acid is the proton, the inverse of the equilibrium constant for the reaction

$$H^+ + X^- \rightleftharpoons HX \qquad ;K_H^o \qquad (6)$$

$$K_a^0 = 1/K_H^o = \{H^+\}\{X\}/\{HX\}$$

is known as the acid dissociation constant (K_a^0) of the acid HX and K_H^o is known as the protonation constant; {X} is the activity of species X. For a tetravalent ligand (L) having four dissociable protons, its proton binding processes are as follows

$$L + H^+ \rightleftharpoons HL^+ \quad (7)$$

$$HL^+ + H^+ \rightleftharpoons H_2L^{2+} \quad (8)$$

$$H_2L^{2+} + H^+ \rightleftharpoons H_3L^{3+} \quad (9)$$

$$H_3L^{3+} + H^+ \rightleftharpoons H_4L^{4+} \quad (10)$$

These processes can be quantified by the following terms

$K^o_{H,1} = \{HL\}/\{L\}\{H\}$ $\quad \beta_1 = K^o_{H,1}$ $\quad K^o_{a,1} = \{H_3L\}\{H\}/\{H_4L\}$

$K^o_{H,2} = \{H_2L\}/\{HL\}\{H\}$ $\quad \beta_2 = K^o_{H,1} K^o_{H,2} = \{H_2L\}/\{L\}\{H\}^2$

$K^0_{a,2} = \{H_2L\}\{H\}/\{H_3L\}$

$K^o_{H,3} = \{H_3L\}/\{H_2L\}\{H\}$ $\quad \beta_3 = K^o_{H,1} K^o_{H,2} K^o_{H,3} = \{H_3L\}/\{L\}\{H\}^3$

$K^o_{a,3} = \{HL\}\{H\}/\{H_2L\}$

$K^o_{H,4} = \{H_4L\}/\{H_3L\}\{H\}$ $\quad \beta_4 = K^o_{H,1} K^o_{H\,2} K^o_{H,3} K^o_{H,4} = \{H_4L\}/\{L\}\{H\}^4$

$K^o_{a,4} = \{L\}\{H\}/\{HL\}$

$K^{o}_{H,1}$, $K^{o}_{H,2}$, ... etc are stepwise (in other words successive) protonation constants, whereas $ß_1$, $ß_2$, ... etc are cumulative protonation constants. It can be seen that the stepwise dissociation constants $K^{o}_{a,1}$, $K^{o}_{a,2}$, ... are reciprocals of some stepwise protonation constants, so for example, $\log K^{o}_{H,1} = - \log K^{o}_{a,4} = pK_{a,4}$.

The second special case is when the Lewis acid is a metal ion (M)[1] and the Lewis base is a ligand (L)[1], then for the reaction

$$M + L \rightleftharpoons ML \qquad ;K^{o}_{ML} \qquad (11)$$

the equilibrium constant K^{o}_{ML} (= {ML}/{M}{L}) is known as a formation constant.

In many cases more than one ligand can coordinate to a given metal ion. Niels Bjerrum first suggested in 1915 and later proved that the formation of complexes occurs in a stepwise manner so that ML is formed first, ML_2 second, and so on. In the general, case it is not possible to form ML_n without first forming ML_{n-1}. Consider the reaction of silver ion with ammonia in which only two complexes are formed,

$$Ag^{+} + NH_3 \rightleftharpoons Ag(NH_3)^{+} \qquad ;K^{o}_{1} \qquad (12)$$

$$Ag(NH_3)^{+} + NH_3 \rightleftharpoons Ag(NH_3)^{+}_{2} \qquad ;K^{o}_{2} \qquad (13)$$

$$K^{o}_{1} = \{Ag(NH_3)^{+}\}/\{Ag^{+}\}\{NH_3\} \qquad (14)$$

$$K^{o}_{2} = \{Ag(NH_3)^{+}_{2}\}/\{Ag(NH_3)^{+}\}\{NH_3\} \qquad (15)$$

---

[1]Throughout this chapter charges are omitted for the sake of simplicity, except when discussing specific metal ions or ligands.

where K_1^o and K_2^o are known as stepwise stability constants. Since we are dealing with equilibrium systems, we can consider the formation of $Ag(NH_3)_2^+$ from silver ions and ammonia.

$$Ag^+ + 2NH_3 \rightleftharpoons Ag(NH_3)_2^+ \quad ;\beta^o \tag{16}$$

where β^o is the overall stability constant.

$$\beta^o = \{Ag(NH_3)_2^+\}/\{Ag^+\}\{NH_3\}^2 \tag{17}$$

If more than two metal ligand complexes are formed, then several stability constants may be defined. In general,

$$K_n^o = \{ML_n\}/\{ML_{n-1}\}\{L\} \tag{18}$$

and the corresponding overall stability constant, β_n^o, is given by

$$\beta_n^o = \{ML_n\}/\{M\}\{L\}^n \tag{19}$$

The overall and the stepwise stability constants are inter-related by

$$\beta_1^o = K_1^o, \ \beta_2^o = K_1^o, K_2^o, ..., \qquad \beta_n^o = K_1^o, K_2^o ....K_n^o.$$

In general,

$$\beta_n^o = \pi_1^n K_i^o \tag{20}$$

It must be noted that the stepwise stability constants usually decrease as the number of ligands in the complex increases. Thus K_1^o in Equation (12) is larger than K_2^o in Equation (13). This trend is expected on the basis of statistical, steric and electrostatic considerations.

If a second ligand B is introduced, the number of possible equilibria increases substantially. In addition to those involving the simple formation of binary complexes, such as MA, MA_2, MB and MB_2, there is also a possibility of the displacement reaction (Equation 21) or mixed complex formation (Equation 22), depending on the nature of the ligands A and B.

$$MA + B \rightleftharpoons MB + A \quad ;K_{MB} \qquad (21)$$

$$MA + B \rightleftharpoons AMB \quad ;K_{AMB} \qquad (22)$$

Thus reaction (21) would be important when one or both of the ligands A and B occupies all or almost all of the metal coordination sites (for example, A = $NH_2CH_2COO^-$ and B = $EDTA^{4-}$). Alternatively, reaction (22) would be important when A and B have a sufficiently small number of donor atoms so that both ligands may coordinate to a metal ion simultaneously.

Consider a reaction where the metal ion reacts with the acidic ligand HL,

$$ML_{n-1} + HL \rightleftharpoons ML_n + H^+ \quad ;{}^*K_n \qquad (23)$$

or

$$M + nHL \rightleftharpoons ML_n + nH^+ \quad ; {}^*\beta \qquad (24)$$

where the stability constant equations are

$$*K_n = \{ML_n\}\{H^+\} / \{ML_{n-1}\}\{HL\} \quad (25)$$

$$*\beta_n = \{ML_n\}\{H^+\}^n / \{M\}\{HL\}^n \quad (26)$$

$$*K_n = K_n^o \cdot K_a^o \quad (27)$$

$$*\beta_n = \beta_n^o \cdot K_{a,n} \quad (28)$$

$*K_n$ = product of stability constant (K_n^o) and dissociation constant (K_a^o) where

$$K_n^o = \{ML_n\} / \{ML_{n-1}\}\{L^-\} \quad (29)$$

$$K_{a\,n}^o = \{H^+\}^n\{L^-\}^n / \{HL\}^n$$

and

$$\beta_n^o = \{ML_n\} / \{M\}\{L^-\}^n \quad (30)$$

STOICHIOMETRIC STABILITY CONSTANTS:

So far all the equilibrium and stability constants are defined in terms of the activities of the species present. However, in practice many analytical techniques yield concentrations rather than activities. Concentrations are related to activities by the expression

$$\{X\} = [X] \cdot \gamma \quad (31)$$

where [X] = the concentration of X and γ = the activity coefficient of X. Therefore the thermodynamic stability constant for reaction (11) may be written in terms of both concentrations and activity coefficients (Equation 32).

$$K^{o}_{ML} = \{ML\}/\{M\}\{L\} = [ML]/[M]\,[L] \times \gamma_{ML}/\gamma_M\gamma_L \qquad (32)$$

Usually the term $\gamma_{ML}/\gamma_M\gamma_L$ in Equation (32) is maintained constant[2] by: (a) having a large excess of an inert background electrolyte present, and (b) using only low concentrations of metal and ligand, so that any change in their concentrations as a result of their reaction has no significant change on the overall ionic strength of the medium. Therefore K_{ML}, defined by Equation (33) would also be a constant, known as a stoichiometric stability constant.

$$K_{ML} = [ML] / [M][L] \qquad (33)$$

The vast majority of stability constants reported in the literature are stoichiometric stability constants (or simply stability constants), in which the ratio of the activity coefficients $\gamma_{ML}/\gamma_M\gamma_L$ is included in the constant K_{ML}

Although constant ionic strength does allow the determination of a reliable stoichiometric stability constant, this constant is only valid at the ionic strength of the measurement.

In conclusion, thermodynamic constants are obtainable by: (a) studying very dilute solutions (less than 10^{-3} M), where the combinations of the activity coefficients are essentially equal to unity, (b) by studying dilute solutions where the activity coefficients can be obtained theoretically (from the Debye-Huckel approach and its extension), and (c) by determining equilibrium constants at different ionic strengths and extrapolating to infinite dilution.

The first method is limited to very stable complexes. In dilute solutions, as in the second and third methods, the activity coefficient of a given solute is the same in all solutions of the same ionic strength.

The ionic strength is defined by Equation (34) where C_i = concentration of ions of charge Z_i. Accordingly, ionic strength

$$I = \frac{1}{2} \Sigma C_i . Z_i^2 \qquad (34)$$

has the units of concentration (mol dm^{-3}). However, it has recently been suggested[3] that ionic strength should be defined by the equation

$$I = \frac{1}{2} \Sigma C_i |Z_i| \qquad (35)$$

The two definitions are identical for univalent ions, but when significant concentrations of multivalent ions are present, the latter may be used. However in this work Equation (34) has been employed.

The ionic strength is usually kept constant by employing a strong electrolyte such as sodium perchlorate or potassium nitrate. The electrolyte must be inert and comply with the following requirements:

(1) It must be a strong electrolyte.

(2) Its cation must not associate with the ligand and with the complex species formed.

(3) Its anion must not associate with the metal ion and with the complex species.

(4) Redox reactions via the inert electrolyte and the central ion or ligand must not take place.

(5) Its solubility has to be very large.

(6) Its contribution to the measured physical or chemical property must be negligible.

TREATMENT OF DATA:

SECONDARY CONCENTRATION VARIABLES:

As discussed above, it is possible to define a series of stability constants for the successive formation of mononuclear complexes involving two species. In order to evaluate these stability constants, it is necessary to find a relationship between them and the experimentally determined variables ([M], [L], etc). This relationship is often established via the definition of secondary concentration variables. It is from these variables that the stability constants are calculated. Only three of these functions are discussed below.

(i) The Complex Formation Function, *n*.

Consider a metal ion, M, and a ligand, L, interacting in a solution of constant ionic strength. The equilibria are

$$M + L \rightleftharpoons ML \quad ;K_1 \tag{36}$$

$$ML + L \rightleftharpoons ML_2 \quad ;K_2 \tag{37}$$

$$ML_{n-1} + L \rightleftharpoons ML_n \quad ;K_n \tag{38}$$

where n is a function of both the maximum coordination number of the metal ion and the multidentism of the ligand. The mass balance equations for both the total metal ion and total ligand concentrations are

$$T_M = [M] + [ML] + [ML_2] + \ldots\ldots + [ML_n] = [M] + \sum_{n=0}^{n=N} [ML_n] \tag{39}$$

$$T_L = [L] + [ML] + 2[ML_2] + \ldots\ldots + n[ML_n] = [L] + \sum_{n=1}^{n=N} n[ML_n] \tag{40}$$

where N is the maximum coordination number for the metal if L is a monodentate ligand. The extent of complex formation can be characterised by the function $\bar{n}$[4, 5] defined as

$$\bar{n} = \text{total bound ligand / total metal} = T_L - [L] / T_M$$

$$= [ML]+2[ML_2]+....n[ML_n] / [M]+[ML]+[ML_2]+....[ML_n] \qquad (41)$$

Taking into consideration Equations (18), (19) and (20) (where {X} = [X])

$$\bar{n} = \frac{\sum_{n=1}^{n=N} n\,\beta_n[L]^n}{1+\sum_{n=1}^{n=N} \beta_n[L]^n} = \frac{\sum_{n=0}^{n=N} n\,\beta_n[L]^n}{\sum_{n=0}^{n=N} \beta_n[L]^n} \qquad (42)$$

Two important conclusions can be drawn from Equation (42), (a) the complex formation function, $\bar{n}$, is solely dependent on the free ligand concentration, [L], and is independent of T_L, T_M and the free metal ion concentration [M], and (b) measuring the free ligand concentration for at least n different total ligand concentrations permits the calculation of a complete set of stability constants.

(ii) The degree of formation, α_c

For any individual component of the system, a variable α_c can be defined such that

$$\alpha_c = [ML_c] / T_M \quad \text{for} \quad c = 0, 1, 2, ...N \qquad (43)$$

This variable α_c is the partial mole fraction of the component ML_c. The degree of formation of the system as a whole may be considered, and another variable, α_T, can be defined

$$\alpha_T = \sum_{c=1}^{c=N} \alpha_c$$

Hence α_T is the fraction of total metal bound to ligand in the form of a complex. By analogy to the derivation of n

$$\alpha_c = \frac{\sum_{c=1}^{c=N} \beta_c[L]^c}{1 + \sum_{c=1}^{c=N} \beta_c[L]^c} = \frac{\sum_{c=1}^{c=N} \beta_c[L]^c}{\sum_{c=0}^{c=N} \beta_c[L]^c} \qquad (44)$$

One interesting solution to Equation (44) is when c = 0 and hence

$$\alpha_o = [M] / T_M \qquad (45)$$

This fraction, α_o, gives the species distribution for the free metal ion in the solution. When no complex formation takes place then α_o is unity. Hence it is possible to plot a series of component distribution curves (N + 1 of them) of α_c versus T_M or T_L.

(iii) The degree of complex formation, ø

The third secondary concentration variable, ø, is defined as

$$\text{ø} = T_M / [M] = 1 + \sum_{n=1}^{n=N} \beta_n[L]^n \qquad (46)$$

This function finds an application in the methods of Leden and Froneaus[1].

The functions, n, α_c and ø are inter-related by

$$\alpha_c = \beta_c[L]^c / \phi \quad (47)$$

and

$$n = \delta \log \phi / \delta \log [L] \quad (48)$$

The above relationships are used to determine stability constants by graphical and numerical methods and by computer.

Determination of stability constants:

Methods for determining stability constants may be classified[6] according to whether or not any of the species $M_qL_pH_j$ occurs in more than one phase, where q and p are zero or a positive whole number. The value of j is also integral and is positive for species which act as Bronsted acid, but negative for those which contain one or more hydroxyl groups. Within each group of techniques, further classification may be based on the way in which the measured property varies with the concentrations of the species being studied. The techniques commonly used are shown in Table 4.1.

Many of the methods listed are of very restricted application. However, potentiometry and spectrophotometry are currently the most widely used .

4.1.2 Calculating dissociation and stability constants using computer programs:

The application of computational methods to the elucidation of solution equilibria has been reviewed up to 1971[7-12]. Subsequently several authors have published powerful computer programs which enable the calculation of stability constants from various types of data. A summary of some of the major published programs for the calculation of such constants is given in Table 4.2. It is clear from this table that most of these programs are based on the non-linear Gauss-Newton or the Newton-Raphson least-squares methods. In these programs, initial guesses are made as to the values of the formation constants and the constants are refined by an iterative

Table 4.1 Some methods for measuring stability constants.

	All species $B_qA_pH_j$ in homogeneous solutions	**At least one species $B_qA_pH_j$ distributed between two phases**
Experimental output (fairly) directly related to conecentrations of individual species	Classical analysis Potentiometry Polarography Amperometry	Solvent extraction Solubility Vapour pressure
Output depends in general on concentrations of more than one species; but in favourable cases method can give single concentrations	Spectrophotometry Kinetics	Ion-exchange
Output always depends on the concentrations of two or more species	Colligative properties Conductivity	

Table 4.2 Summary of some published non-linear least-square programs for the calculation of stability constants[1].

Program	Data treated	Sum of squared residuals minimised	Iterative method used
LETAGROP	Potentiometric	Several ($\bar{n}$, analytical hydrogen ion)	Pitmapping (Newton - Rapheson)
GAUSS	Potentiometric	Analytical hydrogen ion concentration	Gauss - Newton
SCOGS	Potentiometric	Volume of titrant	Gauss - Newton
LEAST	Potentiometric	Analytical concentrations	Gauss - Newton or Newton - Rapheson
LEASK	Potentiometric	Analytical concentrations	Search
STEW	Potentiometric	Analytical hydrogen ion concentration	Fletcher - Powell
MINIQUAD	Potentiometric	Analytical concentrations	Gauss - Newton
SQUAD	Spectrophotometric	Absorbance	Gauss - Newton
DALSFEK	Spectrophtotmetric - potentiometric	Absorbance, e.m.f.	Marquardt

procedure until both the formation constants and the mass balance equations are satisfied to within the specified tolerance. An overall picture of the experimental approach is shown in Figure 4.1.

Two computer programs were used to study the protonation and the formation constants of the cyclic and open-chain macrocycles included in this work and are discussed in some detail (Section 4.1.2.1). The two programs are SQUAD II[13] and SUPERQUAD[14]. SQUAD II was used to process the spectrophotometric data, and SUPERQUAD to process data obtained from potentiometric measurements.

4.1.2.1 The "SQUAD II" computer program:

The program SQUAD II is designed to calculate the best values for the stability constants of the proposed equilibrium model, by employing a non-linear least-squares approach. The program is completely general in scope, having the capability to refine stability constants for the general complex $M_mM_lL_nLq$, where m, l, n, q > 0 and j is positive (protons), negative (hydroxide ions) or zero. The current version of SQUAD II is, in many respects, a distillation of a number of earlier programs[12].

Janca and Have[16] made some improvements and produced SQUAD-G which can read spectra without a constant wavelength increment. Leggett also revised SQUAD II[17] to produce new SQUAD[17] which has "user-friendly" data input to simplify its use. Meloun[18] extended the diagnostic tools in SQUAD[17] for (i) determination of the number of light-absorbing species, (ii) a test for the degree of fit by statistical analysis of residuals of each spectrum and of the whole absorbance matrix, and (iii) a printer plot of estimated molar absorptivities and their standard deviations versus. wavelength. The new version SQUAD 84[19] also contains some additional diagnostics.

THEORY

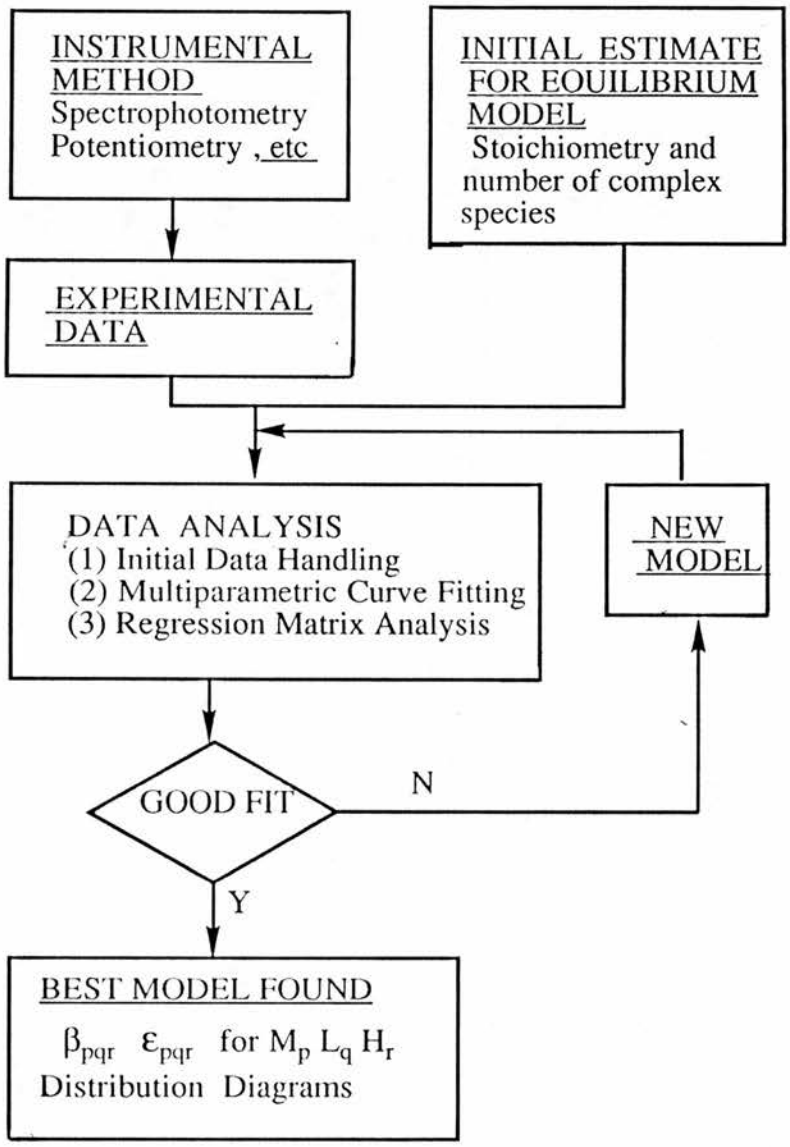

Figure 4.1 Overall scheme for equilibrium model determination .

In absorbance data analysis the Beer-Lambert Law and the Law of Absorbance Additivity are assumed to hold. An equilibrium system consisting of metal M, ligand L and proton(s) H as basic components combined in a species of general formula $M_pL_qH_r$, may be described by the following mass balance equations (charges omitted).

$$C_M = [M] + p \sum_{j=1}^{n_i} (\beta_{pqr}[M]^p[L]^q[H]^r)_j \qquad (49)$$

(n_i = number of coloured species)

$$C_L = [L] + q \sum_{j=1}^{n_i} (\beta_{pqr}[M]^p[L]^q[H]^r)_j \qquad (50)$$

$$C_H = [H] + r \sum_{j=1}^{n_i} (\beta_{pqr}[M]^p[L]^q[H]^r)_j \qquad (51)$$

and the overall stability constant

$$\beta_{pqr} = [M_pL_qH_r] / ([M]^p[L]^q[H]^r) \qquad (52)$$

$$= C / [M]^p.[L]^q.[H]^r$$

For the ith solution measured at the kth wavelength, the absorbance A_{ik} is given by

$$A_{ik} = \sum_{j=1}^{n_i} \varepsilon_{k,j} C_j$$

$$= \sum_{j=1}^{n_i} \varepsilon_{pqr,k} (\beta_{pqr}[M]^p[L]^q[H]^r)_j \qquad (53)$$

where $\varepsilon pqr,k$ is the molar absorptivity of species $M_pL_qH_r$ at the kth wavelength. The absorbance A_{ik} is an element of the $(n_w \times n_S)^2$ absorbance matrix A for n_s solutions with known concentrations C_M, C_L and C_H and at n_w wavelengths. The Beer-Lambert Law can be written in matrix notation as

$$\mathbf{A} = \varepsilon . \mathbf{C}$$

where ε is the $(n_w \times n_c)^2$ matrix of the molar absorptivities and **C** is the $(n_c \times n_s)$ matrix of the concentrations of the species concerned. It is assumed that all n_c species absorb light in the chosen spectral range.

The spectrophotometric equilibrium program is set up to adjust β_{pqr} and ε_{pqr} for any absorbance data by minimizing the residual square sum function U.

$$U = \sum_{i=1}^{n_S} \sum_{k=1}^{n_W} (A_{exp,\,i,\,k} - A_{cal,\,i,\,k})^2$$

$$= \sum_{i=1}^{n_S} \sum_{k=1}^{n_W} (A_{exp,\,i,\,k} - \sum_{i=1}^{n} \varepsilon_{k,\,j} C_j)^2 \approx \text{minimum} \qquad (54)$$

where the dependent variable A_{ik} is an element of the $(n_s \times n_w)$ absorbance response-plane, and the independent variables are the total concentrations C_M, C_L and C_H, which are varied in the n_s solutions.

Statistics

SQUAD II[14, 17] calculates a number of statistical parameters that may be used to judge the validity of a particular model: (a) the correlation matrix, which gives an indication about constants which are not separately defined by the current data, (b) the σ

---

[2] n_w = No. of wavelengths, n_s = No. of solutions; n_c = No. of coloured species.

data (the standard deviation (sd) in the absorbance data), which provides an overall measure of the fit of the model to the data (σ_{data} should have a value of about ±0.001 to ± 0.004 for a good fit), (c) the σ_{const} (the sd of each refined constant), which must be approximately 1% of that constant to indicate a good fit, and (d) σ_{spect} (the sd of each spectrum). In the case where more than one model is insignificantly different, various possibilities may arise. However, in most cases the minimum values of σ_{data} σ_{const}, σ_{spect} and the sum of squares of (A_{obs} - A_{calc}) are usually considered to select the correct model.

Determination of the number of absorbing species in solution.

A knowledge of the total number of absorbing species is necessary in kinetic studies and in the calculation of stability constants of complex species.

A computational method has been adopted for determining the number of species in solution. Such a method, based on simple matrix theory, depends on the fact that the rank of the matrix A of the absorbance values of a series of solutions at several wavelengths gives the number of the absorbing species present in solution.

The rank of the matrix A is given by the number of non-zero elements on the leading diagonal of the reduced absorbance matrix. The criterion used for an element to be considered as a non-zero element is when it is greater than three times the corresponding element in the reduced error matrix (E)[3] (E is the expected error matrix). A range of E values may be used so that the variation of the rank found with error provides an insight into the relevance one can place on the number of species found. The computer program TRIANG[1] was used for this purpose.

4.1.2.2 The "SUPERQUAD" computer program:

The computer program SUPERQUAD[14] is used to calculate formation constants of species in solution equilibria from data obtained by potentiometric titration.

---

[3]Matrices A and E are of same order.

This program has been designed to supercede miniQUAD by providing the additional facilities discussed below.

(1) The program can treat data for substances which are not of high purity.

(2) The model selection criteria have been improved, where the minimisation is based on measured electrode potentials.

(3) New treatment of formation constants, which assume negative values during a refinement, in which a model with a negative formation constant is rejected rather than rejecting the constant itself from a refinement.

(4) The program takes account of some systematic error, and caters for ion-selective electrodes whose response slope is other than Nernstian.

(5) When using miniQUAD it was common practice to omit the calculation data obtained near end points. These data points can now be included as they are assigned small weights.

The basic algorithm in SUPERQUAD can be stated in terms of the set of non-linear equations of mass-balance (55).

$$T_A = [A] + \sum_k a_k \beta a_k b_k \ldots\ldots\ldots [A]^a[B]^b \ldots\ldots$$

$$T_B = [B] + \sum_k b_k \beta a_k b_k \ldots\ldots\ldots [A]^a[B]^b \ldots\ldots \qquad (55)$$

T_A, T_B ..... are the total concentrations of reactants A, B, ... and there are assumed to be k complex species formed. They are solved iteratively by Newton's method. The program uses **s** (the sample standard deviation) and x^2 (goodness of fit factor) to judge the best fit. The best fit is achieved when $s < 1$ and $x^2 < 12$.

SUPERQUAD has many advantages over other computer programs. The main advantages include: (a) the data input are more user friendly, (b) the program can handle data from all known systems of potentiometric titration (for example, batch titrations[15], alkali added or generated coulometrically and determinate systems where

the number of electrodes is equal to the number of reactants), (c) the program uses all titration points therefore no bias results between a certain pH range of the titration, and (d) the program is extremely flexible and can deal with mononuclear, polynuclear, hydrolysed, mixed ligand and mixed metal complexes, with up to 300 titration points and 20 complex species in equilibrium.

4.2 Protonation Constants and Formation Constants for the Ligands [15]aneN$_4$ and [16]aneN$_4$ with Copper(II)

4.2.1 Introduction:

The formation constants of copper(II) and nickel(II) with tet-a (the C-meso isomer of 5,7,7,12,14,14-hexamethyl-1,4,8,11-tetra-azacyclotetradecane) and cyclam are of particular interest because they were determined by Margerum *et al* (20, 21) in his pioneering work dealing with the macrocyclic effect. Cabbiness and Margerum found(20) that log K for the red tet-a complex of Cu(II) was 28, compared with a log K value of only 23.9 for the complex of the open chain polyamine ligand 2,3,2-tet . Hinz and Margerum found(21) that log K for the complex of Ni(II) with cyclam was 22.2, as compared with a log K of 16.4 for the complex of 2,3,2-tet. The approximately four to six orders of magnitude of extra stabilization noted in macrocycles was named the thermodynamic macrocyclic effect (abbreviated as Δlog K(MAC)).

Since Margerum's initial work, log K values have been determined with several macrocycles and different metal ions(22-25).

Recently Kaden *et al* (26) have found that a macrocyclic effect also exists in ligands with mixed N_2S_2 donors. Thus the Cu(II) complex of 1,4-dithia-8,11-diazacyclotetradecane (I) is 10^5 times more thermodynamically stable than the corresponding open-chain ligand 2,13-dithia-6,9-diazatetradecane (II).

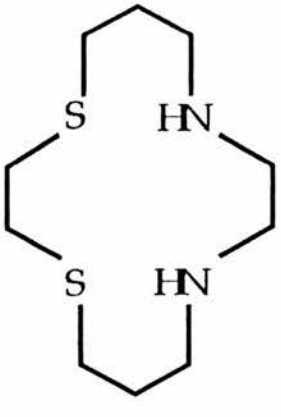

I

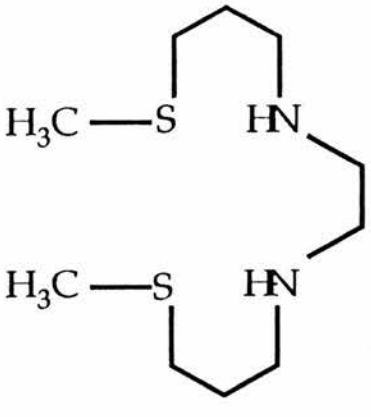

II

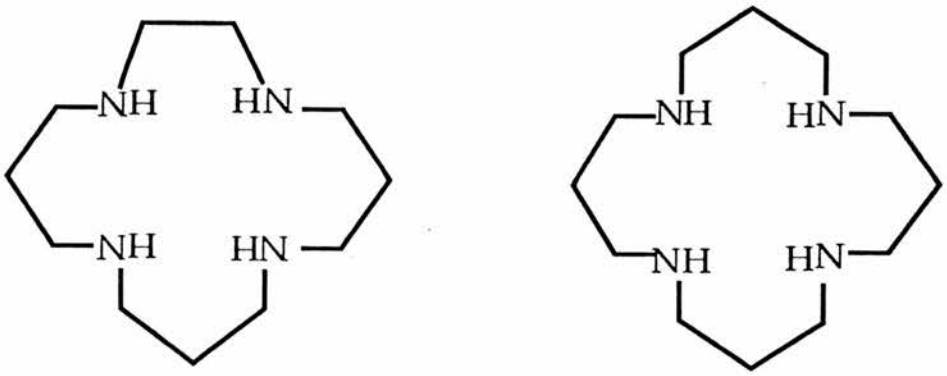

[15]aneN$_4$ [16]aneN$_4$

Figure4.2 15- and 16-membered macrocyclic ligands .

Early work ascribed the macrocyclic effect exclusively to either enthalpic[21] or entropic[27] effects. However, recent direct calorimetric measurements of enthalpy[28] have shown, at least for tetra-aza ligands, that the entropy term is always favourable, whereas the enthalpy term varies in magnitude with the matching size of the metal ion and the aperture of the macrocyclic ligand.

Size-match selectivity[29] has been much used in rationalising the pattern of formation constants of complexes for macrocyclic ligands. The metal might be expected to form its most stable complexes when the match between the cavity size in the macrocycle and the size of the metal ion was closest. However, formation constant studies[25] with the metal ions Cu(II), Ni(II), Zn(II), Cd(II), and Pb(II) with the ligands [12]aneN$_4$ through [15]aneN$_4$ led to the realisation that the macrocyclic cavity was not of great importance in controlling metal-ion size selectivity. The tetra-aza macrocycles are too flexible for macrocyclic cavity size to be an important factor[31]. Several isomers of the macrocyclic complex occur, in some of which the metal ion is coordinated out of the macrocyclic plane. In this situation the factors controlling selectivity are the same as those for open-chain ligands, namely the size of the chelate ring[30]. For tetra-aza macrocycles, macrocyclic ring size increases along the series [12]aneN$_4$ through [16]aneN$_4$. The best fit M-N bond lengths calculated from molecular mechanics (MM)[31] are [12]aneN$_4$, 1.82 Å; [13]aneN$_4$, 1.92 Å; [14]aneN$_4$, 2.07 Å; [15]aneN$_4$, 2.22 Å; [16]aneN$_4$, 2.38 Å. Analysis of formation constants[30] for complexes of macrocyclic and nonmacrocyclic ligands has confirmed that chelate ring size is important in controlling metal ion size-based selectivity and usually outweighs the effect of macrocyclic ring size when flexible ligands are involved.

This work describes the potentiometric determination of the stepwise protonation constants of [15]aneN$_4$ and [16]aneN$_4$ (Figure 4.2) and their formation constants with Cu^{2+}. In addition, the constants were also determined spectrophotometrically by employing the variation in the uv-visible spectrum as a function of pH. The aim was to supplement and check existing formation constants of the tetra-aza macrocycles.

Materials:

The synthesis of [15]aneN$_4$ and [16]aneN$_4$ is described in Chapter 1. Stock solutions of the amines were prepared and the concentrations were checked potentiometrically as described in Chapter 2. The Cu(II) solutions were prepared from the perchlorate salt (Aldrich) (twice recrystallised from water) and standardised potentiometrically against EDTA (Chapter 2). Potassium nitrate (Aldrich; A.R.) was used to maintain the ionic strength at I = 0.4 mol dm^{-3}. Carbonate free solutions of NaOH (0.4 mol dm^{-3}, standardised with potassium hydrogen phthalate) were prepared from 'CONVOLS' ampoules and degassed. All solutions were prepared with distilled CO_2-free water.

Potentiometric Titrations:

The pH titrations were carried out with a Metrohm titroprocessor model 670 equipped with a Metrohm glass electrode and calomel electrode. The titration cell was thermostated at 25.0 ^{o}C by using a Julabo circulator. The buffer solutions (pH 4.00, 7.00 and 9.00, based on the scale of the U.S. National Bureau of Standards)(32) used for calibration were also from Metrohm. The direct pH-meter readings were used in the calculations of the acidity constants. These constants are so-called mixed constants (also known as Bronsted or practical constants), which include both activity and concentration terms. They may also be converted into the corresponding concentration constants by using the hydrogen ion activity coefficients determined in KCl solution(49)[4]. It should be noted that for the formation constants of metal ion complexes no such conversion is necessary. The experimental e.m.f have not been corrected for the liquid-junction

---

[4]Concentration constants may be determined by calibrating the electrodes with solutions of known hydrogen ion concentrations or by conversion of pH values using the appropriate hydrogen ion activity coefficient .

potential[5] because this effect was found to be negligible in the pH range investigated. The protonation and the formation constants were determined by titrating a 25 cm^3 aliquot of the ligand in the absence and presence of copper(II) perchlorate adjusted to an ionic strength of 0.4 mol dm^{-3} (KNO_3). Titrations were carried out in a thermostatted cell at 25.0 ± 0.2 ^oC under the stream of nitrogen, presaturated with water vapour by bubbling it through distilled water. In the protonation constant determinations, 1 x 10^{-2} mol dm^{-3} of the ligand with four equivalents of added acid were titrated with 0.4 mol dm^{-3} NaOH. In the complex formation constant determination, typical concentrations of the metal ion and the ligand (in a 1:1 molar ratio) were in the range 1 x 10^{-2} to 3 x 10^{-2} mol dm^{-3}. Duplicates of each titration curve did not differ by more than ± 0.005 of a pH unit. The potentiometric data were collected by an on-line IBM compatible PC and stored on floppy disk for processing by the SUPERQUAD program. The Fortran Program was adapted to be used by IBM PS/2 80-111 computer (RAM = 4 MB). For the titration curves pH versus B/L, B/L is the number of moles of standard base B per mole of the ligand L. Negative values indicate an excess of acid and positive values an excess of base (for example, - 2 represents 2 equivalents of excess standard acid).

Spectrophotometric Measurements

The formation constants logß were also determined by spectrophotometry. The uv-visible spectra were recorded on a Shimadzu 160 instrument using aqueous solutions, with cells thermostated (25.0 ± 0.1 ^oC) and I = 0.4 mol dm^{-3} (KNO_3). The pH of the

---

[5]When the hydrogen electrode is replaced by a glass electrode and the electrolyte differs from that of the reference electrode, the parallel relationship remains, with additive constants for the liquid-junction potentials, provided that the supporting electrolyte remains as the dominant ionic conductor. Below pH 2 and above pH 12, hydrogen ions and hydroxide ions begin to be responsible for appreciable fractions of the conductance, so that liquid-junction potentials change as the pH is lowered and raised below and above the limits. A useful estimate of the effects of liquid junction potential on the expected accuracy of the pH measurement can be obtained from computations made by Bates[34].

solutions was adjusted by dropwise addition of concentrated HCl or NaOH (*ca.* 6 mol dm^{-3}) and determined with a Radiometer pH-meter type 63 equipped with a Radiometer combined glass electrode, type GK 2311C. The spectrophotometric data were analysed with an IBM PS/2 computer using the SQUAD II (13) computer program. The spectra measured for solutions with $[L] = [Cu^{2+}] = (1 - 3) \times 10^{-3}$ mol dm^{-3} (8 experiments for each system) were evaluated at 15 wavelengths in the wavelength range 450 to 600 nm (pH 3.5 to 10). The test for the number of absorbing species was carried out using the computer program TRIANG (Section 4.1.2.1).

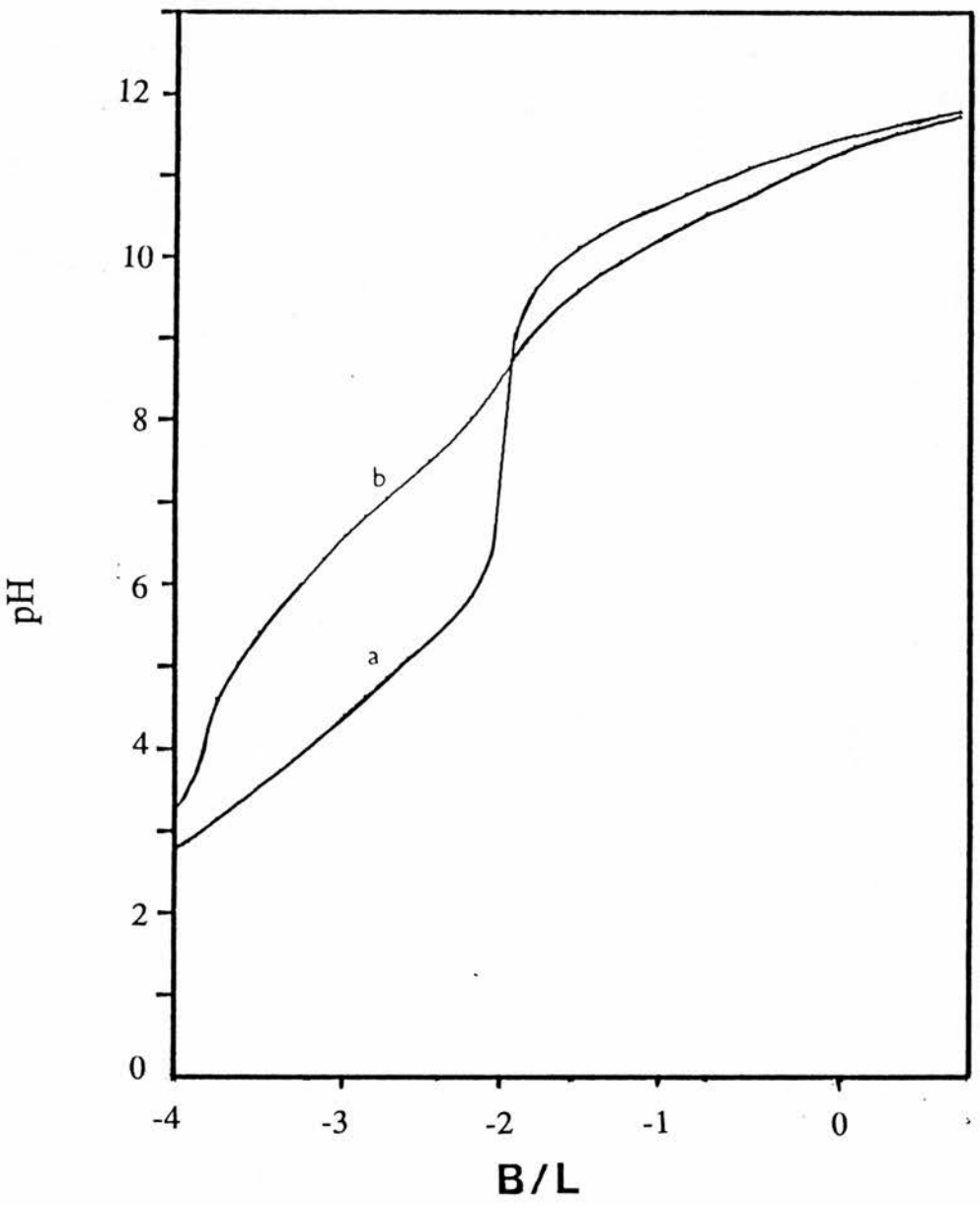

Figure 4.3 pH titration curves for a) [15]aneN$_4$.4HCl (0.01 mol dm^{-3}); b) [16]aneN$_4$.4HCl (0.01 mol dm^{-3})

Table 4.3 Protonation constants of [15]aneN$_4$ and [16]aneN$_4$ at 25.0°C*.

Ligand	I	log K_1	log K_2	log K_3	log K_4	Reference
[14]aneN$_4$	0.15	11.05 (0.3)	10.31 (1)	< 2	< 2	This work (see later)
	0.5	11.83	10.76	< 2	< 2	36
	0.5	11.59	10.62	1.61	2.4	34
[15]aneN$_4$	0.4	11.18 (1)	10.31 (1)	5.21 92)	3.55 (2)	This work
	0.5	11.23 (2)	10.28 (2)	5.32 (5)	3.79 (5)	36
	0.5	11.08	10.38	5.28	3.60	35
	0.2	11.2	10.1	~ 2	~ 2	37
[16]aneN$_4$	0.4	10.69 (2)	9.62 (3)	7.48 (4)	5.78 (4)	This work
	0.5	10.85 (5)	9.80 (5)	7.21 (5)	5.69 (5)	36
	0.1			7.06 (2)	5.30 (2)	38

*Standard deviations are given in parentheses and correspond to the error in the last digit.

4.2.3 RESULTS and DISCUSSION:

Protonation Constants:

For [15]aneN$_4$ and [16]aneN$_4$ there are a maximum of four protonation constants represented by the following reactions:

$$L + H^+ \rightleftharpoons HL^+ \quad ;K_1 \qquad (56)$$

$$HL^+ + H^+ \rightleftharpoons H_2L^{2+} \quad ;K_2 \qquad (57)$$

$$H_2L^{2+} + H^+ \rightleftharpoons H_3L^{3+} \quad ;K_3 \qquad (58)$$

$$H_3L^{3+} + H^+ \rightleftharpoons H_4L^{4+} \quad ;K_4 \qquad (59)$$

The protonation constants were treated as mixed-mode values, as defined by the relationships

$$K_1 = [HL^+] / a_H[L] \qquad (60)$$

$$K_2 = [H_2L^+] / a_H[HL^+] \qquad (61)$$

$$K_3 = [H_3L^+] / a_H[H_2L^+] \qquad (62)$$

$$K_4 = [H_4L^{4+}] / a_H[H_3L^{3+}] \qquad (64)$$

where a_H represents the activity of hydrogen ion as calculated from pH. The log K_i values were calculated from the corresponding pH titration curves (Figure 4.3) of these ligands by the computer program SUPERQUAD[14]. The stepwise protonation constants for the ligands investigated in this work, together with those obtained by others[35, 36], are shown in Table 4.3. The values obtained in this work correspond well with those

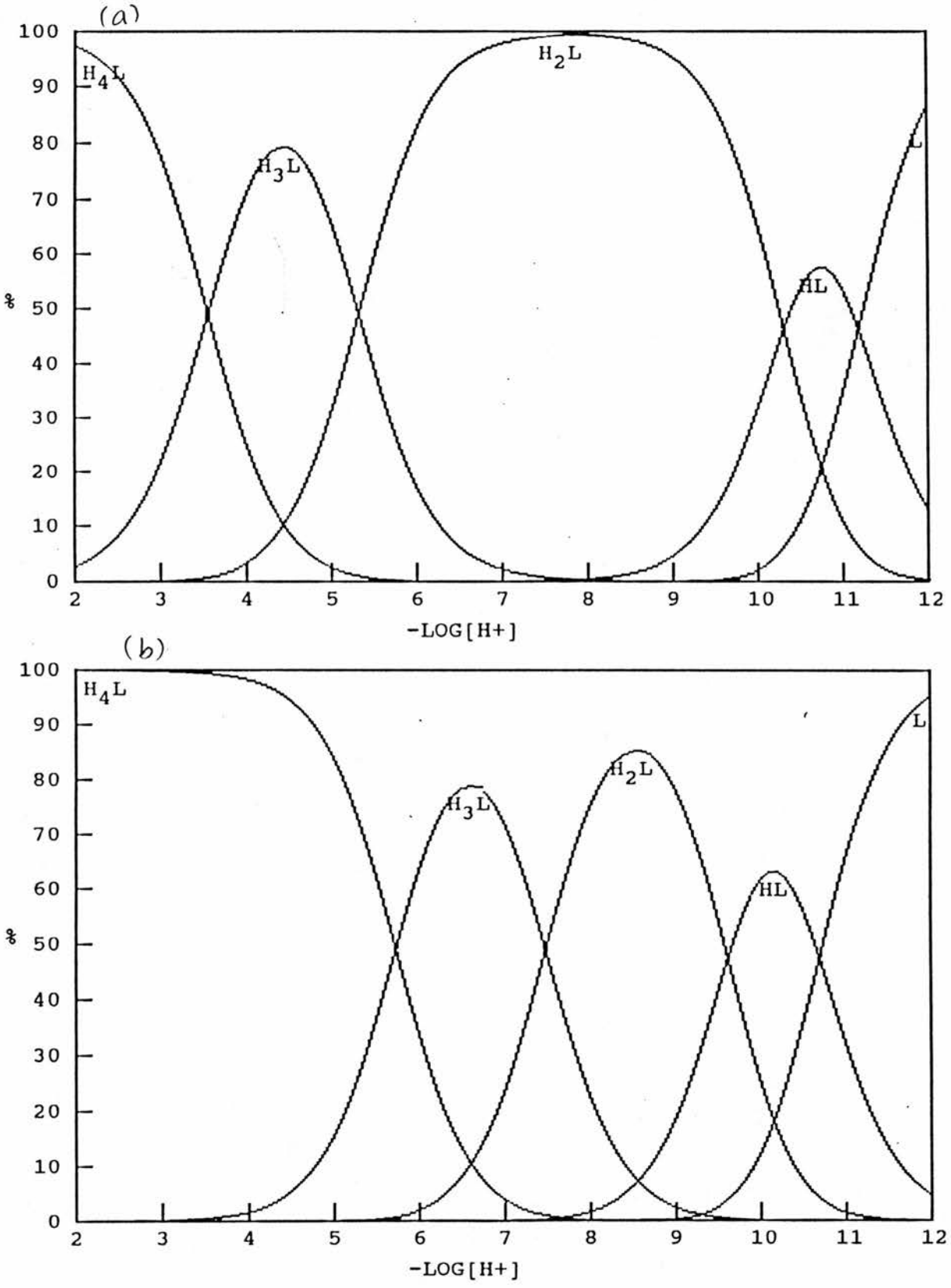

Figure 4.4 Species Distribution Diagrams for a) 0.01 M [15]aneN_4 and 0.01 M [16]aneN_4, at 25.0 ^{o}C and I = 0.4 M KNO_3

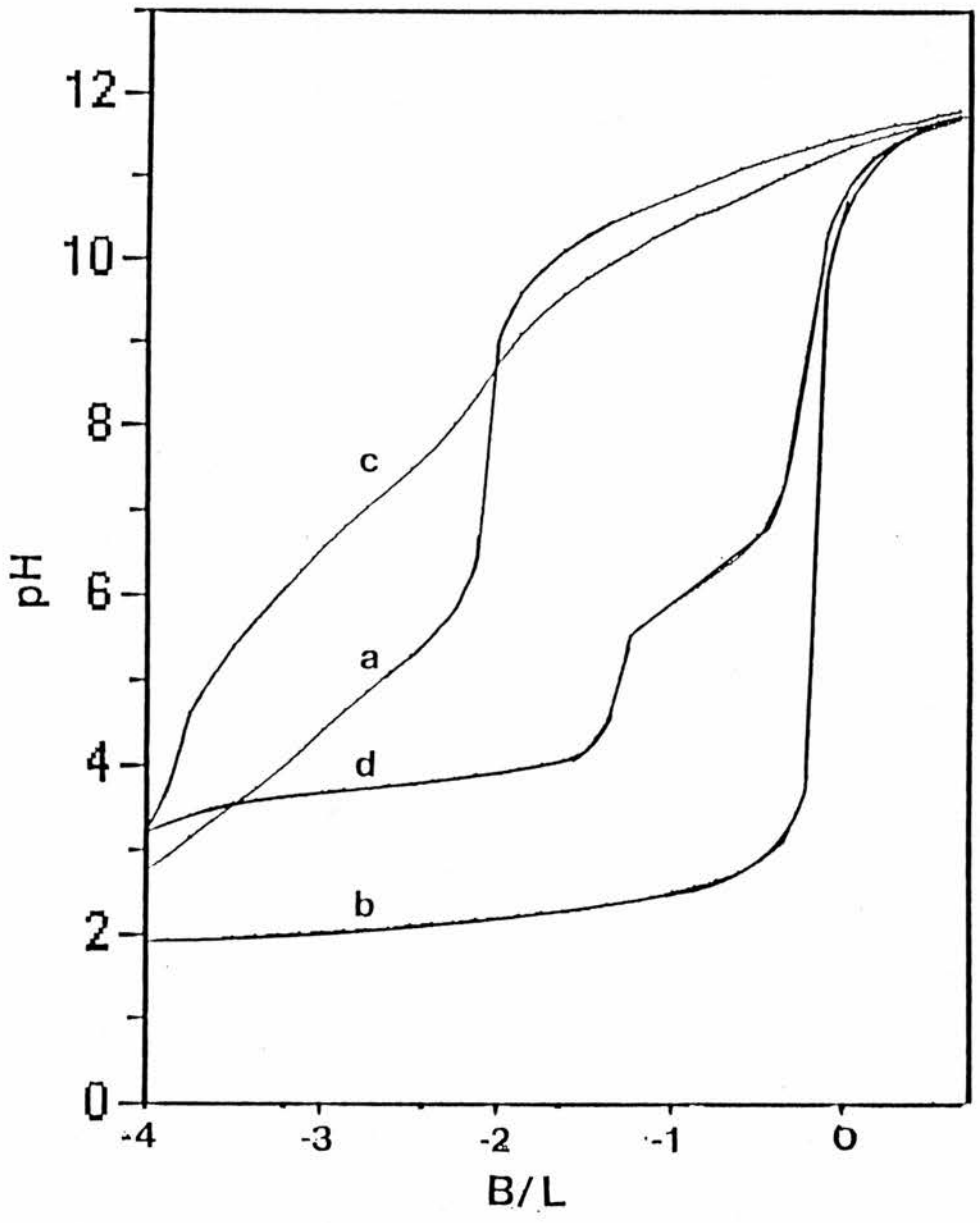

Figure 4.5 pH titration curves for a) [15]aneN$_4$.4HCl (0.01 mol dm^{-3}); b) [15]aneN$_4$ and copper(II) perchlorate (1:1) ; c) [16]aneN$_4$.4HCl (0.01 mol dm^{-3}) and copper(II) perchlorate (1:1) .

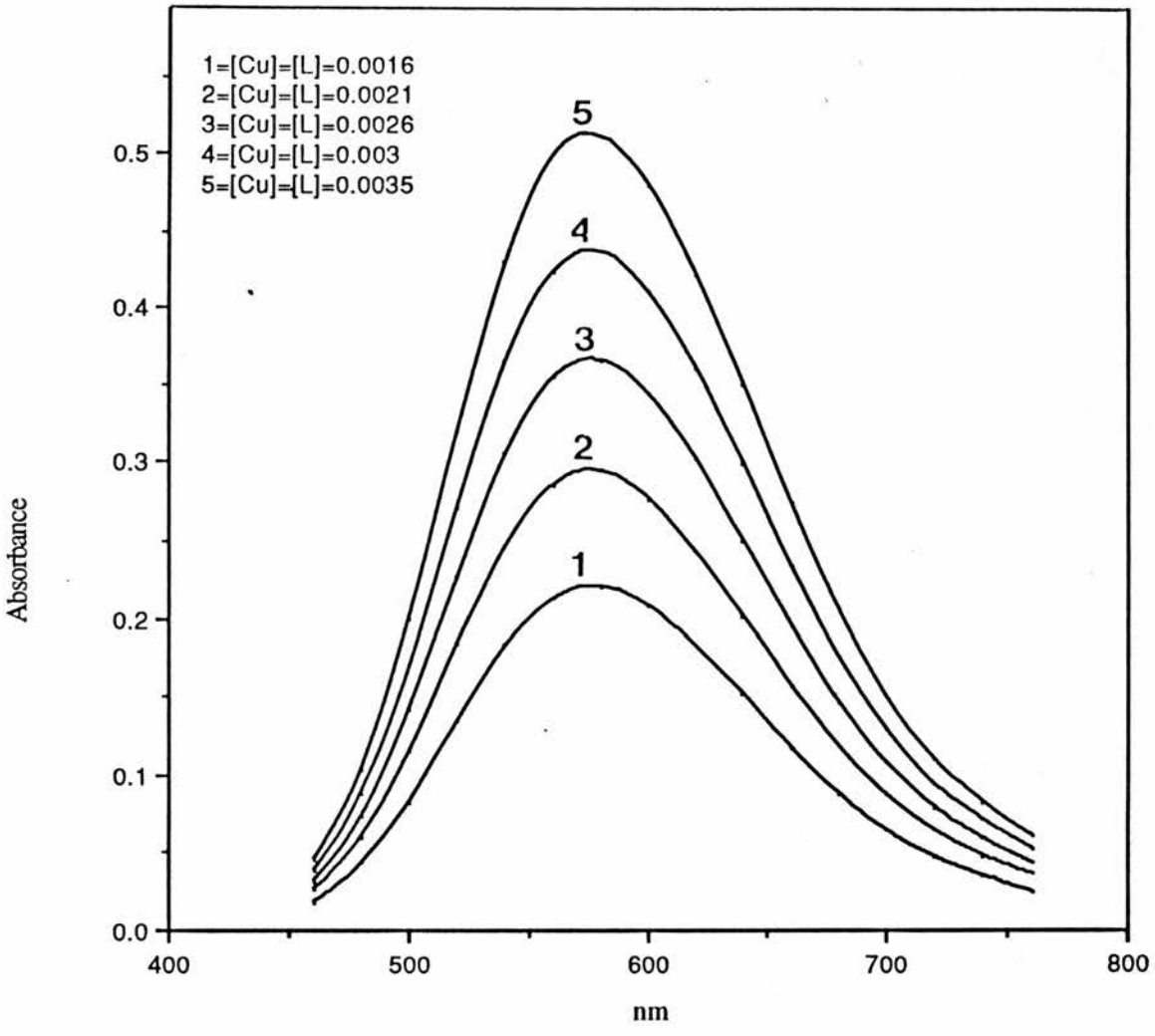

Figure4.6 Typical absorption spectra for Cu-[15]aneN4 as function of concentration at pH 5.4

published in the literature with the exception of values of log K_3 and log K_4 of [15]aneN_4 reported by the Japanese authors[37]. The results in Table 4.3 show that there are two high and two low protonation constants. The variations in log K_1 and log K_2 is minor compared to the change observed in log K_3 and log K_4. The first observation is easily rationalised, the second proton always adds to a nitrogen atom *trans* to the first protonation site. The distances are such that little or no interaction takes place, giving normal log K values. The variation in ring size and the relative arrangement of ethylene and propylene bridges between the amino nitrogens strongly influences the values of the higher protonation constants. The third and fourth protons must bind between two positively charged ammonium groups resulting in a strong electrostatic interaction. Increasing the length of the bridges from two to three carbon atoms and bringing the propylene bridges close to each other leads to easier protonation and log K values increase. It appears that the order of log K_i values arises due to electrostatic repulsion, which is much more important than in an open chain tetraamine. For the largest ring, [16]aneN_4, the log K_i values closely resemble those observed in open chain tetraamines. The species distribution curves at 25 ^{o}C are shown in Figure 4.4 (a) and (b).

Copper(II) Complexes of [15]aneN_4 and [16]aneN_4.

The titration curve of [15]aneN_4 plus 4 equivalents of HCl (Figure 4.5(a)) shows one step inflection at B/L = -2 corresponding to the loss of two acidic protons from the amino salt. The third and fourth protons are too weakly acidic (Table 4.3). For the [16]aneN_4.4HCl amine salt, the four protons are too weakly acidic for an inflection to be observed (Figure 4.4(c)). However, in the presence of Cu(II) both of these ligands behave as strong acids and become fully deprotonated at pH ~ 2.5 and pH ~ 5 for the [15]aneN_4 and [16]aneN_4 respectively. The log β_{pqr} values were calculated from the corresponding pH titration curves (Figure 4.5 (b) and (d)) and from the corresponding absorption spectra (for example, Figure 4.6) by the computer programs SUPERQUAD[14] and SQUAD II[13]. The potentiometric and spectrophotometric studies showed the existence of two complex species (Equations 64 and 65)

$$Cu^{2+} + L \rightleftharpoons [CuL]^{2+} \quad ;\log\beta_{110} = [CuL]^{2+} / [Cu^{2+}]\,[L] \qquad (64)$$

$$Cu^{2+} + H^{+} + L \rightleftharpoons [CuHL]^{3+} \quad ;\log\beta_{111} = [CuHL^{3+}] / [Cu^{2+}]\,[H^{+}]\,[L] \qquad \ldots (65)$$

Table 4.4 lists the formation constants reported here for copper(II) complexes of [15]aneN$_4$ and [16]aneN$_4$, together with the available literature values. In Table 4.5 are shown formation constants for complexes of the set of tetra-aza macrocyles [12]aneN$_4$ through [16]aneN$_4$.

Figure 4.7 shows how the stability of the copper(II) complexes of the tetra-aza macrocyles varies as a function of macrocyclic ring size. The change in complex stability is given by $\Delta\log K$, which is $\log K_1$ for the complex of the particular tetra-aza macrocycle minus $\log K_1$ for the [12]aneN$_4$ complex for copper(II) ion. The pattern in Figure 4.7 is dependent on M-N bond length (although recent studies have shown that such a pattern is dependent on metal ion size for metal ions other than Cu(II)) [38] with the point for the [14]aneN$_4$ (cyclam) complex occupying a pivotal position. The ideal bond length for fitting into [14]aneN$_4$ is 2.07 A^o and for Cu(II) is 2.03 A^o. A similar trend has been observed with the mixed N_2S_2 donor macrocycles[25].

The drop in complex stability when macrocyclic ring size increases beyond 14-membered, probably relates to steric crowding problems. It is no steeper than the drop observed for the open-chain analogues with increasing chain length (section 2.5), and there are no special effects of the macrocyclic ring.

From the ionisation equilibria of the complexes represented in Equations 64 and 65, it can readily be shown that

$$pK_a^{[15]aneN_4} = \log\beta_{111}^{[15]aneN_4} - \log\beta_{110}^{[15]aneN_4}$$

and

Table 4.5 Formation Constants for the the complexation of Cu^{2+} with the set of Tetra-azamacrocycles [12]aneN$_4$ through [16]aneN$_4$.

Ligand	log β_{110}	Ref.
[12]aneN4	23.29	38
[13]aneN4	24.36	38
[14]aneN4	26.50	38
[15]aneN4	24.20	This work
[16]aneN4	18.92	This work

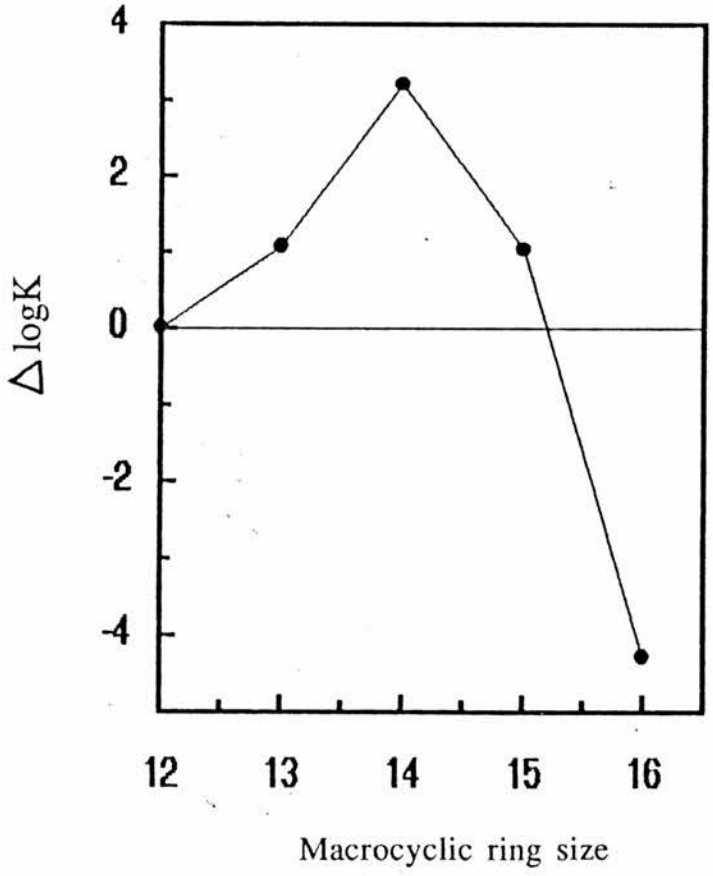

Figure 4.7 Variation of complex stability as a function of macrocyclic ring size for copper(II) with the tetra-aza macrocycles [12]aneN$_4$ through [16]aneN$_4$.

Table 4.4 Formation Constants for the Complexation of Cu^{2+} with Ligands [15]aneN_4 and [16]aneN_4 at 25°C and I = 0.4 mol dm^{-3} (KNO_3). p,q,r are the stoichiometric coefficients of L, Cu, and H^+.

Ligand	Stoichiometric coefficients p	q	r	log β_{pqr} ($\pm\sigma$)[a]	Method	pH range	Reference
[15]aneN_4	1	1	0 [b]	24.15 (3)	potentiometry [d]	1.7 - 3	This work
	1	1	0 [c]	24.58 (2)	potentimetry	1.7 - 3	This work
	1	1	1	26.50 (3)			
	1	1	0 [b]	24.40 (2)	spectrophotometry [e]	2 - 5.5	This work
	1	1	0 [c]	23.45 (4)	spectrophotometry	2 - 5.5	This work
	1	1	1	26.96 (8)			
	1	1	0	24.4	polarography		37
[16]aneN_4	1	1	0 [c]	18.92 (8)	potentiometry [d]	3.5 - 8	This work
	1	1	1	25.15 (6)			
	1	1	0 [b]	14.54 (1)	spectrophotometry [f]	7.5 - 9.5	This work
	1	1	1	20.75 (1)	spectrophotometry [f]	7.5 - 9.5	This work
	1	1	0	20.92	potentiometry		39
	1	1	0	20.01	potentiometry		

[a] Standard deviations are given in parenthesis and correspond to the error in the last digit.

[b] Calculated separately.

[c] Calculated simultaneously.

[d] χi^2 was 16 and s = 0.09. The number of data points 300. The data points were equally weighted.

[e] The standard deviations in absorbance data was $6x10^{-3}$, 16 solutions were used and the wave length range was 450 - 600 nm.

[f] The standard deviations in absorbance data was $7x10^{-4}$, 8 solutions were used and the wave length range was 430 - 890.

$$pK_a^{[16]aneN_4} = log\beta_{111}^{[16]aneN_4} - log\beta_{110}^{[16]aneN_4}$$

giving

$$pK_a^{[15]aneN_4} = 2.35 \quad \text{and} \quad pK_a^{[16]aneN_4} = 6.23.$$

The stability constant $log\beta_{110}$ = 24.58, for the 1:1 complex of [15]aneN$_4$ containing 5,6,6,6-membered chelates is almost 10^6 times greater than the corresponding one formed by [16]aneN$_4$ containing 6,6,6,6-chelates. This may be rationalised in terms of the presence of a five-membered chelate ring in [15]aneN$_4$.

The formation constants for Cu[15]aneN$_4$, determined by potentiometric and spectrophotometric methods differ only slightly. The maximum discrepancy is 0.46 and the average is 0.22 log units. This good agreement also indicates that the equilibria studied are independent of total copper(II) and ligand concentrations, which are 10 times greater in the potentiometric titrations. The reason for the larger discrepancy (~ 4 log units) observed with the Cu[16]aneN$_4$ system is not fully understood.

4.3 Protonation Constants and Formation Constants for the Ligands Dioxocyclam and the Tripeptide Glycylglycylhistidine (glyglyhis) with Copper(II) and Nickel(II) .

4.3.1 INTRODUCTION

The macrocyclic ligand 5,7-Dioxo-1,4,8,11-tetra-azacyclotetradecane (dioxocyclam; H_2L^1) was first characterised in 1978[40] and displays many novel properties. For example H_2L^1 reacts rapidly with metal ions such as copper(II) and nickel(II) and the resulting complexes dissociate rapidly in acidic solution (Chapter 1). The parent ligand 1,4,8,11-tetra-azacyclotetradecane (cyclam) equilibrates extremely slowly with the very labile copper(II) ion and $[Cu(cyclam)]^{2+}$ is not decomposed in 6 mol dm^{-3} HCl over a period of several weeks[41]. The half life of $[Ni(cyclam)]^{2+}$ in 1 mol dm^{-3} $HClO_4$ has recently been shown by Billo[42] to be *ca.* 30 years.

Potentiometric titration of dioxocyclam in the presence of some bivalent metal ions indicated a metal ion promoted ionization of two protons. Quantitatively, the most successful metal ion in promoting the deprotonation is Cu(II), while deprotonation occurs with Ni(II) above pH 7. With Zn(II), Cd(II) or Pb(II) deprotonation is not observed.

Dioxocyclam has a structural resemblance to tripeptides. Both are potential quadridentate ligands featuring two isolated amides between two terminal donor atoms. The coordination of metal ions to the amide nitrogens with displacement of the amide protons in tripeptides is well known[43, 44]. The present study reports the protonation constants of dioxocyclam (H_2L^1) and glyglyhis (H_2L^2) and their complexation equilibria with Cu^{2+} and Ni^{2+} by potentiometric methods. The formation constants of dioxocyclam with copper(II) were also measured spectrophotometrically. The structures of the ligands are shown in Figure 4.8 .

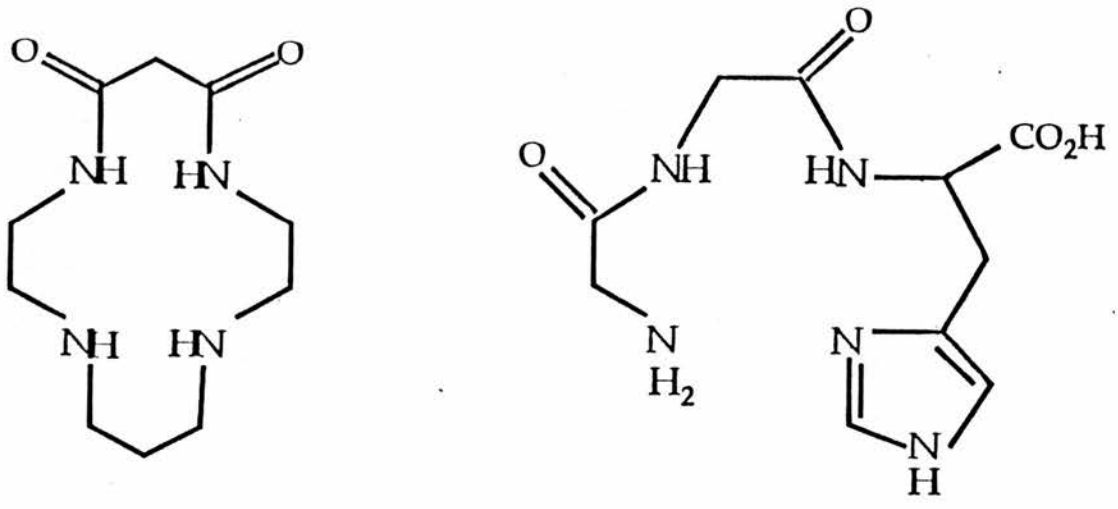

Dioxocyclam Glycylglycylhistidine

Figure 4.8 Dioxocyclam and Glycylglycylhistidine.

4.3.2. EXPERIMENTAL.

Glyglyhis (H_2L^2).

Materials.

The purification of $Cu(ClO_4)_2$ and $Ni(ClO_4)_2$ and the standardisation of Cu(II) and Ni(II) solutions are described in section 4.2.2. The purity of the tripeptide (PEPTIDE INSTITUTE INC, Japan) was checked by elemental analysis (Calc. for $C_{10}H_{15}N_5O_4.0.5H_2O$: C, 43.16; H, 5.80; N, 25.17; Found: C, 43.24; H, 6.01; N, 24.74). Solutions of the ligand were prepared by accurate weighing.

Potentiometric Titrations:

Potentiometric titration of the ligand in the absence and presence of copper(II) and nickel(II) perchlorates were carried out using a Radiometer Titralab System interfaced with an Apple IIe computer. The temperature was maintained at (25 ± 0.5°C) and each titration was performed on a solution volume of 25 cm^3 adjusted to ionic strength of 0.1 mol dm^{-3} with $NaNO_3$. The potentiometric data were processed on a Zenith computer using the SUPERQUAD program. Other experimental details are given in section 4.2.2.

Dioxocyclam (H_2L^1)

The preparation and analysis of the ligand (H_2L^1) is described in Chapter 1. Stock solutions of dioxocyclam were standardised as described in Chapter 2. The equilibrium studies are described in section 4.2.2.

Table 4.6 Equilibrium constants for the stepwise protonation of dioxocyclam (H_2L^1) and glyglyhis (H_2L^2) in aqueous solution at 25 °C.

Equilibrium	log K(± σ) Thiswork	Literature
$H_2L^1 + H^+ \rightleftharpoons [H_3L^1]^+$	9.78 (3)[a]	...
	9.62 (1)[b]	9.51 [c]
$[H_3L^1]^+ + H^+ \rightleftharpoons [H_4L^1]^{2+}$	6.21 (5)[a]	...
	5.87 (2)[b]	5.80 [c]
$[H_4L^1]^{2+} + H^+ \rightleftharpoons [H_5L^1]^{3+}$	1.62 (1)[a]	...
$H_2L^2 + H^+ \rightleftharpoons [H_3L^2]^+$	8.06 (1)[d]	8.10 [e]
$[H_3L^2]^+ + H^+ \rightleftharpoons [H_4L^2]^{2+}$	6.82 (2)[d]	6.75 [e]
$[H_4L^2]^{2+} + H^+ \rightleftharpoons [H_5L^2]^{3+}$	2.80 (3)[d]	2.72 [e]

[a] I = 0.4 mol dm^{-3} KNO_3

[b] I = 0.15 mol dm^{-3} NaCl

[c] Reference 46 (I = 0.1 mol dm^{-3} $NaClO_4$)

[d] I = 0.1 mol dm^{-3} $NaNO_3$

[e] Reference 33 (I = 0.16 mol dm^{-3})

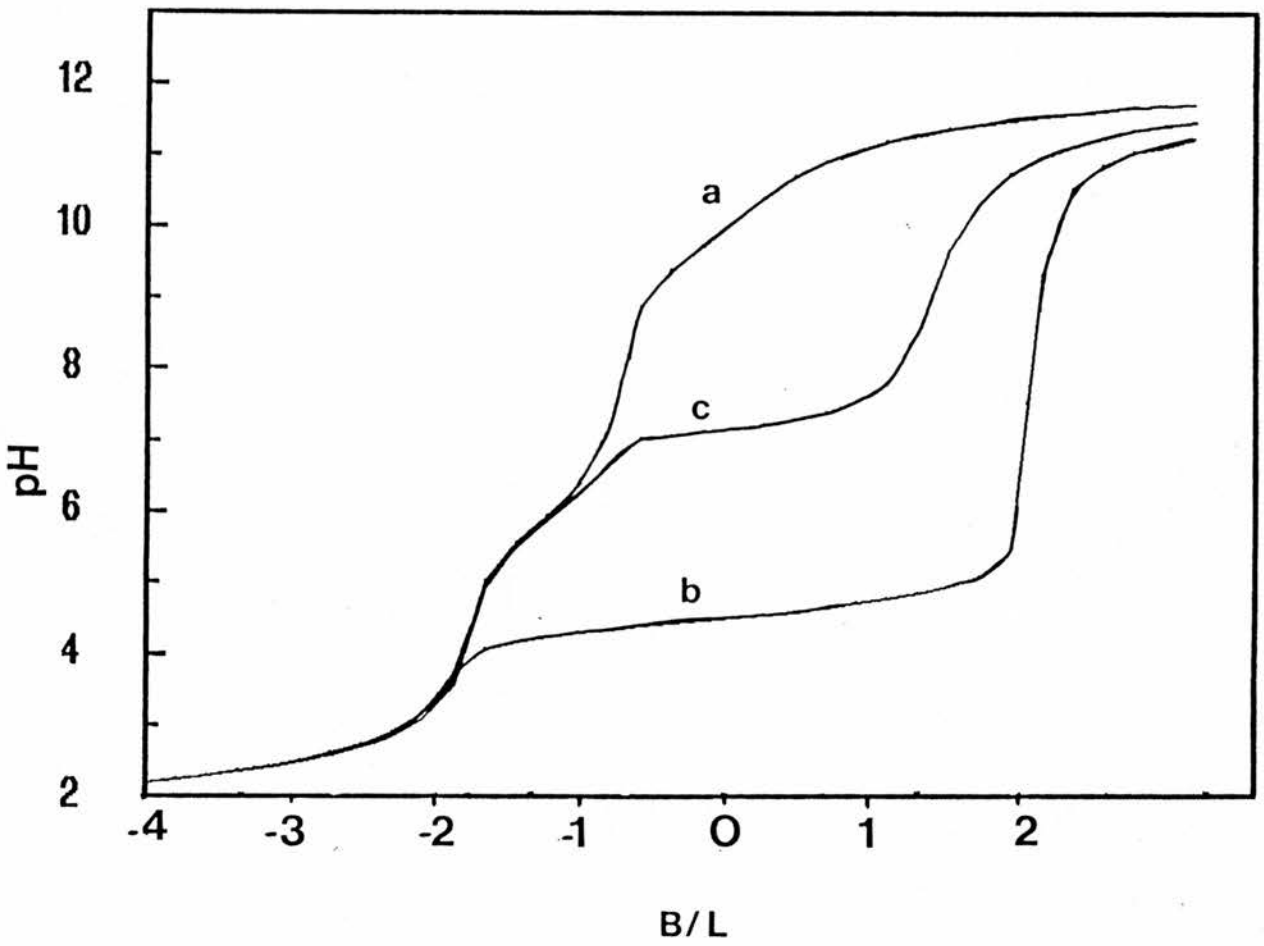

Figure 4.9 Titration curves for dioxocyclam : a) dioxocyclam + excess of acid ; b) dioxocyclam + 1 equivalent of copper(II) + excess of acid ; c) dioxocyclam + 1 equivalent of nickel(II) + excess of acid .

4.3.3 RESULTS and DISCUSSION

4.3.3.1 Copper(II) and Nickel(II) Dioxocyclam Complexes

The acid-base behaviour of dioxocyclam (H_2L^1) in aqueous 0.15 mol dm^{-3} NaCl and 0.4 mol dm^{-3} KNO_3 was investigated by pH titration at 25°C. In a typical experiment, a solution containing the macrocycle and excess acid (4 equivalents of HCl) was titrated by standard base (Figure 4.9a). In the pH range investigated (*ca* 2 to 11.5), dioxocyclam behaves as a triprotic base. The stepwise protonation constants were determined by computer treatment of the titration data (Table 4.6). The first two protonation constants are in good agreement with those reported by Fabbrizzi *et al* (46). Dioxocyclam is a much weaker base than the fully saturated analogue cyclam. Log K_1 is lower than expected on statistical basis. The second protonation step of dioxocyclam (Equation 2; Table 4.6) involves a decrease in log K_2. This effect may arise due to diprotonated dioxocyclam, $[H_4L^1]^{2+}$, having two ammonium ions in adjacent positions where as in cyclam they are trans to each other. Electrostatic repulsion is much less in cyclam.

Formation constants.

The complexation of Cu(II) by dioxocyclam in aqueous solution was first studied by Kodama and Kimura(47), who investigated the equilibria over a very narrow pH range. The system was also studied by Fabbrizzi *et al* in 1984(46).

The titration of an equimolar mixture of copper(II) and H_2L^1 (plus 4 equivalents of acid) is shown in Figure 4.9(b). During the titration, the colour of the solution changes from light blue to deep blue then to purple. In the case of nickel from yellow to intense yellow. Similar colour changes are observed in the tripeptide systems (Section 4.3.3.2).

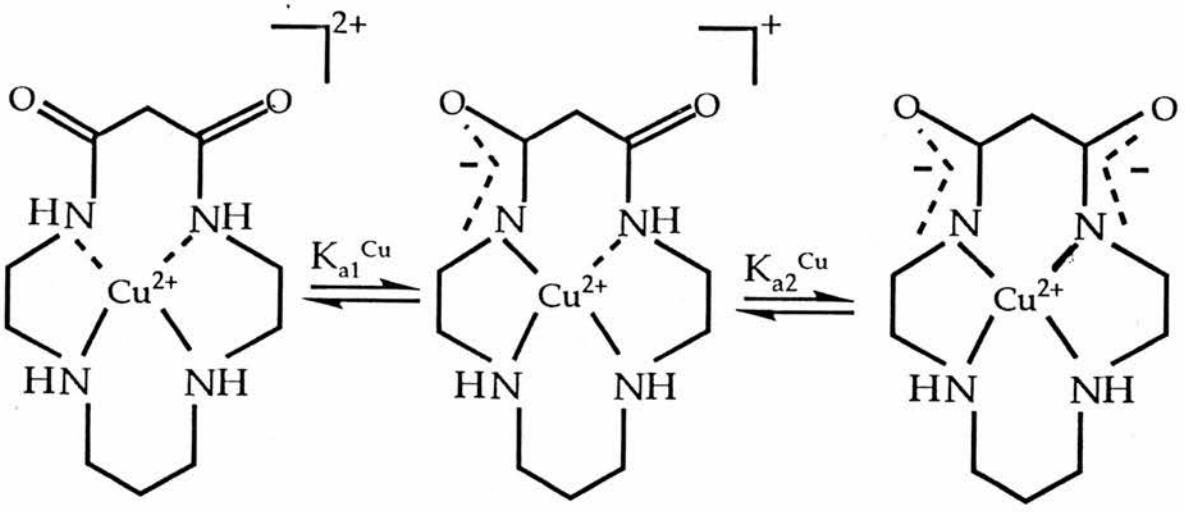

I = $[Cu(H_2L^1)]^{2+}$ II = $[Cu(HL^1)]^{+}$ III = $[Cu\ (L^1)]$

Four moles of base were consumed per 1 mole of Cu(II). Thus, in addition to two protons from the amino groups of the ligand, two other protons are ionised from the two amide nitrogens. Computer analysis showed that the best curve fitting is obtained by assuming that the following species are formed: $[Cu(H_2L^1)]^{2+}$, $[Cu(HL^1)]^{+}$ and $[Cu(L^1)]$ (Formulae I, II and III respectively).

Spectrophotometric measurements of twelve solutions of the copper(II) dioxocyclam complex in the wavelength range 400 to 700 nm (pH 4.5 to 9.5) (Figure 4.10), confirmed the existence of the above three complexes. Log ß values from potentiometric and spectrophotometric measurements are reported in Table 4.7. Again, the agreement between the two techniques indicates that the equilibria studied are independent of total copper(II) and ligand concentrations. The species distribution is shown in Figure 4.11(a). The complex $[Cu(HL^1)]^{+}$ is only a minor species and reaches its maximum concentration, 20.0%, at pH 4.25 and $[Cu(H_2L^1)]^{2+}$ at pH 3.75 (*ca* 30%). The log $ß_{110}$ for $[Cu(H_2L^1)]^{2+}$ (I) is even smaller than that found for trimethylenediamine-Cu(II) (log ß = 10.2)[47], in which the two amino groups are separated by a trimethylene chain, as in the complex (I). The major species $[Cu(L^1)]$ (II) is obtained by deprotonation of the two amido groups. Formation begins at pH 3.5 and is complete at pH 6.0 (Figure 4.11(a)). The Cu(II) lies in the plane of the four nitrogen atoms [47].

It can readily be shown that for the equilibria

Table 4.7 Formation Constants for the Complexation of Cu^{2+} with Dioxocyclam (I = 0.15 mol dm^{-3} NaCl) and Glyglyhis (I = 0.1 mol dm^{-3} $NaNO_3$) at 25° C. p,q,r are the stoichiometric coefficients of L, Cu, and H^+.

Ligand	Stoichiometric coefficients p q r	log $\beta_{pqr}(\pm\sigma)$[a]	Method	pH range	Reference
Dioxocyclam	1 1 0[b]	9.53 (3)[e]	potentiometry[c]	3.9 - 5.2	This work
	1 1 -2	0.52 (1)[e]	potentiometry[c]	3.9 - 5.2	This work
	1 1 -1[d]	4.74 (1)[e]	potentiometry[c]	3.9 - 5.2	This work
	1 1 0[b]	8.45 (5)[f]	potentiometry[c]	4 - 5.2	This work
	1 1 -1	4.24 (2)[f]	potentiometry[c]		This work
	1 1 -2	0.30 (5)[f]	potentiometry[c]		This work
	1 1 0[b]	8.81 (2)[f]	potentiometry[c]	2.2 - 5.2	This work
	1 1 -2	0.35 (1)[f]	potentiometry[c]		This work
	1 1 0[d]	9.46 (2)	spectrophotometry[g]	4.5 - 9.5	This work
	1 1 -1[d]	4.82 (2)	spectrophotometry[g]		This work
	1 1 -2[d]	0.38 (5)	spectrophotometry[g]		This work
	1 1 0	8.75 (1)	potentiometry		46
	1 1 -2	0.44 (1)	potentiometry		46
Glyglyhis	1 1 1	12.40 (1)	potentiometry[c]	2.0 - 7.5	This work
	1 1 0	7.64 (1)	potentiometry[c]	2.0 - 7.5	This work
	1 1 -1	2.55 (3)	potentiometry[c]	2.0 - 7.5	This work
	1 1 -2	-1.55 (1)	potentiometry[c]	2.0 - 7.5	This work

[a] β_{110} is a cummulative formation constant, i.e. for $[Cu(H_2L^1)]^{2+}$, $\beta = [Cu(H_2L^1)]^{2+}/[Cu^{2+}][H_2L^1]$. β_{11-2} is a cummulative formation with two proton loss, i.e. for $[Cu(L^1)]$, $\beta_{11-2} = [Cu(L^1)]/[H_2L^1][H^+]^2$

[b] Computed simultaneously.

[c] Xi^2 was (13 - 19) and s = (0.1 - 0.4).

[d] Computed separately.

[e] I = 0.4 mol dm^{-3} KNO_3.

[f] I = 0.15 mol dm^{-3} NaCl.

[g] The standard deviation in absorbance data was $7x10^{-4}$; 12 solutions were used and, the wavelength range was 400 - 750 nm.

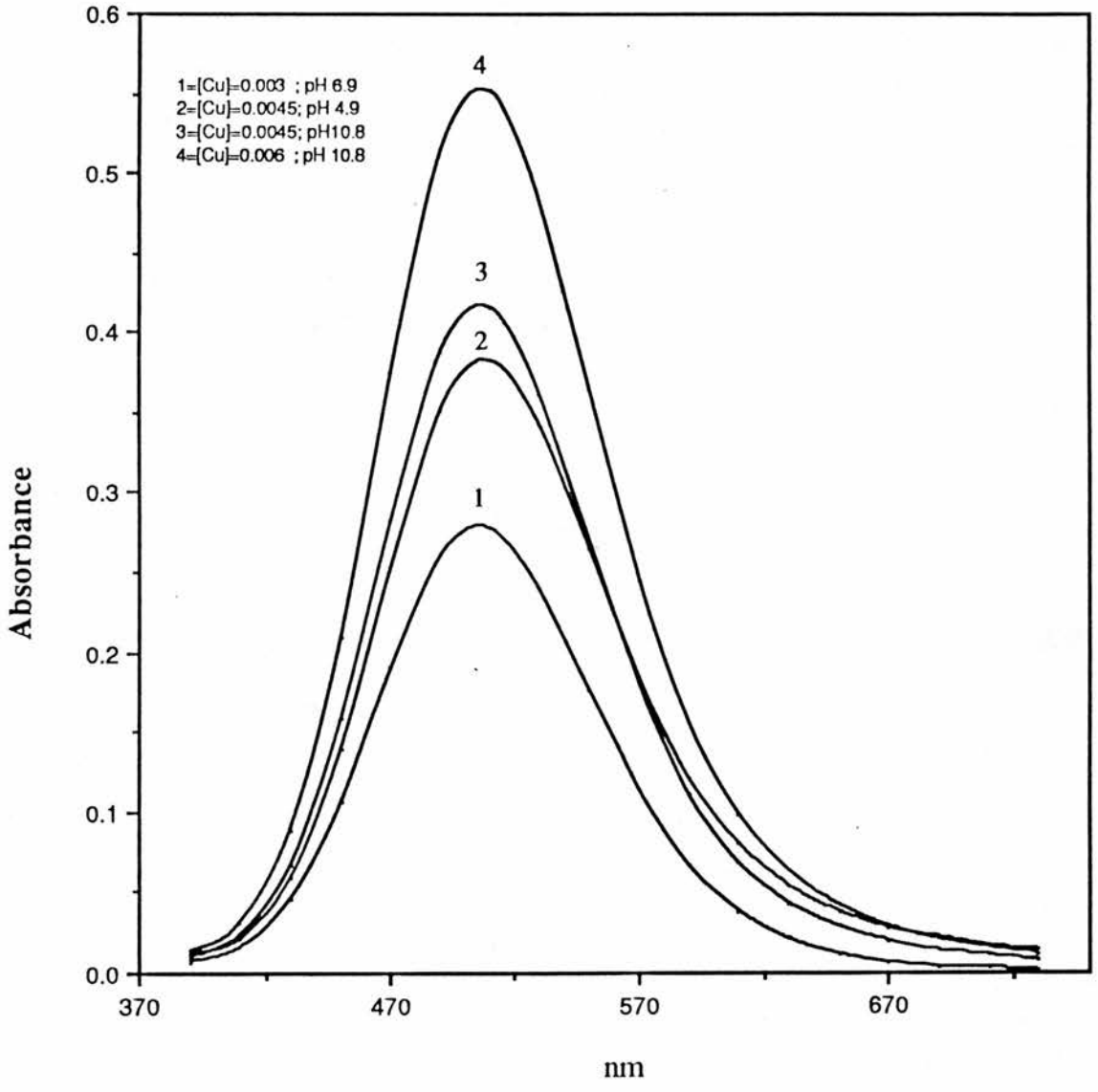

Figure4.10Typical absorption spectra for Cu-dioxocyclam as function of both pH and concentration of metal ion . The ligand concentration was 0.008 M .

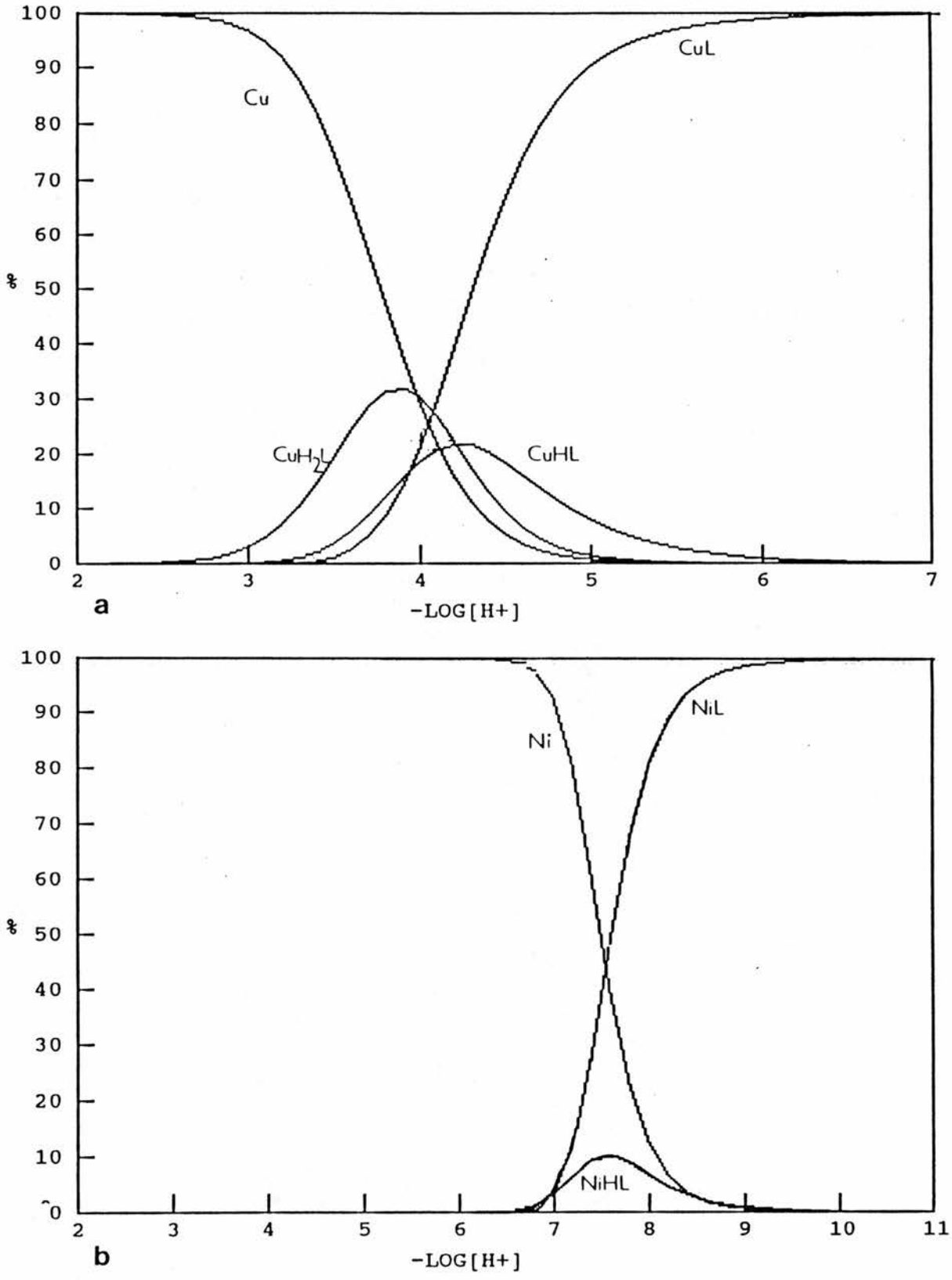

Figure 4.11 Species distribution diagram for a) 0.001 M Cu(II) and 0.001 M dioxocyclam , b) 0.001 M Ni(II) and 0.001 M dioxocyclam at 25.0 ^{o}C .

$$[Cu(H_2L^1)]^{2+} \rightleftharpoons [Cu(HL^1)]^+ + H^+ \quad ;K_{a1}^{Cu} \qquad (66)$$

$$[Cu(HL^1)]^+ \rightleftharpoons [Cu(L^1)] + H^+ \quad ;K_{a2}^{Cu} \qquad (67)$$

$K_{a1}^{Cu} = ß_{11-1} / ß_{110}$ and $pK_{a1}^{Cu} = \log ß_{110} - \log ß_{11-1} = 4.79$ and

$K_{a2}^{Cu} = ß_{11-2} / ß_{11-1}$ and $pK_{a2}^{Cu} = \log ß_{11-1} - \log ß_{11-2} = 4.22$. Similar behaviour was observed with glyglyhis (H_2L^2) .

Somewhat different behaviour was observed with Ni(II). In the pH range 2.1 - 9.5 (Figure 4.9(c)), only two complex species, $[Ni(HL^1)]^+$ and $[Ni(L^1)]$, were detected, arising from the equilibria

$$Ni^{2+} + H_2L^1 \rightleftharpoons [Ni(HL^1)]^+ + H^+ \quad ;\log ß_{11-1} \qquad (68)$$

$$Ni^{2+} + H_2L^1 \rightleftharpoons [Ni(L^1)] + 2H^+ \quad ;\log ß_{11-2} \qquad (69)$$

The log ß values are given in Table 4.8.

The complex $[Ni(HL^1)]^+$ reaches its maximum concentration (*ca.*10 %) at pH 7.8, while at pH 9 the fully deprotonated complex $[Ni(L^1)]$ is almost 100% abundant (Figure 4.11(b)).

It can be readily shown that for the equilibrium

$$[Ni(HL^1)]^+ \rightleftharpoons [Ni(L^1)] + H^+ \quad ;K_a^{Ni} \qquad (70)$$

$$pK_a^{Ni} = \log ß_{11-1} - \log ß_{11-2} = 6.91 \qquad (71)$$

These findings (Equations 67 and 70) indicate that the complex $[Ni(HL^1)]^+$ is a weaker acid than $[Cu(HL^1)]^+$ by a factor of *ca.* 10^3.

The copper(II) ion has a better fit to the 14-membered ring cavity than nickel(II). As a result, copper(II) undergoes stepwise incorporation into the macrocyclic ring. The 'fit' of nickel(II) to the dioxocyclam ring is less favourable. Only two complexes, $[Ni(HL^1)]^+$ and $[Ni(L^1)]$, are observed. Examination of Tables 4.7 and 4.8 shows that the selectivity of the dioxocyclam complexes for Cu(II) over Ni(II) ($\Delta\log \beta_{11-1} = 7.1$; $\Delta\log \beta_{11-2} = 9.8$) is one of the highest yet recorded for any ligand system in the literature(49). A further interesting property of H_2L^1 is its ability to complex rapidly with transition metal ions. Equilibration of H_2L^1 with Cu(II) is essentially instantaneous on the time scale of the potentiometric titrations, with Ni(II) equilibrium was established within two minutes of the addition of base[6].

---

[6]In the B/H_2L^1 scale -1 to +1 (Figure 4.9) the equilibrium with Ni(II) is slow and 10 to 20 minutes are required for the attainment of equilibrium.

Table 4.8 Formation Constants for the Complexation of Ni^{2+} with Dioxocyclam (I = 0.15 mol dm^{-3} NaCl) and Glyglyhis (I = 0.1 mol dm^{-3} $NaNO_3$) at 25°C. p,q,r are the stoichiometric coefficients of L, Ni^{2+}, and H^+.

Ligand	Stoichiometric coefficients p q r	log $\beta_{pqr}(\pm\sigma)^a$	pH range	Reference
Dioxocyclam	1 1 -1	-2.59 (7)	2.1 - 11	This work
	1 1 -2	-9.50 (4)		This work
Glyglyhis	1 1 1	11.33 (2)	3.5 - 7	This work
	1 1 0	4.74 (6)		This work
	1 1 -2	-6.93 (1)		This work

[a] β_{pqr} is a cummulative formation constant.

[b] χ_f^2 was < 13 and s < 0.5.

Table 4.9 Comparative equilibrium data for dioxocyclam and N, N' - bis(2-cyanoethyl) - dioxocyclam.

Dioxocyclam		Bis(2-cyanoethyl) dioxocyclam
pK_1	5.87	3.05
pK_2	9.62	5.94
Copper(II)		
$\log\beta_{110}$	8.45	
$\log\beta_{11-1}$	4.24	-3.43
$\log\beta_{11-2}$	0.29	-9.18
Nickel(II)		
$\log\beta_{11-1}$	-2.59	
$\log\beta_{11-2}$	-9.50	-14.45

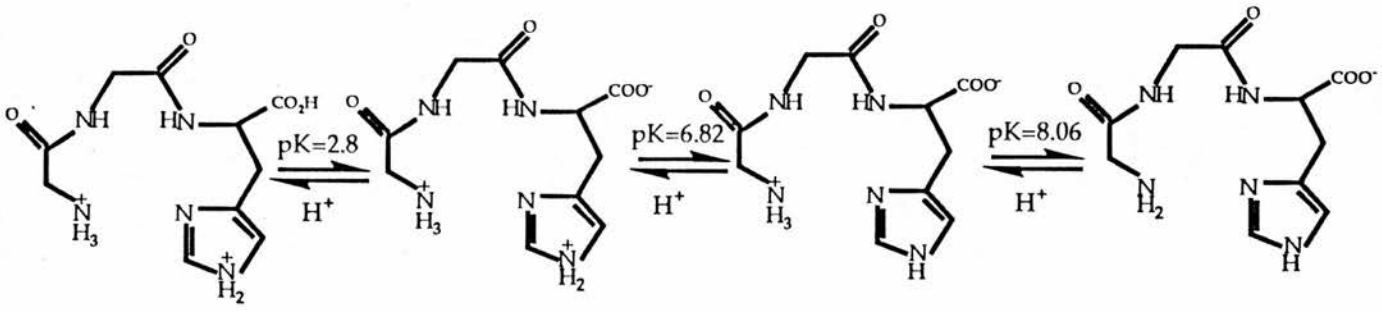

$(H_5L^2)^{3+}$ $(H_4L^2)^{2+}$ $(H_3L^2)^{+}$ H_2L^2

Scheme I. Ionization of glyglyhis.

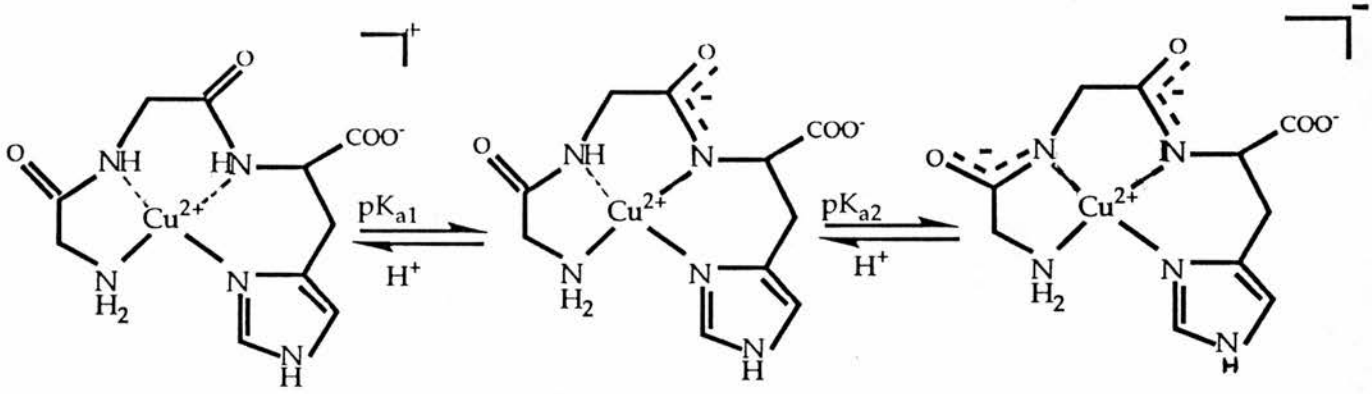

$[Cu(H_2L^2)]^{+}$ $[Cu(HL^2)]$ $[Cu(L^2)]^{-}$

Scheme 2. Deprotonation of $[Cu(H_2L^2)]^{+}$

4.3.3.2. Interaction of Copper(II) and Nickel(II) with Glycylglycylhistidine (glyglyhis).

The acid-base behaviour of glyglyhis (H_2L^2) in aqueous 0.1 mol dm^{-3} $NaNO_3$ was similar to that observed for dioxocyclam (H_2L^1) (Section 4.3.3.1). In a typical experiment (Figure 4.12), a solution of H_2L^2 in excess acid (one equivalent HNO_3 was added) was titrated with standard base. In the pH range investigated (*ca.* 2.0 to 10.5), glyglyhis behaves as a triprotic ligand. The equilibria are illustrated in Scheme I and the protonation constants summarised in Table 4.6 .

Potentiometric studies of the interaction of the tripeptide with copper(II) and nickel(II) indicated different behaviour for the two metal ions. A typical titration curve for 1 : 1 ratios of the ligand to the metal ion is shown in Figure 4.12. In both systems, 4 moles of base were consumed per mole of metal ion, indicating ionisation from the two peptide nitrogens. This displacement reaction is highly specific for Cu(II) and Ni(II) ions, although a much higher pH is required for the displacement of the peptide protons with Ni(II) . Computer analysis of the titration data (Figure 4.12 (b) and c)) showed that the best curve fitting is obtained by assuming that the following species exist in equilibrium: $[Cu(H_3L^2)]^{2+}$, $[Cu(H_2L^2)]^{+}$, [Cu(HL)] and $[Cu(L^2)]^{-}$ in the Cu (II) - tripeptide system and only $[Ni(H_3L^2)]^{2+}$, $[Ni(H_2L^2)]^{+}$ and $[Ni(L^2)]$ in the Ni (II) - tripeptide system. The cumulative formation constants $\log\beta_{pqr}$ are reported in Tables 4.7 and 4.8.

The stepwise ionisation of the peptide protons of the copper complexes are shown in Scheme 2.

It can readily be shown that $pK_{a1} = \log\beta_{11-1} - \log\beta_{110} = 5.09$ and $pK_{a2} = \log\beta_{11-2} - \log\beta_{11-1} = 4.1$.

Comparison of Dioxocyclam and Glycylglycylhistidine.

Copper(II) and nickel(II) promoted amide deprotonation of peptides is well documented[42]. Glyglyhis was chosen for the present comparison not only because of its structural similarities to peptides but also because of its current chemical and

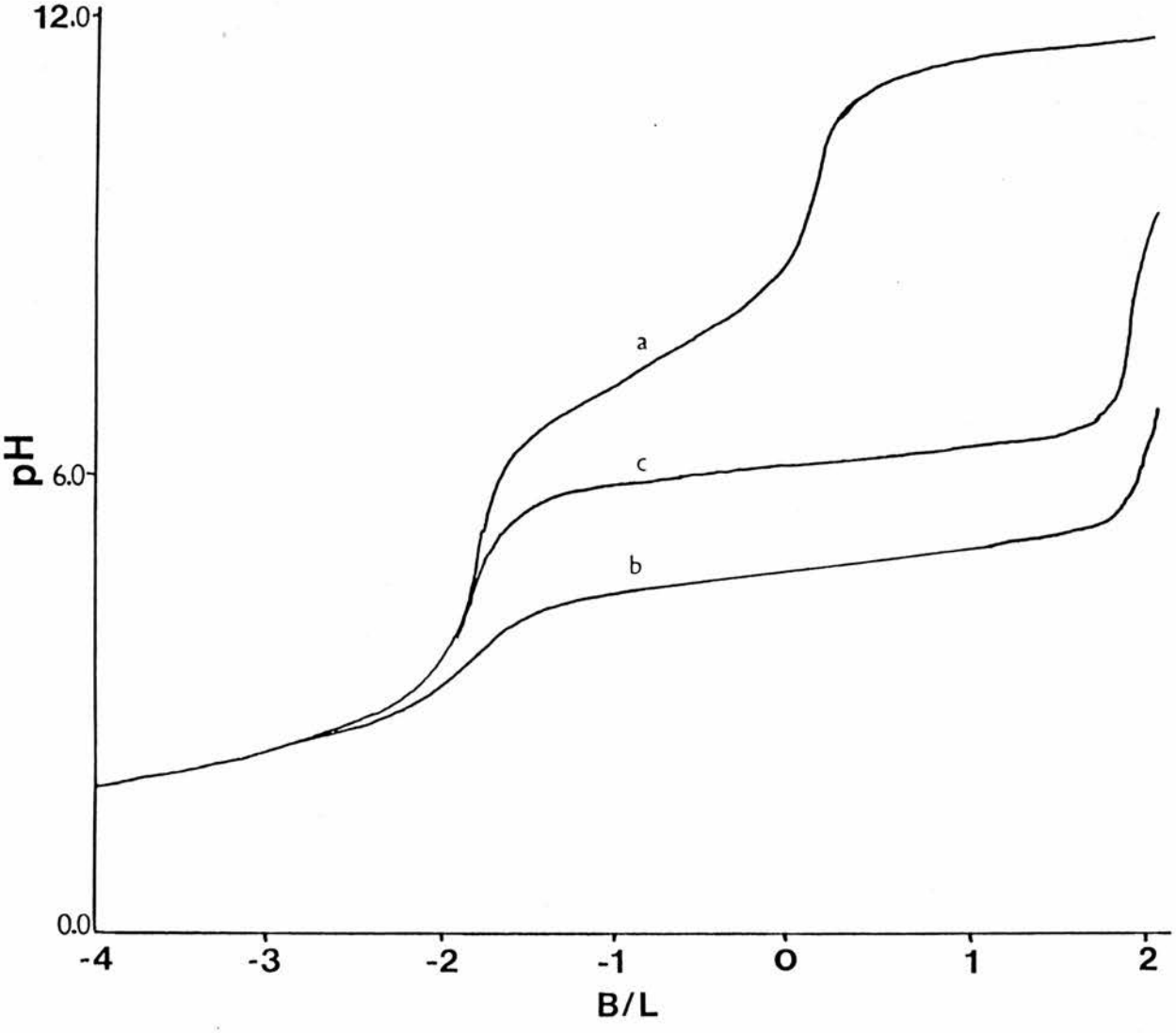

Figure 4.12 Titration curves for glyglyhis : a) glyglyhis + excess of acid ; b) glyglyhis + 1 equivalent of copper(II) + excess of acid c) glyglyhis + 1 equivalent of copper(II) + excess of acid

biological interest in the treatment of Wilson's disease [50]. The dioxocyclam complexes of Ni(II) and Cu(II) when compared with those of glyglyhis show a macrocyclic effect of 2 and 2.5 orders of magnitude respectively.

At acidic pH, complexation with Cu(II) and Ni(II) occurs more readily with the macrocyclic ligand than with the tripeptide (Figures 4.11 (a) and (b)), and 4.13 (a) and (b). Examination of Figures 4.11(a) and 4.13(a) show that at pH 6.0 the [Cu(L)] complex is 100% abundant for both dioxocyclam and glyglyhis. The relative complex stability was investigated by examining visible spectra of solutions of Cu(II) containing equivalent ratios of H_2L^1 and H_2L^2 at pH 5.5 (phosphate buffer). For separate solutions the absorption maxima occur at 500 and 530 nm for Cu(II)H_2L^1 and Cu(II)H_2L^2, respectively. In a mixture of Cu(II) and the two ligands the spectrum completely overlaps with that of the Cu(II)H_2L^1 solutions, thus demonstrating the overwhelming greater stability of the H_2L^1 complex relative to that of H_2L^2.

The present findings may have a potential application in view of the fact that glyglyhis is a molecule designed to mimic the copper(II)-specific transport site of serum albumin[46].

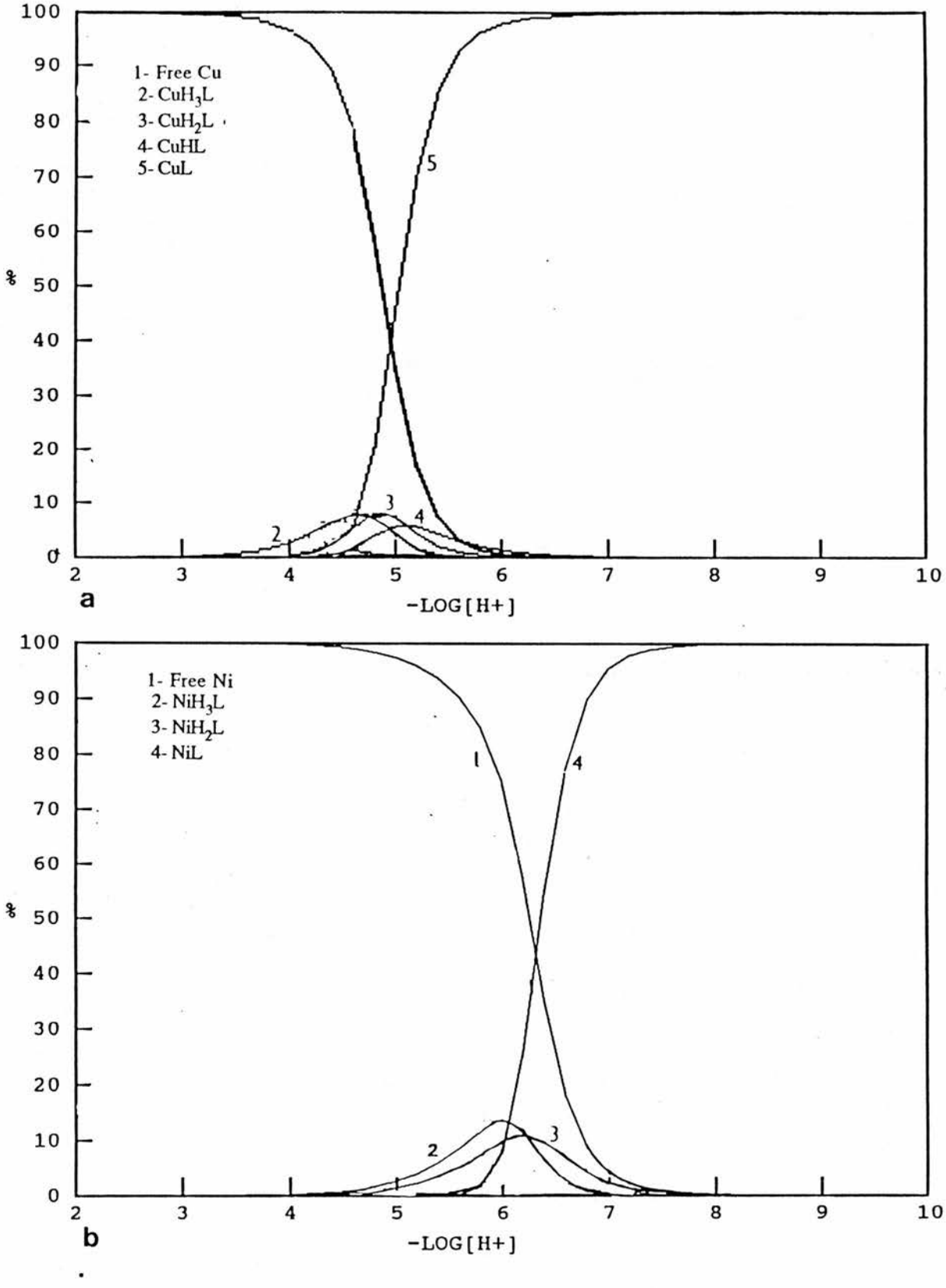

Figure 4.13 Species distribution diagram for a) 0.001 M Cu(II) and 0.001 M glyglyhis , b) 0.001 M Ni(II) and 0.001 M glyglyhis at 25.0 ^{o}C.

4.4 Protonation Constants and Formation Constants for the Ligand N, N'-bis (2-cynoethyl) - 5,7 - Dioxo 1,4,8,11 - Tetra-azacyclo Tetradecane with Copper(II) and Nickel(II) .

4.4.1 INTRODUCTION

Recently the coordination chemistry of pendent arm macrocycles has received considerable attention and the topic has been the subject of several reviews[51-53]. The incorporation of pendent donor groups such as $-(CH_2)_nNH_2$, $-(CH_2)_nCN$, $-(CH_2)_nOH$ and $-(CH_2)_nCONH_2$ to each nitrogen of a tetra-aza macrocycle gives ligands, which exhibit novel coordination modes and in some cases greatly enhanced kinetic lability in the metal complexes[54, 55] (also Chapter 1). The chemistry of tetracyanoethylcyclam (TCEC = I) has been studied in detail by Wainwright[56].

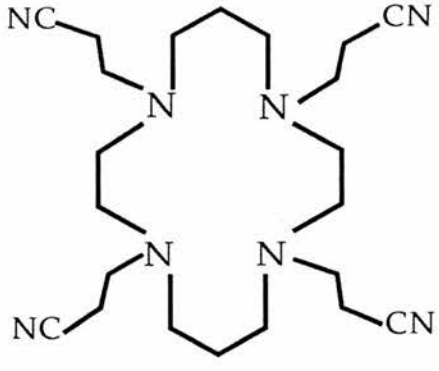

I = (TCEC)

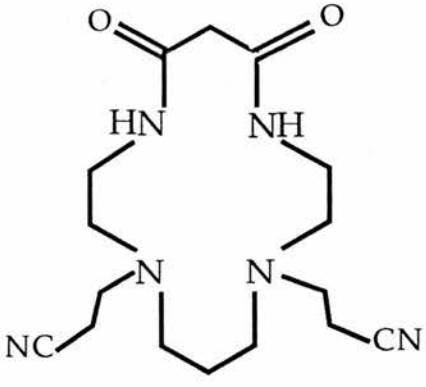

H_2L=N,N'-bis(2-cyanoethyl)-5,7-dioxo 1,4,8,11-tetra-azacyclotetra-decane

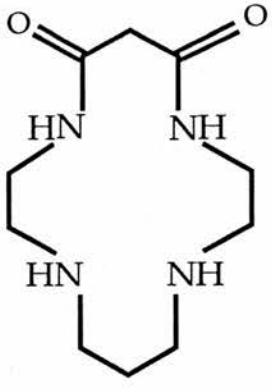

II = dioxocyclam

The present work describes the preparation of the new ligand, H_2L, derived from 5,7-dioxocyclam (II) and the coordination chemistry of this ligand with both copper(II) and nickel(II) ions.

4.4.2 EXPERIMENTAL

Preparation of the ligand

A solution of dioxocyclam (2.5 g) in acrylonitrile (40 cm^3) was refluxed for eight hours and the excess of solvent removed on a rotary evaporator. The resulting sticky solid was recrystallised from ethanol chloroform (9:1, v/v) mixture giving colourless crystals (2.2 g, 61% yield), m.p. 135°C. (Found: C, 57.0; H, 8.2; N, 25.0. $C_{16}H_{26}N_6O_2$. Calc.: C, 57.5; H, 7.8; N, 25.1%). The mass spectrum has M^+ 334, $C_{16}H_{26}N_6O_2$ = 334. ^1H n.m.r. in $CDCl_3$ (ppm downfield from TMS): 6.9δ (broad 2NH), 3.2δ (singlet, 2H), 2.6δ (multiplet, 20H) and 1.6δ (quintet, 2H). I.r., strong bands at 3290 (ϑNH), 2230 (ϑC≡N) and 1680 cm^{-1} (ϑC=O).

Physical Measurements:

I.r. spectra (as KBr pellets) were recorded on a Perkin Elmer 1330 i.r. spectrophotometer. ^1H n.m.r. spectra were obtained using $CDCl_3$ as solvent on a Bruker AM 300 n.m.r. spectrometer using TMS as internal standard. The uv-visible spectra were determined using a Phillips PU 8720 instrument with 1 cm cells.

Potentiometric Titrations:

Potentiometric titrations of the ligand in the absence and presence of copper(II) and nickel(II) perchlorates were carried out using a Radiometer Titralab System interfaced with an Apple IIe computer. Other experimental conditions are described in 4.3.2.

4.4.3 RESULTS and DISCUSSION:

The synthesis of N,N'-bis(2-cyanoethyl)-5,7-dioxo-1,4,8,11-tetra-azacyclotetradecane (LH_2) is straightforward and the ligand is readily prepared in good yield by refluxing a solution of dioxocyclam in neat acrylonitrile for several hours. Cyanoethylation is indicated by the appearance of a strong band in the infrared at 2230 cm^{-1} assigned to νC=N. Dioxocyclam is a cyclic amide and the two amide nitrogens readily deprotonate in the presence of metal ions such as copper(II), nickel(II) (Section 4.3), palladium(II) and platinum(II)[57] to form neutral complexes of the general type (IV).

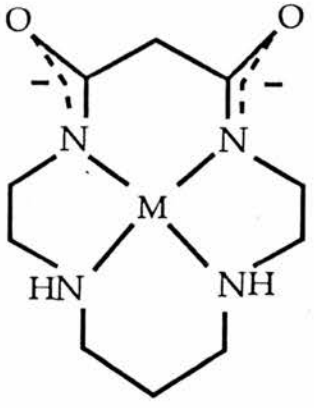

(IV)

Alkylation of the two *sec*-NH donors with electron withdrawing 2-cyanoethyl groups is expected to lower the basicity of the ligand. Potentiometric titration of LH_2 in the presence of two equivalents of acid gives the titration curve shown in Figure 4.14. The stepwise protonation equilibria of the ligand,

$$H^+ + LH_2 \rightleftharpoons LH_3^+ \quad ; K'_1 \qquad (72)$$

$$H^+ + LH_3^+ \rightleftharpoons LH_4^{2+} \quad ; K'_2 \qquad (73)$$

studied by potentiometric titration gives log K'_1 = 5.94 and log K'_2 = 3.05 at 25°C and I = 0.1 mol dm^{-3} ($NaNO_3$). The appropriate pK values for the equilibria,

$$LH_4^{2+} \rightleftharpoons LH_3^{+} + H^{+} \quad ;K_1 \qquad (74)$$

$$LH_3^{+} \rightleftharpoons LH_2 + H^{+} \quad ;K_2 \qquad (73)$$

are pK_1 = 3.05 and pK_2 = 5.94 at 25 °C, giving the speciation curve shown in Figure 4.15(a).

Comparison of pK values with those of dioxocyclam (Table 4.9) indicates a substantial reduction in the basicity of the cyanoethyl derivative compared with dioxocyclam, where pK_1 = 9.62 and pK_2 = 5.87 at 25°C (Table 4.6). Such effects are expected due to the electron withdrawing cyanoethyl substituents. The ratio K_1/K_2 is quite large due to electrostatic repulsive effects in LH_4^{2+}, and a similar effect is observed with dioxocyclam. In the more flexible ethylenediamine molecule log K_1 = 9.98 and log K_2 = 7.28[58], and electrostatic repulsive effects are somewhat less severe.

The interaction of copper(II) with the ligand was studied by potentiometric titration (with standard base) of solutions of the ligand and copper(II) perchlorate (molar ratio LH_2/Cu(II) = 1:1) containing an excess of acid (HNO_3) (Figure 4.14(b)). The titration data can be fitted to the set of equilibria

$$Cu^{2+} + LH_2 \rightleftharpoons [CuLH]^{+} + H^{+} \quad ; \log\beta_{11\text{-}1} = -3.43$$

$$Cu^{2+} + LH_2 \rightleftharpoons [CuL] + H^{+} \quad ; \log\beta_{11\text{-}2} = -9.18$$

The species [CuL] begins to form at pH 5.2 and is some 80% abundant at pH 6.6 (Figure 4.15(b)). The pK_a value for the ionisation can readily be derived as pK_a' = $\log\beta_{11\text{-}1} - \log\beta_{11\text{-}2}$ giving pK_a' = 5.75 at 25 °C.

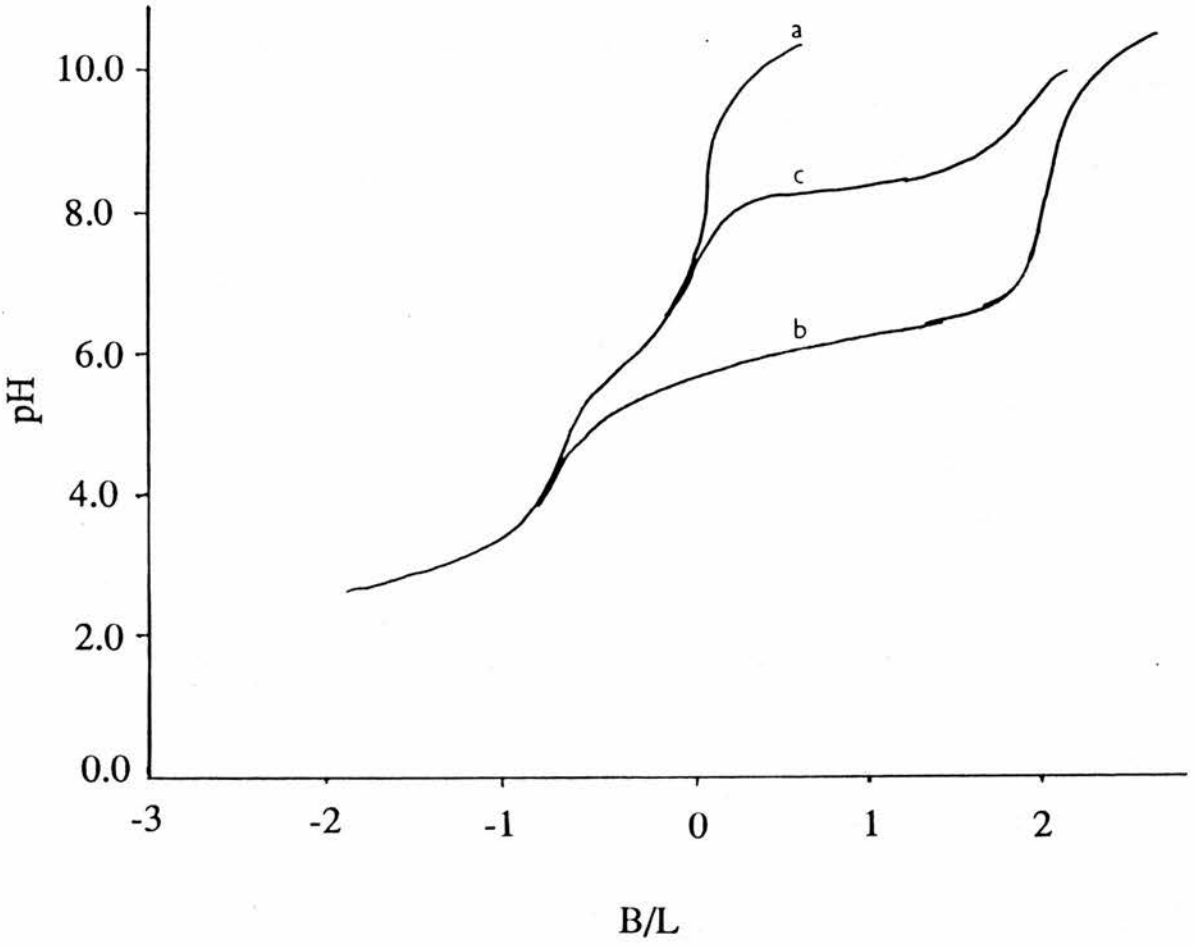

Figure 4.14 Titration curves for N,N'-bis (2-cyanoethyl) -5,7-dioxo-1,4,8,11- tetra-azacyclotetradecane (LH_2) : a) LH_2 + excess of acid ; b) LH_2 +1 equivalent of acid +1 equivalent of copper(II) ; c) LH_2 +1 equivalent of acid +1 equivalent of nickel(II) .

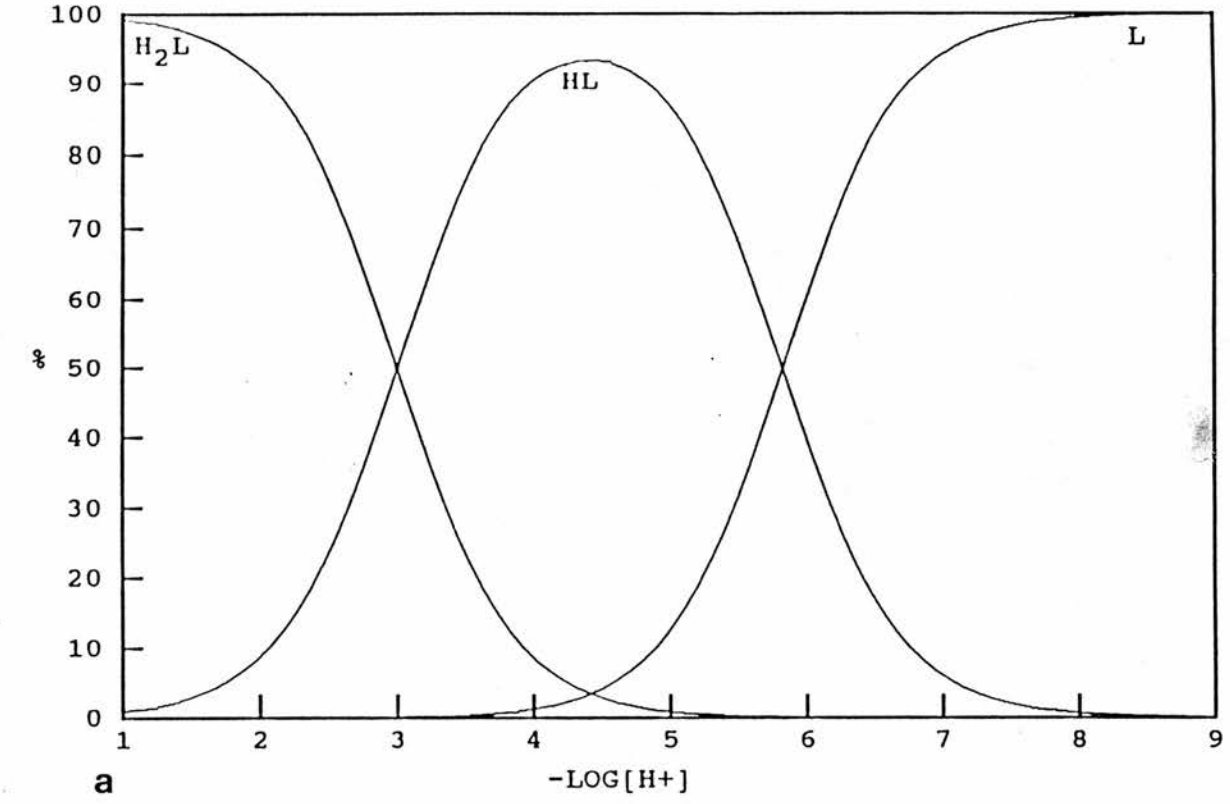

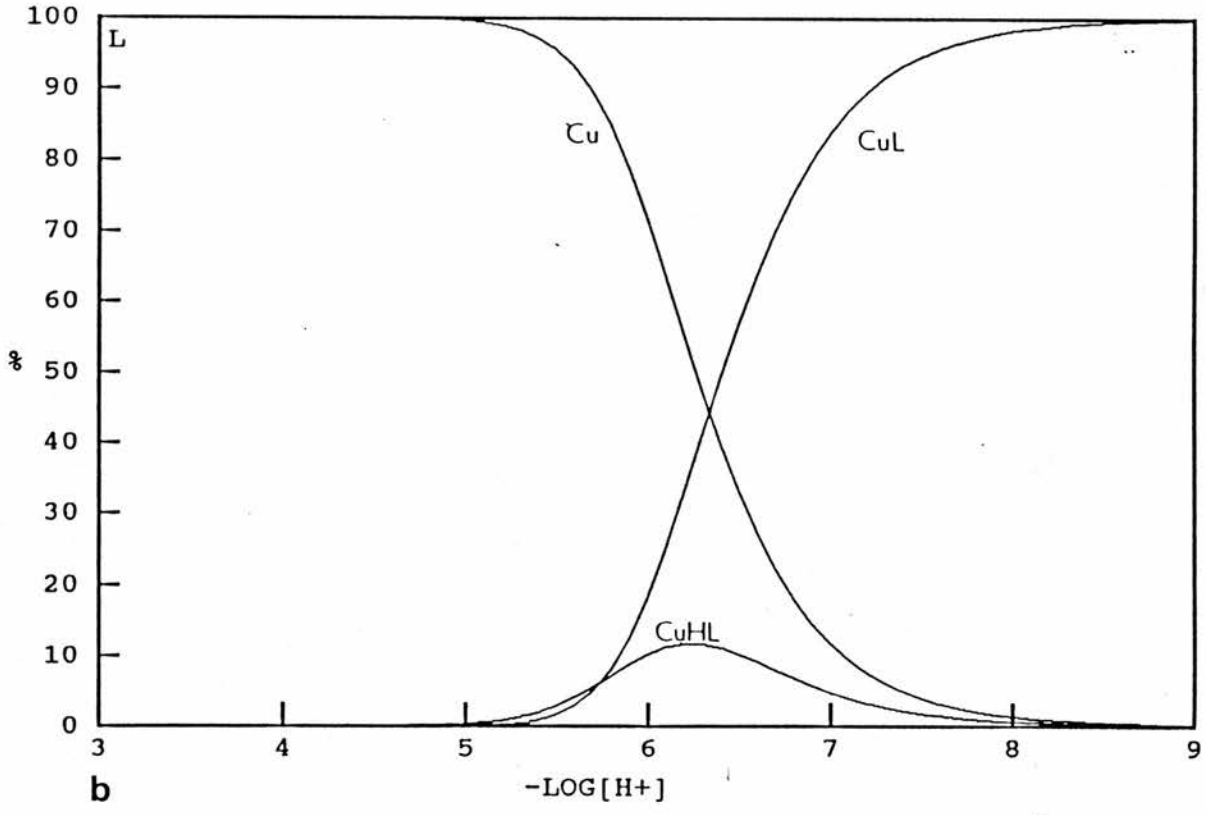

Figure 4.15 Species distribution diagram for a) N,N'-bis (2-cyanoethyl) -5,7-dioxo-1,4,8,11-tetra-azacyclotetradecane (LH_2) b) 0.001 M LH_2 + 0.001 M copper(II) .

Nickel(II), like copper(II), can also induce ionisation of the amide protons. The titration data for LH_2 / Ni(II) = 1:1 (Figure 4.14(c)) can be fitted to the single equilibrium

$$Ni^{2+} + LH_2 \rightleftharpoons [NiL] + 2H^+ \; ; \log\beta_{11-2} = -14.45$$

Deprotonation at the two amide sites occurs with increasing pH to give the orange square planar [NiL] which has λ_{max} 472 nm (ε = 81 $dm^3\ mol^{-1}\ cm^{-1}$) (Figure 4.16), due to the $^1A_{1g} \longrightarrow {}^1E_g$ transition of the singlet-ground state nickel ion.

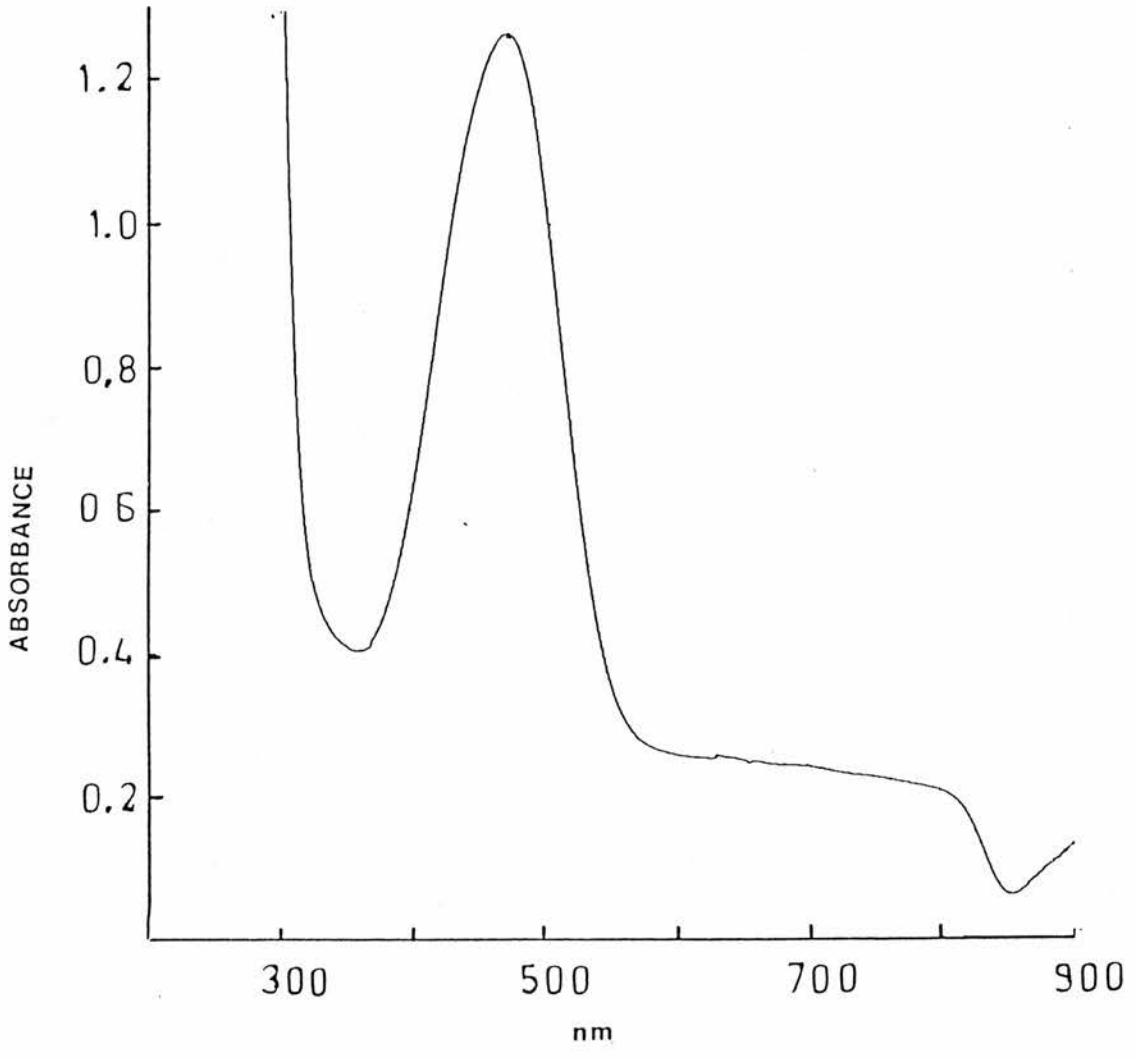

Figure 4.16 Uv.vis spectrum of 0.01 M Ni-N,N' - bis(2-cyanoethyl) -5,7-dioxo-1,4,8,11-tetra-azacyclotetradecane .

4.5 Linear Tetraamines as Reference Ligands for Tetra-aza Macrocycles. Chelating Properties of a Series of Linear Tetraamines with Copper(II) and Nickel(II).

The equilibria between the ligands 2,2,2-tet, 2,3,2-tet, and 3,2,3-tet and the ions H^+, Cu^{2+}, and Ni^{2+} were studied in aqueous solution (0.4 mol dm^{-3} $NaNO_3$) at 25.0 ^oC. The effect on the basicity of the four nitrogen atoms for the progressive and systematic expansion of the aliphatic chain in going from 2,2,2-tet to 2,3,2-tet, 3,2,3-tet, and 3,3,3-tet was also investigated.

The open-chain ligands (Series I) and the homologous cyclic tetraamines [13]aneN_4, [14]aneN_4, [15]aneN_4, and [16]aneN_4 (Series II) are shown in Figure 4.17.

4.5.1 EXPERIMENTAL

Materials:

The preparation of the open-chain tetraamines 2,2,2-tet, 2,3,2-tet and 3,2,3-tet is described in Chapter 1. The corresponding hydrobromide salts of these ligands (L.4HBr) were prepared by adding an excess of hydrobromic acid to a cooled and continuously stirred alcoholic solutions of the amines, as described in Chapter 1. The tetramines L.4HBr were recrystallised twice from water-alcohol and dried *in vacuo*. Stock solutions of the amine salts were prepared and standardised potentiometrically as described in Chapter 2.

Measurements:

Potentiometric titrations of the ligands in absence and presence of copper(II) and nickel(II) nitrates were carried out using a Radiometer Titralab System. The temperature was maintained at 25 ^oC and each titration was performed on a solution volume of 25 cm^3 adjusted to ionic strength of 0.4 mol dm^{-3} with $NaNO_3$. Typical concentrations of the metal ion and ligand (in a 1:1 molar ratio) were in the range 1×10^{-3} to 3×10^{-3} mol dm^{-3}. The potentiometric data were processed on a Zenith computer using the SUPERQUAD program.

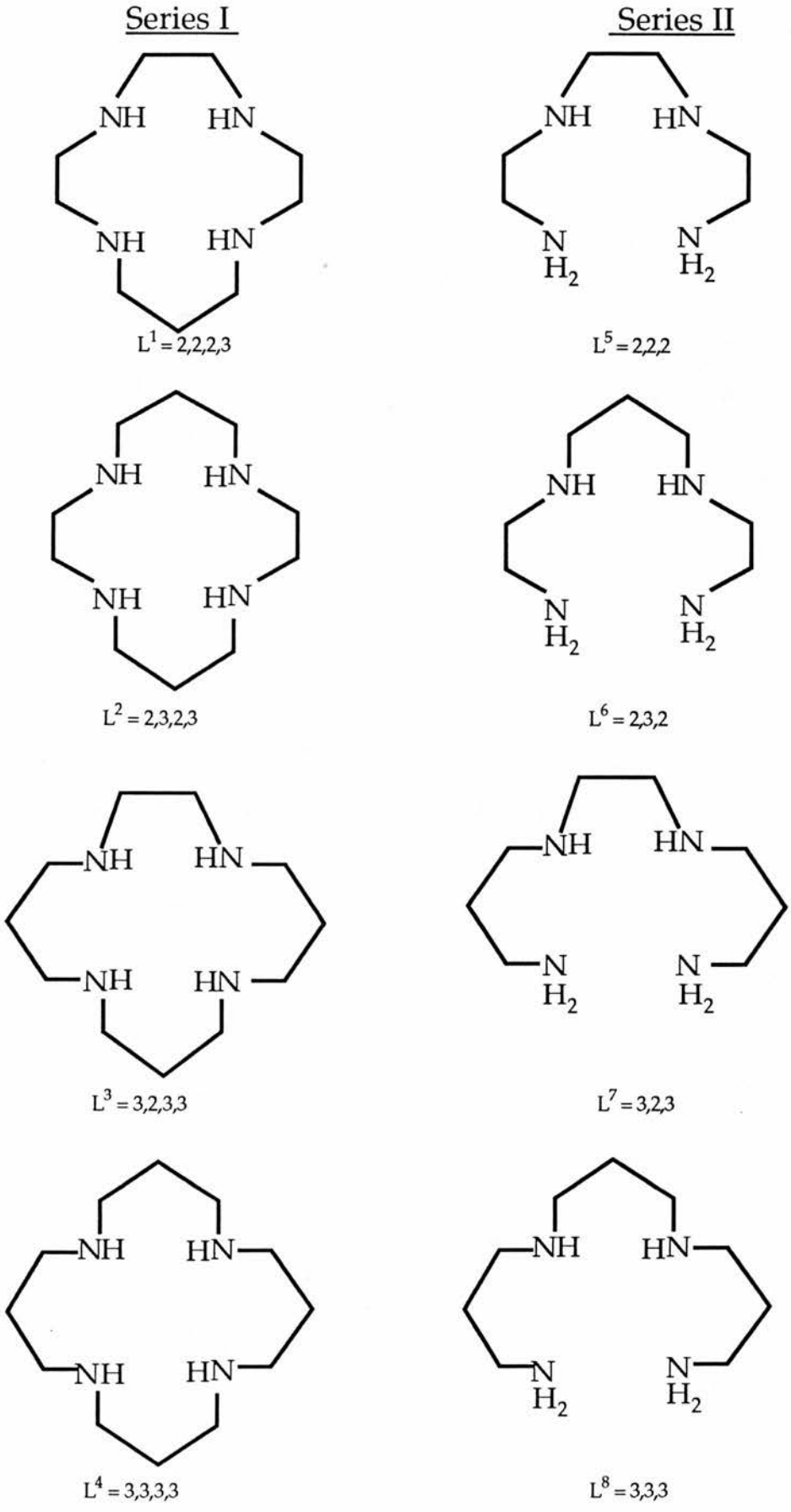

Figure4.17 Compounds discussed in this work .

4.5.2 RESULTS AND DISCUSSION:

Protonation Constants:

Potentiometric titration curves for the ligands (10^{-3} mol dm^{-3}) 2,2,2-tet, 2,3,2-tet and 3,2,3-tet are shown in Figure 4.18. For these ligands there are four protonation constants (Table 4.10). The constant for each successive stage is less than that for the previous stage due to statistical factors and electrostatic repulsion arising from successive protonation. For the purposes of comparison, the corresponding values for the protonation of the homologous cyclic tetraamine [13]aneN$_4$, [14]aneN$_4$, [15]aneN$_4$ and [16]aneN$_4$ are also shown in the Table. For the first three stages of neutralisation, the constants lie in the order 3,2,3-tet > 3,3,3-tet > 2,3,2-tet > 2,2,2-tet, while for the first two stages of neutralisation for the cyclic ligands, the constants are in the order [15]aneN$_4$ > [14]aneN$_4$ > [13]aneN$_4$ > [16]aneN$_4$. Clearly there is no correlation between the two series in terms of protonation constants.

Cu(II) Complexes.

For all three ligands studied in this work, two complexes were found the 1:1:0 complex $[CuL]^{2+}$ and the protonated species 1:1:1 $[CuHL]^{3+}$. A 2:1:2 complex $[(HL)Cu(HL)]^{4+}$ also occurs in the Cu(II)-2,2,2-tet and Cu(II)-3,2,3-tet systems. The formation constants obtained are listed in Table 4.11. Although the 1:1:0 and the 1:1:1 complexes are competitive, the percentage of the complexes in the 2,2,2-tet and 3,2,3-tet systems do not exceed 45% and 20% at pH > 3.5 respectively, Figure 4.19(a) and (b). The ligand 3,3,3-tet is noteworthy in that a protonated species was not detected[60]. The presence of protonated complexes reflects the adverse steric effects associated with coordination, the more strained systems being more readily protonated. Such mono-protonated copper species are also observed with [15]aneN$_4$ and [16]aneN$_4$ (Section 4.2). It is assumed that this protonation involves the opening of one of the two terminal chelate rings. Kinetic studies of dissociation indicate that in Ni(II) complexes with 2,2,2-tet (Chapter 1), it is easier to remove the terminal NH_2 groups than the central[61] ones.

Table 4.10 Protonation Constants (log K_i)[a] of Cyclic and Open-chain tetraamines at 25° C and I = 0.4 mol dm^{-3} ($NaNO_3$).

Reaction	2,2,2-tet [b]	2,3,2-tet [b]	3,2,3-tet [b]	3,3,3-tet [c]	[13]aneN_4 [d]	[14]aneN_4 [b]	[15]aneN_4 [b]	[16]aneN_4 [b]
$H^+ + L \rightleftharpoons HL^+$	9.730 (2)	10.336 (5)	10.820 (2)	10.45	11.10 (3)	11.050 (3)	11.18 (1)	10.69 (2)
	9.95 [c]	10.25 [c]	10.665 [c]					
$H^+ + HL^+ \rightleftharpoons H_2L^{2+}$	9.27 (2)	9.488 (7)	10.035 (5)	9.88	10.12	10.31	10.31 (1)	9.62 (3)
	9.31 [c]	9.50 [c]	9.956 [c]					
$H^+ + H_2L^{2+} \rightleftharpoons H_3L^{3+}$	6.76 (3)	7.214 (9)	8.567 (9)	8.54	< 2	< 2	5.21 (2)	7.48 (4)
	6.86 [c]	7.28 [c]	8.536 [c]					
$H^+ + H_3L^{3+} \rightleftharpoons H_4L^{4+}$	3.50 (4)	5.800 (9)	5.82 (4)	7.22	< 2	< 2	3.55 (2)	5.78 (4)
	3.66 [c]	6.02 [c]	5.837 [c]					

[a] Standard deviations are given in parentheses and correspond to the error in the last digit, Xi^2 = (4 - 8) and S = (0.1 - 1)

[b] This work.

[C] Reference 59.

[d] Reference 36.

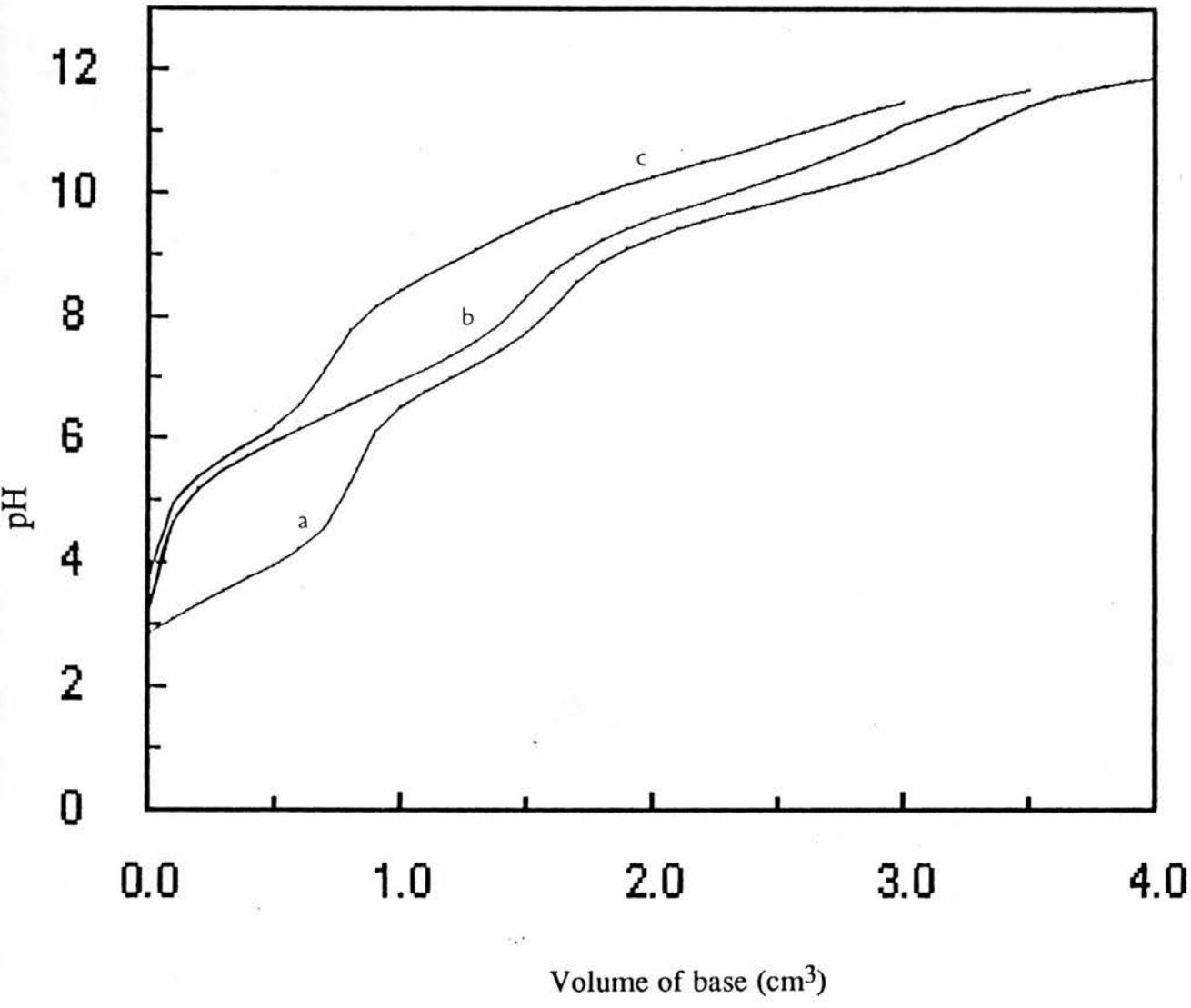

Figure4.18 Titration curves for a) 0.01 mol dm^{-3} 2,2,2-tet.4HBr ; b) 0.01mol dm^{-3} 2,3,2-tet.4HBr; c) 0.01 mol dm^{-3} 3,2,3-tet.4HBr .

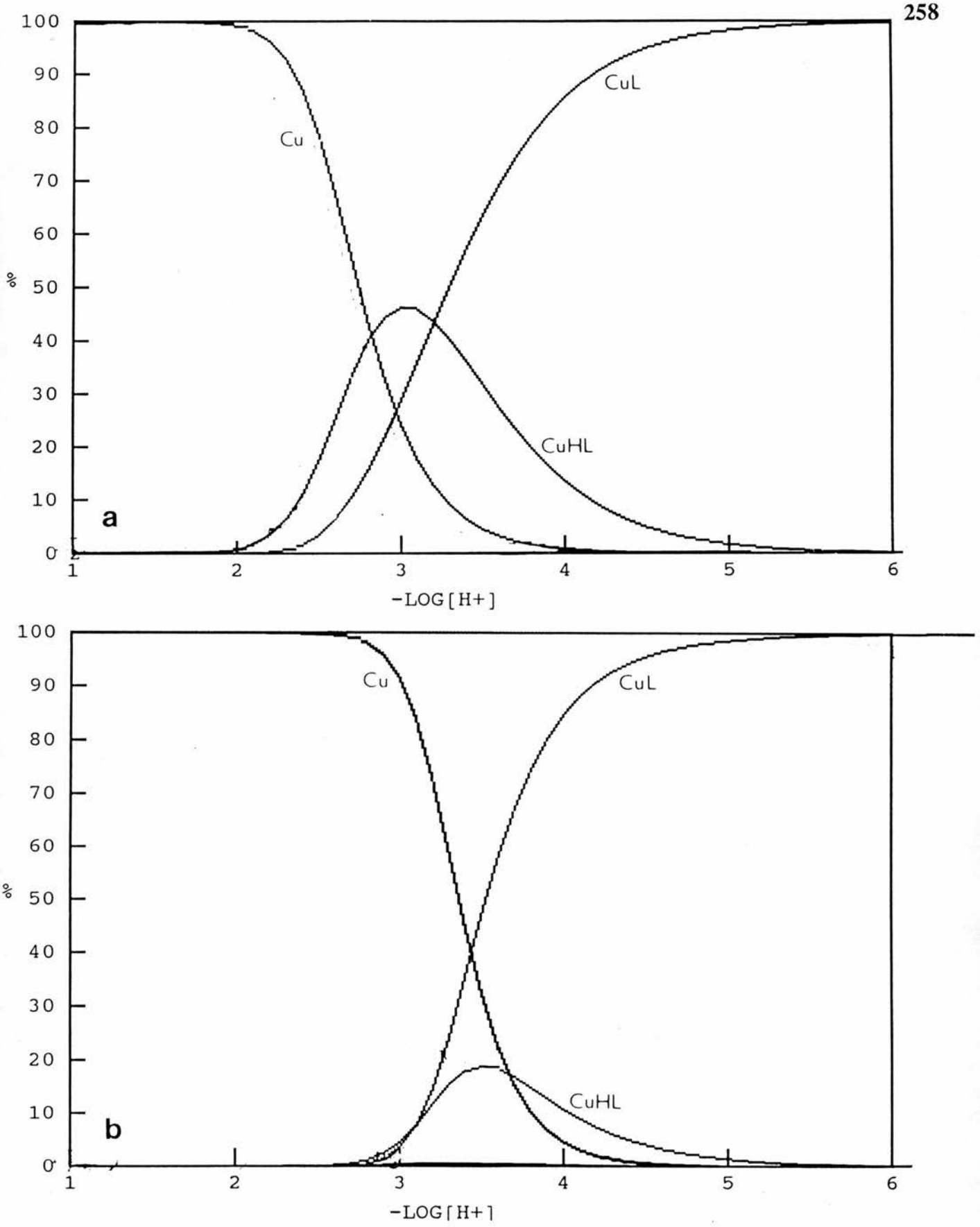

Figure 4.19 Species distribution diagram for a) 0.001 M Cu(II) and 0.001 M 2,2,2-tet , b) 0.001 M Cu(II) and 0.001 M 3,2,3-tet at 25.0 ^{o}C.

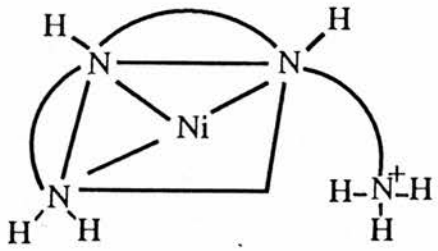

Table 4.11 indicates that the stability order is $[Cu(2,3,2\text{-tet})]^{2+}$ > $[Cu(3,2,3\text{-tet})]^{2+}$ > $[Cu(2,2,2\text{-tet})]^{2+}$ > $[Cu(3,3,3\text{-tet})]^{2+}$ and it can be deduced that an alternating sequence of five- and six-membered chelates increases complex stability. For complexes having chelate rings of alternating size, the one with the larger number of five-membered rings is the most stable. It is noteworthy that the above order of stability (Series II) almost parallels the order of stability in Series I for the macrocyclic ligands having the same sequence of five- and six- membered chelates, (Figure 4.17). Copper(II) complexes of Series I follow the stability order $[Cu([14]aneN_4)]^{2+}$ > $[Cu([15]aneN_4)]^{2+}$ > $[Cu([13]aneN_4)]^{2+}$ > $[Cu([16]aneN_4)]^{2+}$.

Ni(II) Complexes.

Two complexes are also present in solution, the protonated, 1:1:1 $[NiHL]^{3+}$ and the 1:1 complex $[NiL]^{2+}$, however, they form at higher pH than with copper(II) , (Figure 4.20(a) and (b)). Other species such as 2:1:2 $[(HL)Ni(HL)]^{4+}$ and 2:1:0 $[Ni(L)_2]^{2+}$ occur in the Ni-2,2,2-tet and 2,3,2-tet systems. In the Ni-3,2,3 tet system the monoprotonated complex $[NiH(3,2,3\text{-tet})]^{3+}$, diprotonated $[NiH_2(3,2,3\text{-tet})]^{4+}$ and triprotonated $[NiH_3(3,2,3\text{-tet})]^{5+}$ complexes occur. These protonated species were not observed with Cu(II). The formation constants are summarised in Table 4.12. The species $[NiL]^{2+}$ and the monoprotonated species $[NiHL]^{3+}$ are competitive and at no stage is there a large percentage of the protonated species present. As with Cu(II) the stability of these complexes follows the order $[Ni(2,3,2\text{-tet})]^{2+}$ > $[Ni(3,2,3\text{-tet})]^{2+}$ >

Table 4.11 Formation Constants for the Complexation of Cu^{2+} with 2,2,2-tet, 2,3,2-tet and 3,2,3-tet at 25°C and I = 0.4 mol dm^{-3} . p, q, r are the stoichiometric coefficients of L, Cu^{2+} and H^+.

Ligand	Stoichiometry p	q	r	$\log\beta_{pqr}$ (±σ)	S	χi^2	pH range	Reference
2,2,2-tet	1	1	1 [a]	23.49 (1)	0.7	5	2.3 - 5	This work
	1	1	0	20.28 (1)				
	2	1	1 [a]	45.996 (10)	0.20	40	2.3 - 5	This work
	1	1	1	23.486 (7)				
	1	1	0	20.494 (6)				
	1	1	0	20.2				59
2,3,2-tet	1	1	0 [b]	24.300 (3)	0.1	5	2.2 - 3.1	This work
	1	1	1 [b]	26.941 (10)	0.6	16	2.2 3.1	This work
	1	1	0	23.9				59
3,2,3-tet	1	1	1 [a]	25.70 (3)	0.1	10	3.2 - 5	
	1	1	0	22.10 (2)				
	2	1	2	43.95 (10)				
	1	1	1	25.430				60
	1	1	0	21.839				
3,3,3-tet	1	1	0	17.3				60

[a] Computed simultaneously.

[b] Computed separately.

Table 4.12 Formation Constants for the Complexation of Ni^{2+} with 2,2,2-tet, 2,3,2-tet and 3,2,3-tet at 25°C and I = 0.4 mol dm^{-3} . p, q, r are the stoichiometric coefficients of L, Ni^{2+} and H^+.

Ligand	Stoichiometry p	q	r	$\log\beta_{pqr}$ (±σ)	S	χ_i^2	pH range	Reference
2,2,2-tet	1	1	1[a]	18.310 (10)	0.4	22	3.2 - 5.5	This work
	1	1	0	13.837 (10)				
	2	1	2	37.32 (4)				
	2	1	0	25.57 (10)				
	1	1	0	14.1				60
2,3,2-tet	1	1	0[b]	16.4000 (7)	0.3	13	3.7 - 5.1	This work
	1	1	0[a,c]	16.54 (1)	0.6	15	3.7 - 5.1	
	2	1	2	39.69 (17)				
	1	1	0[a,c]	16.500 (6)	0.6	15	3.7 - 5.1	
	2	1	0	29.39 (9)				
	1	1	0[a,c]	16.444 (1)	0.05	13	3.7 - 5	
	1	1	1	20.439 (6)				
	1	1	0	16.4				60
3,2,3-tet	1	1	3[a]	30.932 (8)	0.3	20	4.0 - 7.0	This work
	1	1	1	20.471 (6)				
	1	1	0	14.765 (5)				
	1	1	2[a]	25.45 (2)	0.2	47	4.0 - 7.0	
	1	1	1	20.362 (7)				
	1	1	0	14.763 (3)				
	1	1	1[a]	20.53 (2)	1.5	30	5.0 - 7.0	
	1	1	0	14.67 91)				
	1	1	1	20.42 (1)				60
	1	1	0	14.693 (5)				60
3,3,3-tet	1	1	0	10.7				60

[a] Refined simultaneously.

[b] Refined separately.

[c] Obtained from potentiometric curves of 2:1 molar ratio of 2,3,2-tet to Ni (II).

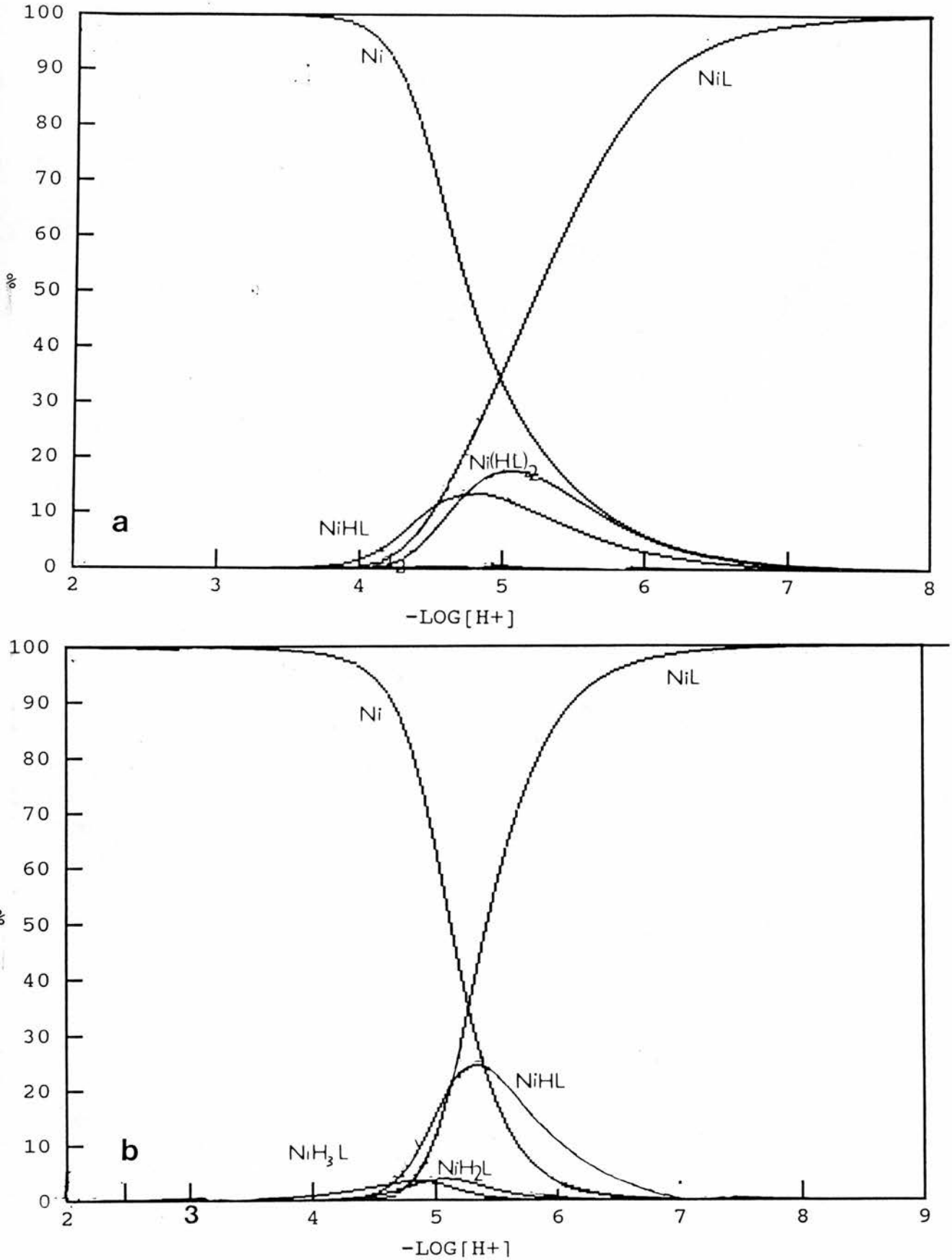

Figure 4.20 Species distribution diagram for a) 0.001 M Ni(II) and 0.001 M 2,2,2-tet , b) 0.001 M Ni(II) and 0.001 M 3,2,3-tet at 25.0 ^{o}C.

$[Ni(2,2,2\text{-tet})]^{2+} > [Ni(3,3,3\text{-tet})]^{2+}$. Interestingly this same order of stability occurs with the macrocyclic ligands of corresponding chelate ring sequence (Figure 4.17, series I and Table 4.14).

The nickel(II) complexes show larger variations in stability than those of copper(II). This effect can attributed to the fact that the copper ion has a greater capacity to adapt to the varying geometrical requirements of the ligands(62).

Macrocyclic Effect.

The additional stability of the macrocyclic complexes of copper(II) and nickel(II) (Series I) compared with those of the open-chain complexes (Series II) is the macrocyclic effect, defined as $\Delta \log ß(MAC)$. The 'macrocyclic effects' for the copper(II) and nickel(II) tetraamines are summarised in Tables 4.13 and 4.14. It can be concluded that the cyclic nature of the ligand has a larger influence on the complexes of nickel(II) than those of copper(II). Again, this reflects the greater capacity of the copper ion to adapt to the varying geometrical requirements of the ligands.

As some of the open-chain complexes of Ni(II) exist as highly protonated species, it was of interest to study the formation of ternary (i.e. mixed ligand complexes) in which two ligands compete for the metal ion Ni^{2+}. The ligands 2,2,2-tet and 3,2,3-tet were selected for two reasons: (1) the 2,2,2-tet ligand forms the octahedral species $[Ni(2,2,2\text{-tet})(H_2O)_2]^{2+}$, which is a *cis-trans* mixture, and (2) the 3,2,3-tet ligand behaves as a mono-, bi- and tetradentate ligand with Ni(II).

Mixed Ligand Complexes (Ni-L^5-L^7).

Potentiometric titrations for the binary Ni(II)-2,2,2-tet and Ni(II)-3,2,3-tet systems and the ternary Ni(II)-2,2,2-tet-3,2,3-tet system are shown in Figure 4.21. In all of these systems the molar ratio of metal to ligand was 1:1 for the binary systems and 1:1:1 for the ternary system. Three complexes are found in the Ni(II)-L^5-L^7 system: the diprotonated 1:1:1:2 (L^5:L^7:Ni^{2+}:$2H^+$), the triprotonated 1:1:1:3 (L^5:L^7:Ni^{2+}:$3H^+$) and the tetraprotonated 1:1:1:4 (L^5:L^7:Ni^{2+}:$4H^+$) species. The formation constants for these

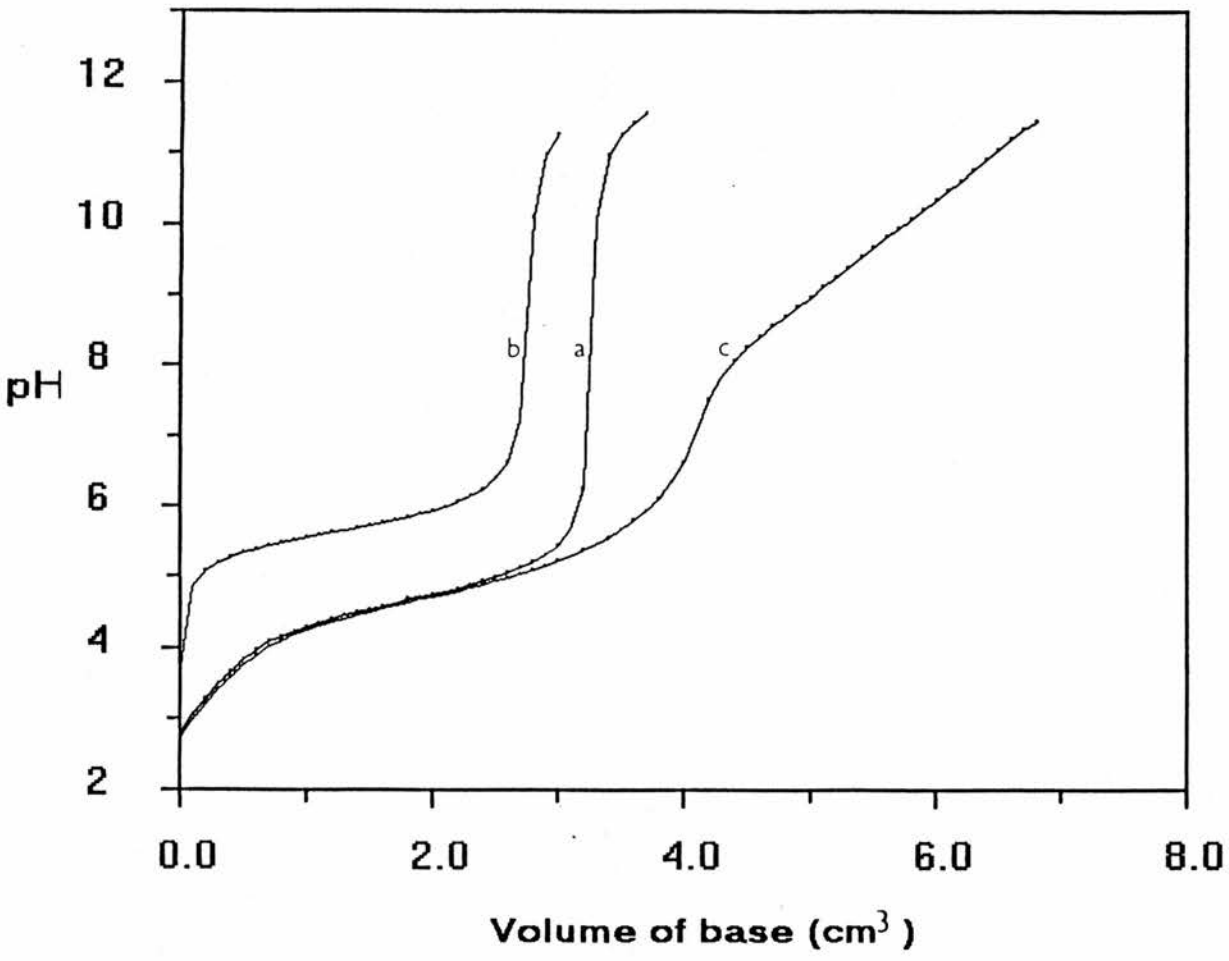

Figure4.21 Potentiometric titration curves of Ni(II) chelates of 2,2,2-tet , 3,2,3-tet , and 2,2,2-tet + 3,2,3-tet at 25.0 ^{o}C and I = 0.4 M NaNO3 . With the following molar ratios of metal to ligand : a) Ni(II) : 2,2,2-tet (1: 1) ; b) Ni(II) : 3,2,3-tet (1:1) ; c) Ni(II) : 2,2,2-tet : 3,2,3-tet (1:1:1) .

Table 4.13 Macrocyclic Effect in Complexes of Cu(II) with Tetra-azamacrocycles.

	Ligand			
	[13]aneN$_4$	**[14]aneN$_4$**	**[15]aneN$_4$**	**[16]aneN$_4$**
logβ_{110}	24.36 [a]	26.5 [a]	24.58	18.92
	2,2,2-tet	**2,3,2-tet**	**3,2,3-tet**	**3,3,3-tet**
logβ_{110}	20.28	24.30	22.10	17.30 [b]
logβ(MAC)	4.08	2.2	2.48	1.62

[a] Reference 38

[b] Reference 60

Table 4.14 Macrocyclic Effect in Complexes of Ni(II) with Tetra-azamacrocycles.

	Ligand			
	[13]aneN$_4$	**[14]aneN$_4$**	**[15]aneN$_4$**	**[16]aneN$_4$**
logβ_{110}	17.98 [a]	20.1 [a]	18.4	13.2
	2,2,2-tet	**2,3,2-tet**	**3,2,3-tet**	**3,3,3-tet**
logβ_{110}	13.84	16.50	14.77	10.7 [b]
logβ(MAC)	4 .14	3.6	3.63	2.5

[a] Reference 38

[b] Reference 60

complexes are listed in Table 4.15. The formation constants of the ternary complexes were obtained by taking into account (a) all protonation constants of the 2,2,2-tet and 3,2,3-tet ligands (b) all formation constants of the two binary Ni(II)-2,2,2-tet and Ni(II)-3,2,3-tet systems. The species considered to be present in solution were (charges omitted): H_4L^5, H_3L^5, H_2L^5, HL^5, H_4L^7, H_3L^7, H_2L^7, HL^7, $[NiHL^5]$, $[NiL^5]$, $[NiH_3L^7]$, $[NiH_2L^7]$, $[NiHL^7]$, $[NiL^7]$, $[NiL^5L^7H_2]$, $[NiL^5L^7H_3]$ and $[NiL^5L^7H_4]$. All of these species are listed in Table 4.15 and are given a refinement key value (a refinement key may be 1, 0, or -1. If the key is zero then $ß_{pqr}$ is held constant, if it is 1, $ß_{pqr}$ is refined, and if it is -1, $ß_{pqr}$ is ignored).

The constants for the ternary species correspond to the following equilibria

$$pL^5 + qL^7 + rNi^{2+} + sH^+ \rightleftharpoons L^5_pL^7_qNi^{2+}_rH_s \qquad (76)$$

$$ß_{pqrs} = [L^5_pL^7_qNi^{2+}_rH_s] / [L^5]^p[L^7]^q[Ni^{2+}]^r[H^+]^s \qquad (77)$$

Stabilities of the Binary and Ternary Complexes.

The parameter generally used to indicate the stability of ternary complexes with respect to the binary ones is $\Delta\log K$. According to Sigel[63], these parameters are used as a measure of stability instead of $\log ß_{pqrs}$ because they are indirectly dependent of ligand basicity. Log K can be calculated by using the equations

$$\log \mathbf{K} = \log K^{ML}_{MLL'} - \log K^{M}_{ML'} \qquad (78)$$

$$= \log K^{ML'}_{MLL'} - \log K^{M}_{ML} \qquad (79)$$

$$= \log K^{M}_{MLL'} - \log K^{M}_{ML} - \log K^{M}_{ML'} \qquad (80)$$

The value of log K is a measure of the coordination tendency of the secondary ligand (L') towards the ML binary complex, relative to $M(II)_{(aq)}$

Table 4.15 Formation Constants of Ligands, Binary and Ternary Complexes and logK at 25°C; Standard Deviations are Given in Paranthesis.

$L^5_pL^7_qNi_rH_5$	p	q	r	s	$\log\beta_{pqrs}$	Refinement[a] key	$\log K_{pqrs}$
Proton -L^5	1	0	0	1	9.73 (2)	0	
	1	0	0	2	9.27 (2)	0	
	1	0	0	3	6.76 (3)	0	
	1	0	0	4	3.50 (4)	0	
Proton-L^7	0	1	0	1	10.82 (2)	0	
	0	1	0	2	10.04 (1)	0	
	0	1	0	3	8.57 (1)	0	
	0	1	0	4	5.82 (4)	0	
Ni(II)-L^5	1	0	1	1	18.37 (1)	0	
	1	0	1	0	13.84 (1)	0	
Ni(II)-L^7	0	1	1	3	30.93 (2)	0	
	0	1	1	2	25.45 (2)	0	
	0	1	1	1	20.47 (1)	0	
	0	1	1	0	14.77 (2)	0	
Ni(II)-L^5-L^7	1	1	1	4	50.22 (9)[b,c]	1	0.92
	1	1	1	3	44.71 (4)	1	1.39
	1	1	1	3	46.16 (7)[b,c]	1	
	1	1	1	2	39.82 (7)	1	1.09

[a] This key may be 1, 0, or -1. If the key is zero then β_{pqrs} is held constant. If it is 1, β_{pqrs} is refined, and if it -1, β_{pqrs} is ignored.

[b] Refined simultaneously.

[c] $\chi i^2 = 5$, $s = 0.5$, pH range 3 - 7.

$$M(L) + M(L') \rightleftharpoons M(L)(L') + M(II) \qquad (81)$$

In general, Equation (81) is expected to be to the left hand side, corresponding to the common rule $K^{M}_{ML} > K^{M(L)}_{MLL'}$ and to statistical considerations[64]. The first ligand to bind has more binding possibilities than the second one. The values of $\Delta\log K_{pqrs}$ (based on the cumulative overall stability constants, $\log ß_{pqrs}$, for example, $\Delta\log K_{1112} = \log ß_{1112} - \log ß_{1011} - \log ß_{0111} = 39.82 - 18.37 - 20.36 = 1.09$) are noted in Table 4.15. It is clear that all the ternary complexes are more stable than expected statistically, with $\Delta\log K_{pqrs} > 0$ indicating that equilibrium (81) is partly displaced to the right. The origin of the greater stability of the present complexes is open to question. It is possible that hydrogen bond formation between the non-coordinated ammonium groups ($-NH_3$) and the coordinated amine groups stabilizes the ternary complex. Table 4.15 shows that the sequence of stability, $\Delta\log K_{pqrs}$, for the ternary complexes follows the order

$$[L^5L^7NiH_3]^{5+} > [L^5L^7NiH_2]^{4+} > [L^5L^7NiH_4]^{6+}.$$

References

1. F.R. Hartley, C. Burgess, R. Alcock, "Solution Equilibria", Ellis Horwood, New York (1980).

2. G. Biedermann and L.G. Sillen, *Ark. Kemi,* **425**, 5 (1953).

3. L. Johansson, *Acta. Chem. Scand.,***A29**, 365 (1975).

4. N. Bjerrum, *Z .Anorg. Allgem. Chem,* **119**, 179, (1921).

5. J. Bjerrum, "Metal ammine Formation in Aqueous Solution (reprinted 1957)". Coppenhagen: P. Haase and Son.

6. H.S. Rossotti, *Talanta,***21**, 809 (1974).

7. C.W. Childs, P.S. Hallman and D.D. Perin, *Tatlanta,* **16**, 119 (1969).

8. S. Feldberg, P. Klotz and L. Newman, *Inorg. Chem,* **11**, 2860 (1972).

9. J.J. Kankare, *Anal. Chem.,* **342**, 1322 (1970).

10. W.E. Grove, "Brief Numerical Methods". Prentice Hall, London (1966).

11. F.J.C. Rossotti, H.S. Rossotti and R.J. Whewell, *J. Inorg. Nucl. Chem.,* **33**, 2051 (1971).

12. D.J. Leggett, "Computational Methods for the Determination of Formation Constants", Plenum Press, New York (1985).

13. D.J. Leggett and W.A.E. McBryde, *Anal. Chem.,* **47**, 1065 (1975).

14. P. Gans, A. Sabatini and A. Vacca, *J. Chem. Soc. Dalton Trans.,* 1195 (1985).

15. L. Bologni, A. Sabatini and A. Vacca, *Inorg. Chim. Acta,* **69**, 71 (1983).

16. L. Jancav and J. Havel, *Scripta Fac. Sci. Nat. Univ. Purk. Brunensis,* **14**, 73 (1984).

17. D.J. Legget, S.L. Kelly, L.R. Shine, Y.T. Wu, D. Chang and K.M. Kadish, *Talanta,***8**, 574 (1983).

18. M. Meloun, "Computation of Solution Equilibria", Conference on Optimization in Analytical Chemistry., *Trencianske Teplice,* **19**, April 1983.

19. M. Meloun, M. Javurek, J. Havel, *Talanta,* **33**, 6, 513 (1986).

20. D.K. Cabbiness and D.W. Margerum, *J. Am. Chem. Soc.,* **91**, 6540 (1969).

21. F.P. Hinz and D.W. Margerum, *Inorg. Chem.,* **13**, 2941 (1974).

22. M. Kodama and E. Kimura, *J. Chem. Soc. Dalton Trans.*, 2269 (1977).

23. M. Micheloni, P. Paoletti and A. Sabatini, *J. Chem. Soc. Dalton Trans.*, 1189 (1983).

24. V.J. Thom, G.D. Hosken and R.D. Hancock, *Inorg. Chem.*, **24**, 3378 (1985).

25. V.J. Thom, and R.D. Hancock, *J. Chem. Soc.Dalton Trans.*, 1877 (1985).

26. M. Micheloni, P. Paoletti, L.S. Hertli and T.A. Kaden, *J. Chem. Soc. Dalton Trans.*, 1169 (1985).

27. M. Kodama and E. Kimura, *J. Chem. Soc.*, Commun., 326 (1975).

28. A. Anichini, L. Fabbrizi, P. Paoletti and R.M. Clay, *J. Chem. Soc. Dalton Trans.*, 577 (1978).

29. L.F. Lindoy, "The Chemistry of Macrocyclic Ligand Complexes", *Cambridge University Press, Cambridge,* 1989, pp. 4-6, 185-191.

30. R.D. Hancock and A.E. Martell, *Comments Inorg. Chem.*, **6**, 237 (1988).

31. R.D. Hancock and G.J. McDougall, *J. Am. Chem. Soc.*, **102**, 6551 (1980).

32. A.K. Covington, R.G. Bates and R.A. Durst, *Pure and Appl. Chem.*, **57**, 531 (1985).

33. A.E. Martell and R.M. Smith, "Critical Stability Constants", *Plenum, New York,* 1974, vol. 1.

34. R.G. Bates, "Determination of pH", John Wiley, New York, 1973, 2nd Ed, p. 38.

35 . M.Micheloni, A. Sabatini and P. Paoletti, *J. Chem. Soc.*, Perkin Trans., **2**, 828 (1978).

36. P. Leugger, L. Hertli and T.A. Kaden, *Helv. Chim Acta.*, **61**, 2296 (1978).

37. M. Kodama and E. Kimura, *J. Chem Soc. Dalton,* 2341 (1976).

38. R.C. Luckay and R.D. Hancock, *J. Chem. soc. Dalton Trams.*, 1491 (1991).

39. E. Gallori, E. Martini, M. Micheloni and P. Paoletti, *J. Chem. Soc. Dalton Trans.*, 1722 (1980).

40. I. Tabushi, T. Taniguchi, H. Kato, *Tetrahedron Lett.*, 1049(1977) .

41. D.K. Cabbiness and D.W. Margerum, *J. Am. Chem. Soc.*, **92**, 2151 (1970).

42. E.J. Billo, *I norg. Chem.*, **23**, 236 (1984).

43. D.W. Margerum and G.R. Dukes, "Metal Ions in Biological Systems", vol. I, ed. H. Sigel, *Marcel Dekker, New York,* p 157 (1974) and references therein.

44. H.A.O Hill and K.A. Raspin, *J. Chem. Soc. (A),* 3036 (1968); 619 (1969).

45. A. Zuberbuhler, S. Fallab and T. A. Kaden, *Helv. Chim. Acta,* **50**, 889 (1967); 51, 1798 and 1805 (1968).

46. L. Fabbrizzi, F. Forlini, A. Perotti and B. Segehi, *Inorg. Chem,* **23**, 807 (1984).

47. M. Kodama and E. Kimura, *J. Chem. Soc. Dalton Trans.*, 325 (1979).

48. F. Holmes and D.R. Williams, *J. Chem. Soc. A,* 1702 (1967).

49. R.W. Hay, M.P. Pujari, W.T. Moodie, S. Craig, D.T. Richens, A. Perotti and L. Ungaretti, *J. Chem. Soc. Dalton Trans,* 2605 (1987).

50. F.P. Bossu, K.L. Chellappa and D.W. Margerum, *J. Am. Chem. Soc.*, **99**, 2195 (1977).

51. R.W. Hay, "Current Topics in Macrocyclic Chemistry in Japan" ed E. Kimura, *University of Horoshima Press, Hiroshima,* 1987.

52. T.A. Kaden, *Top. Curr. Chem.*, **121**, 157 (1984).

53 P.V. Bernhardt and G.A. Lawrence, *Coord. Chem. Rev.*, **104**, 297 (1990).

54. R.W. Hay, M.P. Pujari, W.T. Moodie, S. Craig, D.T. Richens, A. perotti and L. Ungaretti, *J. Chem. Soc. Dalton Trans,* 2605 (1987).

55. R.W. Hay and R. Bembi, *Inorg. Chim. Acta,* **65**, L227 (1982).

56. K.P. Wainwright, *J, Chem. Soc. Dalton Trans.*, 2117 (1980).

57. R.W. Hay and P.R. Norman, *Transition Met. Chem.*, **5**, 232 (1980).

58. A. Vacca and D. Arenare, *J. Phys. Chem.*, **71**, 1495 (1967); R. Barbucci, P. Paoletti and A. Vacca, *J. Chem. Soc.* (A), 2202 (1970).

59. R. M. Clay, S. Corr, M. Micheloni and P. Paoletti, *Inorg. Chem.*, **24**, 3336 (1985).

60. P. Paoletti, L. Fabbrizzi and R. barbucci, *Inorg. Chem.*, **8**, 1861 (1973).

61. G.A. Nelson and R.G. Wilkins, *J. Chem. Soc.*, 2662 91963).

62. J. Gazo, I.B. Bersuker, J. Garaj, M. Kabesova, J. Kohout, H. Langfelderova, M. Melnik, M. Serator, and F. Valach, *Coord. Chem. Rev.*, **19**, 253 (1976).

63. H. Sigel, in Metal ions in Biological Syatems, *Marcel Dekker, New York,* 1973, vol. 2.

64. E. Dubler, U.K. Haring, K.H. Scheller, P. Baltzer and H. Sigel., *Inorg. Chem.*, **23**, 3785 (1984).

APPENDIX 1

The Union Giken stopped-flow spectrometer

A Union Giken, RA-401 stopped-flow spectrometer provided with RA-451 data processor, RA-453 monitor scope, and RA-452 X-Y recorder was used for the kinetic measurements. This instrument utilizes nitrogen gas pressure for driving and stopping the solutions, as shown in Figure A.1. It is designed for convenience of data accumulation (both automatic and manual) and can measure changes of absorbance, fluorescence and optical rotation. The dead time is in the range of 0.5-1.5 ms depending on the flow velocity and dead volume of the cells.

The instrument comprises two main compartments:

a) the detection system, and

b) the fluid handling system.

a) The detection system:

A light source (UV and VIS lamps) and monochromator, photomultiplier and amplifier plus the recording system comprise the detection system. In the recording system, the reaction signal is directly stored in a digital memory, after analog-digital conversion at high sampling rate, and then read out and recorded on a pen recorder. As a result the reaction curve is easily obtained ready for calculation immediately after the measurement. Data accumulation, averaging, and smoothing are also possible. An example of data averaging is shown in Figure A.2.

b) The fluid handling system:

The fluid handling system Figure A.1, is an end-stopping type, and utilizes gas pressure both for driving the solutions and for stopping the flow. A computer-

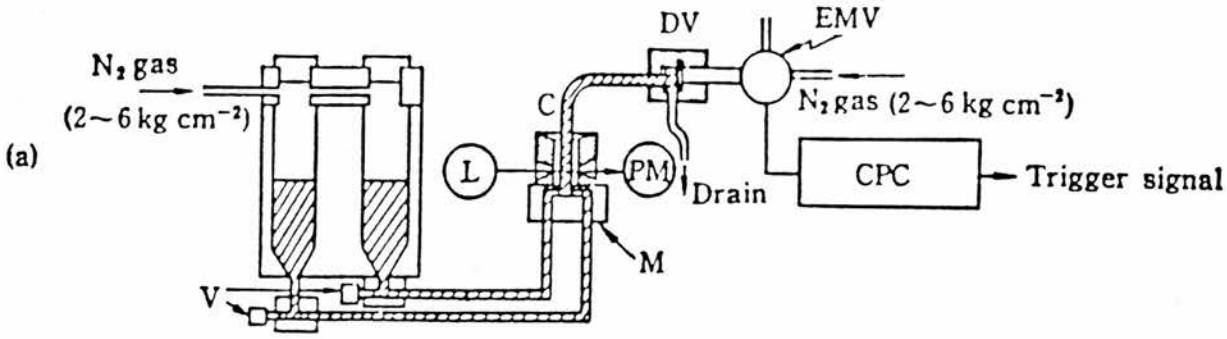

Figure A.1 A stopped-flow diagram of the apparatus of gas pressure-driven type capable of automatic data averaging. Gas pressure (2-6 Kg cm^{-2}) applied to the two solutions in the syringes is used to drive the solutions. The initiation and stopping of the flow is done by opening and closing the diaphragm valve (DV), which is operated by an electromagnetic valve (EMV) controlled by the control-program circuit (CPC). The reaction signal from the photomultiplier (PM) can be automatically accumulated and averaged by the CPC. L, light source and monochromator system; M, mixer; C, cell; V, valve.

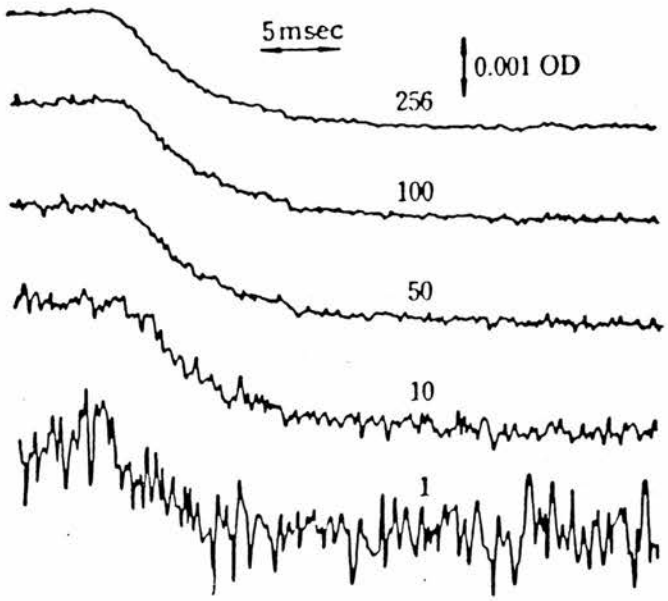

Figure A.2. Data obtained with a gas pressure-driven stopped-flow apparatus capable of automatic data averaging. Reduction of DCIP (2 uM) by L-ascorbic acid (2.5 mM) at pH 4.2 and 20 ^{o}C observed at 524 nm with a 2 mm cell. The numerals in the figure show the number of accumulations of data.

controlled electromagnetic value is used to initiate and stop the flow, opening and closing a diaphragm value by means of nitrogen gas pressure.

Calibration

The instrument calibration and validity of performance was checked by reinvestigation of the Fe(II)-thiocyanate system (published by Meiling and Pardue)[1]. Materials were:

(1) Potassium thiocyanate, a stock solution of 2.0×10^{-4} M, prepared in 1.0M of ($NaClO_4$).

(2) Fe(III) perchlorate, a stock solution of 0.093 M prepared in 0.20 M ($HClO_4$) and standardized potentiometrically at pH = 2 with 0.01 M standard EDTA.

(3) Perchloric acid, a stock solution of 3.88 M prepared and standardized against 0.1 M of standard (NaOH).

(4) Sodium perchlorate, a stock solution of 3.0 M prepared by diluting 3.88 M of perchlorate acid stock solution with water. The pH of the stock ($NaClO_4$) solution was adjusted to 7.0 with Na_2CO_3. The solution was heated to remove dissolved carbon dioxide. The ionic strength was kept constant at 1.0 M by adding the appropriate amount of 3 M $NaClO_4$.

---

[1]G.E. Mieling and H.L. Pardue, Anal. Chem., 1333, 50 (1978).

APPENDIX 2

PUBLICATIONS

Published Papers

EQUILIBRIUM AND KINETICS STUDIES OF THE Fe(III) COMPLEX FORMATION WITH GLYCINE-HYDROXAMIC ACID, M.S. El-Ezaby and M.M.Hassan, *Polyhedron* , **4**, 429(1985).

COMPLEXES OF HYDROXAMATES PART 1. INTERACTION OF METHIONINE-HYDROXAMIC ACID WITH IRON(III) IN AQUEOUS SOLUTION., M.S. El-Ezaby, H.M. Marafie, M.M. Hassan, and H.M. ABU SOUD, *Inorg Chim Acta* , **123**, 53 (1986).

COMPLEXES OF HYDROXAMATES III. EQUILIBRIUM AND KINETIC STUDIES ON THE REACTIONS OF IRON(III) WITH MONOHYDROXAMIC ACIDS., N.M. Shuaib, H.M. Marafie, M.M. Hassan and M.S.El-Ezaby., *J. Inorganic Biochemistry* ,**3**, 171(1987).

COMPLEXES OF HYDROXAMATES V: EQUILIBRIUM AND KINETICS OF THE FORMATION OF THE BINARY AND TERNARY Complexes INVOLVED IN THE NICKEL(II)-HISTIDINE-HYDROXAMIC ACID-PYRIDOXAL SYSTEM., M.S. El-Ezaby, N.M. Shuaib, H.M. Marafie, and M.M. Hassan, *J. Inorganic Biochemistry* , **33**, 161 (1988).

COMPLEXES OF VITAMIN B6 XIX: THE INTERACTION OF Fe(III)-PYRIDOXOL SYSTEM WITH GLYCINE-HYDROXAMIC ACID., M.S.El-Ezaby and M.M. Hassan., *J. Inorganic Biochemistry* , **34**, 241 (1988).

Conference Posters

FORMATION KINETICS FOR THE REACTION OF MACROCYCLIC TETRA-AZA LIGANDS WITH HYDROXYCUPRATE(II) SPECIES., R. W . Hay and M.M. Hassan., 16th International Symposium on Macrocyclic Chemistry (Sheffield,England,1-6-September 1991).

LIGAND EXCHANGE REACTIONS. THE KINETICS OF THE REACTION OF [14]aneN$_4$, [15]aneN$_4$, and [16]aneN$_4$ WITH COPPER(II)-GLYCYLGLYCINATE., R. W. Hay, and M.M. Hassan.Inorganic Mechanisms Discussion Group(York, England, 15-17- December 1991 Meeting).

Papers Submitted for Publication

LIGAND EXCHANGE REACTIONS. THE KINETICS OF THE REACTION OF [14]aneN$_4$, [15]aneN$_4$ AND [16]aneN$_4$ with COPPER(II) GLYCYLGLYCINATE., R. W. Hay, and M.M. Hassan. (*J. Chem. Soc. Dalton*)

KINETICS OF THE ACID DISSOCIATION OF THE COPPER(II) AND NICKEL(II) COMPLEXES OF 5,7-DIOXO-1,4,8,11-TETRA-AZACYCLOTETRADECANE., R. W. Hay, and M.M. Hassan. (*J. Chem. Soc. Dalton*).

A.7

KINETICS AND MECHANISM OF THE REACTION OF 1,4,8,12-TETRA-AZACYCLOPENTADECANE ([15]aneN_4) WITH COPPER(II) IN BASIC SOLUTION., R. W. Hay, and M.M. Hassan. (*Inorg. Chim. Acta.*).